Australian Government
Geoscience Australia

Geoscience Australia Marine Survey 282
Post-Survey Report

Shallow Gas and Benthic Habitat Mapping, Arafura Sea

RV Southern Surveyor April - May 2005

Logan, G.A., Rollet, N., Glenn, K., Grosjean, E., Ryan, G.J., and Shipboard Party

Record
2006/19

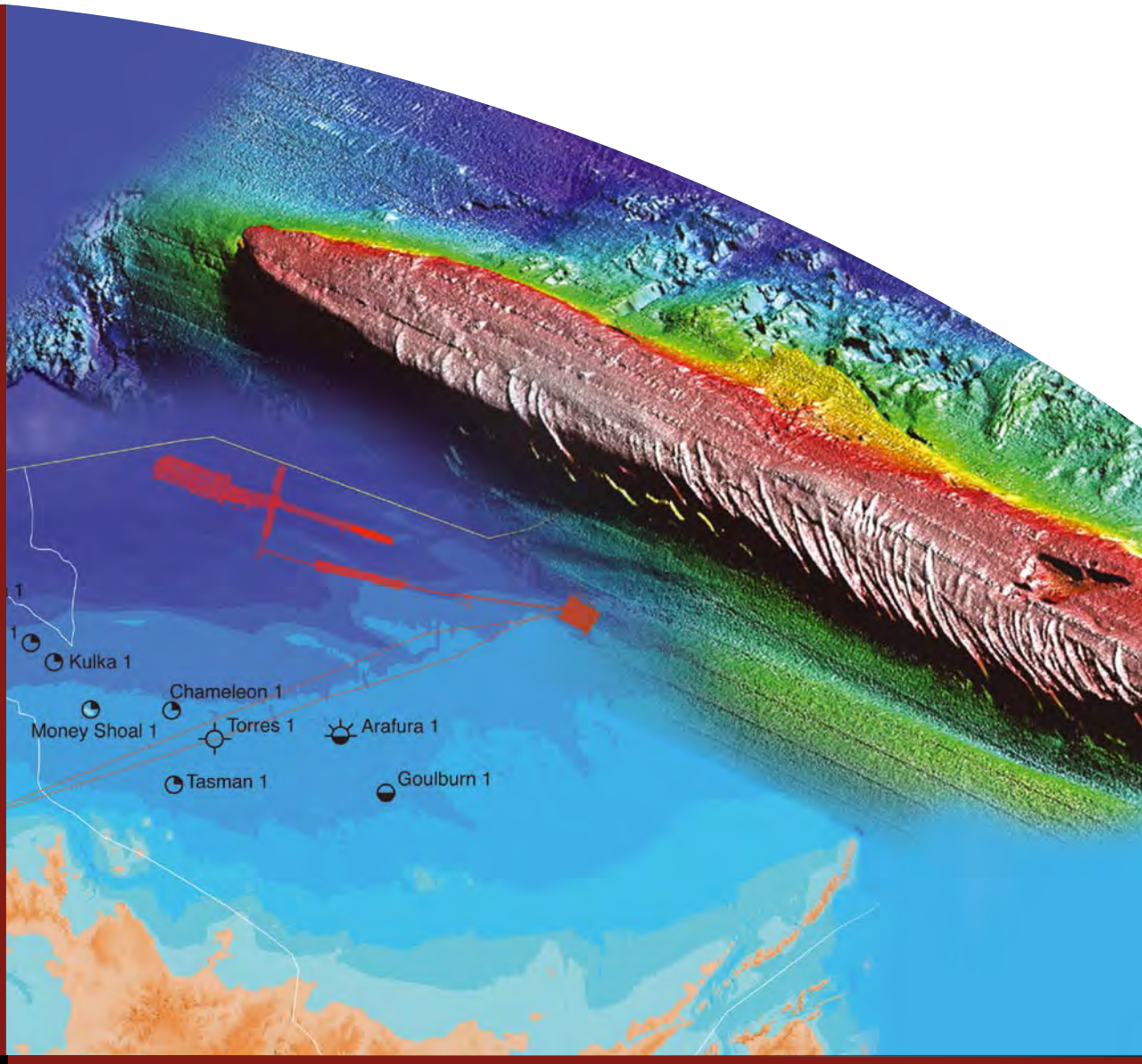

Geoscience Australia Record 2006/19

Geoscience Australia Marine Survey 282 Post-Survey Report

Shallow Gas and Benthic Habitat Mapping, Arafura Sea

RV Southern Surveyor
29th April (Darwin) – 28th May 2005 (Darwin)

G.A. Logan, N. Rollet, K. Glenn, E. Grosjean, G.J. Ryan, and Shipboard Party

Geoscience Australia, GPO Box 378, Canberra, ACT 2601

Australian Government

Geoscience Australia

Department of Industry, Tourism and Resources
Minister for Industry, Tourism and Resources: Senator The Hon. Ian Macfarlane, MP
Parliamentary Secretary: The Hon. Robert Baldwin, MP
Secretary: Mark Paterson
Geoscience Australia
Chief Executive Officer: Dr Neil Williams

ISSN: 1448 2645

GeoCat No. 64003
Bibliographic reference: Logan, G.A., Rollet, N., Glenn, K., Grosjean, E., Ryan, G.J. and Shipboard Party (2006). Shallow Gas and Benthic Habitat Mapping, Arafura Sea - Geoscience Australia Marine Survey 282, Post-Survey Report. Geoscience Australia, Record 2006/19, 342pp.
Correspondence for feedback:
Sales Centre
Geoscience Australia
GPO Box 378
Canberra
ACT 2601

Sales@ga.gov.au

Executive Summary

This report contains the preliminary results of Geoscience Australia Survey 282 conducted between 29th April and 28th May, 2005. One location and three areas were surveyed in the Arafura Sea, between 9° and 10°S and 133° to 135°E, using various geophysical techniques (multibeam, side-scan sonar and sub-bottom profile) and studied using video transects, sea bed and water sampling. A range of geophysical indicators have been used to infer the presence of shallow gas in the Arafura Sea. The existence of shallow gas has been confirmed by the analysis of core material obtained during the survey. This sampled gas has a microbial origin related to decay of organic matter in Holocene mud-filled channels. However, geophysical data indicates that another source of gas exists in deeper parts of the sedimentary section and this gas appears to be migrating up from depth. Intense pockmark fields (~350/km^2) are developed above the mud-filled channels but they have also been recorded away from these channels. The development and density of the pockmark fields appears to be related to sea bed sediment type, microbial gas production within the mud-filled channels and supply of fluids from deeper within the sedimentary section. Correlation of sub-bottom profile data with conventional seismic data also indicates that there are links between deep first-order Proterozoic faults, second-order Jurassic faults and third-order faults to sea bed observed in sub-bottom profiles.

The detailed sea bed mapping carried out during the survey has also shown correlations between habitat and biodiversity of various benthic fauna. Areas of high biodiversity and abundance generally correlated with harder substrates. In these areas, sea whips and fans, soft corals, hydroids, crinoids and octocorals were frequently identified, with sessile benthos extending up to ~50cm in height. The extensive areas of soft substrate commonly exhibited low-relief benthos which often covered less than 5% of the surface area. Such areas were also frequently noted for pockmark fields and the general uniformity of the environment.

1. Introduction

This report contains the preliminary results of Geoscience Australia Survey 282 in the Arafura Sea. The survey focused on four areas between 9° and 10°S and 133° to 135°E. These areas were selected to coincide with existing conventional seismic data, interpreted hydrocarbon slicks on the sea surface (based on synthetic aperture radar data) and bathymetric information. The primary goals of the survey were to improve understanding of the petroleum resources and to assess the modern sedimentary and environmental settings within this area of the Arafura Sea. To address these goals a variety of digital datasets was acquired to map the sea bed and sub-surface in detail, including side-scan and multibeam sonar. Based on these new datasets, a sampling program was undertaken to collected sea bed cores, rock and biological samples, along with video footage of the sea bed.

The selected survey areas have not previously been explored for petroleum and the survey was intended to provide a range of new data that can be correlated with conventional seismic and remote sensing data acquired by exploration companies. These new data are ideal for the study of shallow gas and natural hydrocarbon seepage, which in turn can provide evidence of an active petroleum system. Coupled with the biological sampling and video footage, these new data also provide a unique record of the sedimentary environments and benthic habitats. A range of different water depths and habitats were studied during the survey which will allow a much better understanding of the biodiversity in this part of the Arafura Sea.

1.1. BACKGROUND

1.1.1. Geological Setting

The Arafura Basin is a Neoproterozoic to Palaeozoic basin, extending from onshore northern Australia into Indonesian waters, and covering approximately 200,000 km^2

in Australia waters (**Figure 1**). Water depths typically range from about 70 m to 230 m.

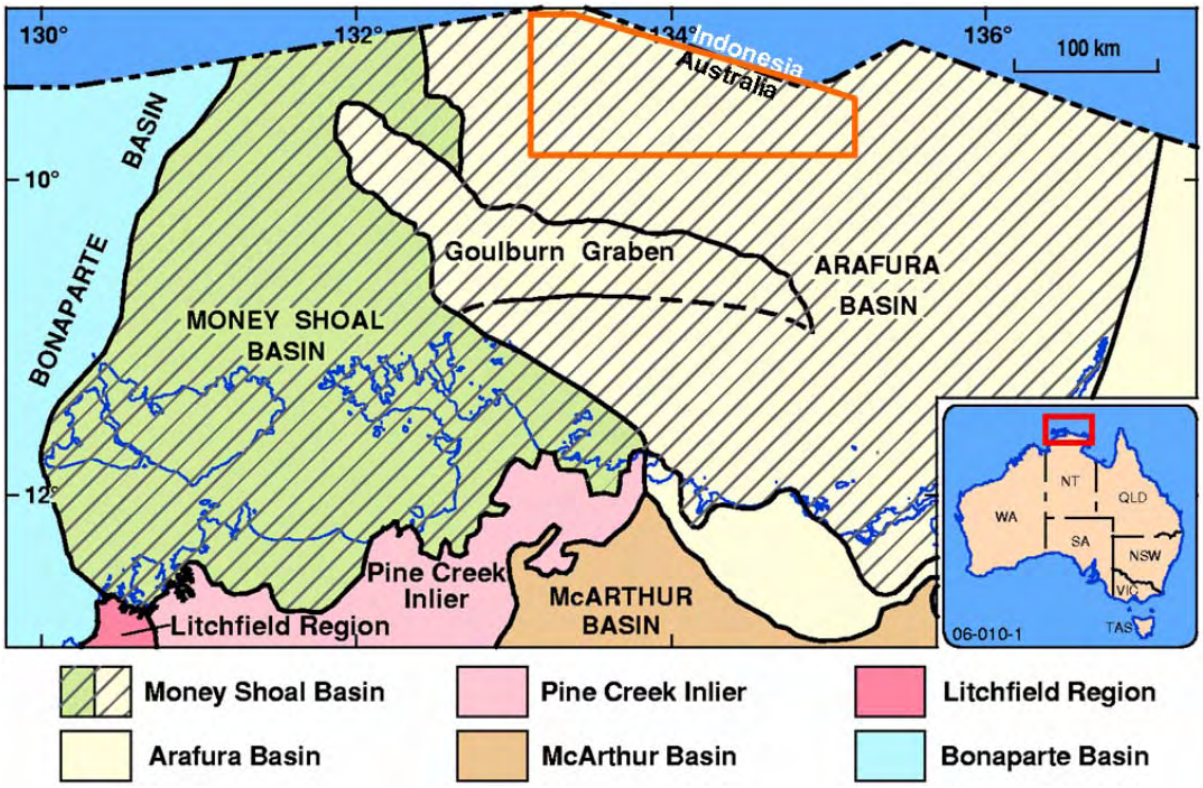

Figure 1 Arafura Basin regional setting. The survey area of Figure 2 is shown in the orange polygon.

The stratigraphy, structural architecture and petroleum systems of the Arafura Basin are covered in greater detail in Struckmeyer (2006). The Arafura Basin formed in the Neoproterozoic as a result of NW-SE upper crustal extension that produced a series of NE-SW trending half graben across much of the basin. During this time the dominantly clastic sediments of the Wessel Group were deposited. Subsequent periods of subsidence in the Cambro-Ordovician, Late Devonian and Late Carboniferous to Early Permian were separated by long, tectonically quiescent periods of non-deposition and erosion. The predominantly marine carbonates of the Cambro-Ordovician Goulburn Group are overlain by shallow marine to non-marine clastics and carbonates of the Devonian Arafura Group and fluvio-deltaic clastics of the Late Carboniferous to Early Permian Kulshill Group equivalent.

The most striking feature of the Arafura Basin is the Goulburn Graben, which divides the basin into southern and northern parts. The Eastern part of the Arafura Basin is obscured because of poor seismic quality data. The Goulburn Graben is approximately 350 km long and up to 70 km wide, and contains a sedimentary section more than 10 km thick. The graben formed in the Late Carboniferous to Early Permian in response to NE-SW extension related to the break-up of Gondwana. The region north of the Goulburn Graben is the main basin depocentre and contains up to 15 km of sediment. The southern region forms a north-dipping, relatively undeformed ramp overlain by up to 3 km of sediment.

Subsequent compression and crustal shortening in the Triassic resulted in oblique inversion of the Goulburn Graben, accompanied by uplift and erosion of up to 3.5 km of sediment. This deformational event did not affect areas to the north and south of the Goulburn Graben as significantly. Subsequent basin-wide erosion resulted in formation of a peneplain upon which the sediments of the Money Shoal Basin were deposited in the Jurassic to Quaternary.

The Arafura Basin unconformably overlies the Palaeoproterozoic to Mesoproterozoic McArthur Basin in the south and east, and the highly deformed Archaean-Palaeoproterozoic Pine Creek Inlier in the west. In turn, it is overlain by the Mesozoic to Recent Money Shoal Basin. Sediments of the Money Shoal Basin onlap the Arafura Basin section from the west, forming a time-transgressive sediment wedge the base of which ranges in age from Middle Jurassic in the west, to Late Cretaceous in the east.

1.1.2 Modern depositional setting

The majority of the recent terrigenous sediments deposited in the survey area probably originated from the Gulf of Carpentaria (GC). This is based on bathymetry data, which shows a major palaeo-channel extending from the GOC into the Arafura Sea (**Figure 2**). The Arnhem Land rivers in the Arafura region may also supply

sediment to the survey area to a lesser extent, and some biogenic sediment may be produced in situ.

The Arnhem Land region is dominated by the 200-300m high Arnhem Land Plateau, composed mainly of Mesoproterozoic sandstone of the McArthur Basin (Nott and Roberts, 1996). Outliers of Cretaceous strata form scattered plateaux throughout the on-shore parts of the Arafura Basin (Plumb and Roberts, 1992). Rivers drain onto the topographically lower-lying Arafura Basin. Most of the coastal plain is composed of laterites, overlain by sand, deposited on Cretaceous strata of the overlaying Money Shoal Basin (Plumb and Roberts, 1992). Onshore Tertiary deposits include coastal silt, sand, evaporates, residual soil, alluvium, laterite, and ferricrete (Plumb and Roberts, 1992).

1.1.3 Palaeo-Environmental Setting

The palaeo-environmental setting is important for understanding the depositional environment of sediments in the survey area. The Quaternary in Arnhem Land was a period of intense erosion resulting from changes in climate and sea level accompanying glacial-interglacial cycles (Nott and Roberts, 1996).

During the last glacial maxima sea-level low-stand (~ 20 000 years BP), and the earlier Quaternary low-stand (**Figure 3**), the GC was isolated from the open waters of the Indian and Pacific oceans, forming Lake Carpentaria, with outlet channels to the Arafura Sea to the west (Chivas et al., 2001). The present river systems also drained across an extensive exposed shelf, transporting sediments to areas which are now submerged (Woodroffe, 1993).

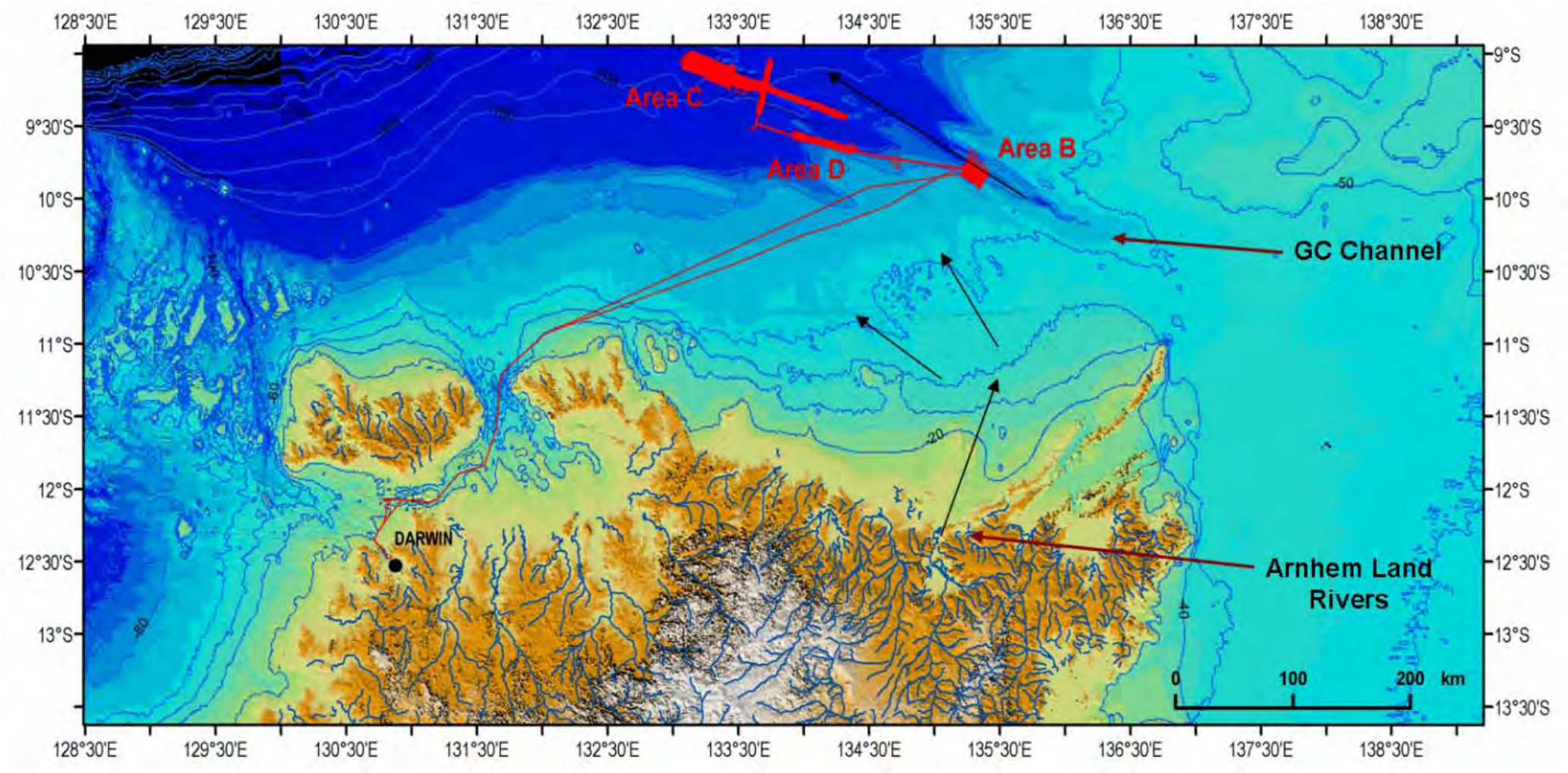

Figure 2 Bathymetry showing a major drainage channel beginning in the Gulf of Carpentaria (GC). Onshore drainage routes from Arnhem Land are also illustrated.

The last Interglacial shoreline has been interpreted to have been about 6 m above the present level at its peak (Woodroffe, 1993). This would have produced similar environments of deposition in the survey area as are observed today. The period between 20 000 and 125 000 years BP was characterised by a gradual oscillating fall in sea level (**Figure 3**). This period was characterised by a wet climatic phase where alluvial deposits formed extensive river or coastal terraces (Woodroffe, 1993).

Sea level was at its lowest during the glacial maximum between 22 000 and 19 000 years BP (Yokoyama et al., 2001; **Figure 3**) at which time the shoreline was 120 m below its present level (Woodroffe, 1993) (**Figure 3**). During this period, the Arafura region was characterised by widespread erosion (leading to calcrete and soil development), fluvial channelling (forming banks and terraces), and coral reef development near the shelf edge are known to have occurred in the Arafura region (Lavering, 1993; Jongsma, 1970). A dry and arid climate produced allowed formation of dunes, open grasslands, and eucalyptus woodlands close to the coastline, while some mangrove forests formed in intertidal areas (Lavering, 1993).

Rapid sea level rise (30mm/yr), began ~12 000 years BP, causing the shoreline to transgress several tens of metres per year (Woodroffe, 1993). Sea level was close to its present level by 6000 years BP and mangrove forests were initially widespread. However, the mangrove forests have since been replaced by broad, convex clay floodplains supporting a freshwater wetland vegetation dominated by grasses and sedges around the margins of the Arafura Sea (Woodroffe, 1993). Today, tidal flats are most extensive around the estuaries of the rivers. They are subject to tidal and seasonal flooding and act as repositories for fine sand, silt, and evaporite deposits (Plumb and Roberts, 1992). Tidal streams meander through these flats and extensive coastal dunes are developed, which are rarely more than 6m high on the north coast of Arnhem Land. Some of these are in the form of emergant offshore bars and act as

barriers enclosing the seaward edges of the tidal flats; others are normal beach and dune deposits built up at sea level by wave and wind action (Plumb and Roberts, 1992).

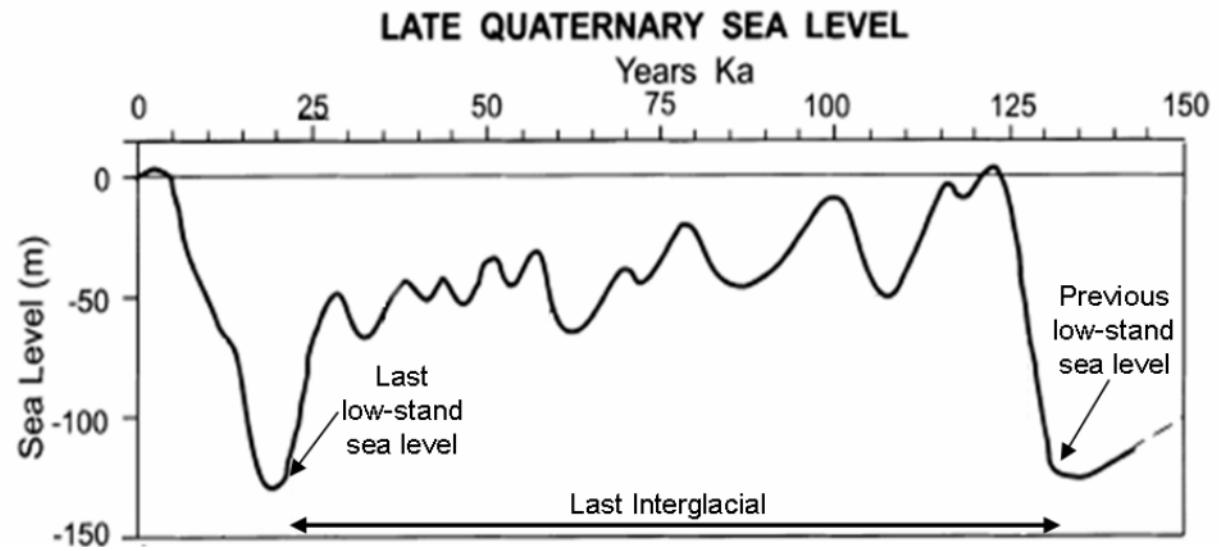

Figure 3 Quaternary sea level curve from Chappell and Shackleton (1986) and James et al. (2004).

1.1.4 Survey Objectives and Area

The scientific objectives of Survey 282 were:

1. to identify and sample natural hydrocarbon seepage;
2. to improve our understanding of the petroleum resources in the Arafura Sea;
3. to document modern sedimentary/environmental settings of the Arafura Sea for bio-regionalization and regional marine planning

Sample sites were selected based on a series of datasets including:

1. Areas of interpreted hydrocarbon slicks using Synthetic Aperture Radar (INFOTERRA Global Seeps Database, see Chapter 6 of this report)
2. Geophysical features identified in seismic surveys [Veritas Arafura 2002 (AR2002); Geoscience Australia Surveys 94, 106, 118]. These features include:
   - acoustic blanking and poor data quality zones
   - faults close to sea bed
   - mounds
3. Pockmark fields identified using side-scan sonar data collected during the survey.
4. Faults at the sea bed based on sub-bottom profile data collected during the survey.
5. Bathymetric features interpreted using multibeam sonar data collected during the survey.

Pre-survey data analysis identified areas for the collection of geological and biological samples to help provide a better understanding of both potential sites of natural hydrocarbon seepage, as well as deep and shallow tropical water shelf habitats. The areas were selected to provide insight to both habitat and biodiversity, and are referred to as Areas A, B, C and D (**Figure 4**).

Deeper parts of the shelf (>120 m water depth) have remained inundated throughout the late Quaternary providing relatively stable environmental conditions, whereas shallower areas have been exposed for part of the Holocene (Since 12 000 years BP) and have undergone dramatic environmental change as sea level rose, inundating the landscape. Comparing these two environments gives an insight into the colonisation and adaptation of species to the new shallow environment as it became available with the rising sea level.

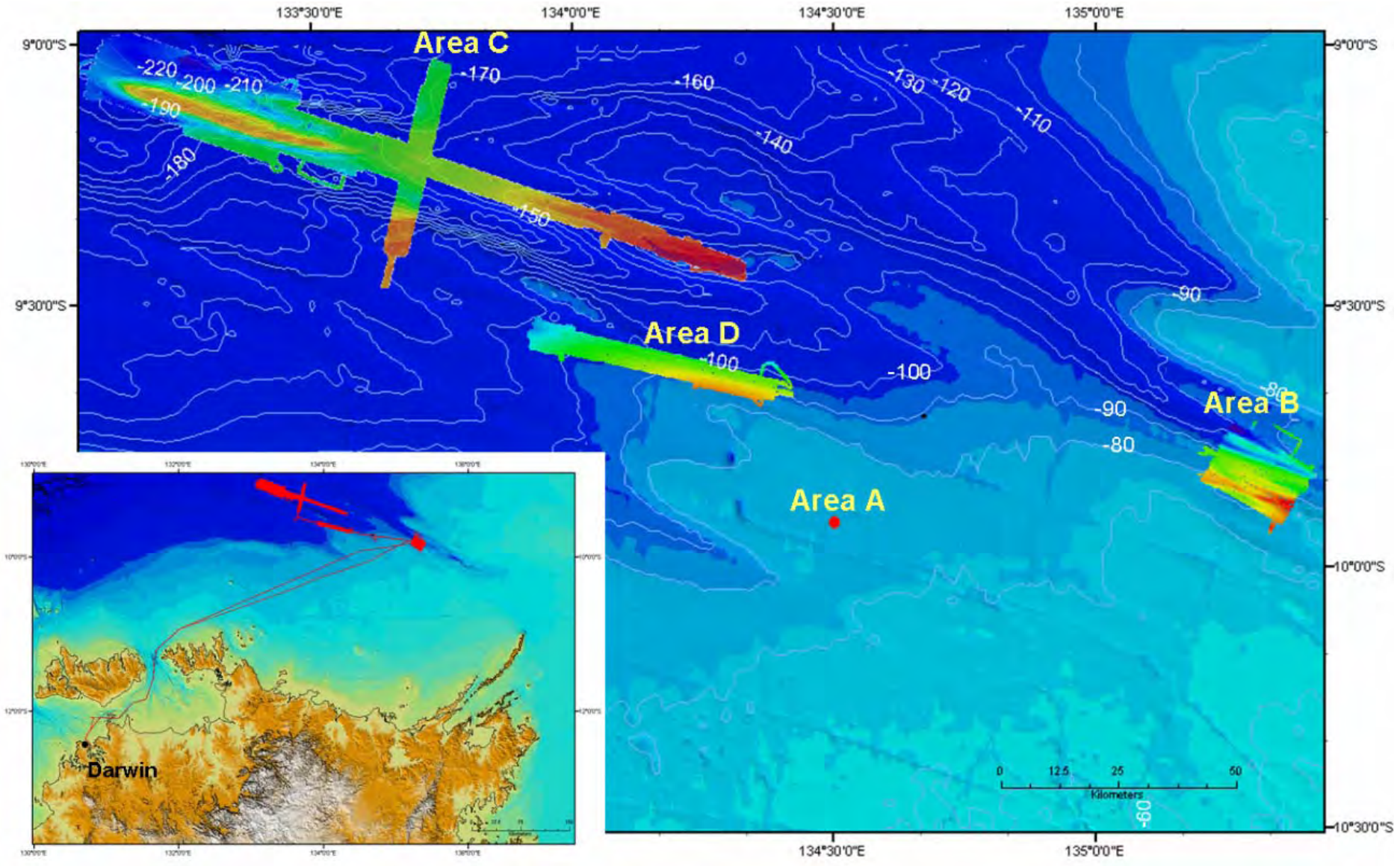

Figure 4 Multibeam bathymetry image over the surveyed areas A, B, C and D. Inset shows ship track of GA survey 282. Bathymetric contours in pale blue are in meters.

Area A was selected as the site to deploy an Acoustic Doppler Current Profiler; this was to provide information on tides and currents in the Arafura Sea. However, the acoustic release did not work when tested on board and it was decided not to deploy the instrument without this capability. Sediment and core samples were collected at this site. Area B was selected for sedimentological and biological objectives. Because it is a relatively shallow water area, it would have been exposed during low sea-level stands and the biological population would comprise organisms that have colonised the area since previous low stands. Area C and D were selected on the basis of geophysical features in conventional seismic and the presence of mapped hydrocarbon slicks interpreted in SAR data. The geochemical sampling was concentrated in Areas C and D, north of the Goulburn Graben. These areas were also sampled for sedimentology and biology to examine the relationships between sub-strait and habitat types. The biological data collected on this survey are still undergoing analysis by multiple research facilities across Australia and consequently are not the subject of this report. The initial analysis is contained within a separate biological report of the survey presented for the Department of the Environment and Heritage (Wilson 2005).

1.1.5 Data and Sample Acquisition

The sampling conducted on this Survey 282 consisted of: 15 benthic sleds, 15 Diamantina and chain bag dredges, 86 Smith-McIntyre grabs, 101 gravity cores, 24 CTD profiles, 62 camera sites (**Appendix 1**). ~4,600 kilometres of sub-bottom profiles and multibeam bathymetry and 165 km of seismic data were collected. **Figure 4** shows the swath maps generated for the survey areas and their locations.

Further information on the sediment samples is found in the online Geoscience Australia Marine data base, MARS; go to http://www.ga.gov.au/oracle/mars/, click on either the simple or advanced version, and type in '282' into survey ID.

1.2 SURVEY PARTICIPANTS AND VESSEL

1.2.1 Vessel Description

The vessel used for the survey was the National Facility Research Vessel *Southern Surveyor*. The RV *Southern Surveyor* is a converted trawler, with accommodation for 24 participants (including 12 ships crew). Detailed information on the vessel can be obtained at http://www.marine.csiro.au/nationalfacility/features/vessel.htm

1.2.2 Scientific Personnel

Graham Logan	Chief Scientist	Geoscience Australia
John Kennard	Scientist	Geoscience Australia
Kriton Glenn	Scientist	Geoscience Australia
Andrew Heap	Scientist	Geoscience Australia
Michele Spinoccia	Multibeam processing	Geoscience Australia
Karen Earl	Scientist	Geoscience Australia
George Bernardel	Scientist	Geoscience Australia
Jon Stratton	Science technician	Geoscience Australia
Craig Wintle	Mechanical technician	Geoscience Australia
Andrew Hislop	Mechanical technician	Geoscience Australia
Franz Viligranz	Electronic technician	Geoscience Australia
Karen Gowlett-Holmes	Biologist	CSIRO
George Wilson	Biologist	Australian Museum
Lindsay Pender	Voyage manager	CSIRO
Drew Mills	Electronics support	CSIRO

1.2.2 Ship's Crew

Les Morrow	Master
Samantha Durnian	Chief Officer
Brent Middleton	2nd Officer
Roger Thomas	Chief Engineer
Rinaldo Di Vitis	1st Engineer
Chris Heap	2nd Engineer
Malcolm McDougall	Bosun
Tony Hearne	IR

Tony Van Rooy	IR
John Baker	IR
Paul O'Grady	Greaser
Charmayne Aylett	Chief Steward
Pat Wainwright	Chief Cook
Angela Zutt	2nd Cook

2. Methods

A geophysical survey was conducted to collect data on sea bed characteristics and sub-surface geology. The geophysical data allowed the selection of sample sites and a link to previously recorded regional 2D conventional seismic data.

2.1 EQUIPMENT AND PROCESSING

A range of different data sets were recorded during the survey. The acquisition and processing parameters are outlined below.

2.1.1 Multibeam Sonar

Multibeam bathymetric data was collected using a Kongsberg Simrad EM 300 multibeam echo-sounder fitted on a gondola beneath the vessel hull. The nominal sonar frequency is 30 kHz with 135 beams, each with a 1° beam width, giving a total angular coverage of 135°. The system provides roll and pitch stabilization, with optional yaw compensation. In typical water depths of 100 m, a swath width of ~700m was achieved; in 230m of water the swath width was around 1000 m.

2.1.2 Sub-bottom Profiling

A TOPAS PS 18 Parametric Sub-bottom Profiler fitted in a gondola below the hull was used to collect sub-bottom profile data. Acquisition involved a ping interval of 450 ms, using a Ricker pulse at 1.5 kHz frequency, pitch, roll, and heave were internally corrected. In water depths of 30 – 250 m, penetration of up to 100 ms (i.e., 75 m) was achieved in good sea conditions, depending on the sea bed and sediment types. Data were saved in the RAW TOPAS format, while processed data were output in SEG-Y format. DISCO/FOCUS seismic software was used to generate concatenated SEG-Y lines of sub-bottom profile data, from which hard copy plots were produced. Hardcopy plots of SEG-Y files were subsequently used for selection of sampling sites.

2.1.2.1 General Operating Procedure

As the survey took place in water depths less than 250 m, the TOPAS transmission pulse was set as a Ricker wavelet form and the ping triggering was set to internal mode. Apart from occasional modifications for experimental purposes, the following parameters were maintained throughout the survey:

- transmit mode: normal (ie one pulse for each internal trigger)
- sample rate: 40 μS (ie 25 kHz)
- ping interval: dependant on ship speed but generally 450 ms
- transmitted pulse frequency: 1.5 kHz
- transmitted power level: mostly 0 dB
- beam stabilisation for ship movement: always on
- sound velocity in water: 1500 m/s
- receiver gain: 9-21 dB depending on bottom hardness and sub-bottom penetration

2.1.2.2 General Processing Procedure

The processing procedure for TOPAS refers to the processing chain applied to the incoming ping data in real-time for on-screen display purposes. The parameters used dictate the appearance of the sub-bottom profiles. What is seen on-screen is written to the associated SEG-Y file – the 'RAW' file format is unaffected by the processing stream. Apart from the occasional modification for experimental purposes the following processing parameters were maintained throughout the survey:

- filters: bandpass 1000-5000 Hz with roll-on and roll-off. The bandpass filtering is performed in the frequency domain by applying a window to the complex Fourier-transformed time series of the acquired signal and performing a subsequent inverse Fourier transform. The window characteristic is defined by four frequencies: lowstop (LS), highpass (HP), lowpass (LP) and highstop (HS). These

frequencies are defining full stop and full pass points. The transition between these points has a cosine shape. Typical values used for this cruise were LS 0.8 kHz , HP 1.2 kHz and LP 5.0 kHz, HS 5.5 kHz

- bottom-tracker: mostly enabled in auto-mode
- time-variable gain: on
- stacking: a 2-trace mix was applied

Areas of highly rugose sea bed interfered with the ability of the bottom-tracker to correctly track the sea bed. Therefore, in these areas the operator disabled the tool.

2.1.2.3 Data Quality

Data quality was very good with low noise levels and generally good sub-bottom penetration. Low to moderate sea conditions produced noise levels and ship-roll/heave/pitch movements which were effectively handled by appropriate choices of filtering and compensating parameters.

Continuous blank, or very low amplitude, sub-vertical zones in the processed data are probably due to loss of bottom tracking and, consequently, time-variable gain-amplitude enhancement was applied. The raw data can be re-processed with a new set of parameters at any time.

2.1.3 Side-scan Sonar

An EdgeTech 4200-FS 120/410 kHz dual-frequency side-scan sonar was used to collect water column and sea bed data. Generally the sonar fish was operated using only 120 kHz in high-speed mode, as this provided a swath width of 200-400 m depending on the height of the sonar fish above the sea bed, at a speed of around 6 kts. The height above sea bed varied depending on the bathymetric conditions. Where the sea bed was flat with minimal topographic relief a height of 30 m was aimed for. In areas of variable relief the sonar fish was towed higher in the water column to avoid possible grounding.

Signal was received through a 1500 m co-axial cable and processed on a 466 Topside PC-based processor using EdgeTech's Discover 4220FS acquisition software. Data were stored initially on an i-Omega external hard drive before files were backed up and stored the vessel's computer network drives. Navigation was supplied by the vessel's Trimble GPS Nav Trac XL and manual offset correction for the sonar fish was computed within CARIS software after completion of the survey. Mosaics were then completed within CARIS software, which was used for post-processing of both the multibeam and side-scan sonar data.

2.1.4 Echo-Sounder

A Simrad EK 500 echo-sounder (12, 38 and 120 KHz transmission frequencies) was used to provide water column and water depth information. The 38 kHz frequency was continuously recorded, while the 120 kHz frequency was only used when water column targets were observed to be abundant. Data from the 120 kHz echo sounder was collected, simultaneously with the 38 kHz echo sounder, south of Pillar bank around survey sample sites 50, 51 and 52.

2.1.5 Seismic

The seismic source was provided by 2 x GI airguns, each with 25/105 cubic inch volume with compressed air at 2000 psi supplied from a DC330/2000 diesel compressor. A 450 m *Stealtharray* solid seismic cable with 300 m of active section and 24 channels was used for acquisition at a speed of 5 to 6 kts.

A compressor failure curtailed the collection of seismic data after about 24 hours of operation. As parts could not be readily obtained it was decided to abandon seismic operations after ~165 km of seismic data had been acquired.

2.1.6 Hydrodynamic Measurements (BRUCE deployment)

The hydrodynamic conditions at Area B were recorded using a current meter deployed to measure sea-level, waves and currents. The *Benthic Research for Underwater sediment Concentration Experiment* (BRUCE) was constructed at Geoscience Australia, with a 300 kg weighted steel frame, and for this deployment contained

only a Nortek™ acoustic current meter. BRUCE was deployed at 9° 48.014' S, 135° 22.000' E at a water depth of 92 m water depth. The record commences at 0119 30-Apr-2005 GMT (Julian Day 119.056), and continues until 2130 27-May-2005 GMT (Julian Day 146.90).

The Nortek™ acoustic current meter recorded currents at 1 m above the sea bed. Water velocity readings were collected for 10 mins at 8 Hz every hour in order to resolve waves and turbulence. The 3-dimensional velocity components (east, north, and vertical), pressure, and temperature were logged internally and downloaded to a PC after recovery.

2.2 PHYSICAL SAMPLING AND EQUIPMENT

2.2.1 Water Samples and Profiles

A Seabird SBE 911 plus, with a rosette of twelve 10 litre Niskin bottles, was used for water column sampling and to provide conductivity, temperature and depth profiles. Two litres of sea water, collected in the Niskin bottles at the surface and at 1m above the sea bed, were filtered through pre-weighed 0.45 μm mesh glass filter papers using a vacuum system. The filter papers were then stored in a dry freezer and on return from the survey were oven dried at 60° C in the laboratory and re-weighed to ±0.0001 g to obtain suspended sediment masses. 19 of these samples were collected and the results are listed in **Appendix 2**.

Water column profiles were also obtained while underway by deploying Expendable Bathythermographs (XBT) supplied by CSIRO. These were deployed to provide temperature and conductivity measurements to allow multibeam data to be processed. Data from these deployments is reported in **Appendix 3**.

2.2.2 Surface Sediment Samples

Surface sediments were collected using a Smith-McIntyre sediment grab deployed from the side A-frame. In soft muddy sub-strates the grab did not operate efficiently and failed to activate on several occasions. When this occurred, surface sediment samples were collected using a small epi-benthic sled, supplied by CSIRO.

2.2.2.1 Smith-McIntyre sediment grab

The grab is mounted on a sturdy, weighted, steel frame, suspended from the lowering wire, with springs to force the two-jaw bucket into the ocean bottom when released. Tripping pads, positioned below the square-based frame on which the bucket is suspended, make contact with the sea bed first and are pushed upward to release two latches holding the spring-loaded bucket jaws. Rewinding the deployment wire exerts tension on cables connected to the end of each bucket-jaw arm causing the jaws to pivot tightly shut.

2.2.2.2 Epi-benthic sled

A benthic sled provided by CSIRO was used at selected sites to collect samples of benthic organisms. The benthic sled comprised a plastic fine mesh net attached to a 0.5 m high x 1 m wide metal frame that was lowered to the sea bed and then dragged along the surface for approximately 200 m. The sled was also used to sample muddy environments where the sea bed was too soft to trigger the Smith-McIntyre grab. Mud collected in the epi-benthic sled was sub-sampled for sedimentology and then the bulk of the sample was seived to obtain macroscopic biological samples.

2.2.2.3 Rock Dredge

The rock dredge, consisting of a 0.5 x 1 m rectangular metal collar to which a 1 x 1 m chain bag was attached, was used to sample lithified and cemented sediments on the sea bed, mostly over the hard-ground environments. The dredge was operated using the coring winch, and was lowered to the sea bed and dragged along the sea bed for approximately 100-200 m.

2.2.2.4 Diamantina Dredge

The Diamantina dredge has a wide toothed rectangular mouth and narrows into delta-shaped funnel that feeds into a removable box, where the rocks and sediments are captured. The box can be unbolted to remove the dredged material. The dredge was operated using the coring winch, and was lowered to the sea bed and dragged along the sea bed for approximately 100-200 m.

2.2.2 Sub-Surface Sediment Samples

Cores were colleted using a gravity corer with a 1 tonne core head and a PVC core barrel liner deployed from the stern A-frame. The length of the core barrel was varied depending on the sediment type; typically a 3 m barrel was used, as penetration generally varied between 2 to 3 m. In soft sediments a 6 m barrel was used. The corer was deployed and retrieved using a hydraulically-operated cradle and the ship's coring winch.

2.2.3 Video Camera

Video footage of the sea bed was collected to provide a continuous visual recording of the substrate, morphology, habitats, and benthic biota in the survey area. The digital video camera was contained in a watertight housing attached to a steel frame. Four battery-powered 25W halogen lights were used to illuminate the sea bed. The underwater camera recorded on digital videotape in the camera housing and was also fed to a VHS tape recorder and a monitor on board the vessel. This "live" video feed enabled the winch control operator to raise and lower the camera in order to image a representative area of the sea bed and specific features while the vessel drifted beam on to the swell, to reduce vertical camera movement. Each camera lowering recorded a minimum of three minutes of video footage, and usually up to 30 minutes. A total of 62 camera deployments were conducted during the survey, which totalled approximately 24 hours of footage. Sea floor video footage from the survey is being edited and will be available on the Geoscience Australia MARS data base (http://www.ga.gov.au/oracle/mars/).

2.2.4 Sampling and Handling During Survey

2.2.4.1 Bulk Sediment samples

Sediment samples were collected from both the Smith-McIntyre grab and epi-benthic sled for sedimentological analysis. Between 0.5-1 kg of sediment was placed in clear plastic bags and given a Munsell colour and grain size description. Samples were then labelled, double-bagged along with an aluminium sample tag and stored at 4˚C. The remaining sediment collected by the grab was sieved on a 5 mm screen to obtain a course fraction, which was then stored in the same way as the bulk sediment samples.

2.2.4.2. Biological Sampling of Sediments and Preservation

Where possible, a full grab sample was obtained for biological processing. This was then sieved and elutriated using filtered seawater. Each grab taken for sedimentology purposes was also sub-sampled for visible surface biota. Specimens were preserved in either a ~4% Formaldehyde sea water solution or in 80% ethanol. Within 4 days the formaldehyde-fixed samples were washed in fresh water and transferred to a 100% ethanol for future DNA work. Macroscopic specimens were photographed and described before preservation. Microscopic specimens were preserved in methanol for sorting and description after the survey. Mud obtained from the epi-benthic sled was processed in the same manner as grab samples.

2.2.4.3 Biological Photography

Macro invertebrates were photographed fresh before preservation to record colours. All specimens were photographed using a Nikon Coolpix 995 camera with an attached macro ring light mounted on a copystand. Specimens were placed on a black cloth background with a millimetre scale for photography. Fish were pinned to extend their fins, and the fins fixed in place using formalin painted on. The fish were then photographed using the same camera on a white background with a millimetre scale and a Kodak colour bar, according to standard CSIRO Marine Research fish photography protocols. All specimens were then fixed in appropriate preservatives with an ID label including the site number. All images were transferred to a

computer, then cropped and colour balanced in Photoshop CS. Files were renamed with the specimen CAAB code, site/accession number and taxon identification. Files were arranged in directories taxonomically. These files were then stored on the computer hard drive with backups on CD. CDs were distributed to all participating institutions. Images were printed on board using a colour-corrected Canon PIXMA 5000 printer.

2.2.4.4 Core handling

A total of 103 gravity cores (http://www.ga.gov.au/oracle/mars/) were collected during the survey for stratigraphic and geochemical sampling. At sites of geochemical interest an additional core was taken to provide a stratigraphic record because the geochemical sampling did not allow intact stratigraphy to be collected.

Once the core barrel was secure on deck the stratigraphic cores were cut into 1 m sections starting at the base of the core. Each section was sealed with PVC end caps, labelled and stored horizontally at 4˚C.

Cores taken specifically for geochemistry were sub-sampled in the lab as outlined in the *Geochemistry Sampling* section below and material was then frozen at -20˚C. Lengths of core taken for geochemistry that were not sub-sampled and frozen were disposed of during the survey.

2.2.4.5 Geochemical Sampling

Cores taken specifically for geochemical analysis were also initially cut into 1 m sections on deck. These sections were immediately sub-sampled in the on-board laboratory. The lower 30 cm of each 1 m section of core was sampled as shown in **Figure 5**. Care was taken to remove mud that had been in contact with the PVC liner, to avoid organic contamination, and only the interior portion of the core was collected for any of the geochemical analyses.

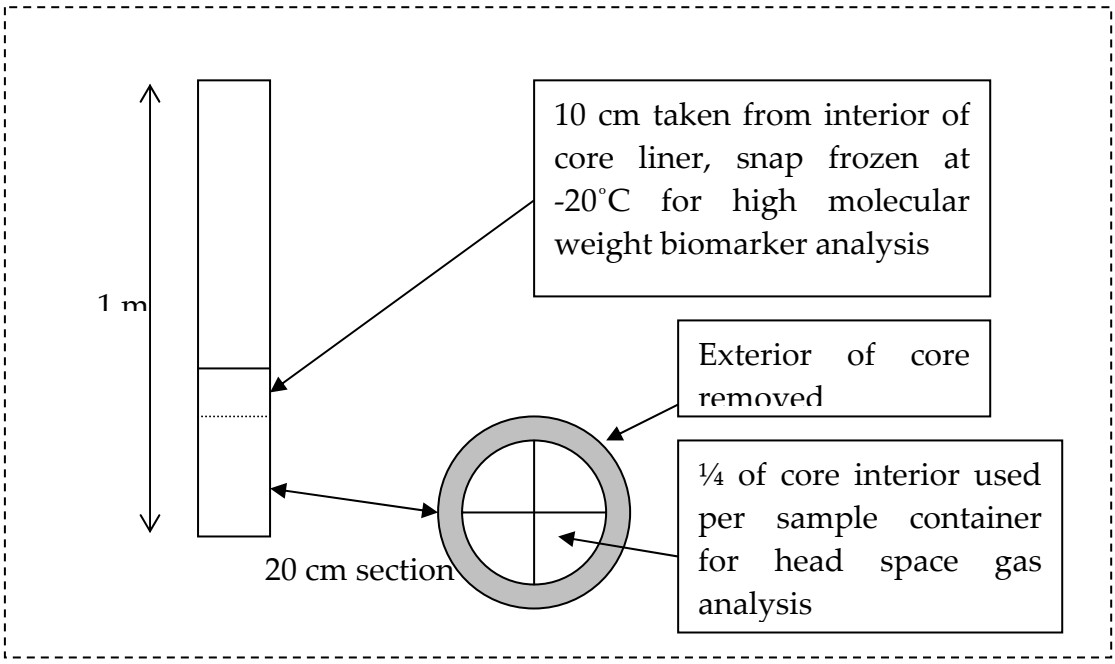

Figure 5 Illustration of samples taken from 1 m gravity core section. The upper 70 cm of each core section was discarded after sampling.

Samples collected for high molecular weight biomarker analysis were double bagged within plastic zip lock bags and snap frozen at -20 ˚C. These samples will be analysed using protocols outline in the *University of Utah* study *Surface Geochemistry Calibration Study* (Abrams et al., 2004).

Two methods for head space gas collection/sampling were tested during Survey 282. The lower 20 cm of each 1 m core section was extruded from the PVC liner by pushing a metal cutting device up through a 20 cm section of core liner. The cutting device has two intersecting metal plates that divided the extruded core into quarters. After extrusion, the exterior of the core was trimmed to remove mud that had been in contact with the core liner. Each quarter was then removed from the cutter and placed in either a 500 ml tin (duplicate samples; tins provided by TDI-Brooks) or a plastic disrupter canister (duplicate samples; disrupters provided by EGI).

2.2.4.5.1. Sampling Using Tins

The 500 ml metal paint tins used for the head space gas analysis were provided by TDI-Brooks and are the same as used during their surface geochemical sampling surveys. One quarter of a 20 cm section of core filled a tin to around one-third full. This was the volume of mud required for head space gas analysis. Once the mud was placed inside a tin, a further one-third of the volume was then filled with filtered sea water which had been poisoned with sodium azide and degassed by bubbling with chemical-grade nitrogen. The head space of the tin was then flushed with nitrogen and the lid of the tin was sealed. Once sealed the tin was briefly shaken and placed inverted on the bench. The tins were labelled with core number and depth, then snap frozen inverted at -20 ˚C.

2.2.4.5.2. Sampling Using Disrupters

The plastic disrupters were provided by EGI to compare with the more traditional tin containers for head space gas analysis. The disrupters are designed to be re-used and also contain a plastic insert used to disrupt the mud during analysis.

During sampling, each disrupter received one-quarter of the mud from the bottom 20 cm of each one-metre core section. This volume of mud filled about one-third of the disrupter. If loose mud was collected in the core the volume could be checked using a mould line on the canister body. Once the mud had been placed in the canister the plastic insert was pushed into the mud. Then a further one-third of the canister volume was then filled with filtered sea water which had been poisoned with a bacteriocide, sodium azide, and degassed by bubbling with nitrogen. While the volume of mud and liquid could be judged against a second mould line on the canister side, it proved more efficient to mark a graduated measuring cylinder with the known volume of seawater needed for both the tins and disrupters and use this to measure the required water volume. The head space of the disrupter was then flushed with nitrogen and the lid was secured. Once sealed, the disrupter was

shaken and then placed upside down in the -20 ˚C snap freezer. Results from the disrupter analysis will form part of a separate larger study *University of Utah* study *Surface Geochemistry Calibration: Phase III* and will not be reported in this study.

2.2.4.6 Dredge samples

Two different dredges were used during the survey. The small Diamontina dredge was used initially. However, the larger chain dredge was used to obtain more sample material once work began around Pillar Bank. The contents of each dredge were sorted on deck and representative rock samples were then selected for return to Geoscience Australia. These samples were then trimmed using a small rock saw and described on board before storage. Biological material collected in dredges was photographed and described before preservation and archiving.

3. Results and Discussion

3.1. GEOMORPHOLOGY AND SITE DESCRIPTIONS

Four main Areas (A, B, C and D) were surveyed, which represent different water depths and environments (**Figure 4**).

3.1.1 Area A

Area A contains a single site at approx. 9.9°S / 134.5°E. The water depth at this site was 95 m, indicating it was exposed at the Last Glacial Maximum (LGM). A CTD was cast and a benthic sled was used to collect sediment, because it was too soft for the Smith-McIntyre grab to pick up.

3.1.2 Area B

Area B was selected for sedimentological and biological purposes and is rectangular in shape (~20 km x 14 km) and covers an area of ~300 km^2 (**Figure 6**). As it is a relatively shallow water area, it would have been exposed during sea-level low stands. Thus the biological population would represent organisms that have colonised the area since previous low stands.

In this area almost 100% multibeam coverage was obtained and a total of ~570 line-km of sub-bottom profiles were recorded in water depths ranging from 67 to 105 m. Water depth increases to the northwest, and the bathymetry shows a distinct series of large-scale, gentle undulations (~ 10 m of amplitude and ~ 2 km of wavelength) with an azimuth of ~290 degrees. The area is located on the edge of a channel system that was a conduit for both water and sediments during periods of low sea level. After deployment of GA's benthic current meter (BRUCE), the area was swath-mapped concurrently with side-scan sonar and sub-bottom profiling. This information assisted with targeting the subsequent sampling program. Area B includes survey sites 2 - 12, and 64 (**Figure 9**). Multiple sampling activities were carried out at each site. A suite of 36 sediment samples and cores were collected from these sites, including 2 benthic sled samples, 23 grab samples and 11 gravity cores. A detailed

tabulation of site locations and sample activities is provided in **Appendix 1**. In addition, six CTD (conductivity, temperature, depth) profiles recorded properties of the water column and video captures were taken at all sites, except one (**Figure 9**).

3.1.3 Area C

Area C was selected on the basis of geophysical features in conventional seismic data (faults to seafloor, high amplitude reflectors near the sea bed) and the presence of mapped hydrocarbon slick interpreted in SAR data (INFOTERRA Global Seeps Database; Chapter 6). It also covered a range of different bathymetric features that provide various benthic habitats. Area C is an elongate rectangle ~140 km in length and orientated WNW-ESE, with a second rectangle ~45 km in length orthogonal to the larger rectangle (**Figure 7)**. It covers a total area of ~1,875 km^2 and includes ~1,800 line-km of multibeam and sub-bottom profile data. Water depths in Area C range from 84 to 246 m, with a general trend showing deepening to the northwest. The southeast part of the area is the shallowest (84 to 110 m) and would have been sub-aerially exposed during the LGM.

The sea bed in the east appears to be a hard-ground. To the west of this, a slightly deeper bank bounded by an apparent structurally-controlled escarpment drops off into a relatively flat terrace. Detailed multibeam mapping showed slump features on the southern edge of the escarpment and multiple, deeper scours and depressions on the northern and western edges. A submarine plain dominates the central part of Area C which lies at ~150 to 170 m water depth and is draped in sediment. The plain is featureless, with one topographically positive feature or rock sub-crop. The southern part of the smaller survey rectangle shows a shallow area (~110 m) of hard-ground with rock sub-crops, with a sharp drop off onto the plain.

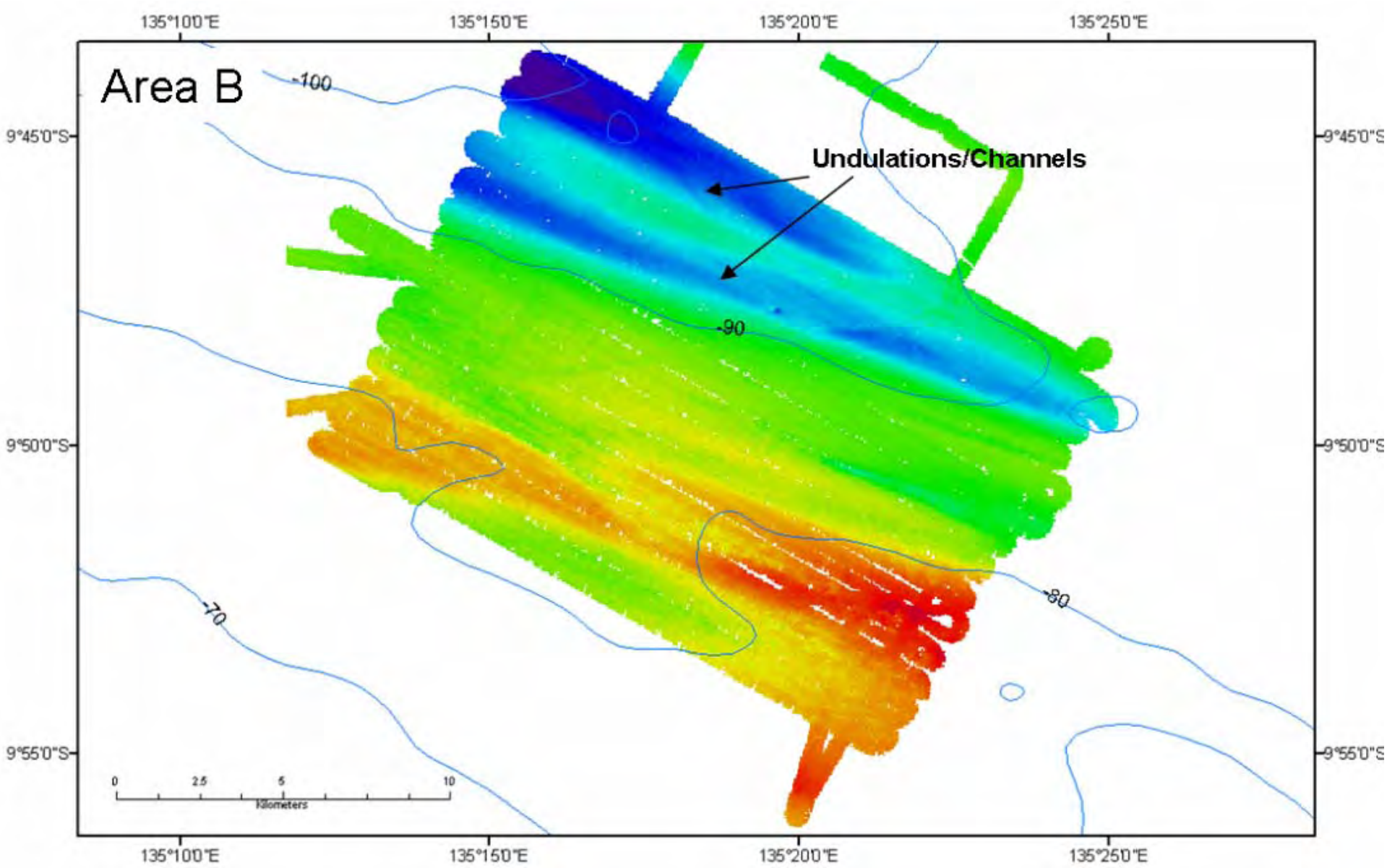

Figure 6 Multibeam bathymetry image of Area B. Contours in blue, show regional bathymetry in meters.

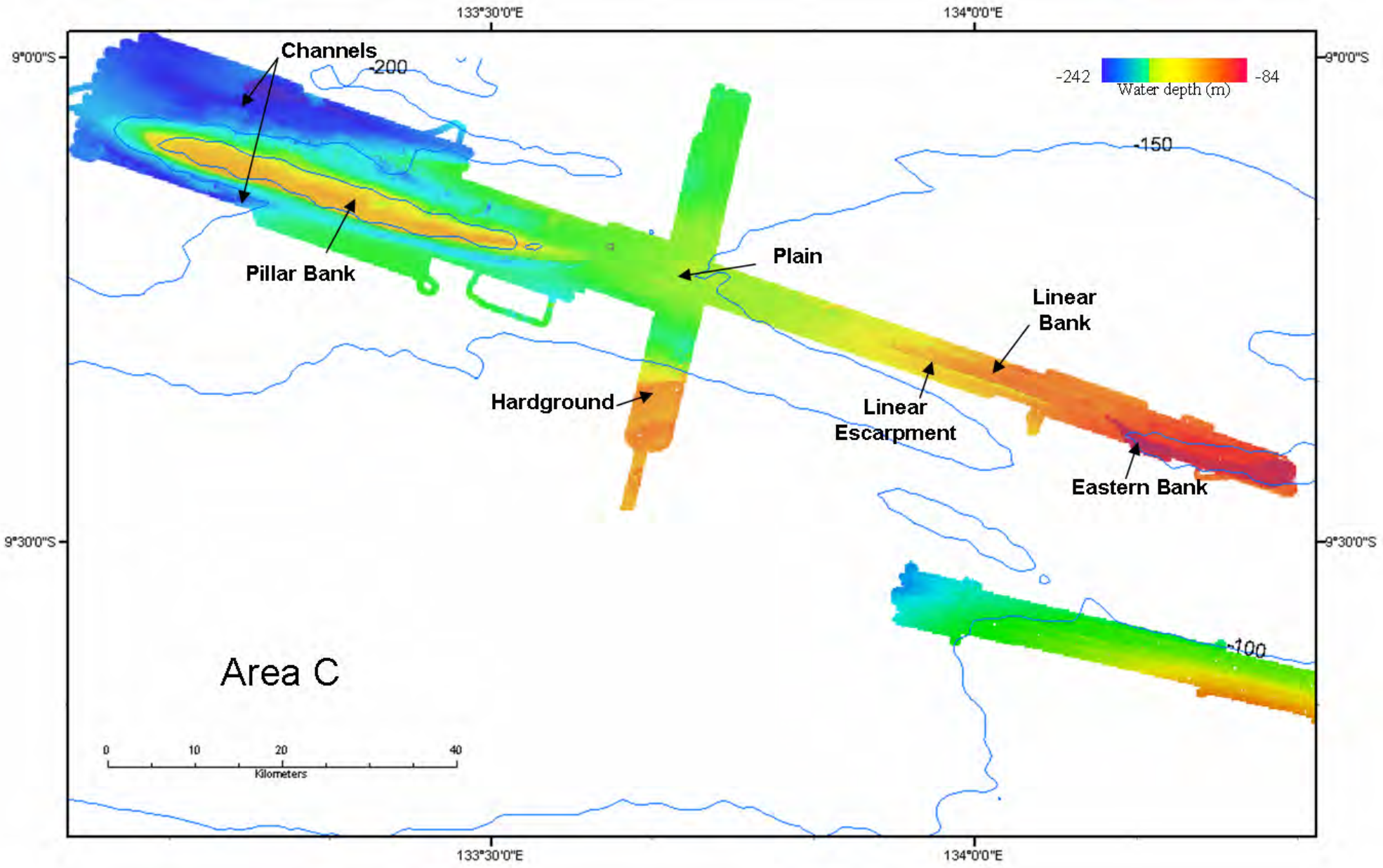

Figure 7 Multibeam bathymetry image of Area C. Contours in blue show the regional bathymetry in meters.

The western part of Area C is dominated by the topographically positive Pillar Bank. It is an elongated bank that rises from 200 m water depth in the east and 220 m in the west. The crest of the bank lies ~125 m below sea level, indicating that it was either exposed or near sea level during the LGM. Its southern flank is characterised by curvilinear ridges, whereas to the north it has a more subdued morphology. Pillar Bank is flanked by channels to the north and south, and slump features are present on its northern flank. To the northwest of Pillar Bank, the morphology grades into a broad, deep shelf.

Area C was extensively sampled with sites 13 - 56 occupied in the area (**Figure 10**). A suite of 159 sediment samples and cores were collected from these sites, including 9 benthic sled samples, 15 dredge samples, 62 grab samples and 73 gravity cores. In addition, 15 CTD profiles were recorded and the video camera was deployed 43 times.

3.1.4 Area D

Area D was selected on the basis of geophysical features in conventional seismic data and the presence of mapped hydrocarbon slicks interpreted in SAR data (INFOTERRA Global Seeps Database, see Chapter 6). Area D is narrow and rectangular in shape (**Figure 8**) and covers an area of ~385 km^2. A total of ~ 480 line-km of sub-bottom profiles and multibeam data were acquired in the area on lines approximately parallel to the bathymetric contours at an azimuth of ~290^0. Water depths range from 81 to 112 m, indicating that the area was exposed at the LGM. Area D contains sites 57 – 63 (**Figure 11**). 21 sediment samples and cores were collected from these sites, including 3 benthic sled samples, 1 grab sample and 17 gravity cores. In addition, two CTD profiles casts were recorded and the video camera was deployed 7 times.

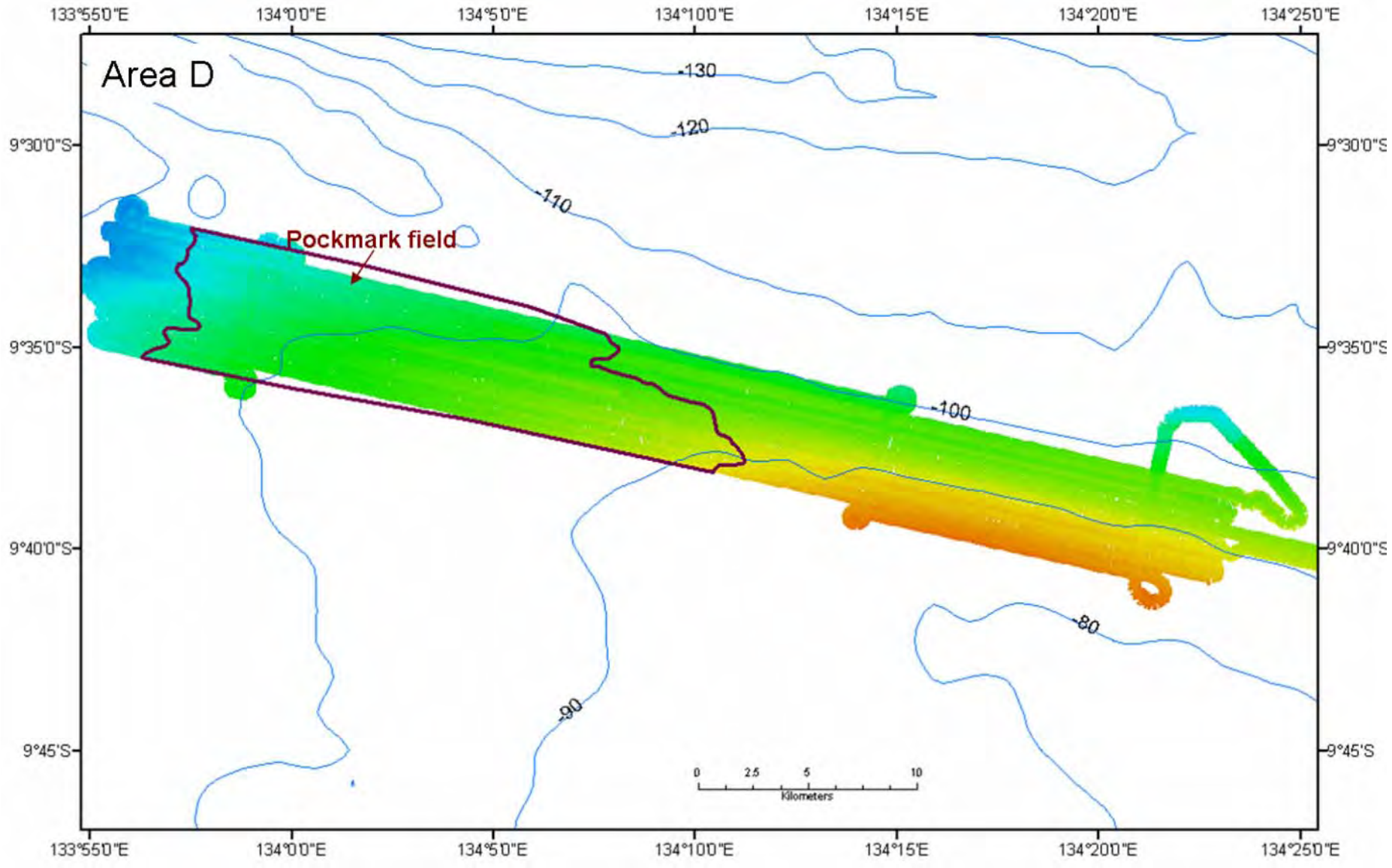

Figure 8 Multibeam bathymetry image of Area D. Contours in blue, show regional bathymetry in meters.

3.2 METEOROLOGY AND OCEANOGRAPHY

Onboard measurements of surface salinity, temperature and fluorescence were taken throughout the survey using the on-board thermosalinograph and are presented in **Appendix 3**. The hydrodynamic conditions were recorded with an oceanographic mooring designed to measure localised currents in Area B at site 2. As processes involving sediment transport occur near to the sea bed, currents were measured at a height of 1 m above the sea bed. Maximum tidal current velocities of 42 cm/s 120°True were experienced on a flood tide. Flood tide currents were directed to the ESE (~120 ° True), and ebb currents were directed WNW (~300 ° True). Four of the five bedload transport formulae tested indicate a net bedload transport in a direction consistent with flood tides. This indicates that flood tide currents provide most of the bedload transport.

3.2.1 Meteorology

Throughout the survey, the onboard meteorological log recorded atmospheric temperature, relative humidity, wind speeds and direction, and atmospheric pressure. These Datasets are embargoed except to the Principal Investigator (PI) for 2 years from date of processing. For datasets out of embargo, contact the Divisional Data Centre for authorisation to access this dataset via the Data Link (see "Links" section). http://www.marine.csiro.au/marlin/ click 'search', click 'voyage/survey', southern surveyor SS05/2005 then go to 'underway data'.

The wind speed ranged from 10-30 knots for the period of the survey and the air temperature exhibited a diurnal signal with magnitude of approximately 4.0 ˚C. A strong diurnal signal is also observed in the atmospheric pressure, with variation of approximately 4 hPa. Similarly, the humidity displays a diurnal signal of magnitude of approximately 5 %. This data is presented in **Appendix 3**.

3.2.2 Conductivity Temperature and Depth (CTD) Profiles

Using the onboard Seabird SBE911 CTD, 29 deployments were carried out during the survey. Three water masses were identified: a warm fresh water mass (A); a warm saline water mass (B); and a cool saline water mass (C). The surface mixed layer had consistent temperatures of approximately 28 °C with variable, low salinity of approximately 32.5‰. The water column profiles indicate that the surface mixed layer extends to approximately 60 m depth. The water column profiles also indicate that no light reaches more than 80 m below sea level. While transmission is typically high in the surface mixed layer, values of less than 20 % are recorded in the near-sea bed layer. Transmission drops sharply in the near sea bed layer, suggesting the presence of suspended material close to the sea bed.

In Area B (**Figures 4 and 6**), an intermittent warm layer is observed between approximately 40 and 60 m depth, with maximum temperatures of about 30 °C. The mixed layer depth shows variation from approximately 25- 80 m. Lowest temperatures (15 °C) and highest salinities (34.6 ‰) are observed near the sea bed at the deepest sites.

3.3 SEDIMENTOLOGY

The sediments of the Arafura Sea have been described in some detail in a previous study of the region (Jongsma, 1974). Geoscience Australia Survey 282 targeted specific areas of sea bed thought to be representative of different facies or habitats as opposed to the previous grid-based approach. A targeted approach can yield a better understanding of the diverse environments and habitats. The details of the sedimentology can be accessed in MARS. Go to http://www.ga.gov.au/oracle/mars/, click on either the simple or advanced version, and type in '282' into survey ID.

3.3.1 Area B

36 sediment grab samples and cores were collected in Area B, comprising 2 benthic sled samples, 23 grab samples and 11 gravity cores (locations in **Figure 9** and **Appendix 1 and 4**). Analysis of sediment samples shows that sediments are generally calcareous, medium- to fine-grained sand and sandy mud, and include minor amounts of mollusc and foraminifera fragments.

3.3.2 Area C

159 sediment samples and cores were collected in Area C, comprising 9 benthic sled samples, 15 dredge samples, 62 grab samples and 73 gravity cores (locations in **Figure 10** and **Appendix 1 and 4**). An analysis of sediment samples and video footage shows that sediments are generally muddy, fine- to medium-grained sand and gravel in the shallow southeast part of Area C. Sediments on the plain in the central part of Area C are generally muddy sand to sandy mud, with video footage showing bioturbated soft sediment and occasional hard surfaces. Sediments on Pillar Bank comprise sand and gravel, with areas of cemented hardgrounds and a diverse biota coverage seen in video footage. The channel to the north of Pillar Bank contains calcareous mud and muddy sand.

3.3.3 Area D

21 sediment samples and cores were collected from sites in Area D, comprising 3 benthic sled samples, 1 grab sample and 17 gravity cores (locations in **Figure 11** and **Appendix 1 and 4**). Initial analysis of samples shows that sediments are generally sandy or shelly calcareous mud, with some areas of muddy fine sand.

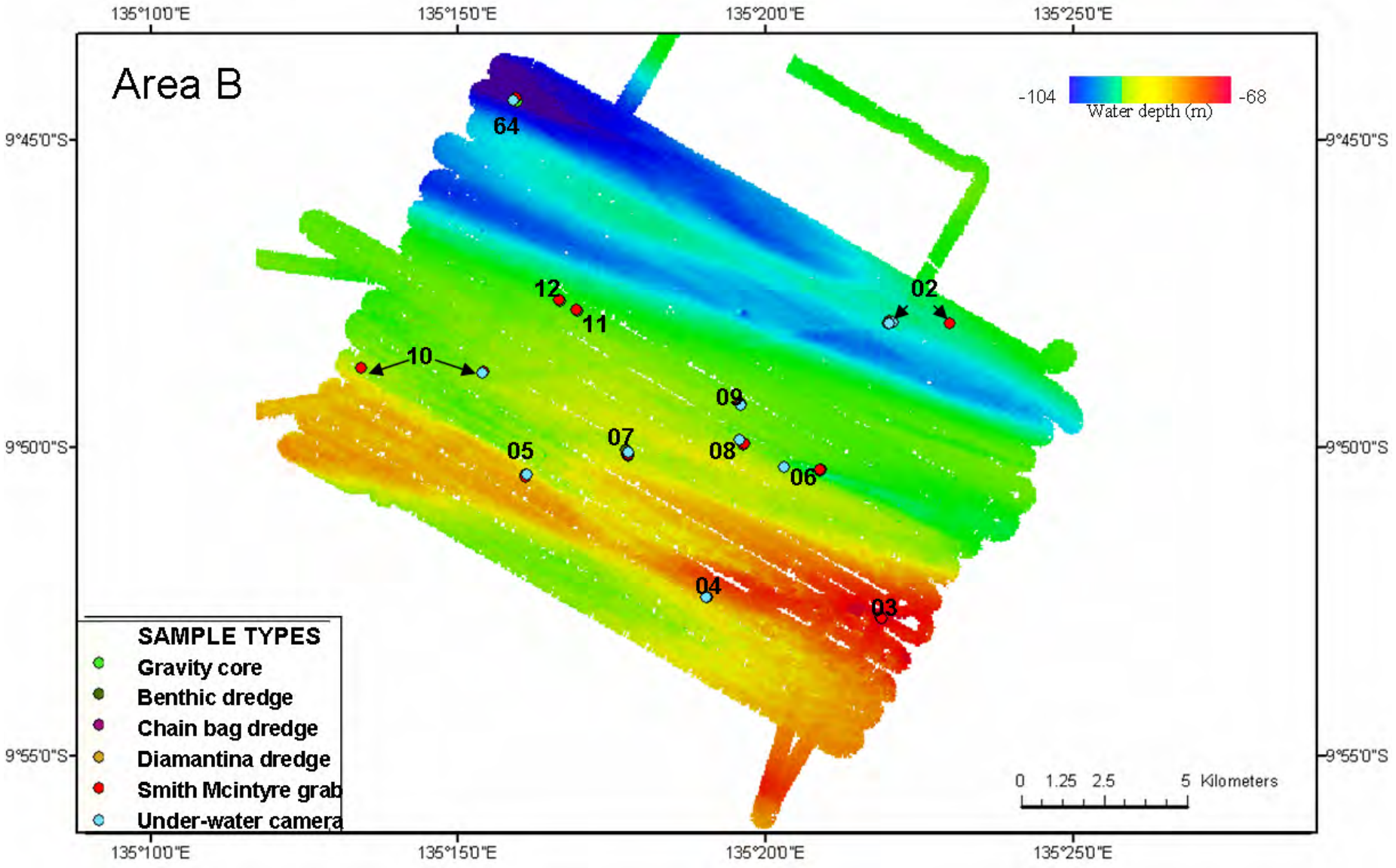

Figure 9 Multibeam bathymetry image and sample sites location in Area B.

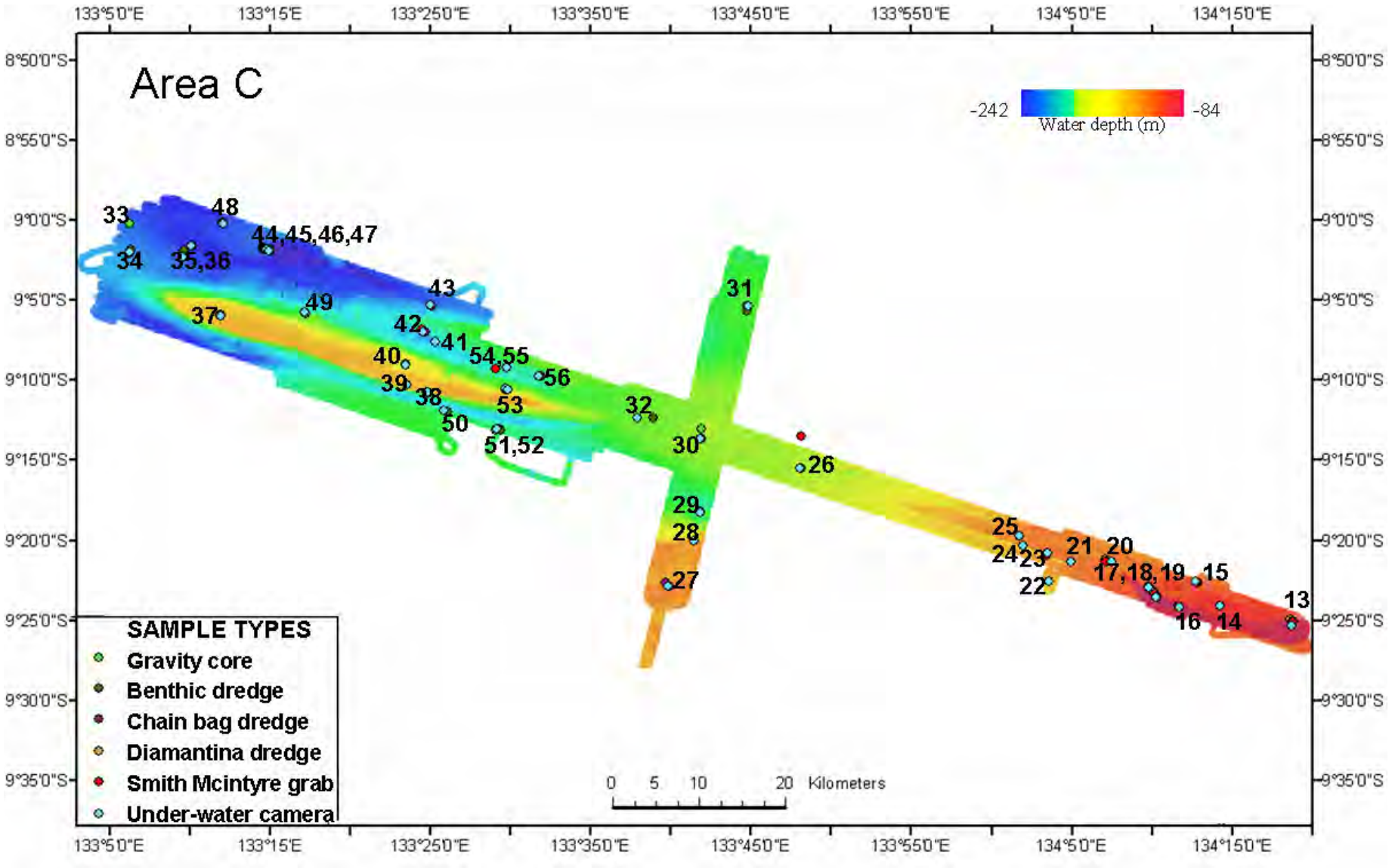

Figure 10 Multibeam bathymetry image and sample sites location in Area C.

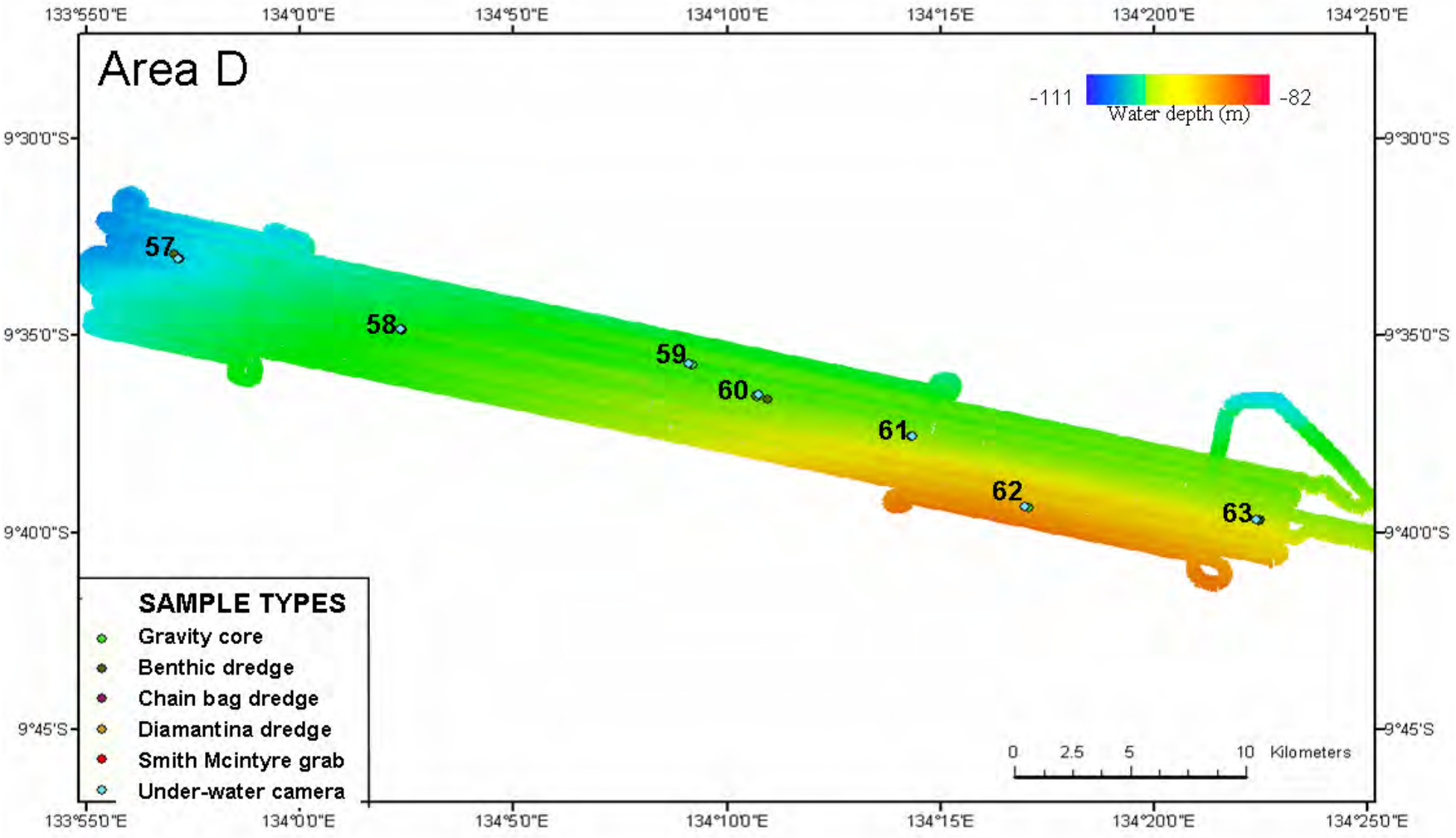

Figure 11 Multibeam bathymetry image and sample sites location in Area D.

3.3.4 Sediment accumulation rate in cores.

Five of 103 gravity cores, acquired during the survey, were selected for radiometric dating, three from Area B, and one each from Areas C and D. Each core was sub-sampled and 30 of these samples were processed (see **Appendix 4** for complete list). The carbon dates ranged from 34,770 ± 357 to 739 ± 78 years BP, with several of these dates indicating a significant amount of reworking. For each of the cores, an average linear sedimentation rate has been obtained. However, as many of the cores show facies variations, a linear sedimentation rate is not representative of the actual accumulation rate. While these dates provide insights into sediment accumulation rates throughout the survey area, more detailed dating is needed to provide further information on the Holocene (and older) evolution of Australia's central northern margin. Dating was carried out on fresh, unstained biogenic carbonate (benthic forams and molluscs) which were living as the sediment was being deposited. This method tries to avoid reworked material and provides the most accurate depositional dates.

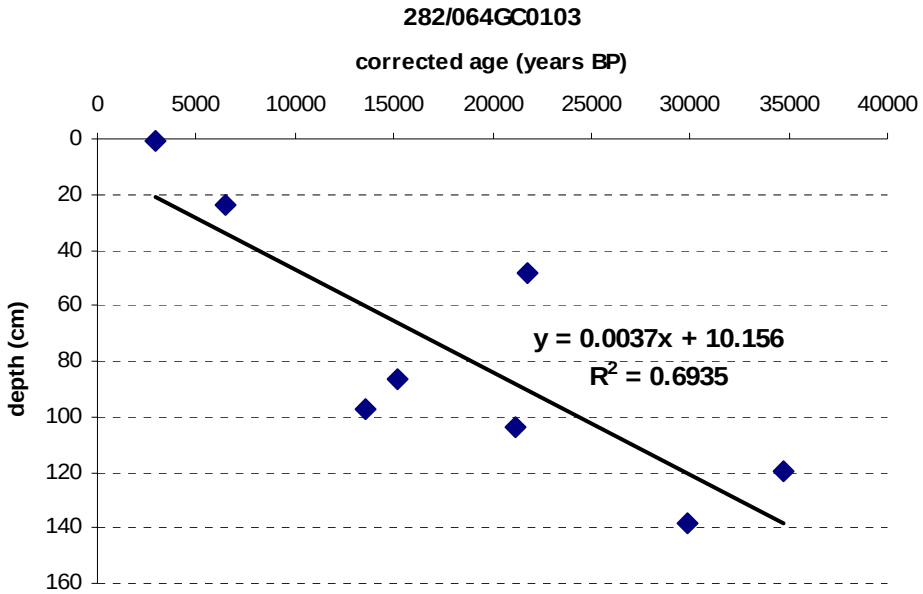

Figure 12 Core 282/064GC103 Corrected ^{14}C- age *v's* depth plot

Core 282/064GC103 (**Figure 12**) located in Area B, is ~1.40 m long and has eight corrected ^{14}C-radiometric ages ranging from the oldest of 34,770 ± 357 to 2,921 ± 78 years BP. The non-sequential dates down the core indicate either that the sediments have been subject to significant reworking or there is significant carbon contamination. Reworked sediments are redistributed and redeposited due to a range of physical inputs, including bioturbation, fluvial erosion/deposition and the impacts of changing sea level with wave, wind and current action. The dates infer a linear sedimentation rate for this core averaging 3.7 cm per thousand years.

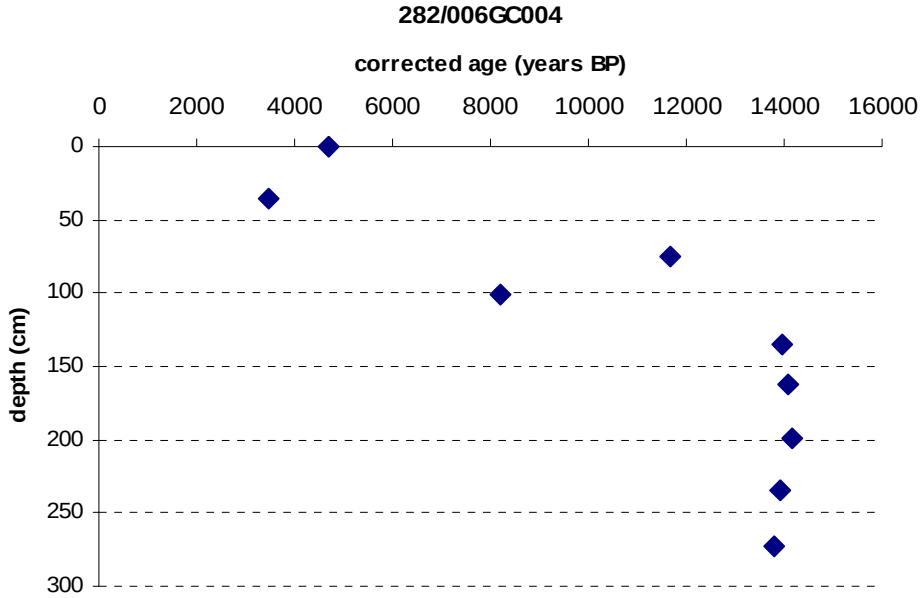

Figure 13 Core 282/006GC004 Corrected ^{14}C- age *v's* depth plot

Core 282/006GC004 (**Figure 13**) located in Area B, is ~2.75 m long and has corrected ^{14}C-ages ranging from 14,178 ± 90 to 3,474 ± 78 years BP. These dates indicate rapid linear accumulation or substantial reworking (below ~1.30m) from the 13,805 ± 90 to 13,943 ± 93 years dates. The top 1.25 m of the core also has some non-sequential dates, again indicating either significantly sediment reworking or contamination from older carbon. This reworking is to be expected in the fluvial-dominated environment in 'Area B' where sediments are deposited, reworked then redeposited

due a range of physical inputs including bioturbation, fluvial erosion/deposition and the physical impacts of changing sea level including wave and current energy.

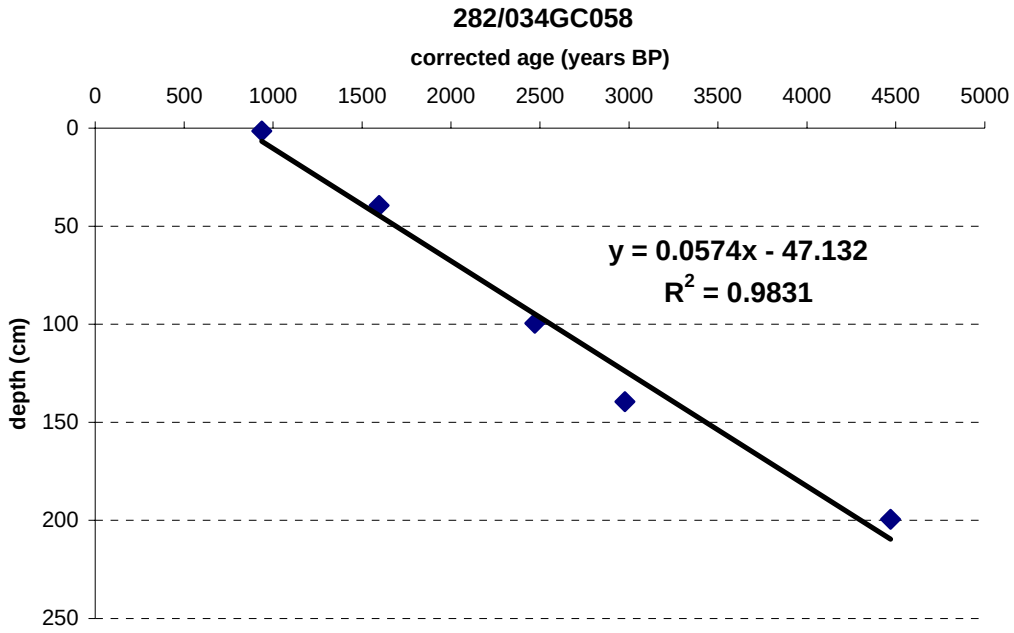

Figure 14 Core 282/034GC058 Corrected ^{14}C- age *v's* depth plot

Core 282/034GC058 (**Figure 14**) located in Area C, is ~2.0 m long and has five corrected ^{14}C-ages ranging from 4470 ± 80 to 937 ± 80 years BP. These dates show a steady and continuous lineal sedimentation rate of 57 cm per thousand years. As the surficial sediments are dated at 937 years BP, this infers that either a lack of sedimentation, palimpsest reworked material, or contamination from older carbon, is present in the surface layer.

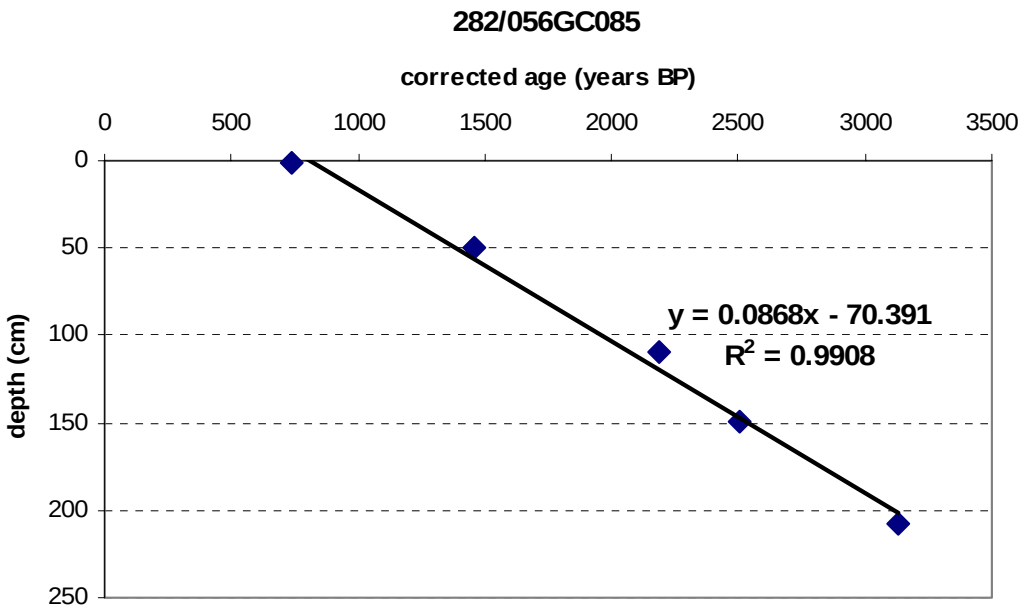

Figure 15 Core 282/056GC085 Corrected ^{14}C- age *v's* depth plot

Core 282/056GC085 (**Figure 15**) located in Area B, is ~2.75 m long and has five corrected ^{14}C-radiometric ages ranging from 3,131 ± 80 to 739 ± 78 years BP. The ages show that sedimentation at this site has been steady at 87 cm per thousand years.

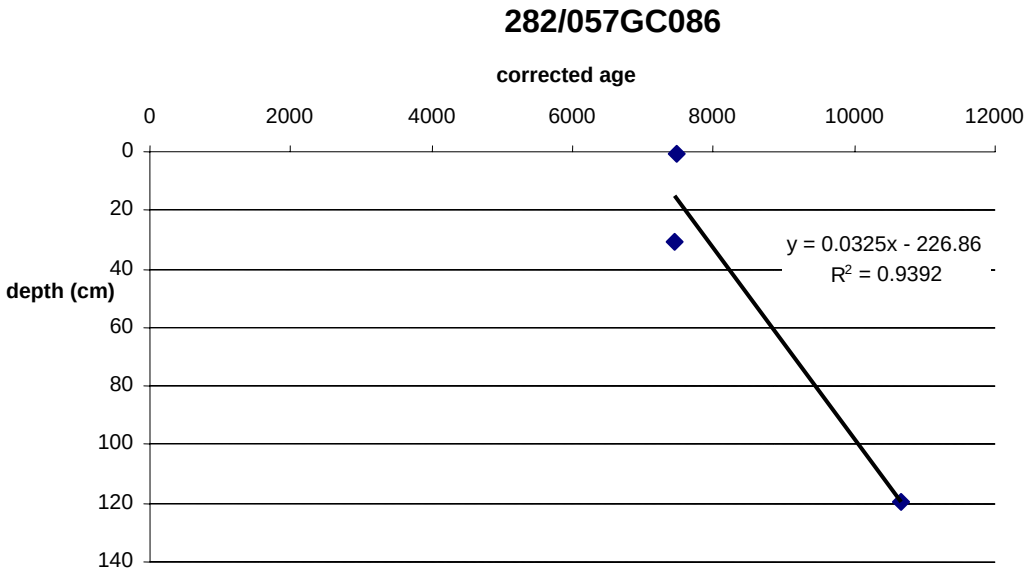

Figure 16 Core 282/057GC086 corrected ^{14}C- age *v's* depth plot

Core 282/057GC086 (**Figure 16**) located in Area D, is ~1.20 m long and has three corrected radiometric ages, ranging from 10,670 ± 82.3 to (7461 and 7477) ± 78 years BP at the surface. The top 30 cm of the core is of the same age within the error bars and indicates reworking of the upper sediment. A calculated deposition rate of 33 cm per thousand years is derived from the data; however, this is based on one point at the base of the core and must be considered highly unreliable.

3.4 VIDEO OBSERVATIONS

During the Arafura survey, approximately 24 hours of benthic video footage were recorded at 61 sites (**Appendix 5**), detailing scenes recorded down to water depths of 237m. Topography in the survey area ranged from sharp escarpments to flat sea bed and the substrate varied from unconsolidated soft muddy sands and sandy muds to lithified pavements with frequent cobbles. Biota was also varied and areas of high biodiversity and abundance generally correlated with harder substrates. In these areas, sea whips and fans, soft corals, hydroids, crinoids and octocorals were frequently identified with sessile benthos up to ~50cm in height.

The extensive areas of soft substrate commonly exhibited low relief benthic communities which often covered less than 5% of the surface area. Depressions, interpreted as pockmarks, were also frequently noted in soft muddy sea bed sediments. Visibility and the identification of organisms was sometimes heavily impeded by fine, suspended marine detritus, although it was possible to determine surface features such as mounds, depressions and small scale ripples of less than 5cm height and with varying alignment and direction. Potential fluid escape structures were also identified at sites, where the camera appeared to enter or pass pockmarks. Across all sites (**Appendix 5**), epifaunal species (fixed or sessile) and nektonic/planktonic species were seen only sporadically and were often solitary. Video will be made available through the MARS database: http://www.ga.gov.au/oracle/mars/

3.5 BIOLOGY

While not covering all habitats and ecosystems of the region, the survey collected more than 50 distinct taxa in the 2-10 cm size range and many smaller specimens. The shipboard biologists recorded 245 species from 107 grab/dredge sites and photographed and identified the larger biota. **Appendix 6** contains a photographic summary of the digital images of collected macro-fauna arranged by taxon according to the CSIRO CAAB (Codes for Australian Aquatic Biota) system (Yearsley et al. 1997; Rees et al. 1999). Wilson (2005) estimates that there may be an additional 500 species yet to be identified during post-survey analysis of grab and dredge samples.

Some of the biota highlighted in the biology report (Wilson 2005) included stomatopod crustacean species ("mantis shrimps") that appear to represent two different families. The abundant thallassanidean crustaceans ("ghost shrimp") appear to be a major bioturbator of the sediment. The thalassanideans may include five distinct species in two different families (Callianassidae, Upogebiidae), and additional species are expected to be found. At least six species of Ophiuroidea ("brittle stars", Echinodermata), were identified, probably belonging to at least three different families. Two species of the ophiuroids were found to be unusual, displaying a small central disk (only 2-3 mm wide) attached to long arms (30-40 mm). Across the benthos, the principal group is polychaetous annelids ("bristle worms") and, like the macrofaunal samples derived from the elutriation of the sediment, many of these species may be previously unknown to science.

As stated by Wilson (2005), the data derived from the ongoing study of the sedimentary macrofauna will provide an excellent first step toward an improved understanding of the distribution of benthic biodiversity in the Arafura Sea, and this will help reveal how it relates to regional diversity.

The biological data collected on this survey are still undergoing analysis by multiple research facilities across Australia and consequently are not the subject of this report. The initial analysis is contained within a separate biological report of the survey presented for the Department of the Environment and Heritage (Wilson, 2005).

3.6 SUB-BOTTOM PROFILES

3.6.1 Seismic Stratigraphic Units in sub-bottom profile data

The sub-bottom profiler data acquired over Areas B, C and D was used to define the youngest stratigraphic units, down to 300 ms two-way time (twt), in the Money Shoal Basin, within the survey areas. Sub-bottom data was collected while transiting between survey areas. It allows interpretations to be tied between survey areas, but only to a limited extent (**Figure 17**). Area C is linked to Area D by tying strike lines across Area C to the transit line to Area D. The transit line towards Area B ties with the sediment packages between Area D and Area B. However, this transit line and the link between Area B and D have not been studied for this report.

In the deepest part of the surveyed areas (Area C) ten units (from A to J) bounded by nine unconformities (from U1 to U9) and the sea bed have been interpreted down to 330 ms twt (**Figure 18**). Four main progradational sediment units (C, E, G, I) back step southeast towards the coastline, indicting an overall transgressive trend. Internally these sediment packages are composed of northwest-dipping reflectors, prograding basinwards towards the Timor Trough, and overly a major unconformity (U1). These different units and unconformities are probably 4th or 5th order compared to the ones bounding the main basin packages in the Arafura and Money Shoal basins.

The details of the different unconformities and sediment units described in this study are summarized in **Table 1**.

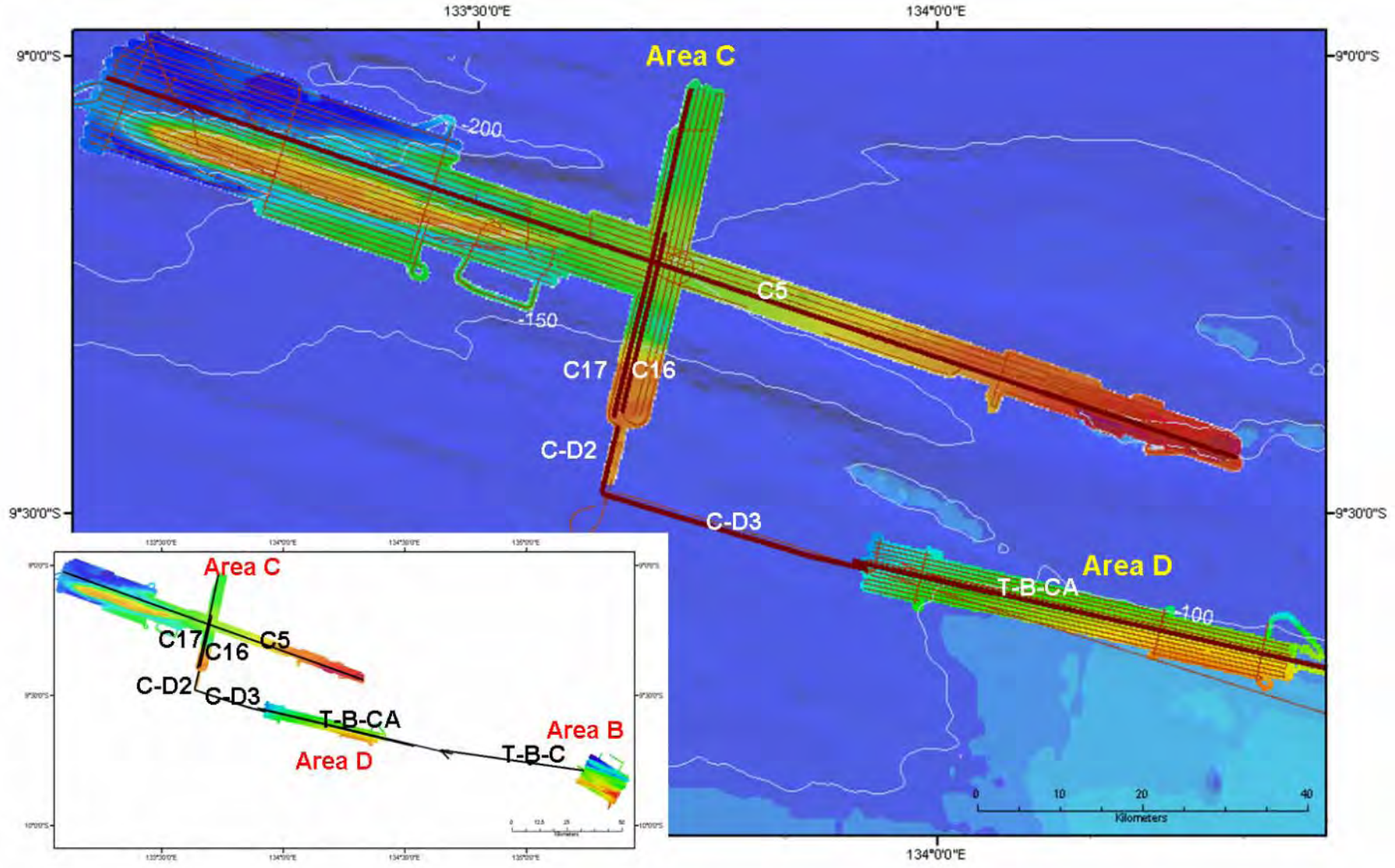

Figure 17 Multibeam bathymetry image of Areas B, C and D with overlying Topas data location. The highlighted lines show the locations of the cross-sections presented in more detail in other figures which were used to develop the seismic stratigraphic unit interpretation.

Seismic stratigra-phic units	Maximum observed thickness	Internal Characteristics	Upper boundary	Lower boundary	Facies Interpreta-tion	Jongsma's equivalent unconfor-mities (1974)	Gas Indicators
Unit J	~ 15 m	Low amplitude, discontinuous and parallel	Concordant	Concordant	Open marine, shallow water	Holocene	Seabed pockmarks; small- scale mud diapir (3m high and 140m wide); horizontal high amplitude, phase reversed, low frequency reflections
U9				Last Glacial Maximum?		SH	
Unit I	~ 45 m	Variable amplitude, high continuity and oblique prograde	Toplap to truncational erosion	Downlap	Progradation		Dipping, bedding-conformable high amplitude, phase reversed, low frequency reflections
U8							
Unit H	~ 15 m	Variable amplitude and discontinuous (3 different facies)	Concordant	Downlap	Transgression	Pleistocene	Injectites; potential Methane Derived Authigenic Carbonates
U7						S1	
Unit G	~ 52 m	Variable amplitude, high continuity and oblique prograde	Toplap to trucational erosion	Downlap	Progradation		Dipping, bedding-conformable high amplitude, phase reversed, low frequency reflections associated with a widely distributed cross-cutting enhanced, phase reversed, low frequency reflection
U6							
Unit F	~7 m	Low amplitude, discontinuous	Concordant	Downlap to concordant	Short transgression	Pliocene	
U5						S2	
Unit E	~ 22 m	Variable amplitude, moderate continuity and oblique prograde	Truncational erosion	Downlap	Progradation		Dipping, bedding-conformable high amplitude, phase reversed, low frequency reflections
U4							
Unit D	~ 7 m	Variable amplitude, moderate continuity and oblique prograde	Concordant	Downlap	Short transgression		
U3							
Unit C	~ 15 m	Moderate amplitude, high continuity and oblique prograde	Toplap	Downlap	Progradation		Dipping, bedding-conformable high amplitude, phase reversed, low frequency reflections
U2							
Unit B	~ 11 m	High amplitude, high continuity and many parallel reflectors	Concordant to eroded	Concordant to downlap	Basal Sand transgressive system tract	Late Miocene-Early Pliocene	
U1						S3	
Unit A	Undeter-mined	Moderate amplitude and weak reflections; Acts as an acoustic basement	Concordant	Not visible	?		

Table 1: Characteristics of the different seismic stratigraphic units and unconformities observed on sub-bottom profile data, from the seabed down to 330 ms twt.

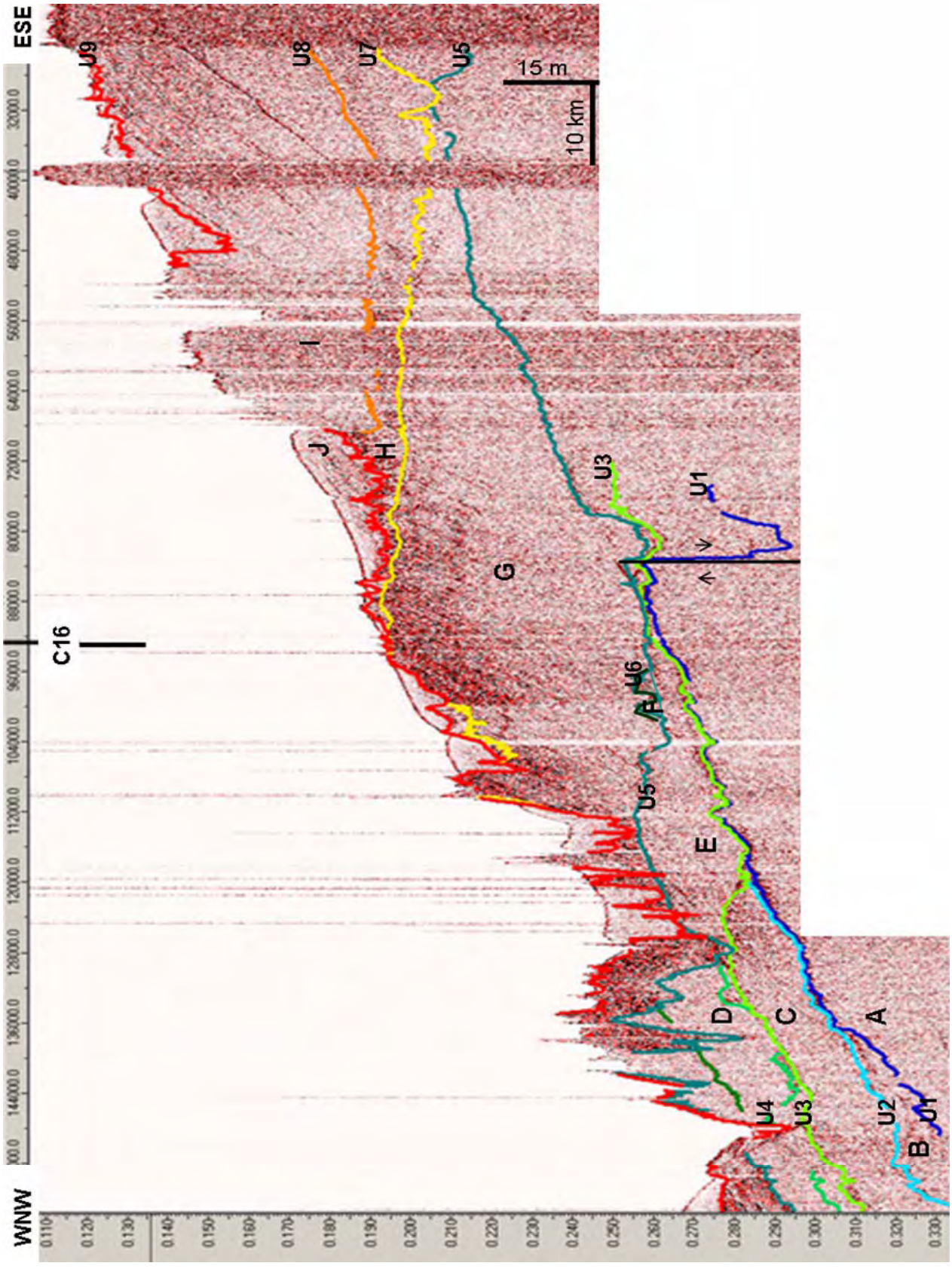

Figure 18 Sub-bottom profile line C5 showing the broad seismic stratigraphic units (A-J) and unconformities (U1-U9) in Area C (Location shown in **Figure 17**). U1 (dark blue) major erosional unconformity and base of onlap units; Seismic penetration beneath U1 is minimal. Unit A is considered as an acoustic basement. U2 (light blue) base of the first NW- dipping prograding unit; U3 (light green) base of a transgressive unit; U4 (green) base of the second NW-dipping prograding unit; U5 (dark green) base of another transgressive unit; U6 (olive green) base of the third NW-dipping prograding unit; U7 (yellow) base of the sand ridges unit; U8 (orange) base of the fourth NW-dipping prograding unit; U9 (red) the mud unit.

3.6.2 Major unconformities observed in the surveyed areas

The deepest unconformity (U1) is a strong reflection present on most seismic lines in the western and central parts of Area C, where the signal penetration is deeper (down to 270-300 ms twt). This unconformity dips gently to the northwest.

1. Unconformity U1 is an erosional surface marking a strong acoustic contrast between Unit A and the overlying units. It is possible that U1 is strongly indurated. It is overlain by either concordant or downlapping units. U1 shows some irregularities which may be caused by structural deformation. In the central-eastern part of Area C, U1 is offset by normal faults (**Figure 19**). It becomes harder to define this unconformity southwards as U1 becomes deeper and is covered by thicker sediment packages.
2. Unconformities U2, U3 and U4 separate downlapping progradational units and are restricted to the northwest, in the deeper part of Area C.
3. U5 and U6 are present throughout Area C at 210-260 ms twt and disappear progressively under Area D where the seismic penetration is degraded. U5 is an erosional surface dissected by channels, which in some places have cut down to the underlying U3.
4. U7 is an erosional surface. It is present over Area C and Area D, usually at a depth of 160-220 ms twt, except when it has been incised by the younger unconformity U9 (**Figures 19 and 20**).
5. U8 is present only in the southeast part of Area C, the eastern part of Area D and Area B, in the shallower parts of the region (**Figures 21 and 22**).
6. U9 is the most recent unconformity below the seabed and forms the base of channels observed in sub-bottom profiles to the north and south of Pillar Bank.

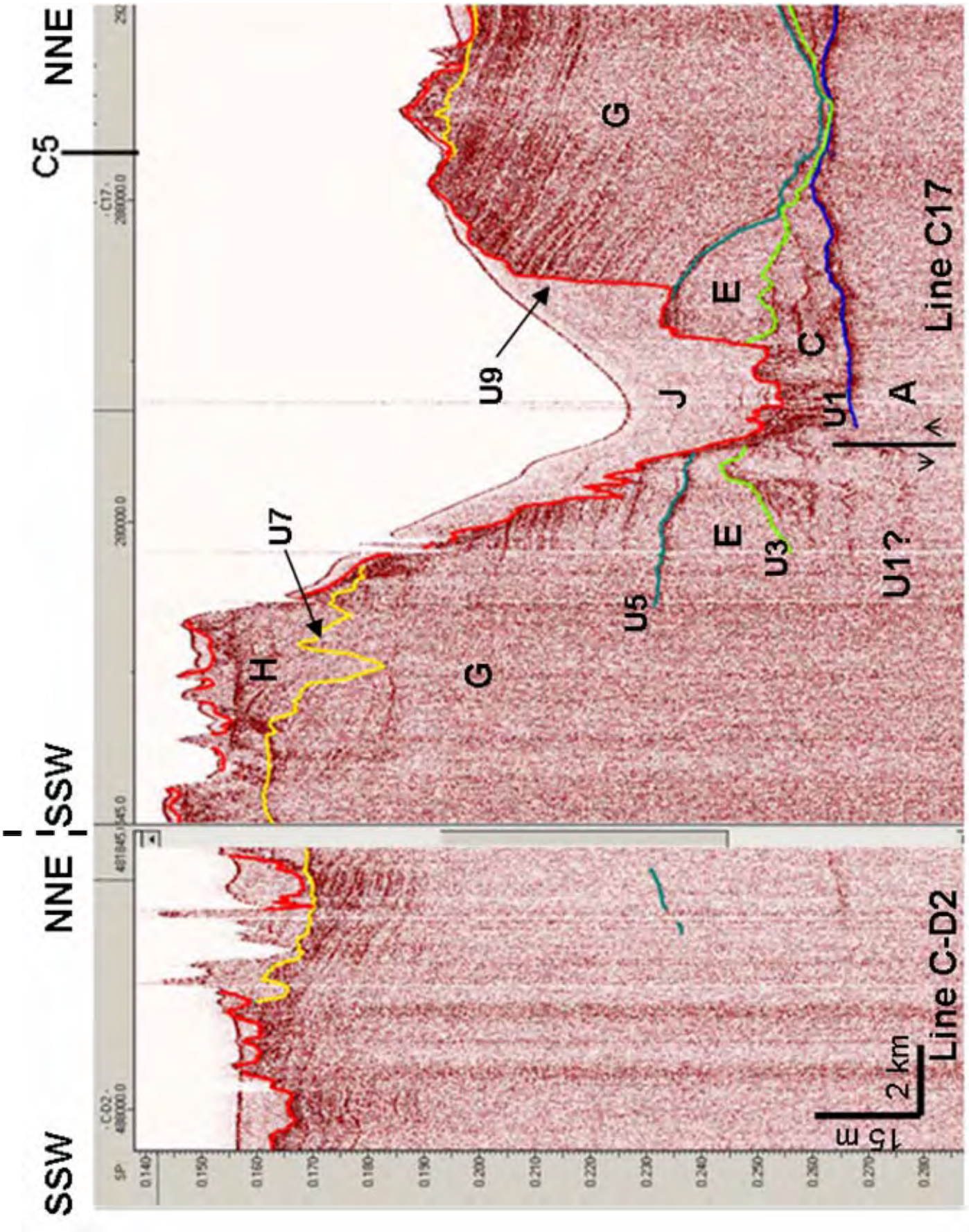

Figure 19 Line C-D2 and C17, from SSW to NNE, are strike lines across Area C. U8 an U2 are not observed on these lines. Location shown in **Figure 17**.

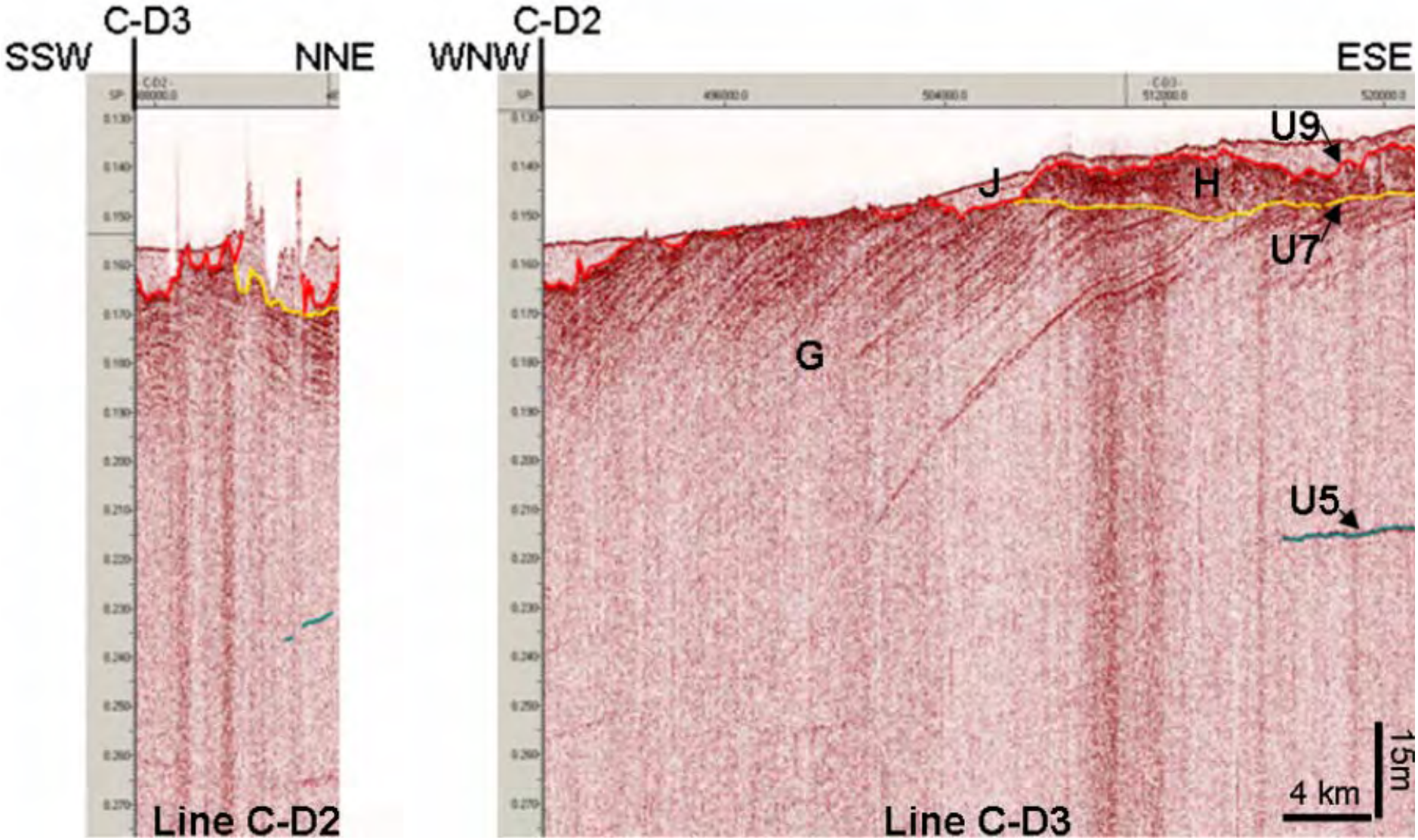

Figure 20 Intersecting lines C-D2 and C-D3. Unconformity U8 and Unit I are not observed in this area. Location shown in **Figure 17**.

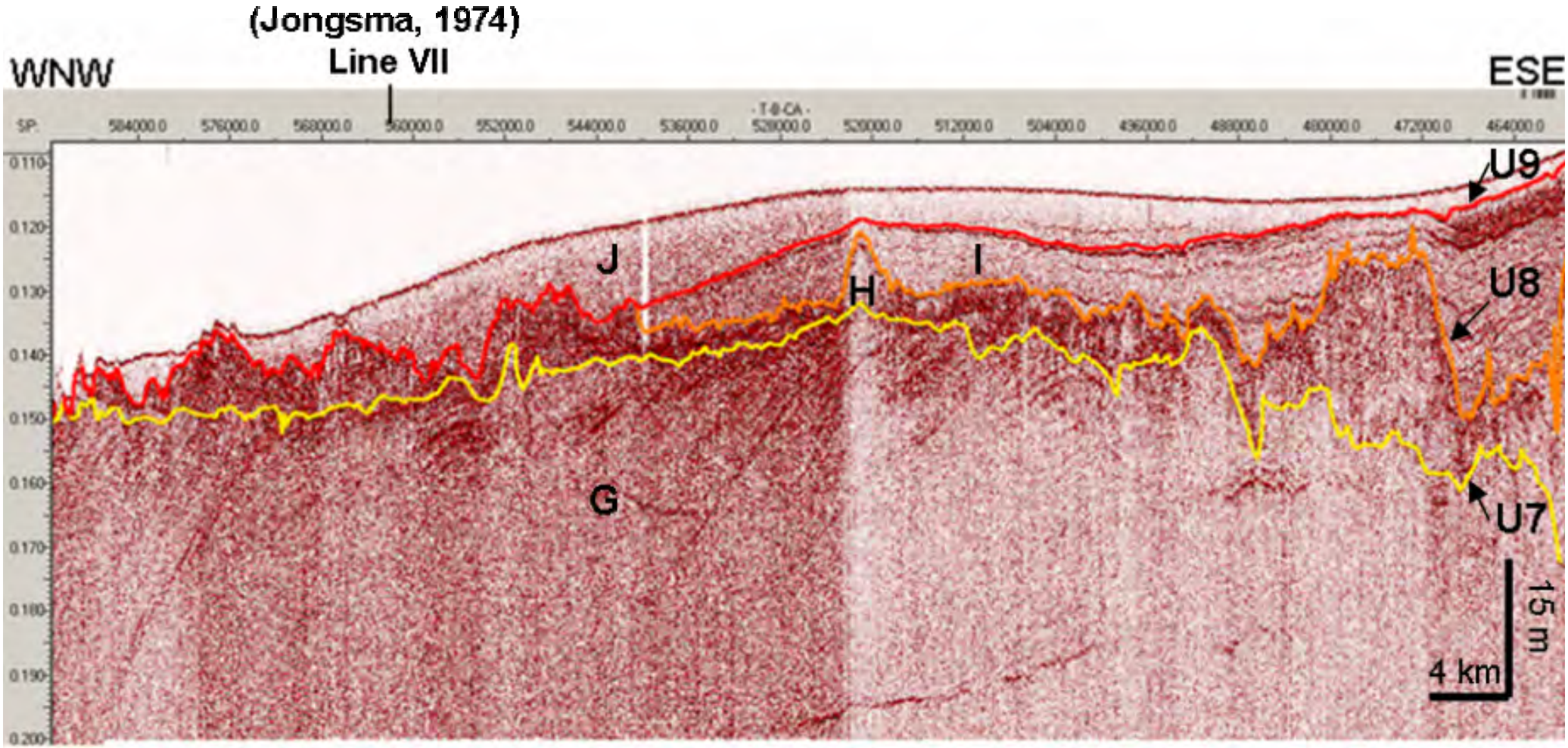

Figure 21 Line T-B-CA in area D showing the onlapping of the NW-dipping prograding Unit I above unconformity U8. Unit I is limited to the eastern part of Area D. Location shown in **Figure 17**.

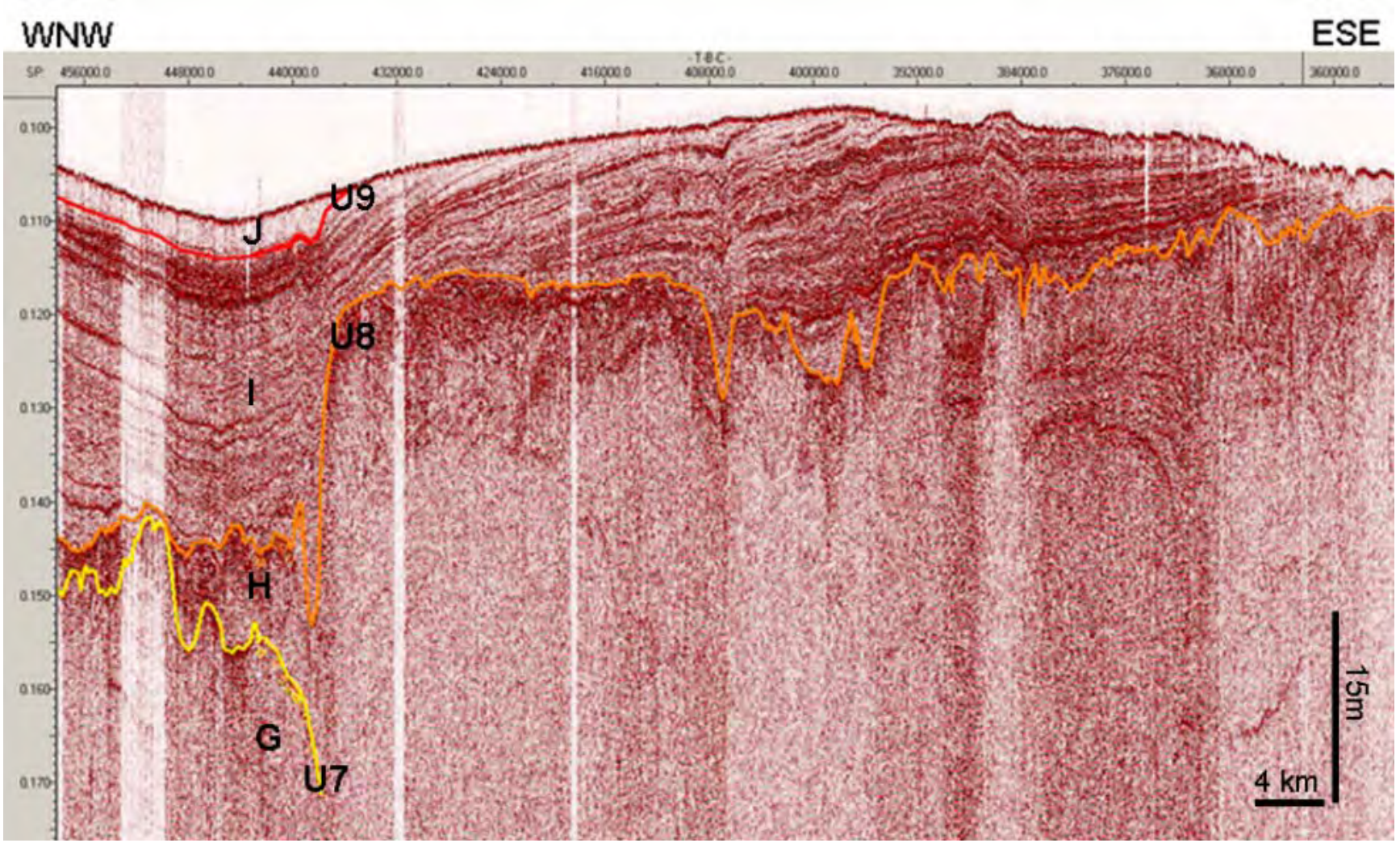

Figure 22 Line T-B-C in the eastern part of area D, showing the seabed truncation at the top of the NW-dipping prograding Unit I. This line provides a tie between Area D and Area B to the east. Location shown in **Figure 17**.

3.6.3 Seismic stratigraphic units in Area C

Most seismic stratigraphic units are stacked in an overall transgressive trend with a northwest-wards progradation internal geometry. They are described from oldest to youngest below and summarised in **Table 1**:

1. Unit A is acoustic basement within Area C. It exhibits moderate amplitudes with weak reflections (**Figure 23**).
2. Unit B contains a transparent seismic facies at the base and more reflective discontinuous reflectors at the top (**Figure 23**).
3. Unit C downlaps on to U2 and is truncated at the top by U3 (**Figure 23**). Its internal geometry is oblique prograding and shows some structural or depositional deformation in the east, particularly in the shallower part of the unit, with coincident increase of amplitude within the internal reflectors.
4. Unit D is only observed in the north-western parts of Area C and has a variable amplitude facies. It has limited geographical extent and appears to form isolated mounds.
5. Unit E has similar seismic characteristics to Unit C, except that an increase reflection amplitude and deformation are observed in the deepest parts of the unit, in the southwest (**Figures 23 and 24**).
6. Unit F is only interpreted in the central part of Area C and has low amplitude reflections. It appears to form isolated mounds.
7. Unit G comprises a north-westerly dipping reflector package which down-laps onto U5 and is truncated above by U7 or U9, where it shows top-lap relationships (**Figures 24 and 25**). The general geometry of Unit G is oblique progradational. Reflection amplitudes are markedly higher in the upper part of the unit. In detail, a series of enhanced reflectors often composed of en echelon segments, gives the appearance of a cross-cutting reflector ~10ms below U7 (**Figure 24**). Unit G is the most deformed layer, showing minor faults and folds (**Figures 24 and 25**).

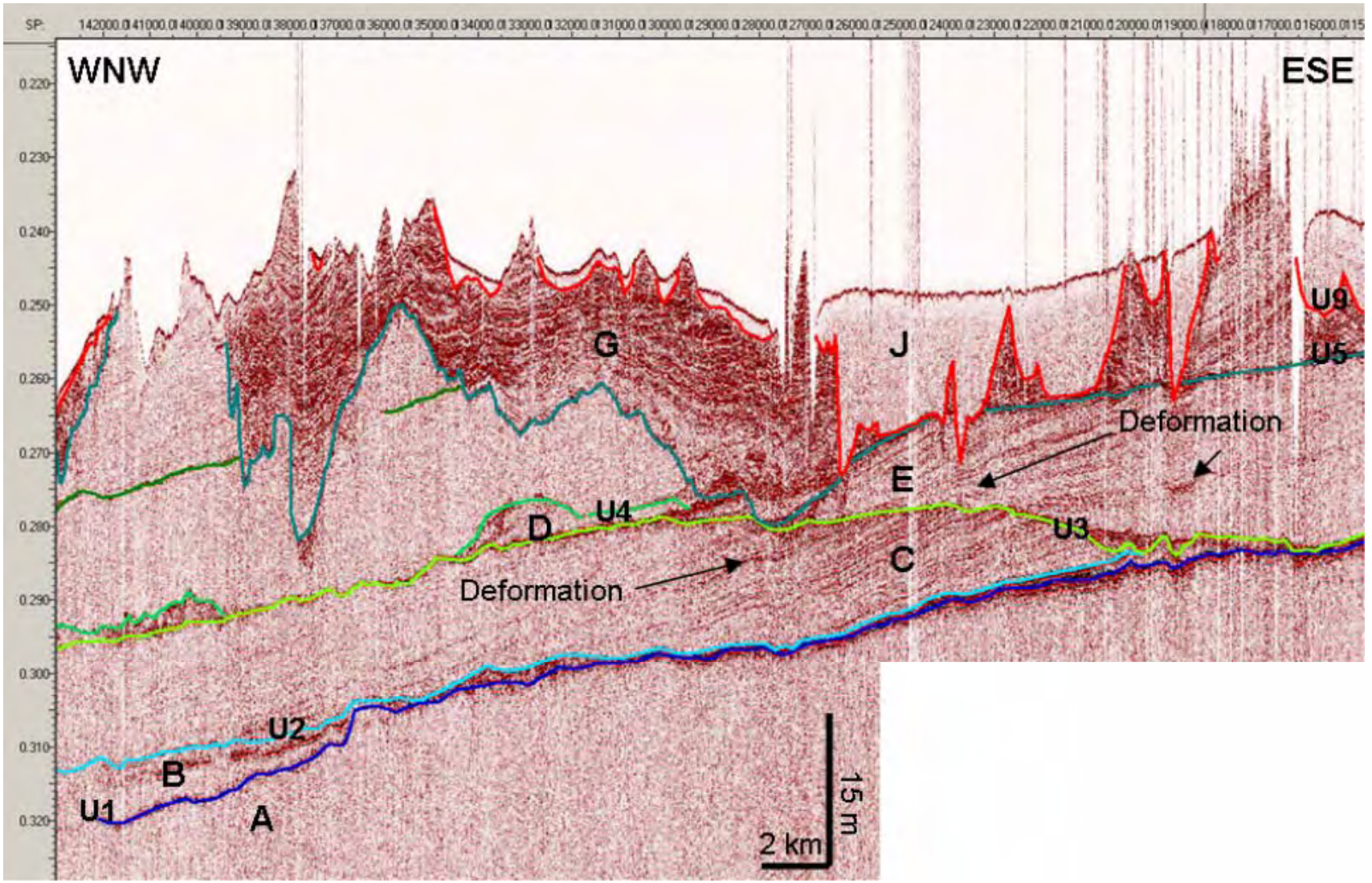

Figure 23 Western part of Line C5 showing a concordant Unit B above U1 that thickens in the deepest NW part of the area. Unit C is truncated at the top by the unconformity U3 and onlaps U2 at the base.

8. Unit H is characterised by complex internal seismic facies (**Figure 26**). This unit contains three different seismic facies depending on the nature of the overlying Unit. The first two seismic facies are present in Area D and in the central part of Area C, when Unit I is not present. These two facies include an acoustically transparent facies, interpreted as massive deposition of sand (**Figure 26a**), and a layered facies with internal cross-bedding, interpreted as deposits associated with either fluvial or tidal channels. A third seismic facies is observed in the eastern part of Area C, when Unit H is overlain by Unit I, and consists of transparent, small-scale blocks separated with bedded asymmetric infill, roughly 50 m across (**Figure 26b**). They are interpreted as representing sand ridges.

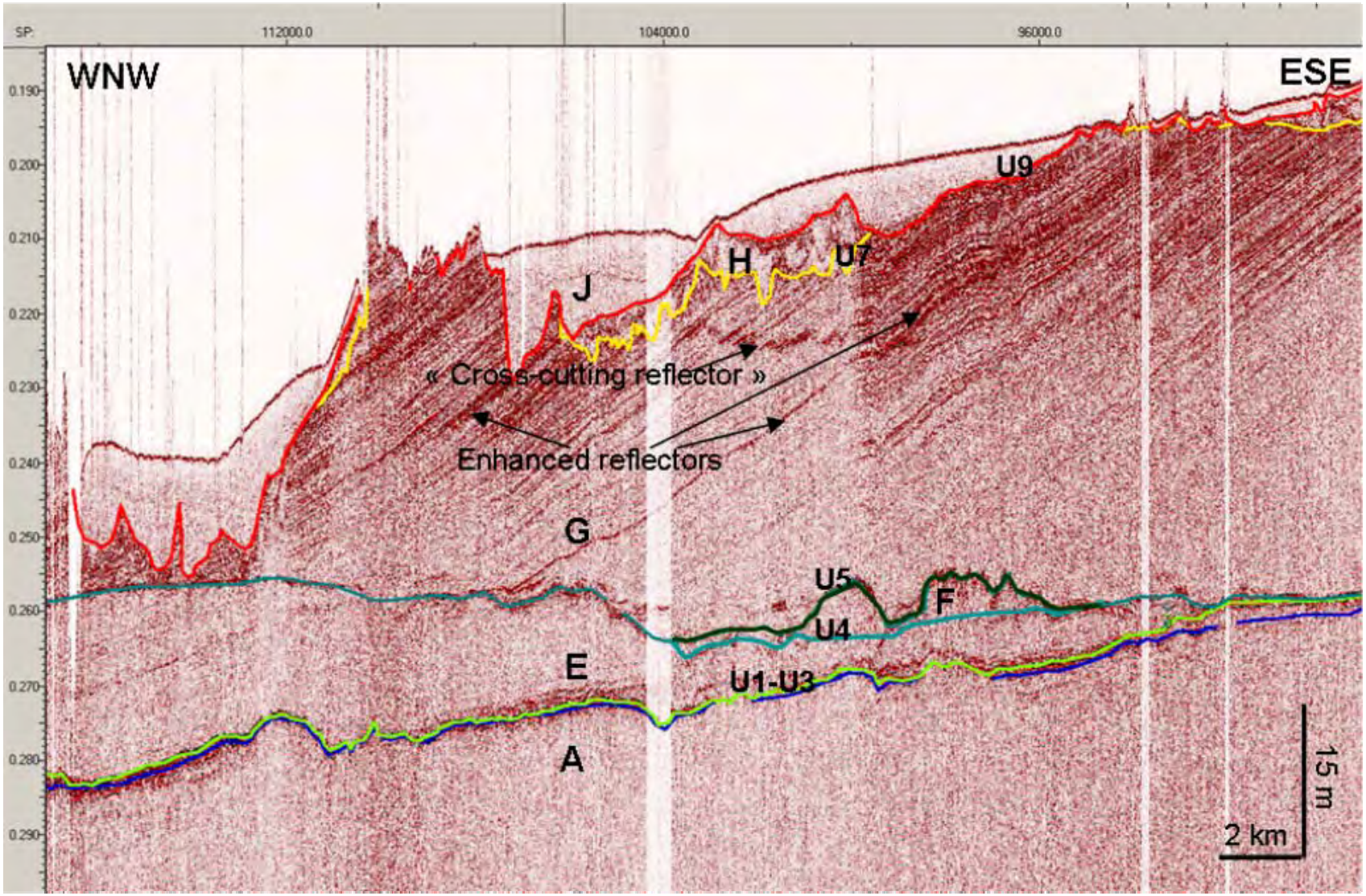

Figure 24 Western-central part of Line C5 showing the NW-dipping prograding Unit E which is bounded below and above by the erosional surfaces, U3 and U5. Enhanced reflectors are visible in the upper part of Unit G, sometimes forming a pseudo-cross-cutting reflector (in the centre of the figure).

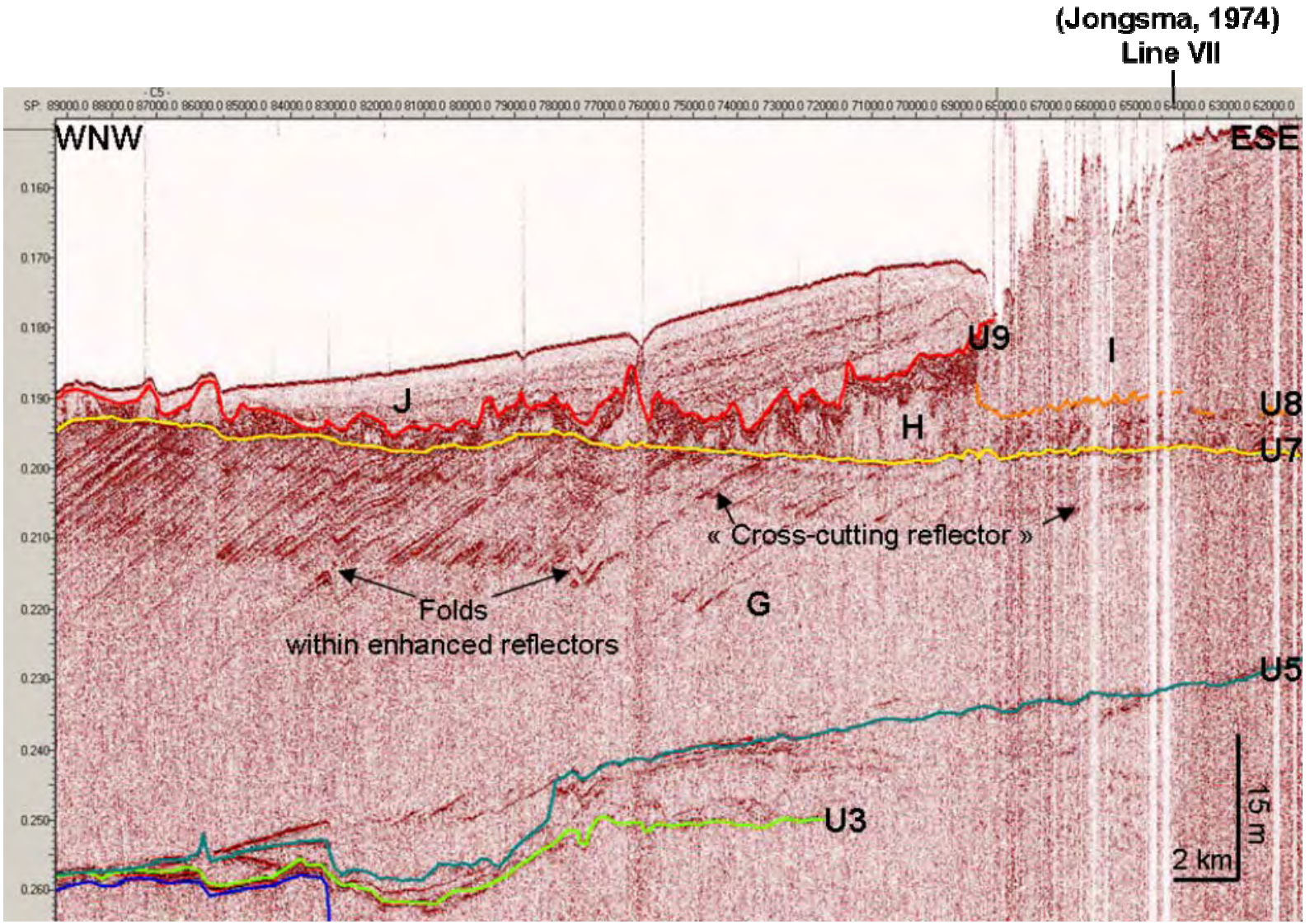

Figure 25 Central-eastern part of Line C5 showing the NW-dipping prograding Unit G which is bounded below and above by the erosional surfaces, U5 and U7. The package G is truncated at the top and onlaps U5 at the base.

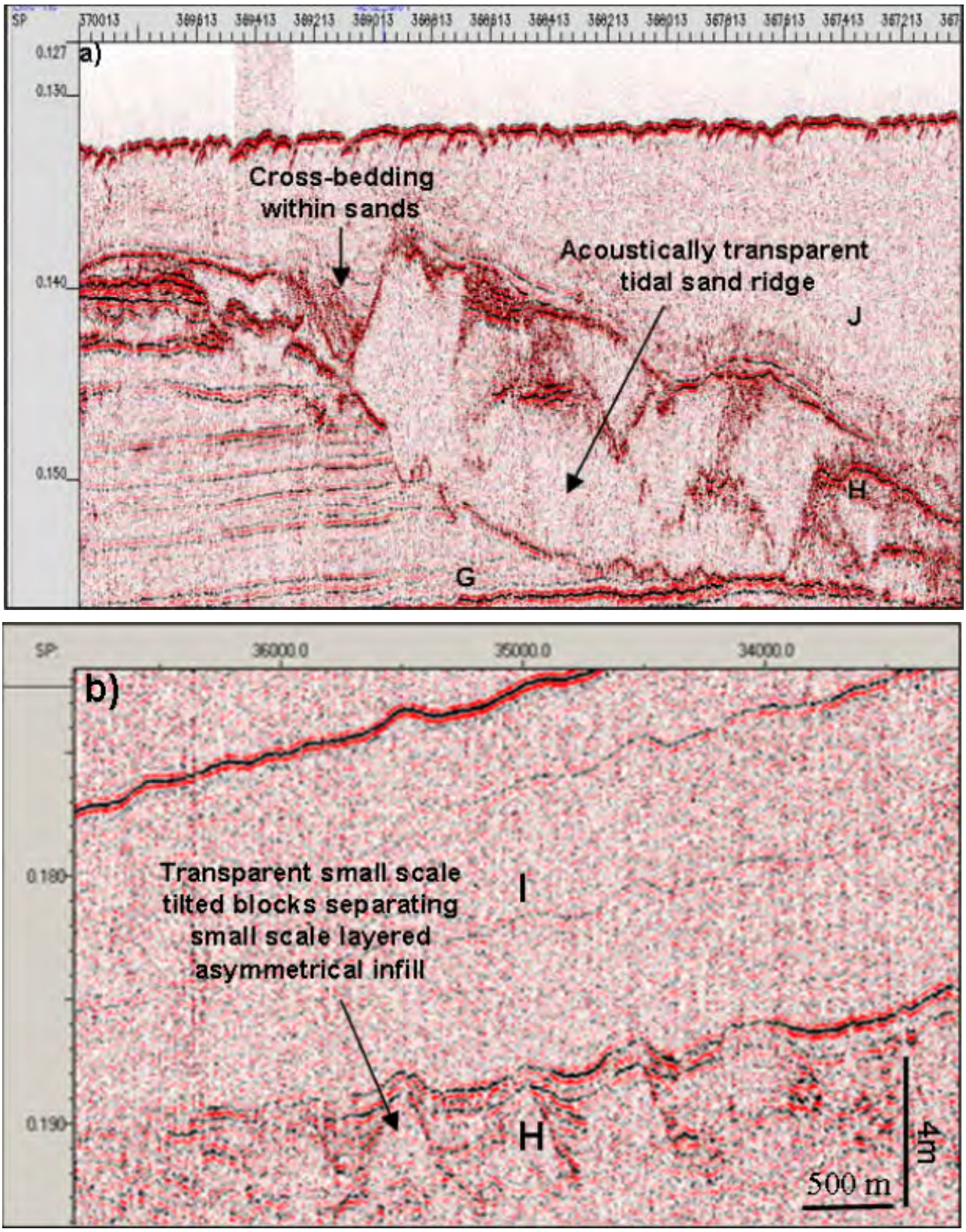

Figure 26 Various seismic facies of Unit H reflecting different lithologies; a) in Area D and central part of Area C, where Unit I is absent; b) in eastern part of Area C, where Unit I is present.

Outcropping mounds of Unit H are prominent topographic features, and are apparently capped by hard material, as indicated by the strong sea bed reflections and absence of seismic signal from the underlying section (see **Figure 27**, vertical white bands). These mounds may be reefs that formed during a sea-level low-stand. An alternative interpretation is that they may be cemented sand waves. Further sampling would be required to confirm the origin of these features.

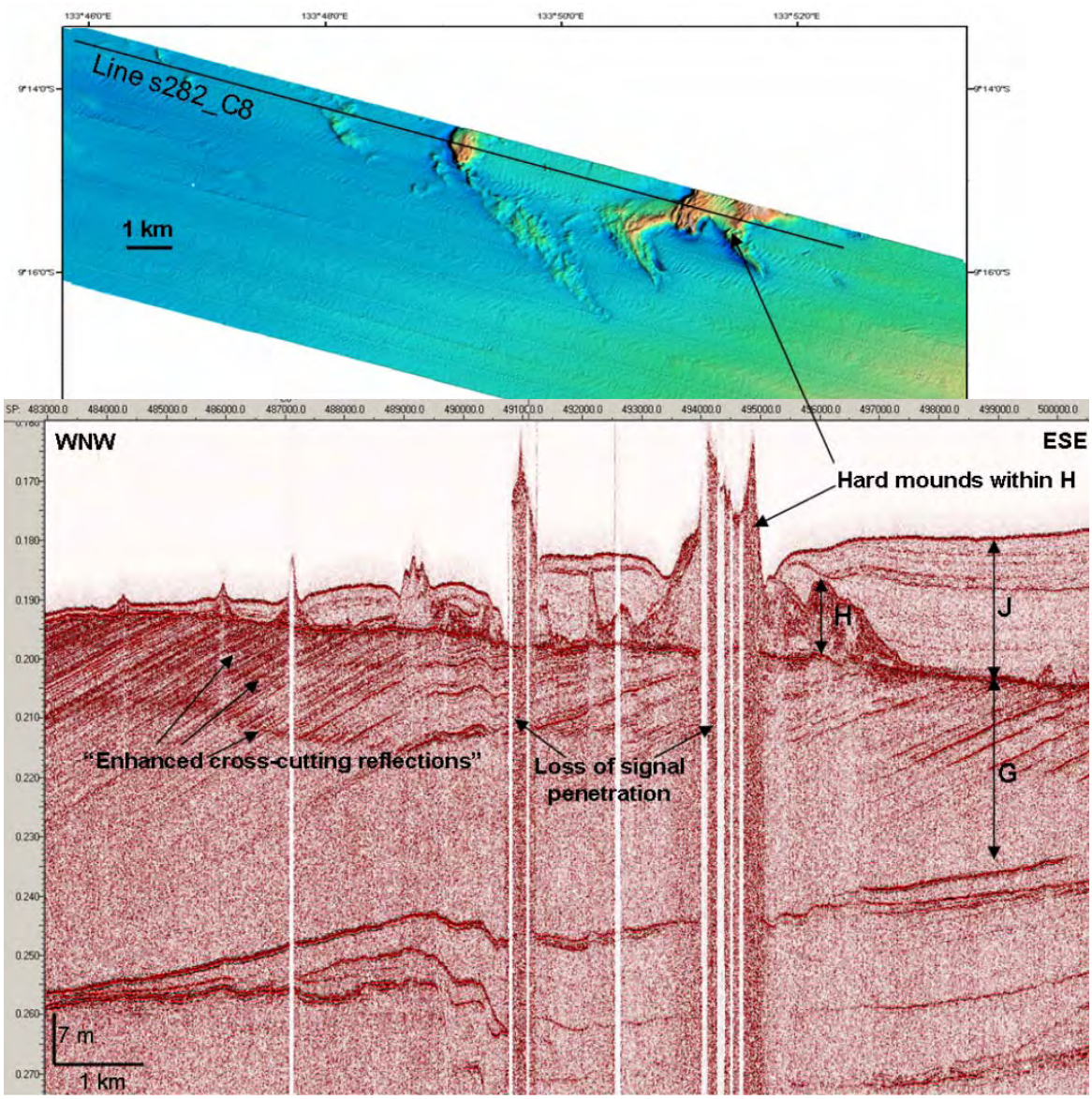

Figure 27 Line S282_C8 in Area C, showing Unit H mounds that outcrop on the sea bed and cause the loss of seismic signal below. Location shown on the multibeam bathymetry above.

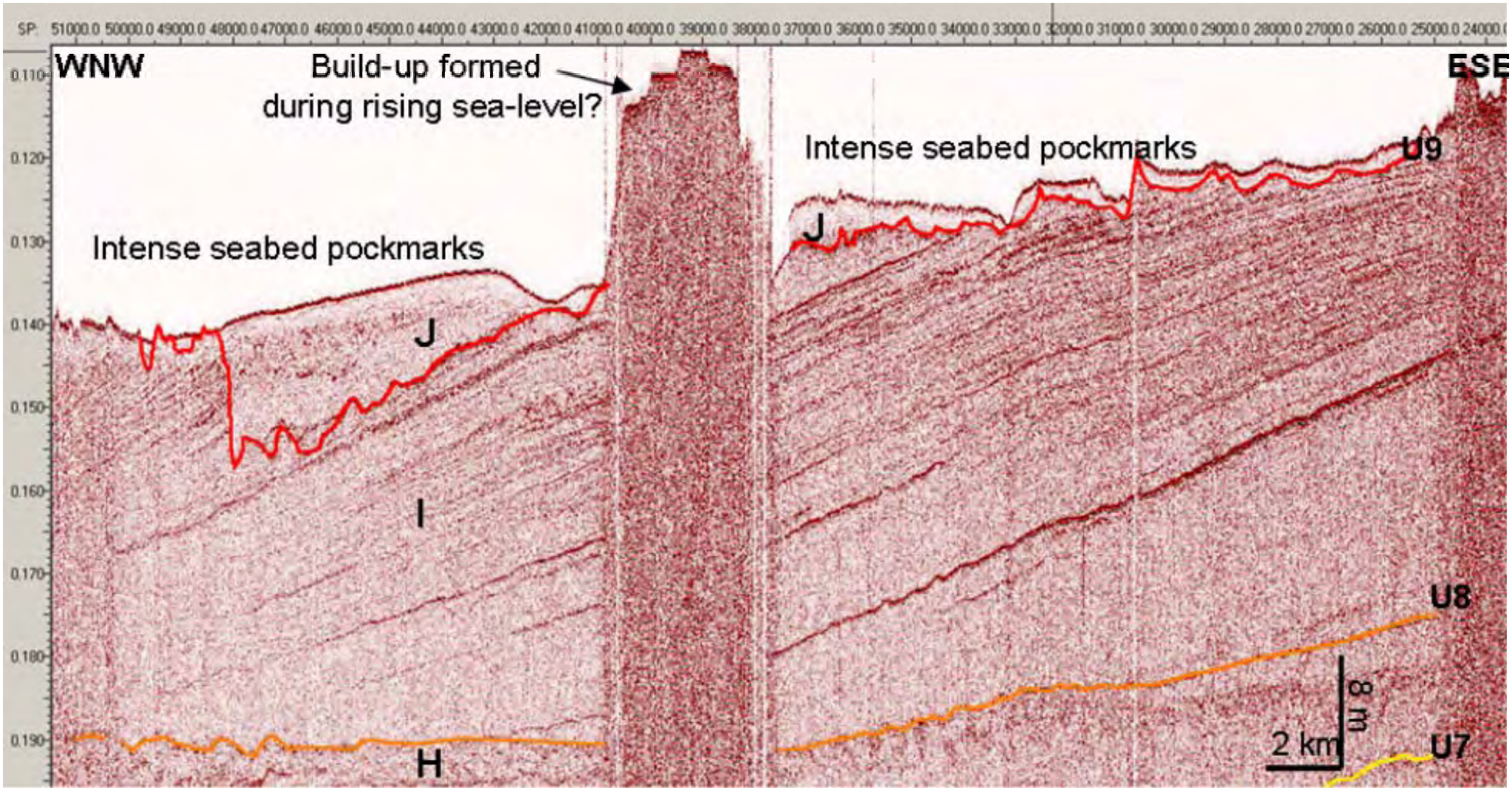

Figure 28 Eastern part of Line C5 in eastern part of Area C, showing the NW-dipping prograding Unit I which is bounded below and above by erosional surfaces, U8 and U9.

9. Unit I is a progradational package containing NW- dipping reflections which are downlapping onto U8 at the base and are truncated by U9 above (**Figure 28**). This unit is mostly restricted to the eastern part of Area C.
10. Unit J is generally seismically transparent but shows, in some places, a more reflective layer near the base of the unit. This deeper layer is composed of disrupted reflective segments, giving a chaotic appearance. Often, the sea bed is intensely pockmarked where this unit is present (**Figures 26a, 27 and 28**).

3.6.4 Seismic stratigraphic units in Area D

In Area D, only the units G to J are observed because of the reduced seismic penetration in this area. These units have similar facies characteristics to those previously described for Area C. These units are described below, from the oldest to youngest.

1. Unit G downlaps onto the unconformity U5 at about 200-220 ms twt, where this unconformity is visible (**Figures 20 and 21**). U5 deepens to the northwest and cannot be distinguished in the central part of Area D.

2. Unit H is present throughout Area D but is not present on to the western half of the transit line between Areas C and D (**Figures 20 and 21**), where it has either not been deposited or is absent due to erosion.

3. Unit I is only present in the eastern part of Area D. It downlaps onto U8 and forms a wedge shaped unit that pinches out on the central part of Area D.

4. Unit J is present throughout Area D but is absent due to erosion or non-deposition to the east and west. Unit J is thickest in the western part of Area D (up to 20 ms twt), coincident with a sea bed pockmark field.

3.6.5 Seismic Units in Area B

Analysis of Area B is being undertaken for a separate report on benthic habitat and biodiversity of the Arafura Sea prepared by Geoscience Australia for the Department of the Environment and Heritage.

3.6.6 Correlation of seismic stratigraphic unit interpretation with previous studies

The unconformities recognised in the Areas C, D and B can be correlated with shallow seismic profiles previously acquired in the area (Jongsma, 1974; see location in **Figure 29**).

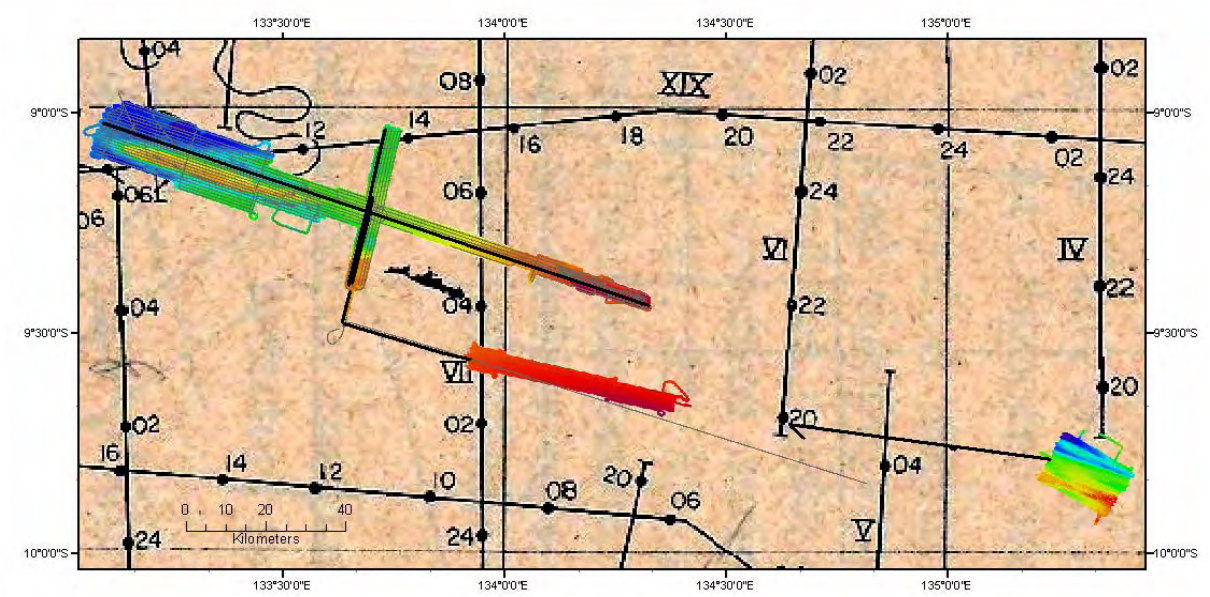

Figure 29 Multibeam bathymetry image of Areas B, C and D and locations of shallow seismic reflection profiles acquired previously in the area (from Jongsma, 1974).

Profile VII (**Figure 30**) extends through Areas C and D from north to south, while profile XIX (**Figure 31**) extends through Area C obliquely the from WSW to ENE. The unconformities S1, S2 and S3 interpreted by Jongsma (1974) can be correlated with the unconformities U7, U5 and U1 described in this current study (**Table 1**).

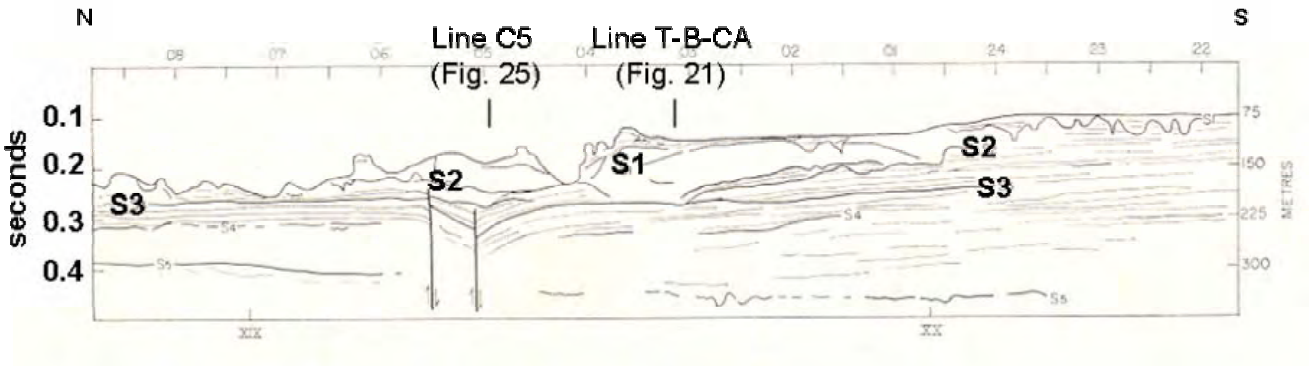

Figure 30 Line VII from Jongsma (1974) extending through Areas C and D.

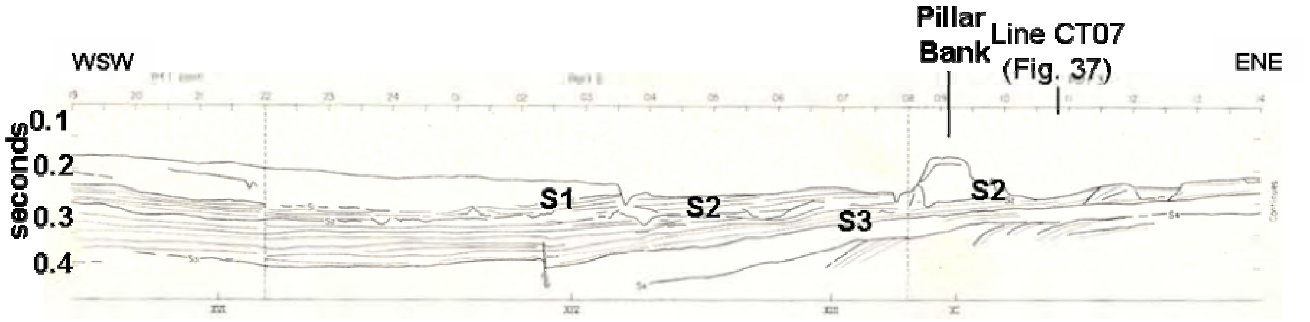

Figure 31 Line XIX from Jongsma (1974) extending through the western part of Area C. S3 and S2 interpreted by Jongsma correlate with U1 and U5 interpreted in this study.

In Jongsma (1974), S3 (U1 in this study) is described as a strong reflector which has been correlated with a Late Miocene to Early Pliocene unconformity at Ashmore Reef (Veevers, 1971) and on the North West Shelf (Jones, 1971). S3 is a major widespread erosional unconformity that may be related to regression in the Lower Pliocene. This event could also be associated with uplift of the margin during the collision of Timor and Australia which started in the Late Miocene to Pliocene (Keep and Moss, 2000).

Unconformity S2 of Jongsma (1974) (U5 in this study) was recognized throughout most of the Arafura region. Above this surface, Plio-Pleistocene sediments have been observed on the upper continental slope around Melville Island. Tectonic events are interpreted to have produced the unconformity S2, our U5, during folding in Timor and New Guinea, on the Arafura Shelf (Jongsma, 1974).

Unconformity S1 of Jongsma (1974), correlates with our U7, and is interpreted as Pleistocene. Unconformity U7 is overlain by Unit H, which has not been sampled, but its reflection character of laterally migrating channels, interbedded with tidal sand ridges, indicates a high-energy shallow-marine or near-shore environment, at the start of a transgression. This surface is observed to be regionally extensive across the whole of the Arafura Sea (Jongsma, 1974). However, it is difficult to define the age U7 age without direct dating of the units.

U9 in this study underlies the acoustically transparent surficial sediments of Unit J, and correlates with Jongsma's unconformity SH (Holocene surface). Sediment cores acquired during this survey sampled the uppermost part of the sediment package, down to 3-4 m, giving a range of radiometric dates between 34,770 ± 357.3 to 739 ± 78 years (Late Pleistocene-Holocene; **Figure 32**). These sediments show varying degrees of reworking and have been redistributed and redeposited due to a range of physical inputs including bioturbation, fluvial erosion / deposition and the impacts of changing sea level. Further discussion of these cores and their radiometric dates is included in **Section 3.3.4**.

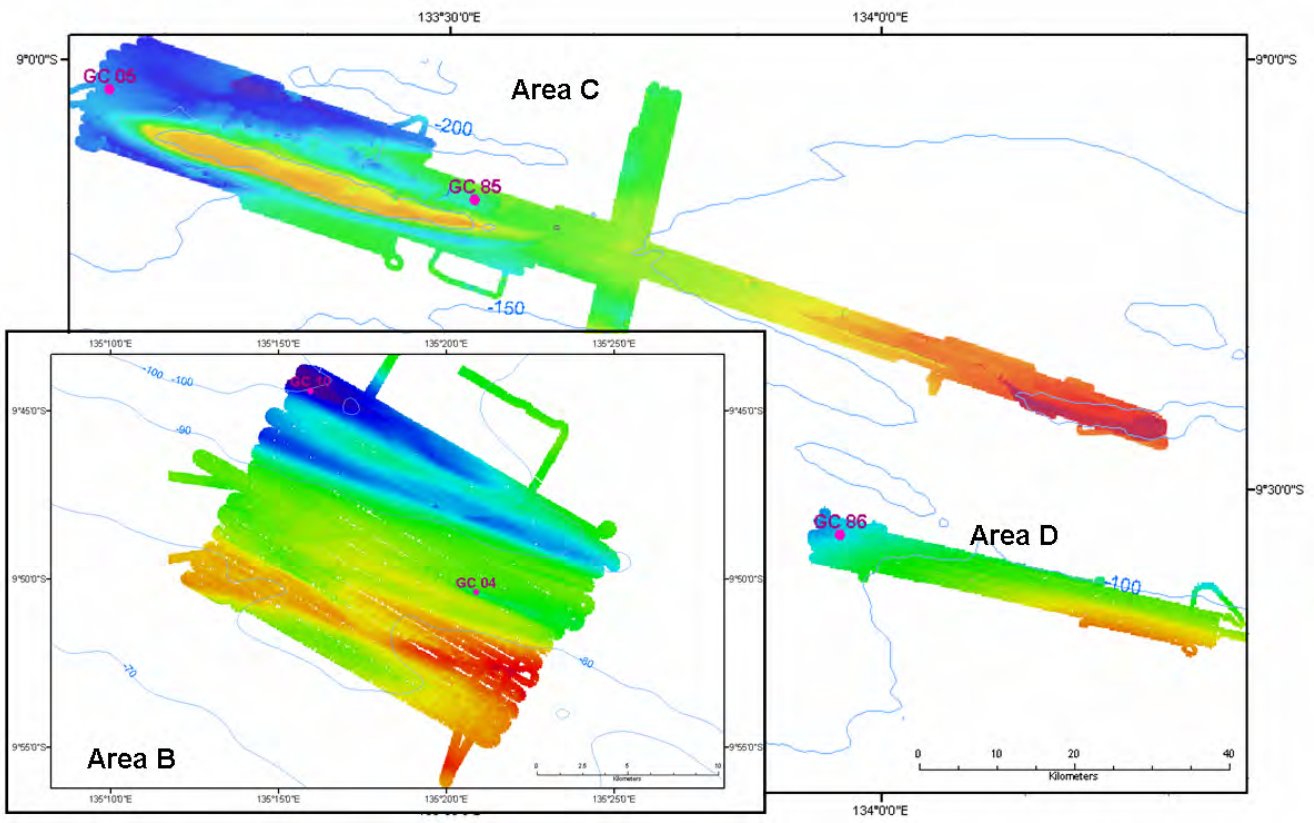

Figure 32 Location of sediment cores used for dating in Areas B, C and D.

The general distribution of the seismic stratigraphic units in the survey areas suggests that, after a major erosional event (U1), correlated with the onset of the collision of the Australian and Eurasian plates convergence, four or five transgression events occurred (Units B to G). Between these transgressive events, sea-level appears to have stabilized, allowing the deposition of thick prograding packages (15-50 m thick). Subsequently, these prograding sediment packages have been sub-aerially exposed and eroded. The nature and dating of these packages is uncertain. They can be attributed to global eustatic sea-level rises or regional tectonic events (sea-level curve from the Miocene; Haq et al., 1986; **Figure 33**, and in the Quaternary; Chappell and Shackleton, 1986; **Figure 3**). The deepest palaeo-shoreline at the LGM is widely taken as 120 m below the present sea-level (Yokoyama et al., 2001.). On the shelf off the north coast of Australia, evidence indicates a deeper palaeo-shoreline at 150-165 m (Jongsma, 1970; Veeh and Veevers, 1970). However, this difference could reflect the influence of local tectonic.

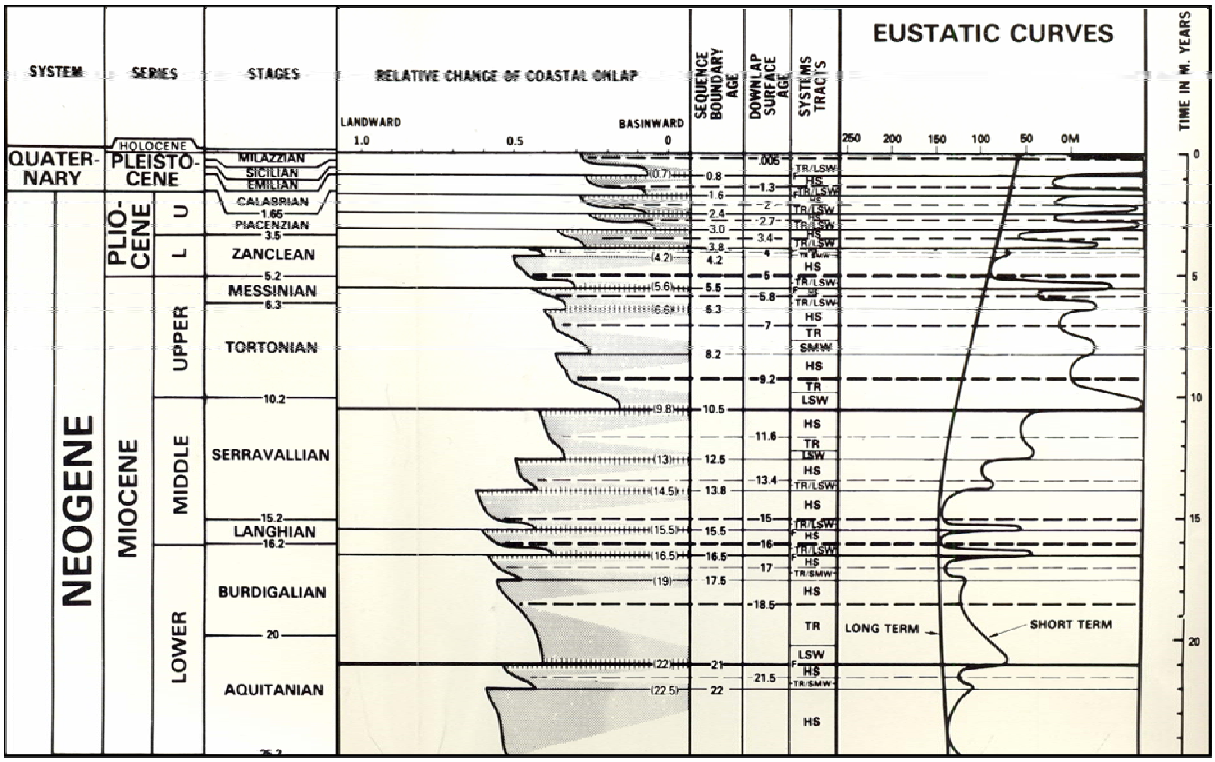

Figure 33 Late Cainozoic sea level cycle chart (after Haq et al., 1986).

A strong erosional event has subsequently incised all the prograding NW-dipping packages (Units B to I). This last major erosional surface (U9 in our study) incised the stratigraphy down to the oldest erosional unconformity in some places (U1, ~300 ms twt). This erosion occurred before the deposition of Unit J (Holocene) and most probably during the LGM (Pleistocene). Such erosion has shaped high-standing features, forming channels up to 40 m deep and banks with up to 100 m of relief. Some of this relief could be due to remnant erosion features and/or reef builds-up (**Figure 28**). Pillar Bank (**Figures 34 and 35**) appears to show cut and fill features at the base (above the unconformity U1), formed from either migrating fluvial or tidal channels. These features are overlain by thick progradational units and finally covered by possible reef builds-up on the top. The hard upper surface inhibits seismic imaging of underlying sediments, suggesting that Pillar Bank may have been sub-aerially exposed during the LGM.

The sides of Pillar Bank have been dredged and cored (282/038DR009; 282/039GC069; 282/053DR015) providing samples of packstone and limestone (**Figure 34**). Coarse-grained, semi-lithified limestone has also been sampled in the core catcher (282/017GC021) on the Eastern Bank in Area C (**Figures 36 and 37**). The nature of the samples suggests that Pillar Bank may be exhibit limestone karst structures towards the top. Strong tidal currents and waves generated in the sub-tidal environment may also have eroded these features. Unit J is deposited over a strong relief, formed after the erosional event U9.

3.6.7 Depositional model

Above the unconformity U1, Units B to I can be interpreted as four progradational cycles, each with a transgressive system tract (reef or basal transgressive sands, most developed within Unit H), followed by the dominant prograding facies. The dip of the prograding units suggests that they formed either in a submarine environment or as dramatic fluvial events forming low-stand deltas fed from the palaeo-Gulf of Carpentaria. However, the youngest Unit J (deeper water mud) has been deposited in a shallow marine environment. In between these progradational cycles, several periods of erosion appear to have occurred, probably during eustatic low stands (U1, U3, U5, U7 and U9). Many incised valleys are observed, in-filled by some fluvial facies.

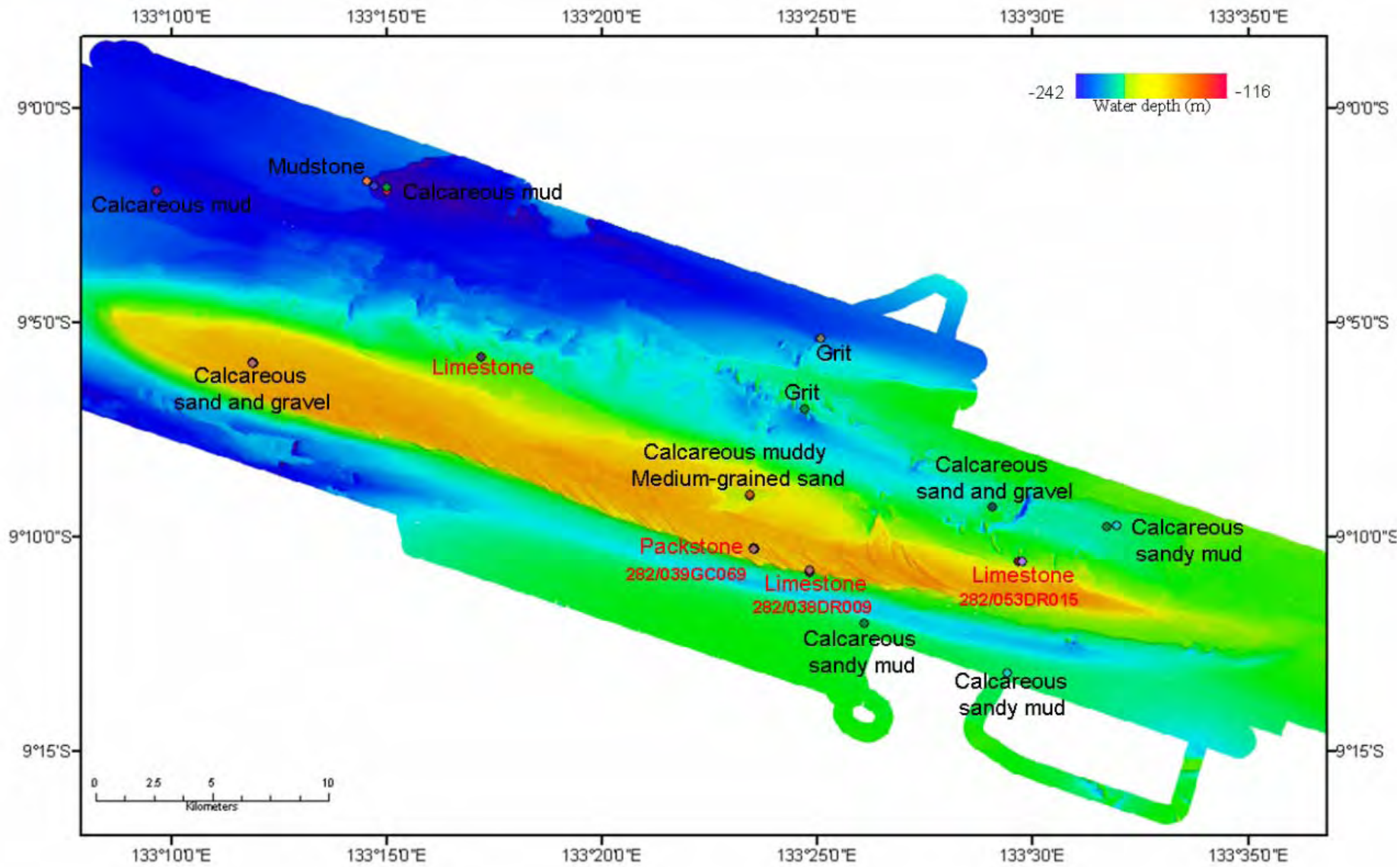

Figure 34 Nature of the sediments recovered over Pillar Bank, in Area C. Samples collected by grab and dredge.

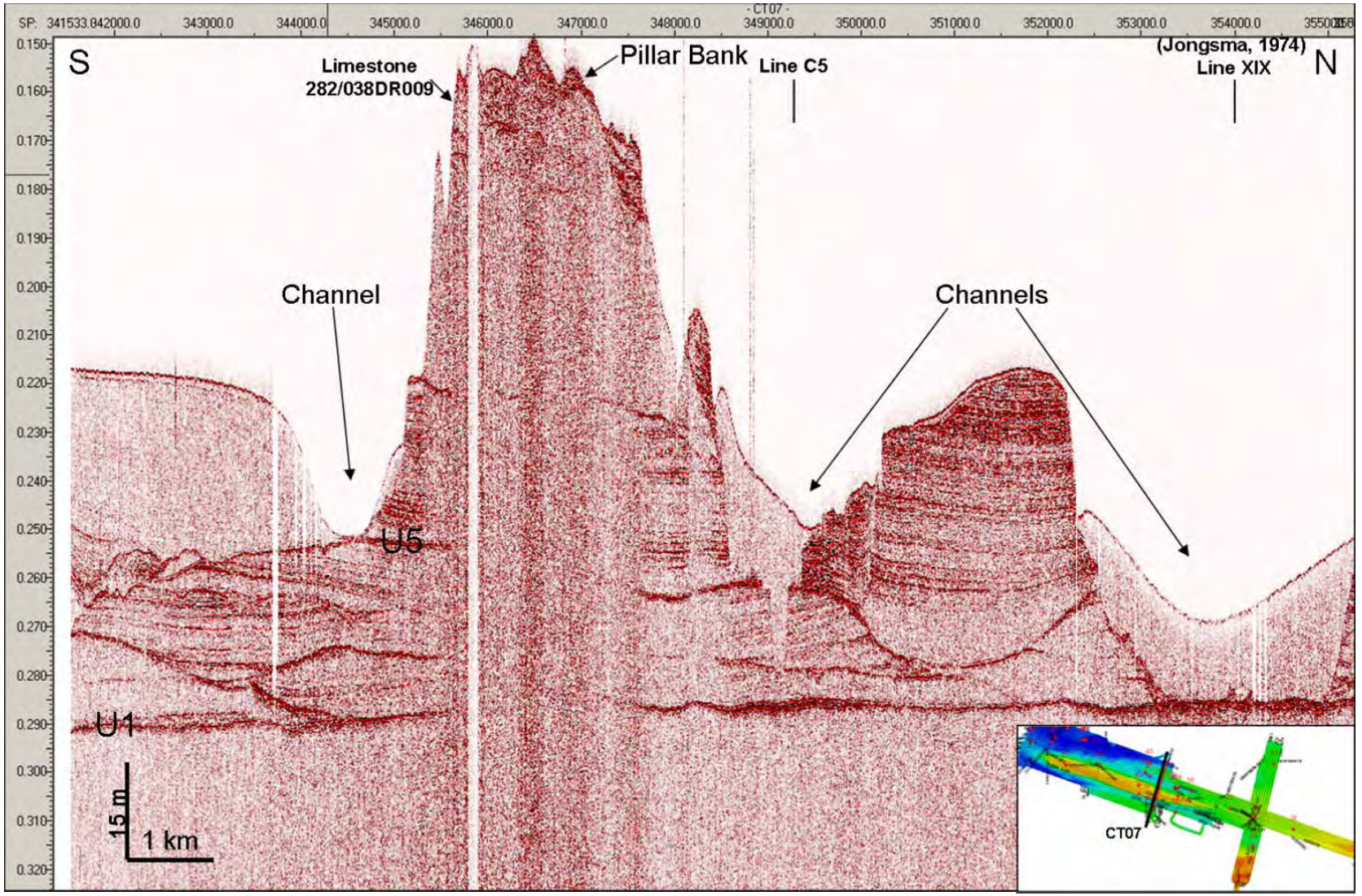

Figure 35 Sub-bottom profile cross-line CT07 showing the N-S structure of Pillar Bank incised by channels, to the north and the south. Pillar Bank is composed, from the base to the top, of interfluve deposits from a palaeo-fluvial system (between U1 and U5), covered by thick progradational packages (above U5) and with possible carbonate build-ups at the top. Limestone was dredged (282/038DR009) on the southern escarpment of Pillar bank.

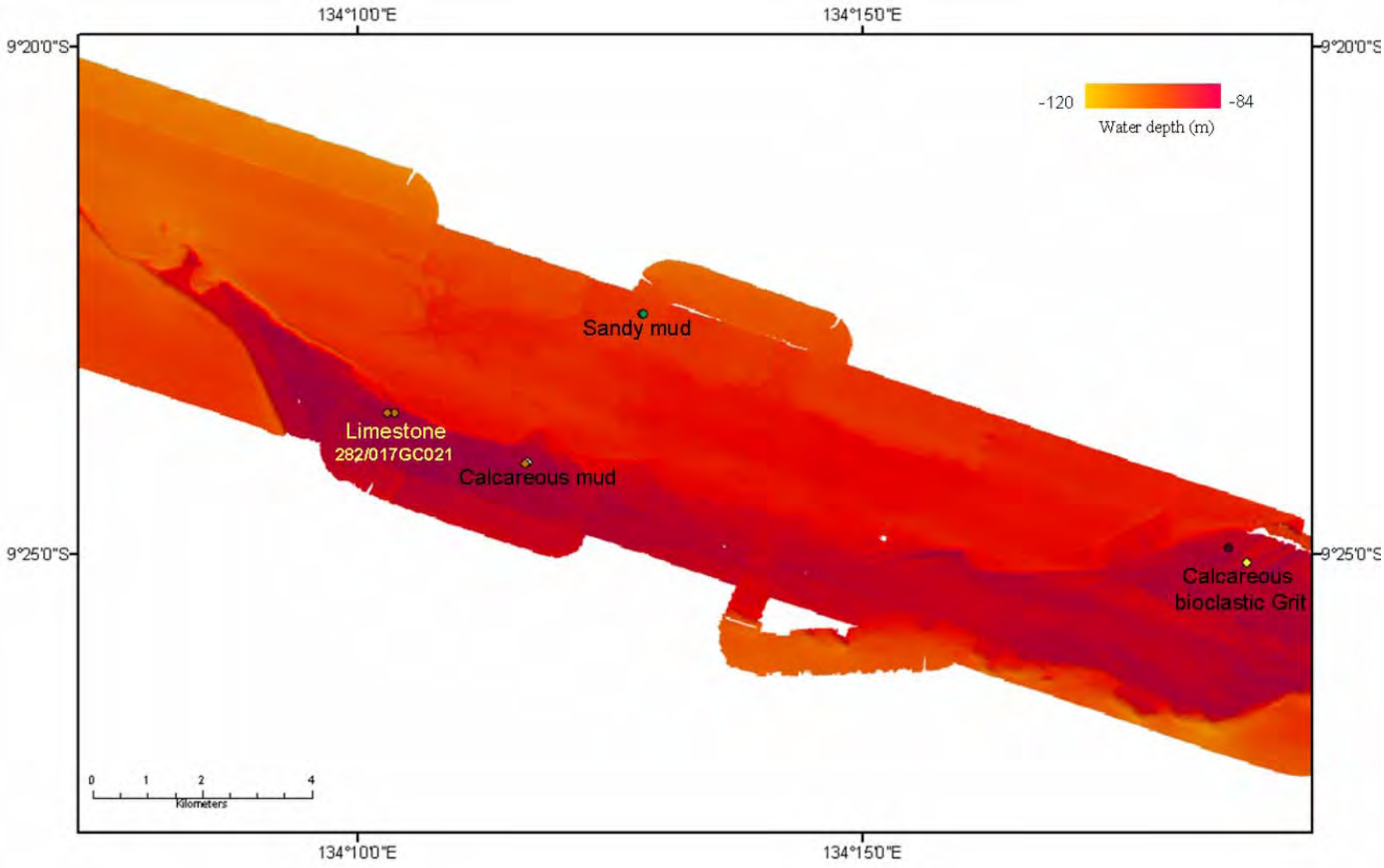

Figure 36 Nature of the sediments recovered over the Eastern Bank, in Area C. Samples collected by grab and gravity core.

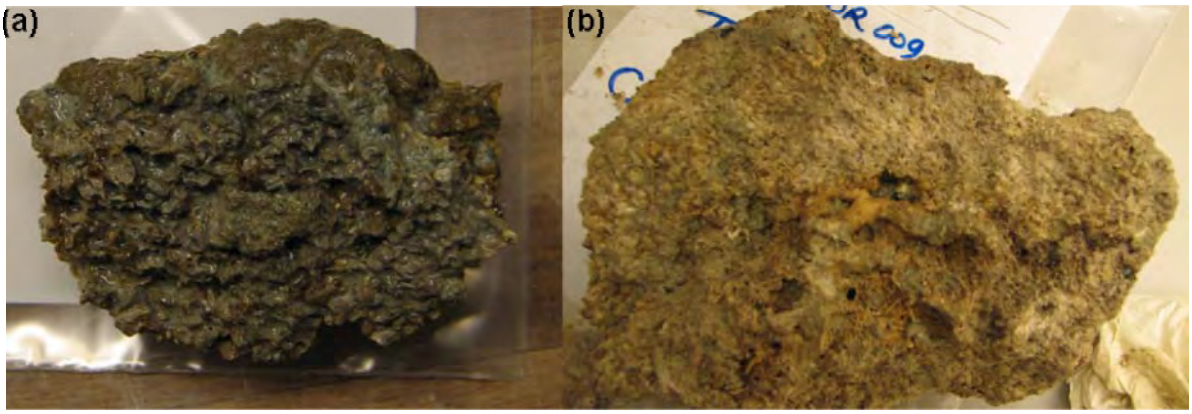

Figure 37 (a) Limestone sample from site 17 (282/017GC021). (b) Limestone sample from site 38 (282/038DR009). Samples location is shown on **Figures 34 and 35**.

These different units can be tied to the Quaternary sea level curve where:

- Unit J was deposited during the latest transgression (from 19 000 years BP until present);

- Unconformity U9 corresponds to the major erosional surface occurring during LGM;

- Unit I corresponds to a small scale regression around 35 000 years BP, as suggested by the oldest carbon dates collected above Unit I (site 64, see **Figures 9 and 12**).

- The older units cannot be tied to the sea level curve without constraint on their ages.

3.7 GEOCHEMISTRY

A range of samples were collected for gas and lipid geochemistry analysis. One of the primary aims of the survey was to identify areas of gas in near-surface sediments and collect sediment samples to allow the analysis of pore-space gases. This was achieved using gravity cores taken at specific sites. Site selection was undertaken using survey data, including side-scan sonar, multibeam and previously collected seismic data. Targets were chosen based on the identification of features, such as pockmark fields, faults to sea bed and geophysical attributes that are often associated

with shallow gas, including enhanced reflections, reverse polarity, and acoustic blanking (see **Section 3.10**).

At each site targeted for head-space gas analysis, replicate samples from within each core were taken for lipid biomarker extraction. Therefore, sampling within each core involved removing sediment for both pore space gas and lipid extraction at similar levels to allow comparison of results. Generally two to three samples were taken within each core at metre intervals for geochemical analysis. As samples were collected starting from the base of each core, and each core varied in length, the depth of sampling varied between cores. Stratigraphic cores were also taken at most sample sites but they have not been analysed for geochemistry.

Grab samples were also collected at each site and several have been analysed for lipid biomarkers to provide geochemical signatures for the surface sediments. These signatures can be compared to sub-surface core material to help understand environmental change. Only 4 grab samples were analysed during this study as these types of sample were often heavily bioturbated and contained components of macro-fauna, such as shell material, which can strongly influence recent faunal lipids and therefore dominate the sedimentary biomarkers.

3.7.1 Head Space Gas Analysis

Samples collected for pore space gas were transported frozen and analysed by TDI-Brooks, College Station, Texas, USA. Concentration data (ppm) was reported for C_1-C_5 hydrocarbons and CO_2 for one set of replicate tins. The second set of tins was retained at Geoscience Australia at -80°C to provide a back-up in case of shipping problems or sample loss.

Over the survey area, methane (C_1) and wet gas (C_2 to C_5) were generally found to be in very low abundance with most samples containing less than 10 ppm methane and much lower levels of wet gas components. Only four sample sites had methane levels in excess of 100 ppm (**Figure 38**).

Abundant pockmarks up to 10m across and ~1m deep were identified on side-scan sonar and sub-bottom profile data, with a field density of up to 350/km^2. The highest density pockmark fields were found above palaeo-channels filled with organic-rich Holocene muds. For example, south of Pillar Bank, the Sites 50 and 51 provided three separate cores with elevated methane levels (**Figure 39**). Below 1 to 2 m depth, samples from these cores produced methane levels of 100 to 1,200 ppm. The gas is interpreted to be microbially derived from *in situ* methanogenesis due to the low levels of wet gas components (ethane, propane and butane levels all below 1ppm).

At Site 31 in Area C, methane levels in 3 cores ranged between 400 and 700 ppm for samples collected below 2 m depth (**Figure 38**). The ethane levels and other wet gas components were all below 1 ppm. The gas sampled from this level is also interpreted to be microbially derived because of the low levels of wet gas relative to methane. Near-surface sediments at this site were heavily pockmarked and also consisted of Holocene mud.

The highest methane concentrations were found at Site 22 at the eastern end of Area C (**Figures 38 and 39**). Below 2m depth, methane concentrations ranged from 42,000 to 71,000 ppm in three cores. As with other locations, all ethane levels were below 1 ppm. At this site methane concentrations were high enough to obtain $\delta^{13}C$ measurements for methane, which was found to be -95.9‰. The isotopic composition, together with the very low wet gas concentration levels, indicates that the gas at this site is microbially derived. As with Sites 31, 50 and 51, Site 22 is characterised by a thick Holocene mud package (**Figure 39**).

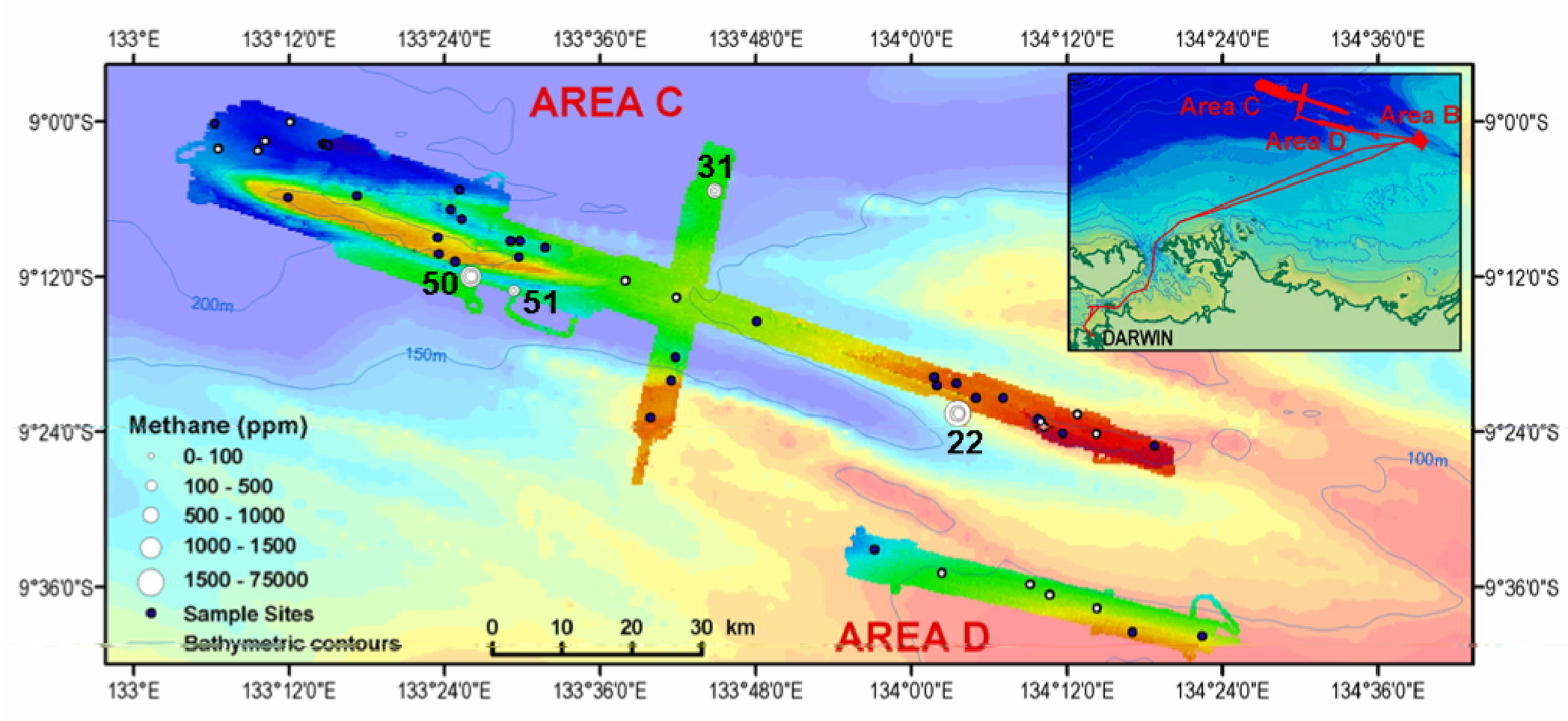

Figure 38 Methane concentrations plotted on the multibeam bathymetry image of Areas C and D.

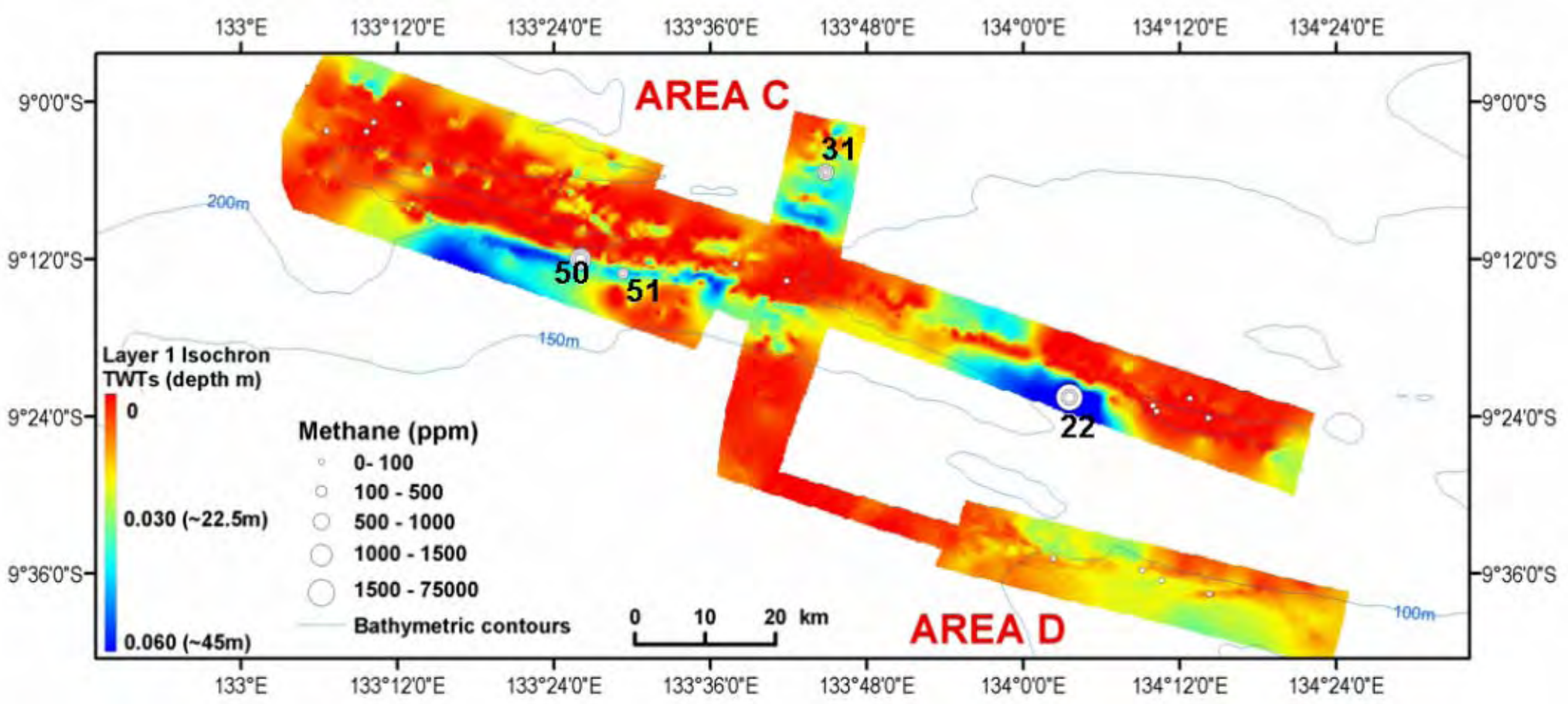

Figure 39 Isochron map of Unit J showing the samples with highest methane concentrations related to thick sections of Holocene mud.

Despite the high gas concentrations, the surface sediments at Site 22 did not appear to be heavily pockmarked based on side-scan sonar data. Although hydrogen sulfide (H_2S) levels were not measured, cores taken at all the sites mentioned above all had a strong H_2S smell when opened for sampling. This is consistent with high levels of bacterial sulfate reduction (BSR), either related to anaerobic oxidation of methane (AOM) or break-down of sedimentary organic matter.

Much of the western half of Area D is intensely pockmarked. The pockmarks were observed in side-scan sonar data and were generally 5-10 m in diameter and 1-2 m deep. Within the areas of intense pockmarking the abundance was ~350/km^2, compared to ~ 30/km^2 outside this pockmark field. Sub-bottom profiles across the pockmark field also show an irregular pitted sea bed due to pockmarks formed across the surface. The area of intense pockmarks partly coincides with a mud-filled Holocene channel. However, pockmarks are observed outside of this channel, where the mud package is thin, and in some areas where the mud is thick, pockmarks are rare. The high density of pockmarks provides evidence of fluid flow (either gas or water).

Core penetration within the pockmark field of Area D was greater than any other area of the survey, with recoveries between 3-4 m. Methane levels were all below 10 ppm at Sites 58, 59 and 60, where the Holocene mud package was thickest. These values are similar to background levels observed at other sample sites in Area C. However, some samples at Sites 58 to 60 taken between 2 -4 m depth had anomalously high CO_2 levels with values ranging from 18,000 to 62,000 ppm. The $\delta^{13}C$ values of the CO_2 measured in these cores were around -32‰, indicating that the carbon was derived from oxidation of an organic substrate. This must be related to Anaerobic Oxidation of Methane (AOM) and/or the oxidation of *in situ* organic matter. The high density of pockmarks and the high CO_2 levels suggest that this is

an area of very active fluid flow and also rapid carbon oxidation within the sub-surface.

3.7.2 Surface Sediment Lipid Geochemistry

Four grab samples taken from different water depths in Areas C and D were processed and analysed for their lipid contents. The sediments are characterized by a high proportion of biomarkers derived from marine sources, predominantly of algal origin (**Figure 40**). Sterols, long-chain alkenones and linear alkanols dominate the biomarker distributions. Differences in composition observed between samples indicate that a diverse biota contributes to the present-day organic matter.

Grab sample 282/061GR082A contains an exceptional amount of cholesterol (**Figure 40a**), which is likely to reflect a large input of macrofauna to the sediment as this sterol is the major sterol in most marine animals (Volkman, 1986). The elevated amounts of C_{27} sterols are consistent with the original sediment containing abundant shelly material. This sample was recovered in shallow water (~90 m) in Area D.

Cholesterol and cholestanol were also detected in the other three grab samples in Areas C and D, but in much lower abundances. Dinosterol, produced predominantly by dinoflagellate algae (Boon et al., 1979; Robinson et al., 1984), is the major constituent in the mixtures of sterols and stanols found in these grabs, suggesting that dinoflagellates were an important component of the phytoplankton community at the time of deposition. However, the enhanced signal of dinosterol may also be partly related to its greater resistance to degradation compared to A-ring-desmethylsteroids (Harvey et al., 1989). The diversity of steroids in the surface samples indicates inputs from a variety of marine organisms, although some, such as 24-ethyl-5α-cholest-5-en-3β-ol (sitosterol), may derive from higher plants (Volkman, 1986; Volkman et al., 1998). However, pentacyclic triterpenoids derived from higher

plants are only found in very low amounts in surface samples. This suggests that the sitosterol is predominantly derived from algal sources in these surface sediments.

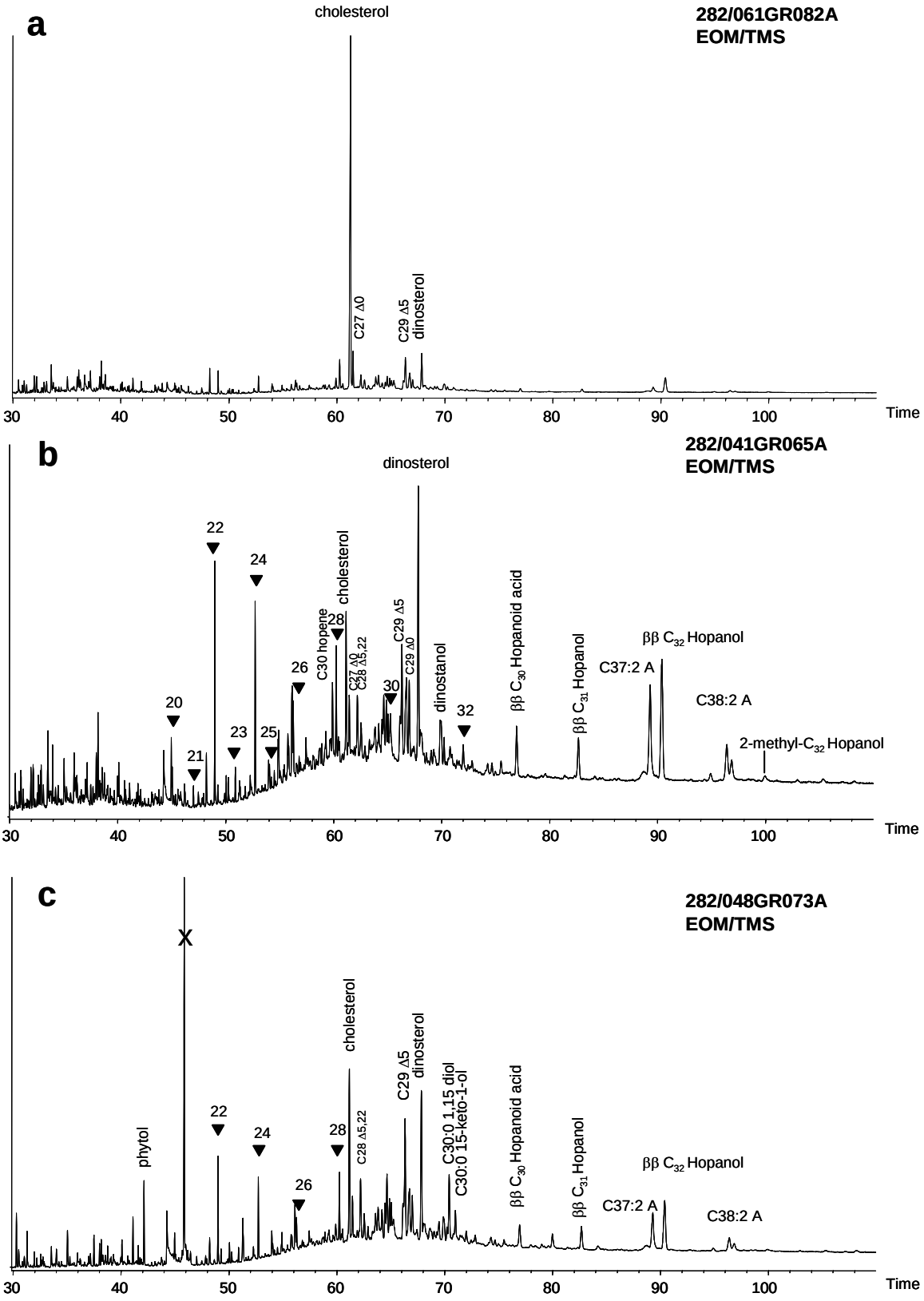

Figure 40 Reconstructed ion chromatograms of the silylated extractable organic matter fractions from surface samples a) 282/061GR082A, b) 282/041GR065A and c) 282/048GR073A.

Diunsaturated C_{37} and C_{38} ketones derived from haptophyte algae (Marlowe et al., 1984; Brassell et al., 1981; Conte et al., 1994) are substantial components of the total biomarker distributions. C_{37} alkenones are commonly used to estimate past sea surface temperatures based on the ratio of tri- to di-unsaturated C_{37} alkenone, which increases as surface water temperature decreases (Brassell et al., 1986). However, the applicability of this ratio is restricted to the temperature range 5-27°C (Herbert, 2003; Pelejero and Calvo, 2003), which limits the use of these compounds for SST reconstruction in warm tropical waters. The triunsaturated C_{37} alkenone is absent in all the surface samples analysed due to the high SST in this region.

Bacterially derived hopanoids, homohopanol and bishomohopanol, were detected in all the surface samples analysed in relatively high abundances. The presence of 2-methylbishomopanol is probably related to a cyanobacterial contribution to the sediments (Summons et al., 1999).

Linear alkan-1-ols contribute significantly to the biomarker distributions of the grab samples. Their distributions range from C_{12} to C_{32} and present a bimodal pattern maximizing at C_{22} for the first mode and at C_{28} for the second, with an even-over-odd predominance observed throughout. The strong even-over-odd predominance of *n*-alkanols in the C_{26}-C_{32} range is attributable to terrigenous plant input (Eglinton and Hamilton, 1967; Pancost and Boot, 2004). The high relative abundance of C_{22} *n*-alkanol, compared to other *n*-alcohols, suggests a primarily marine origin, plausibly from algae (Volkman et al., 1998). It is the major alcohol in Arabian Sea sediments (Smallwood and Wolff, 2000) and in a phytoplankton sample from the Baltic Sea (Morris and Brassell, 1988) supporting the idea that it has a marine source.

C_{30} 1,15-diol and 15-keto-1-ol were present in only two surface samples 282/021GR036 and 282/048GR073A (**Figure 40c**). Even though their source is still a matter of debate, these compounds are likely to represent microalgal biomarkers. Eustigmatophyte microalgae from the genus *Nannochloropsis* have been found to biosynthesize long-chain alkyl diols but their distributions differ quite substantially from those observed in marine sediments (Volkman et al., 1992; Versteegh et al., 1997), and consequently another yet unidentified algal source has been suggested (Gelin et al., 1999). Ketols have never been found in organisms and are therefore thought to derive from the oxidation of the corresponding diols (Ferreira et al., 2001).

Lycopane appears to be present in all surface samples. It is resolved from the linear alkane *n*-C_{35} on the 60 m DB1 column, and easily detected by means of the *m*/*z* 85 ion current. Although lycopane is often found in Recent marine sediments (Brassell et al., 1981; McCaffrey et al., 1991; Farrington et al., 1988), its origin remains uncertain. Intact lycopane has been detected in sponges of the class Hexactinellida (Thiel et al., 2002) and it has been attributed to sponge symbionts, possibly archaea which are thought to be a likely source for lycopane (Brassell et al., 1981). Underwater video footage and analysis of grab samples identified this class of sponge as common across the survey area. Marine phytoplankton has also been suggested as an alternative source for lycopane in marine environments based on stable carbon isotopic composition and concentration profiles in oceanic water columns and shallow cores (McCaffrey et al., 1991; Wakeham et al., 1993). However, no marine algae have yet been analysed that produce this compound. Potential precursors of lycopane in recent settings, such as lycopadienes, have so far only been found in freshwater microalgae Botryococcus Braunii (Metzger and Casadevall, 1987). Lycopane was detected in relative low abundances when compared to linear alkanes indicating oxic conditions of deposition.

Marine/agal inputs dominate over a minor contribution of land-plant material in the extractable organic matter in surface sediment grabs taken across the survey area. This pattern is observed in sample sites in a variety of water depths (80 to 230 m) and distances from the coast (250 to 350 km), and indicates that organic input to surface sediments across the region is dominated by marine sources. A strong metazoan contribution is recognized by the abundance of cholesterol in grab 282/061GR082A, consistent with the presence of shelly material within this sample.

3.7.3 Sub-surface Lipid Geochemistry

3.7.3.1 Area D samples

Area D is a relatively shallow (70-80 m) part of the shelf. The sea bed and associated biota indicate a generally calcareous medium- to fine- grained sand through to a sandy mud, and includes minor amounts of mollusc and foraminifera fragments. Video footage shows occasional ripples and burrows, and a range of biota, including octacorals, sea pens and small fish. Sub-bottom profile data, collected during the survey, show that this region was exposed during previous low stand periods and a channel developed running NE-SW (**Figure 39**). The channel filled with mud during the Holocene and the entire area was draped by soft muds during the last transgression. Initial ^{14}C-dating from a sediment core taken in this area indicates that accumulation rates have been rapid, up to 33 cm/1000 yrs (**Figure 16**).

Two end-member biomarker distributions are identified in cores from Area D. The upper samples (0.5 to 2.5 m) present distributions fairly similar to extracts analysed from surface sediment grabs, described above. In contrast, the deepest samples (>2.5 m) are characterised by a strong terrigenous input, as illustrated in **Figure 41** for core 282/060GC095. The main difference between the upper core samples and the surface samples is the higher proportion of long-chain alkyl diols and ketols, with the C_{30} 1,15-diol and 15-keto-1-ol dominating the overall biomarker distribution. C_{32} 1,15-diol and 15-keto-1-ol were also detected along with C_{28} 1,14-diol. Unlike 1,15-diols,

the 1,14-diols are not produced by eustigmatophyte algae and diatoms are a likely biological source for these compounds (Sinninghe Damsté et al., 2003b). The higher proportion of long-chain diols and ketols in core samples, as compared to surface samples, may arise from their enhanced resistance to oxic degradation, as they have been shown to be more refractory than other compound classes (alkenones, steroids and triterpenoids) to post-depositional diagenetic processes (Hoefs et al., 2002). Among other contributors to the biomarker distributions are diunsaturated C_{37} and C_{38} alkenones and linear alkan-1-ols, the latter displaying the same bimodal pattern described for the surface samples with an unusual abundance of C_{22} and C_{24} homologues. As with the grab samples, a complex suite of sterols and stanols is observed with a significant contribution of dinosterol. A homologous series of *n*-fatty acids is also identified.

In most of the cores from Area D, the biomarker distribution of the deepest core samples differs significantly from the upper samples and is characterised by a strong input of terrigenous organic matter, typified by a strikingly large amount of taraxerol (**Figure 41c**). Taraxerone, a diagenetic product of taraxerol, is also present in minor amounts. On average, taraxerol abundance increases by a factor of 4 at depths below 2.5 m in cores from sites 59, 60 and 61 (**Figure 42**). This down-core increase in the relative input of terrestrial to marine organic matter sources, and the parallel drop in algal contribution, is illustrated by the down-core decline of C_{30} 1,15-diol abundance (**Figure 42**), as well as by the increase in the ratio of taraxerol to dinosterol (T/D ratio) (**Figure 43**).

The bimodal pattern observed in the linear alkan-1-ol distributions of the shallow samples (0 to 2.5 m) with the predominance of the C_{22} homologue is replaced in the deeper core samples (>2.5 m) by a unimodal distribution with a maximum at C_{28} and a strong odd-over-even predominance in the range C_{22}-C_{34} (**Figure 44**). Additionally, high molecular weight linear alkanes displaying an odd-over-even predominance in

the range C_{25}-C_{33} become relatively much more abundant in the deepest core section and are easily detected in the total ion chromatograms (TIC) as evidenced in **Figure 41c**, whereas they are hardly visible in the TICs of the upper core samples (**Figures 41a and 41b**). These features are an additional argument supporting significant contributions from terrestrial higher plants in the deeper core samples (>2.5 m) of Area D (Pancost and Boot, 2004).

The strong terrestrial input signal appears to decrease towards the north-west (site 58, location in **Figure 43**) where the buried channel shallows, and is strongest at sites where the channel fill is thicker. Indeed, the relative increase of the taraxerol in the deepest core samples at site 58 is not as sharp as in the other sites (**Figure 43**) and the distributions of linear alkanols in the deepest samples present a bimodal pattern (**Figure 44**) similarly to the one in the upper samples.

3.7.3.2 Palaeo-environmental Change and Mangrove Inputs

Taraxerol has been used as a proxy for mangrove inputs (Sikes et al., 1991; Versteegh et al., 2004; Scourse et al., 2005), as it occurs abundantly in mangrove leaves, in particular in leaves of the genus Rhizophora (Killops and Frewin, 1994; Versteegh et al., 2004). Taraxerol occurs in a wide variety of higher plants along with other higher plant biomarkers, such as long-chain odd *n*-alkanes, and even *n*-alkanol homologues, whereas the latter compounds constitute a minor portion of Rhizophora leaves. Therefore, the ratios Taraxerol/*n*-C_{29} or Taraxerol/*n*-C_{28}-ol have been developed by Versteegh et al. (2004) to identify substantial mangrove contributions. The fact that taraxerol predominates largely over *n*-alkanols and *n*-alkanes in the lowermost unit of Area D cores and is detected along with β-amyrin and germanicol, also known as Rhizophora leaf wax constituents (Killops and Frewin, 1994), point to a mangrove source for these compounds.

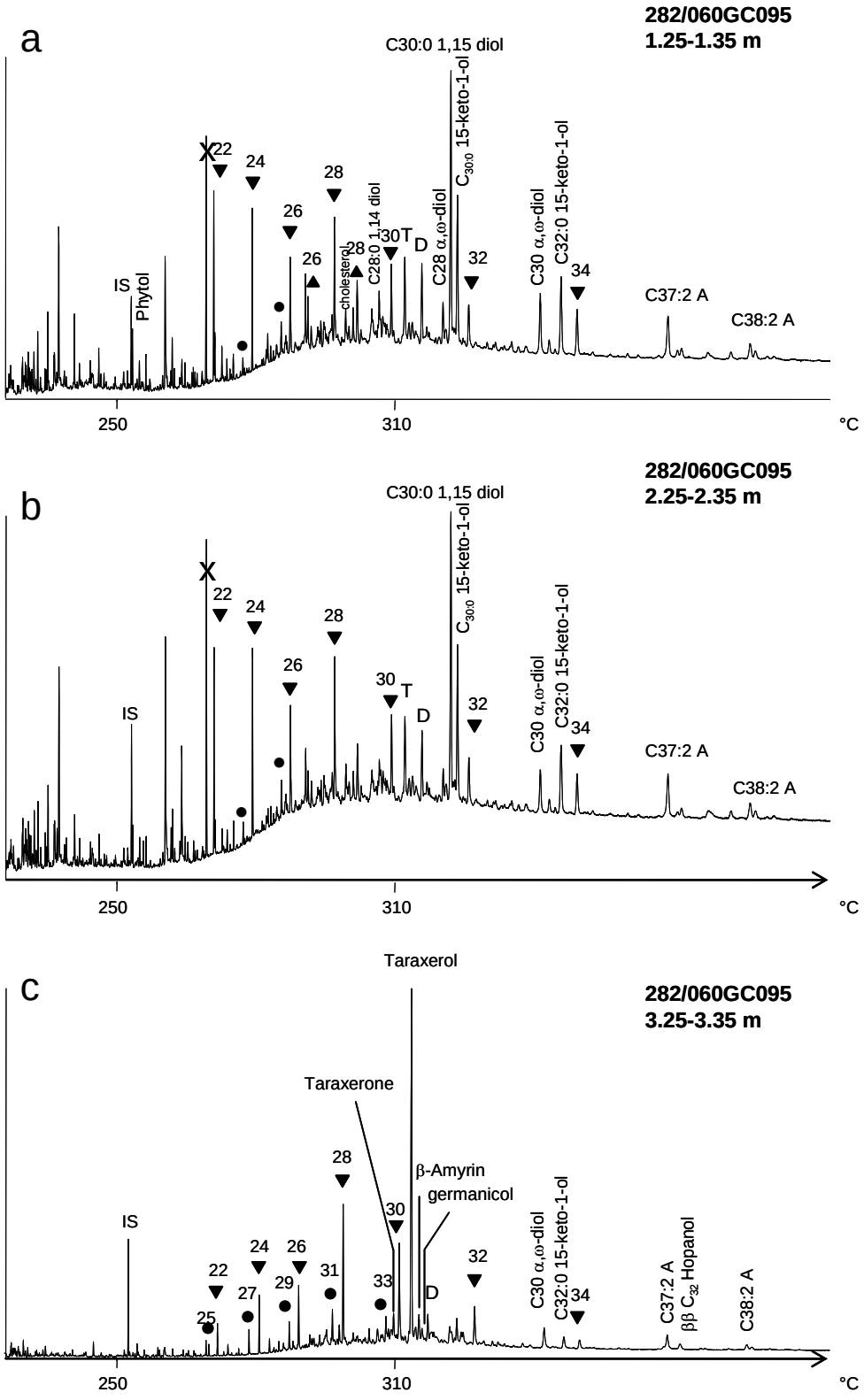

Figure 41 Total ion chromatograms of the silylated extractable organic matter fractions from samples of core 282/060GC095. ▼ : *n*-alkan-1-ols; : ▲ : fatty acids; ●: n-alkanes; T: Taraxerol; D: Dinosterol; A: Alkenones; IS: internal standard.

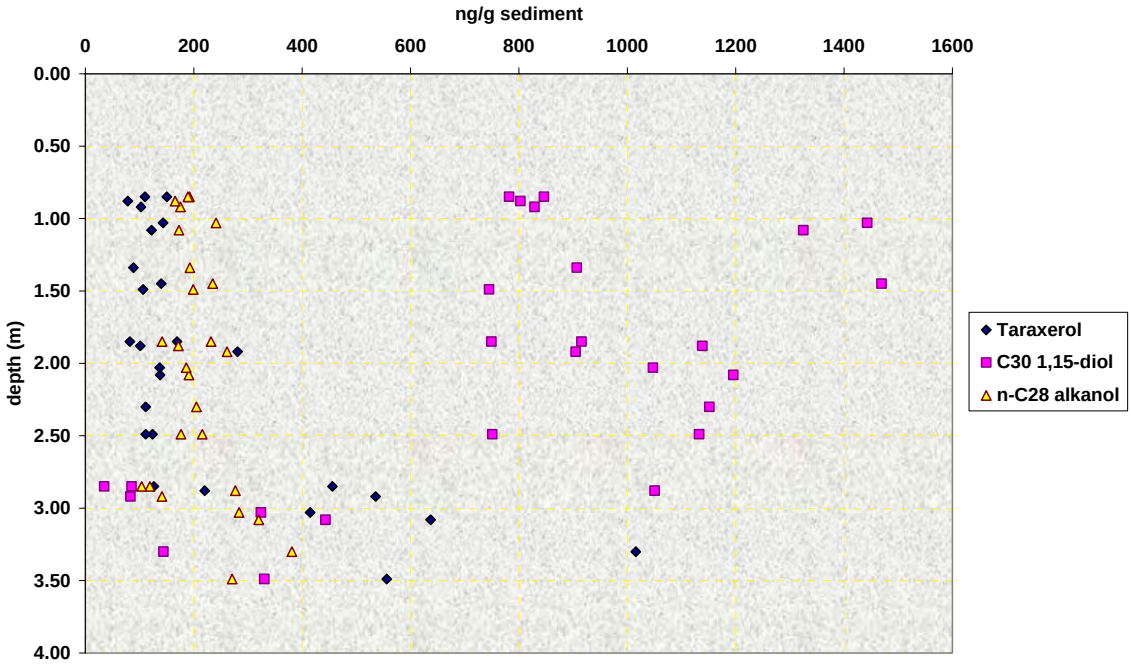

Figure 42 Profiles of taraxerol show an increase with depth and a decrease for C_{30} 1,15-diol concentrations in cores from sites 59 to 61, in Area D.

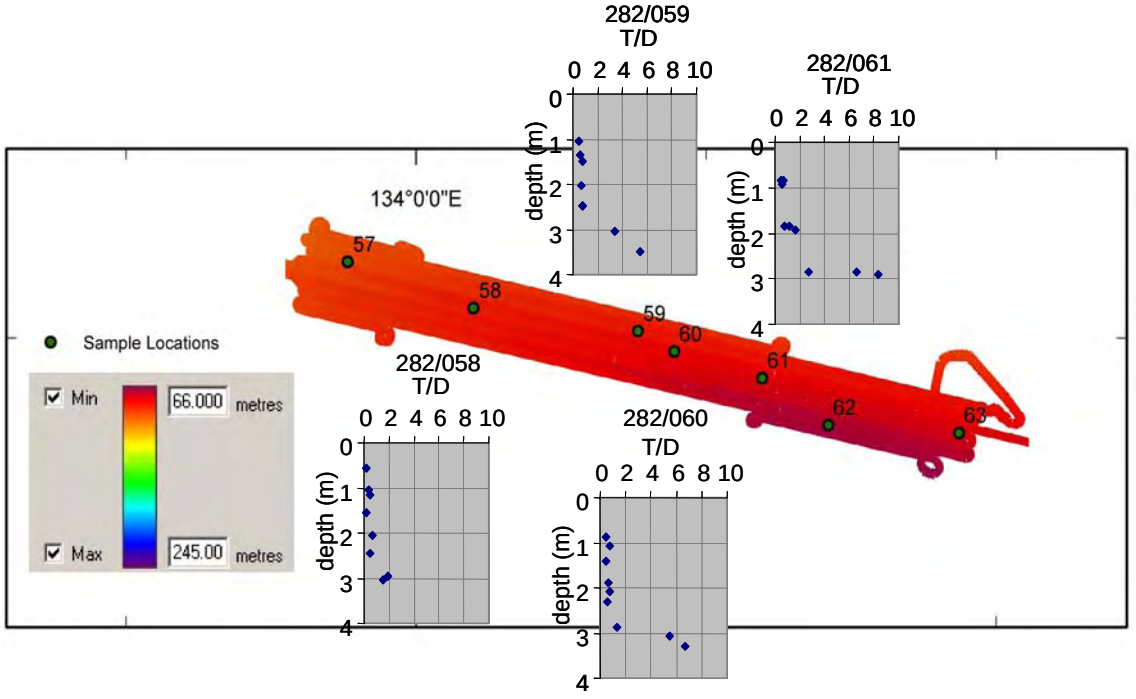

Figure 43 Depth profiles of taraxerol to dinosterol ratios (T/D) in cores from sites 58 to 61, in Area D.

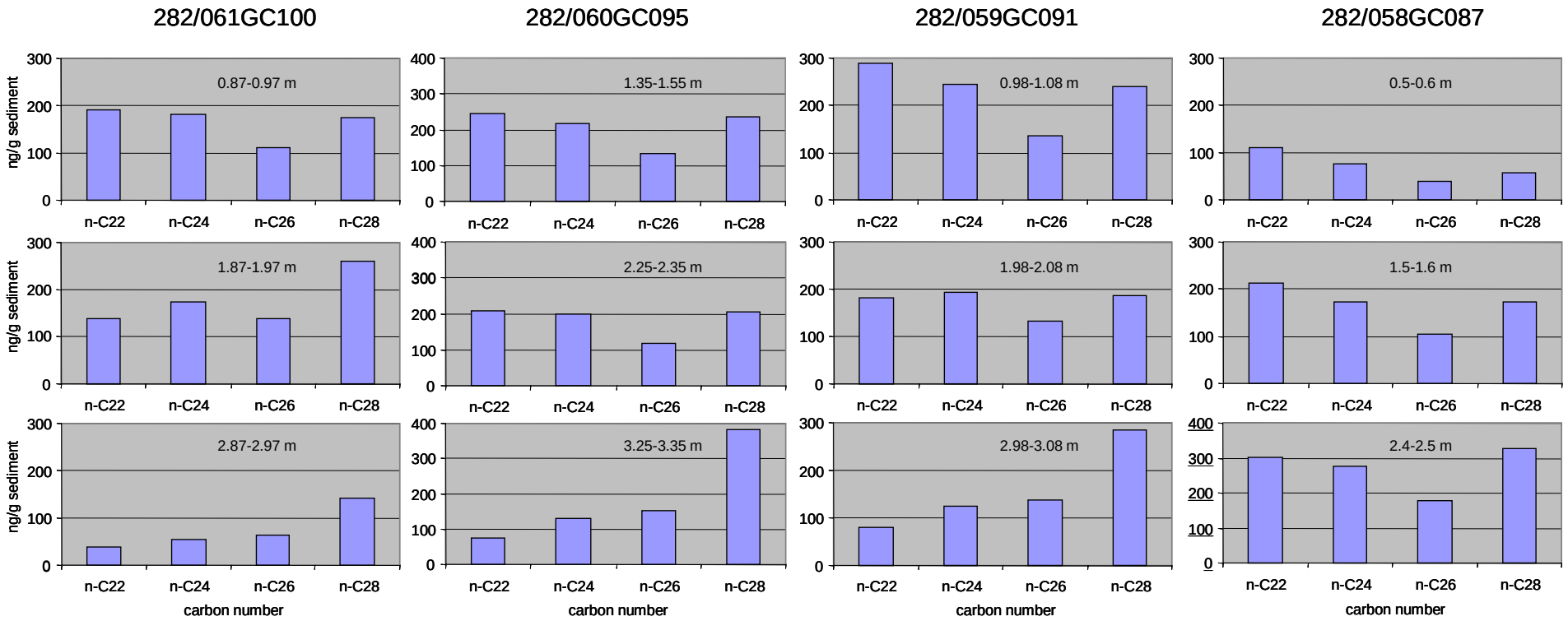

Figure 44 Distributions of even-numbered linear alkan-1-ols in the range C_{22}-C_{28} for representative cores at sites 58 to 61, in Area D.

Pollen records in sediments underlying coastal and estuarine plains of northern Australia attest that mangrove forests were widespread and dominated by Rhizophoracae at the end of the post glacial marine transgression when sea-level stabilized around 6000 years BP (Woodroffe et al., 1985). After 6000 years BP mangroves were replaced by floodplains supporting freshwater wetland vegetation dominated by grasses and sedges (Woodroffe, 1993). Radiocarbon dates indicate an age of ~10,600 years BP for the base of Core 282/057GC086, the only dated core in Area D, which corresponds to a period before the LGM. This core was not taken within the mud-filled Holocene channels and may not represent the depositional phase of channel fill. However, mud taken from below 2.5 m in cores collected within the Holocene channel is derived in part from mangrove forests across the region which flourished before 6000 years BP. Taraxerol is also present in the upper samples, but to a much lower extent, suggesting a small contribution from mangroves to these sediments. This may reflect the continued reworking of older mangrove muds or more recent material derived from the present-day coastal zone.

3.7.3.3 Area C samples

This survey area was further off-shore than Area D and much of the eastern part of Area C is composed of a lithified carbonate structure, called Pillar Bank. On either side of this bank palaeo-channels developed during a regression and then filled with mud during the Holocene transgression. Review of sediment samples and video footage shows that sediments are generally muddy fine- to medium-grained sand and gravel in the shallow south-eastern part of Area C, with relatively high amounts of biota and bioturbation at some sites. Sediments on the submarine plain in the central part of Area C are generally muddy sand to sandy mud, with video footage showing bioturbated soft sediment and occasional hard surfaces. Sampled sediments on Pillar Bank were sand and gravel, with areas of cemented hard-grounds and video footage showing biota covering ~5 - 10% of the sea bed. The deeper channel to

the northwest of Pillar Bank contains calcareous mud and muddy sand, and video footage shows heavy bioturbation and large burrows, with occasional areas of rocky substrate.

The extractable organic matter in Area C core samples presents distributions similar to those described above, with an additional end-member encountered mostly in the eastern, shallower end of Area C (80 – 120 m). This end-member is characterized by a high proportion of C_{37} and C_{38} alkenones together with a relatively low abundance of alkyl-diols and alkyl-ketols and a highly complex steroid mixture as shown in **Figure 45**. This sterol distribution differs substantially from those described so far. Distinctive features include a high abundance of stanols and ketosteroids as compared to sterols. In core 282/018GC025, the ratio of cholestanol to cholesterol jumps from 0.3 in the upper samples at 0.53-0.63 m and 1.53-1.63 m to 6.6 in the lower sample at 2.53-2.63 m (**Figure 45**). Stanols and steroidal ketones may derive from direct biogenic inputs (Volkman et al., 1998) or from microbial transformation processes from sterols (Wakeham, 1987). The latter alternative is more likely to account for the occurrence of these compounds in samples from Area C. Steroidal ketones have been shown to be intermediate products in the reduction of stenols to stanols (Gagosian et al., 1980). The presence of abundant diagenetic steroids is consistent with the core material being older than that sampled in Area D at equivalent depths (**Figure 46**).

Both end-members noted in Area C are dominated by marine biomarkers but reflect changes in the dominant algal inputs. The more sterol-, diol- and ketol-dominated samples reflect a stronger diatom and dinoflagellate input to the sediments and this is more commonly observed in the upper, more recent, parts of cores taken in this survey area. The stronger alkenone signal is developed deeper in most of the cores and reflects a stronger input from Haptophyte algae. On longer time scales than sampled by our cores, a change in silicious to calcareous marine algae has been noted

in relation to dust input to marine sediment (Calvo *et al*., 2004). This change is thought to be driven by iron which is an important nutrient and can enhance diatom growth compared to other marine algae (Hutchins and Bruland, 1998).

The distinct change in biochemical compositions observed in Area D cores, from mangrove-dominated patterns at the base of the core to more marine distributions upwards, is not seen in the eastern end of Area C. Although, the relative increase of taxaxerol is observed at the base of longer cores from Area C at site 32. This may simply be a function of core depth (only 2 meters average in Area C, as opposed to 3 m for Area D).

3.7.4 Samples with high methane concentrations

Up to 80% of the methane produced in marine sediments is estimated to be consumed through AOM before reaching the sea bed, thus reducing the contribution of the marine environment to global methane atmospheric emissions (Reeburgh, 1996). AOM occurs in methane-rich sediments with concomitant seawater sulfate reduction and is effective at the methane-sulfate interface, where both substrates are depleted. Studies suggest that a prokaryotic consortium of methanotrophic archaea and sulfate-reducing bacteria mediate this process (Hinrichs et al., 1999; Boetius et al., 2000). We studied various sediment samples for evidence of AOM looking for evidence of enhanced levels of this bacterial activity. The primary reason for this assessment was to look for any signals of enhanced methane fluxes through the upper sediments that might be related to natural hydrocarbon seepage.

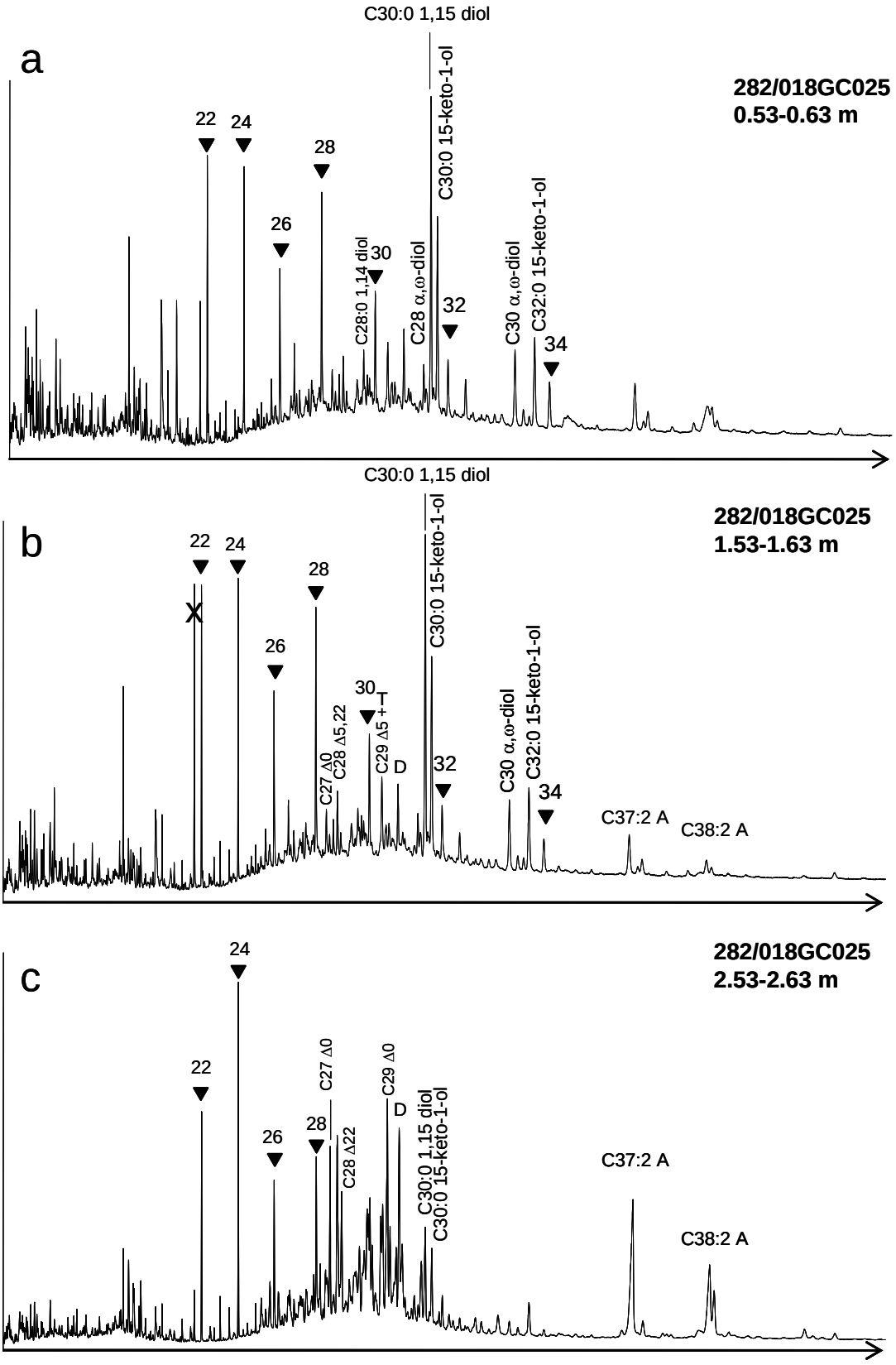

Figure 45 Reconstructed ion chromatograms of the silylated extractable organic matter fractions from samples of core 282/018GC025.

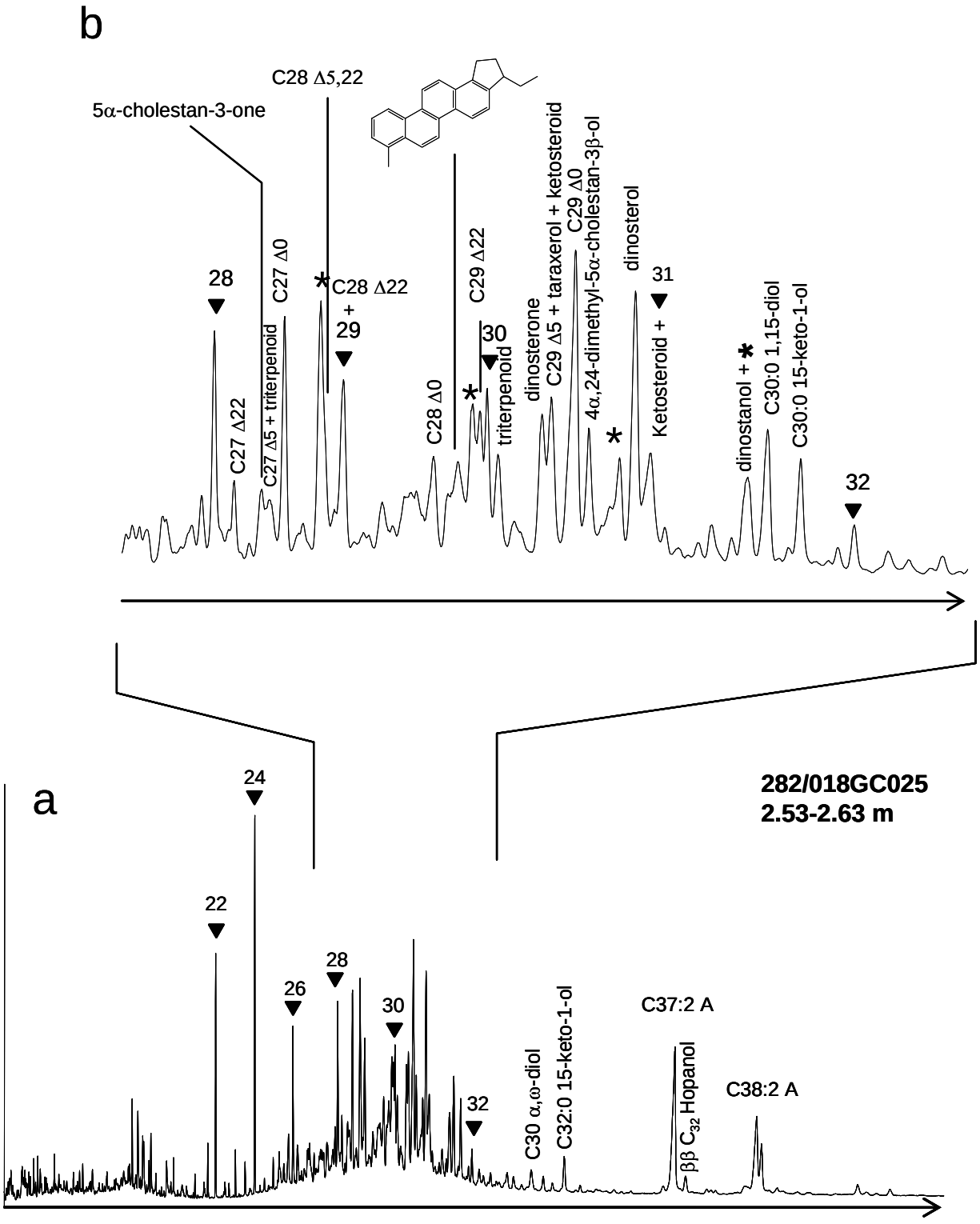

Figure 46 Reconstructed ion chromatograms of the silylated extractable organic matter fraction from core sample 282/018GC025 2.53-263 m showing the complex distribution of steroids and triterpenoids.

Headspace gas analyses of samples from the base of cores at site 22 revealed very high concentrations of microbial methane (up to 71,000 ppm). Methane concentrations decrease considerably in the corresponding upper samples. The sediments with high methane concentrations were analysed to investigate the occurrence of lipids commonly associated with AOM. Globally, where AOM rates are high, specific biomarkers have been detected (Brocks and Pearson, 2005). The presence of methanotrophy is recognised by the significant ^{13}C depletion of certain biomarkers found in these settings, such as the isoprenoidal glycerol diethers archeol and hydroxyarcheols, which are known constituents of archaeal membranes. These archaeal lipids together with corresponding depleted carbon isotopic compositions are used as proxies for AOM.

Very distinctive biomarker assemblages have been noted at cold seeps which are related to AOM (Pancost et al., 2001). However, analysis of core samples at site 22 did not show strong AOM signals. Biomarker distributions in these cores are very similar to those observed in the upper samples from cores taken in Area D, with prominent long-chain alkyl diols and ketols, linear alkan-1-ols, long-chain alkenones and dinosterol. A range of biomarkers possibly related to AOM were detected in relative low abundances. Archaeol was identified based on mass spectral data and on relative retention times (Teixidor and Grimalt, 1992) (**Figure 47**). A range of non-isoprenoidal dialkyl glycerol diethers evidenced using current ion *m*/*z* 130 is also observed (**Figure 47c**). Two main homologues C_{33} I and C_{35} II are present in our samples and several isomers of C_{33} DGD I are detected at slightly later elution times. These compounds have been identified in carbonate crusts in the vicinity of cold seeps on the East Mediterranean Ridge and are thought to be related to sulfate-reducing bacteria (Pancost et al., 2001). However, similar biomarker assemblages are also found in marine settings where methanogenesis occurs.

Methanotrophy via AOM can be differentiated from methanogenesis by using carbon isotopic compositions of archeal biomarkers. Where these lipids are derived from organisms feeding on methane they are highly depleted in ^{13}C. Unfortunately, archeol was not abundant enough in our samples to get reliable carbon isotopic compositions and to allow the distinction between methanogenesis and methanotrophy. Moreover, the high methane levels at this site are direct evidence that an active microbial methanogenic community is present in these sediments. Interestingly, archaeol and non-isoprenoidal dialkyl glycerol diether concentrations appear to increase with depth, i.e. with increasing concentrations of methane (**Figure 48a**). This rise is fairly modest, about three-fold. These compounds also increase down-core relatively to algal biomass as exemplified by C_{33} DGD/$C_{37:2}$ alkenone and archaeol/$C_{37:2}$ alkenone ratios (**Figure 48b**). Analogous distributions of archeal biomarkers and non-isoprenoidal glycerol diethers, at comparable concentrations, are observed in marine sediments characterized by a diffusive flux of methane (i.e. slow AOM rates) where abundances reach a maximum near the sulfate-methane transition zone and are several orders of magnitude lower than observed at cold seeps (Pancost et al., 2005).

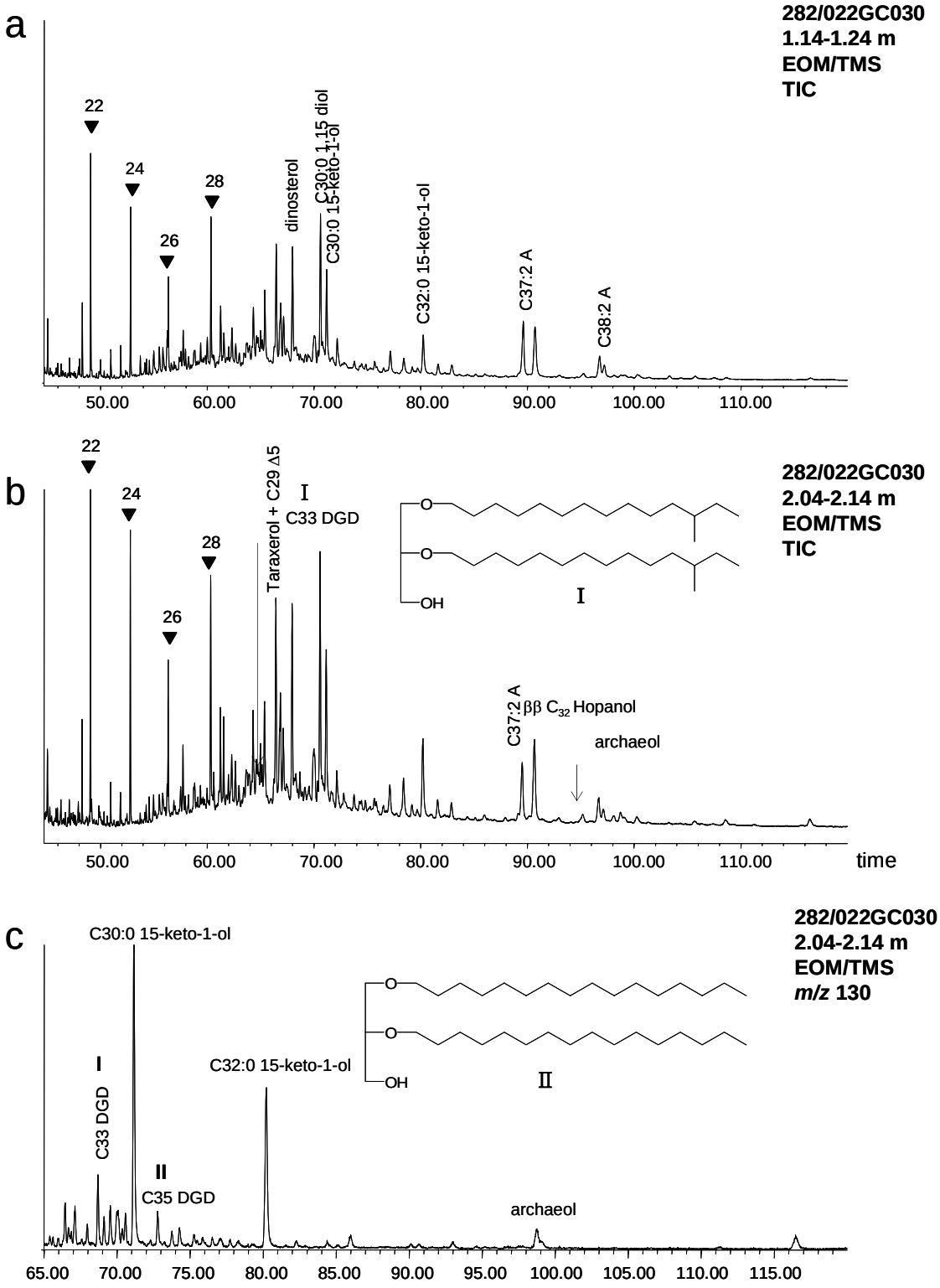

Figure 47 Reconstructed ion chromatograms of the silylated extractable organic matter fractions from samples of core 282/022GC030, CH4 cc = 658 ppm for 282/022GC030 1.14-2.14 m (a) and 47513 ppm for 282/022GC030 2.04-2.14 m (b).

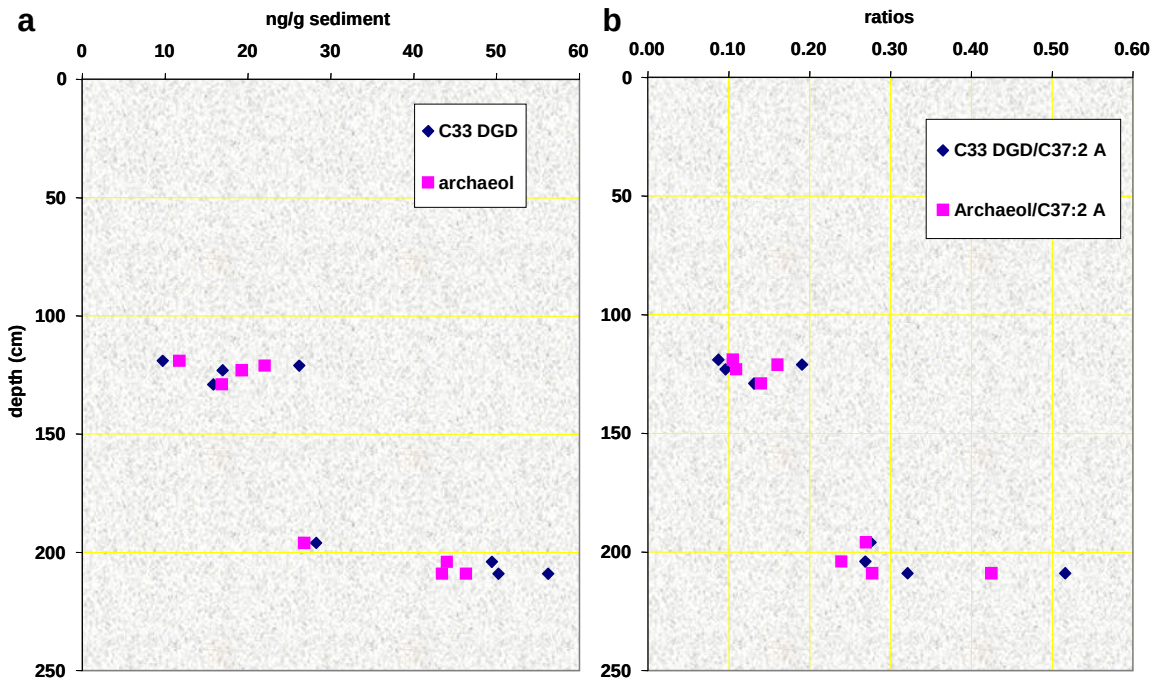

Figure 48 Plots of : a) concentrations of C_{33} dialkyl glycerol diether I and of archaeol versus depth; b) C_{33} DGD/C37:2 alkenone and Archaeol/C37:2 alkenone ratios versus depth in core sediments from site 22.

3.8 SEA BED CHARACTERISATION AND ENVIRONMENTS

The sea bed features in Areas B, C and D have been characterised by integrating various datasets, such as multibeam, side-scan sonar and sub-bottom profile data. Some of these features have been ground-truthed by core, grab and dredge sampling, and also with video camera footage. The spatial distribution of these features is mapped in **Figures 49 and 50**.

The various sea bed features are observed at different scales:

a) Large-scale features (< 50 km) include channels and banks forming relief along a major depression extending west from the Gulf of Carpentaria. Some banks form rectilinear escarpment features, mostly following a WNW direction.

b) Small-scale features (< 10 km) include lithified ridges, mounds and pockmark fields, often superimposed upon large-scale features.

3.8.1 Large-scale sea bed features

3.8.1.1 Channels and banks

Channels are observed in the northern part of Area B (**Figure 50d**) and in the north-western part of Area C, particularly adjacent to the northern and southern flanks of Pillar Bank (**Figure 50a**). They have 10-20 m of relief, and are at water depths of 100-200 m.

Four banks are observed in the surveyed areas: three are in Area C (Linear Bank, Eastern Bank and Pillar Bank; **Figures 50a, c and 51**) and one is in Area B (**Figure 50d**). Pillar bank is an elongated feature, approximately 50 km long, 3 km wide, and 60 m high (between 125-185 m of water depth). Pillar Bank is orientated WNW-ESE, parallel to major drainage channels shown in **Figure 51**. It is composed of several stacked, lenticular sediment packages that overlie the erosional surface U1 (**Figures 52 and 53)**.

The banks are bounded by escarpments that are particularly steep on the northern and southern flanks (**Figure 54**). The main scarp slopes have a strong WNW trend and some are rectilinear suggesting possible tectonic inheritance (**Figure 53**). Two orthogonal sub-bottom profiles over the Eastern Bank show that a shallow-rooted fault controls this escarpment (**Figure 55**). The fault separates Unit I to the north from the younger Unit J to the south. The fault appears to be currently active as it affects Unit J to the sea bed and the hanging wall exhibits a roll-over structure. An alternative explanation for this feature is current scour along the edge of the fault scarp. The fault affects Unit I and possibly Unit H but it does not appear to affect the surface U7 (**Figure 55 inset**). During the last sea level low stand, Pillar Bank and Eastern Bank were subaerially exposed (**Figure 56**). Sampling at site 17, on top of the Eastern Bank, and at site 38 on top of Pillar Bank recovered cemented, calcareous, gritty limestone (**Figure 36**). Given the exposure of these banks during the low-stand this limestone is most likely to be attributed to beach rock or calcrete formation.

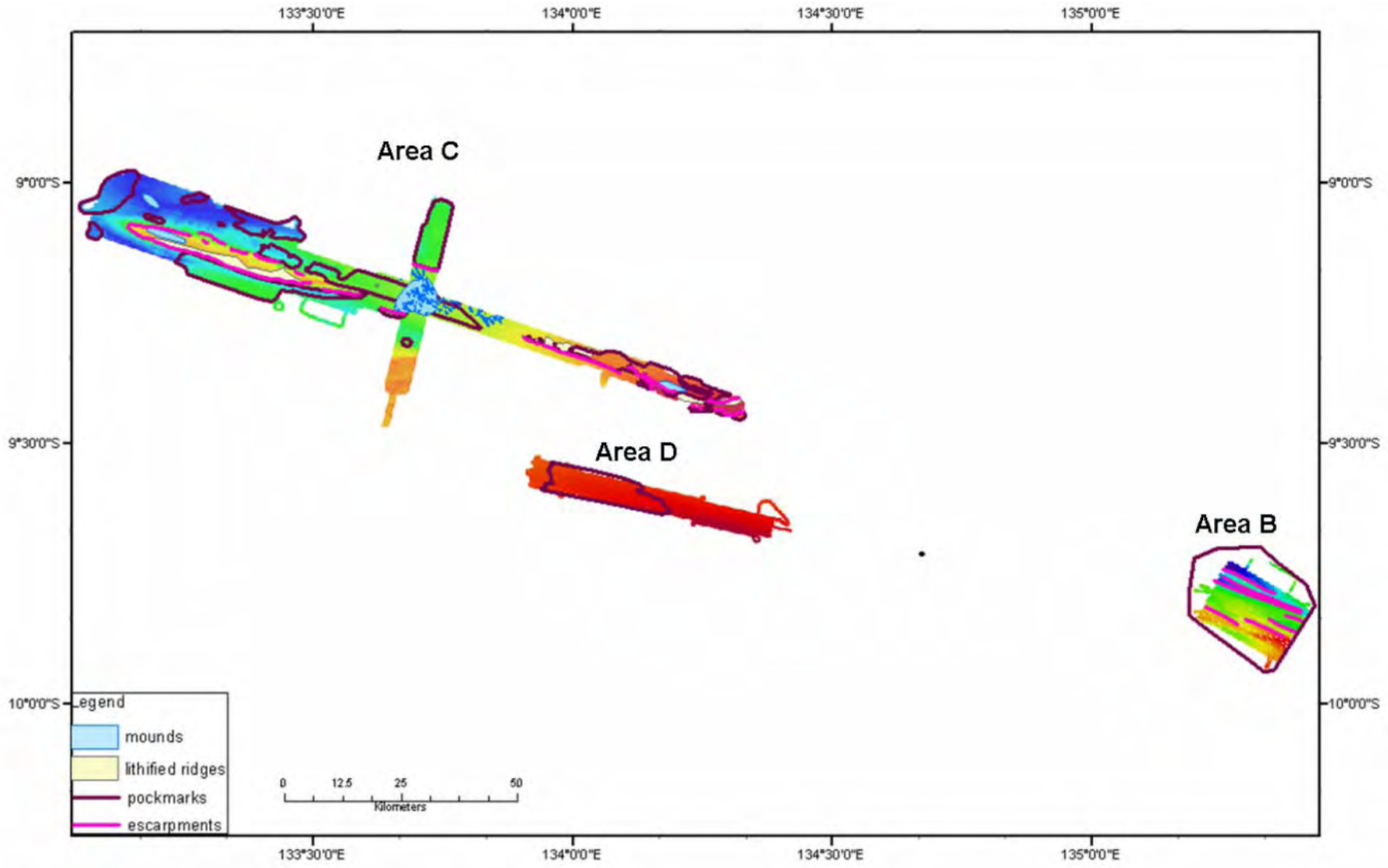

Figure 49 Seabed features in Areas B, C and D. Over banks and channels, smaller features, such as escarpments (dark blue line), lithified dunes (yellow filled polygons), mounds (blue filled polygons) and pockmark fields (green polygons) are observed. Enlargements of the survey areas are shown in **Figure 50**.

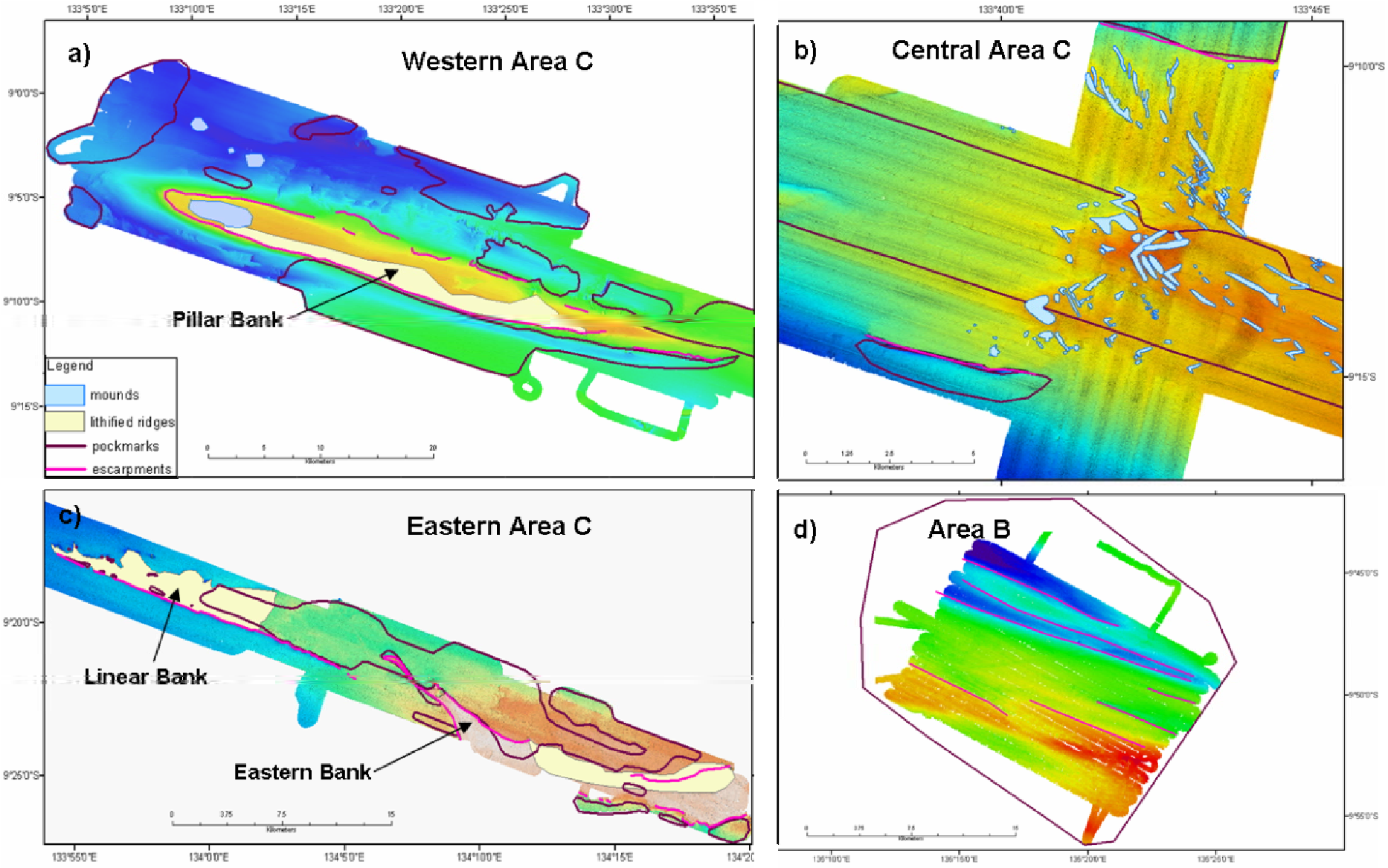

Figure 50 Enlargement of the different surveyed areas: a) Western part of Area C; b) Central part of Area C; c) Eastern part of Area C; d) Area B.

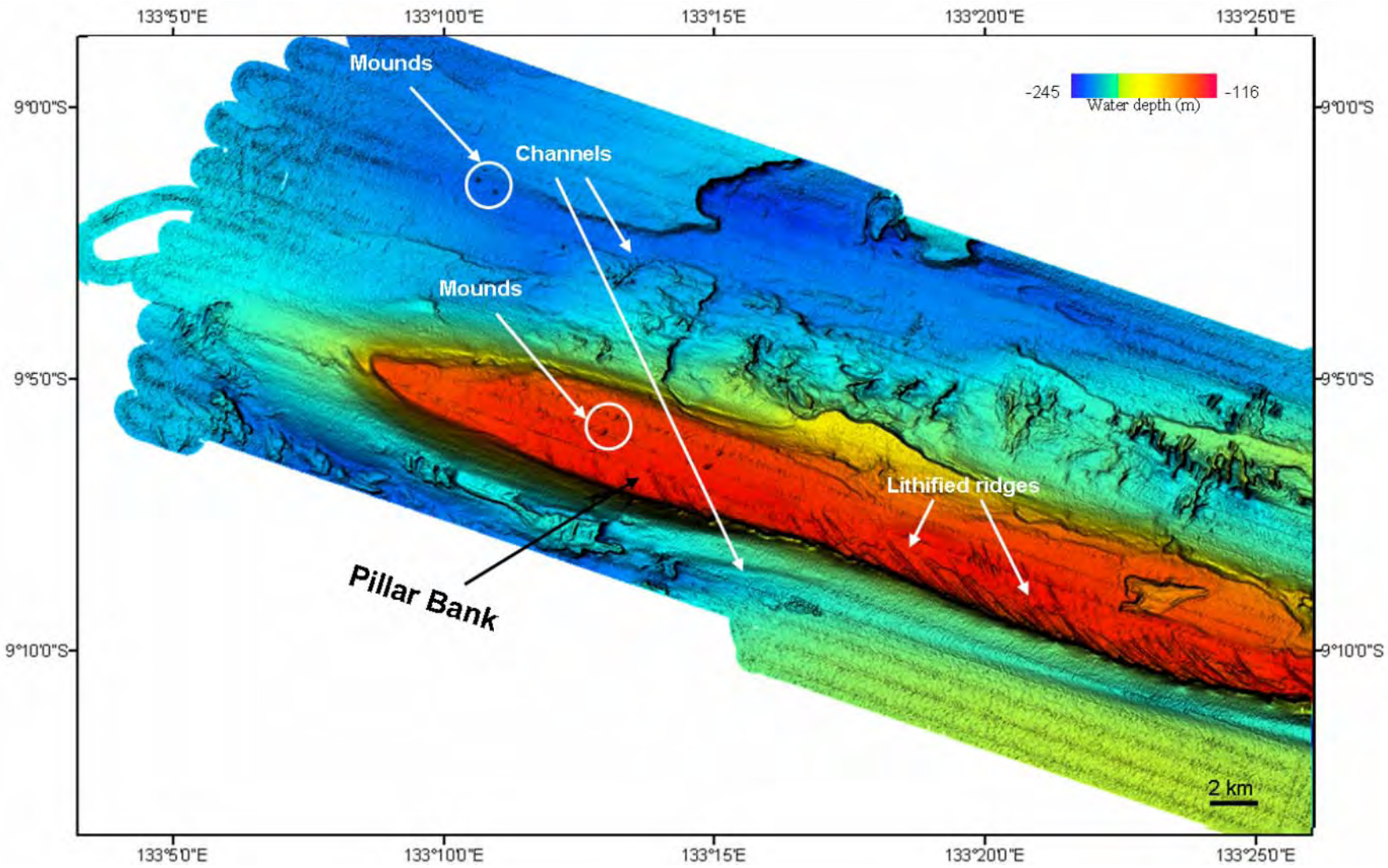

Figure 51 Multibeam bathymetry image of Pillar Bank, in the western part of Area C. Channels north and south of Pillar bank are 20 m and 10 m deep, respectively. Illumination from the northwest.

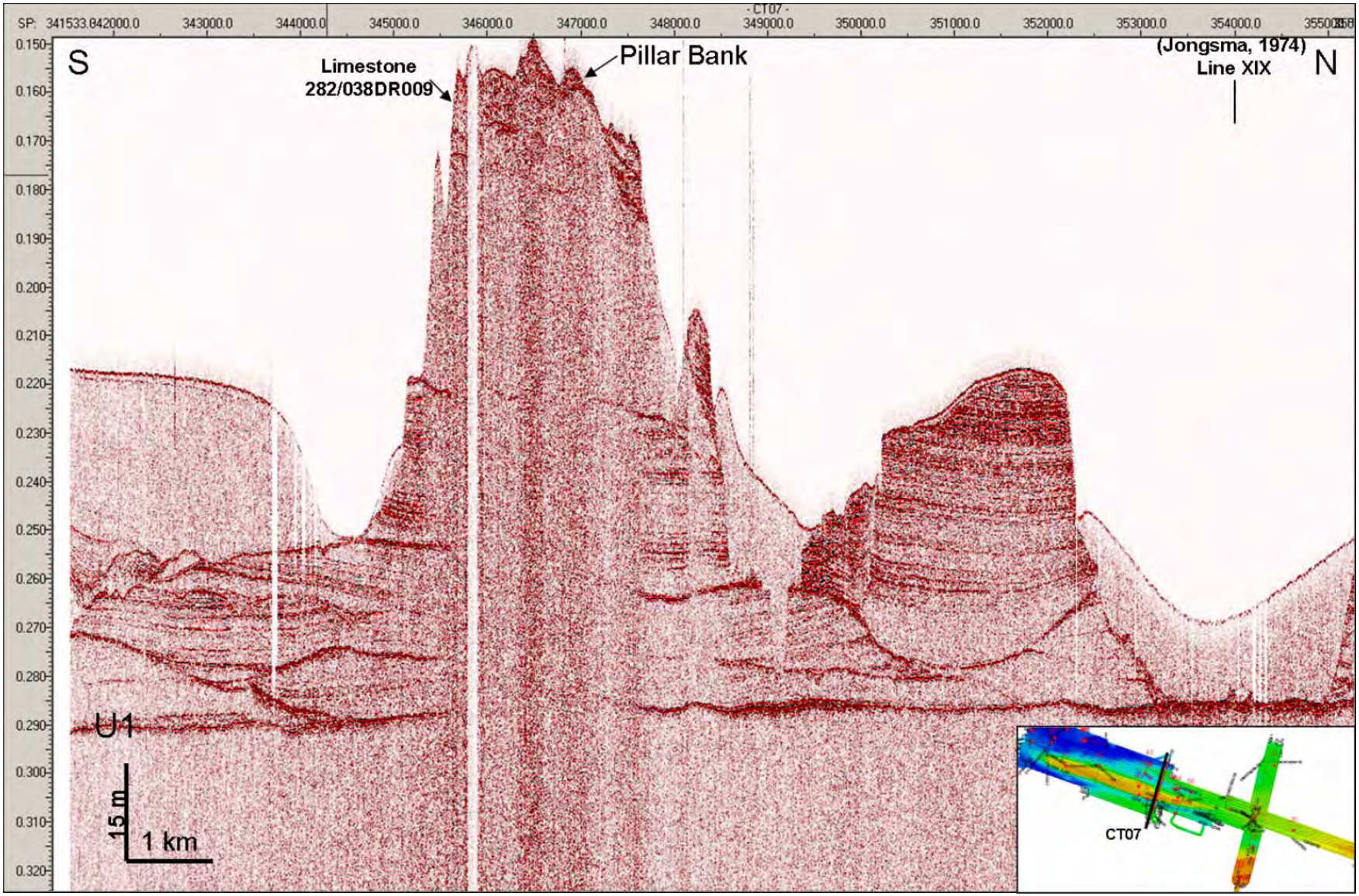

Figure 52 Sub-bottom profile CT07 across Pillar Bank. The bank is flaked by channels and is constructed from several different lenticular sediment packages.

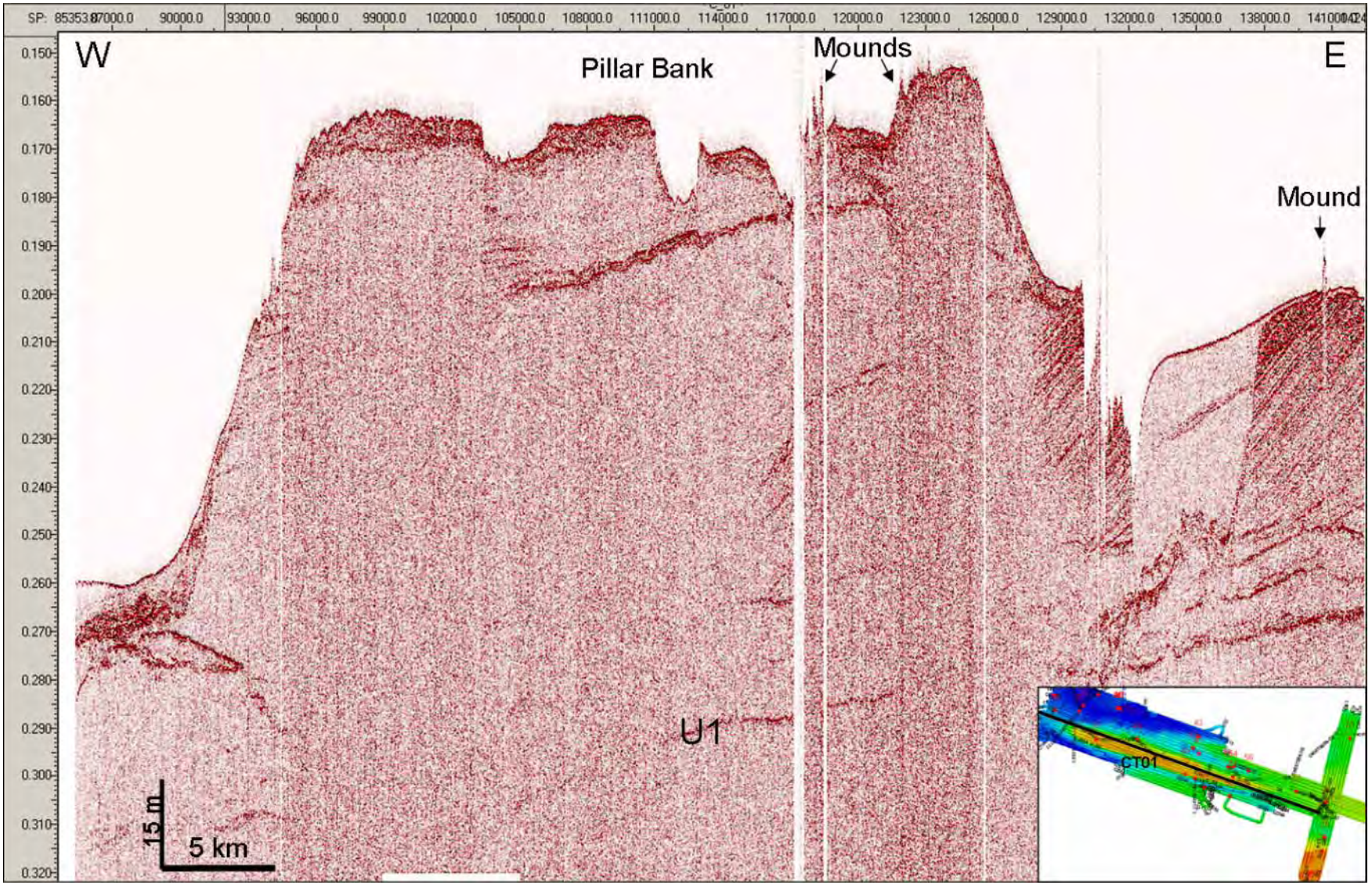

Figure 53 Sub-bottom profile C_01 along the axis of Pillar Bank. This bank is bounded by steep escarpments at either end and is capped by hard-grounds and local hard mounds. These mounds are up to 8 m high, and strongly attenuate the seismic signal.

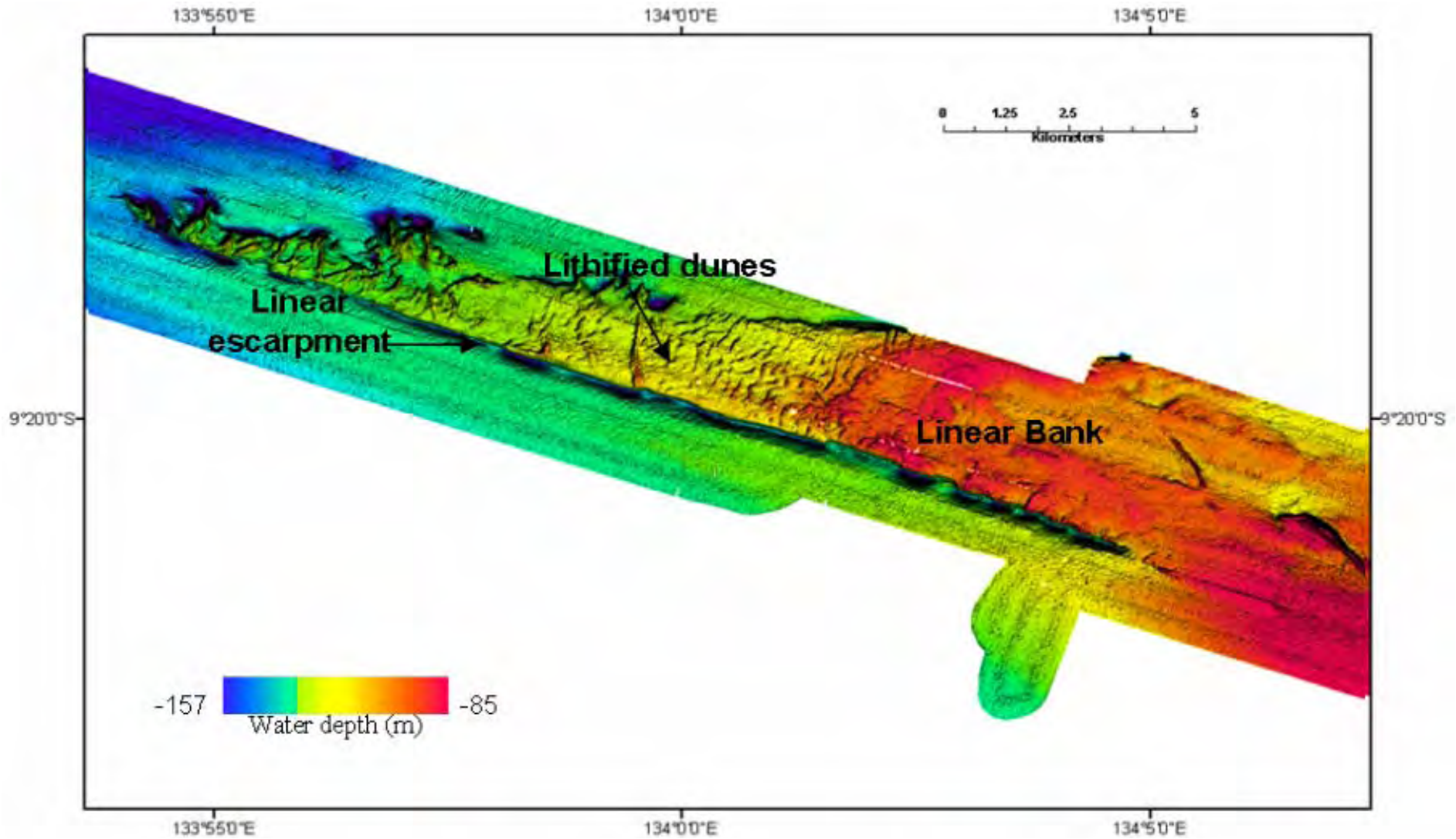

Figure 54 Linear escarpment on the southern edge of Linear Bank, in the eastern part of Area C (see location on **Figure 7**). Small-scale, NE-SW lithified dunes (up to 2 km long, less than 100 m wide and 2-6 m high) are observed on the top of the bank, orthogonal to the elongation of the bank. See also **Figure 59**.

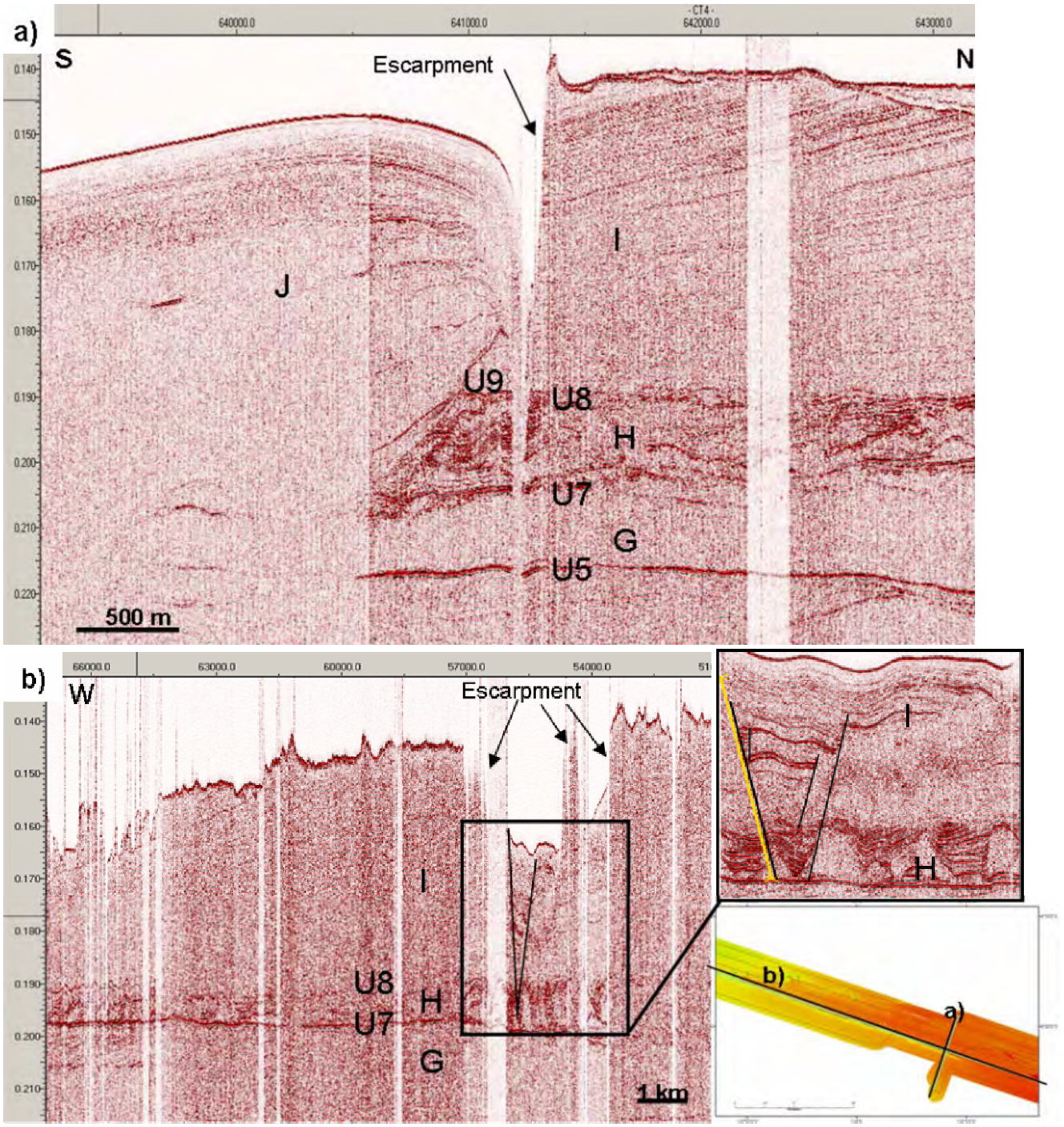

Figure 55 a) Sub-bottom profile CT4 showing the recent escarpment fault affecting the most recent sediment package Unit J (roll-over geometry or current scour). b) Sub-bottom profile C5 showing the faulted origin of the rectilinear escarpment. This fault, which has been intersected several times on the deep line, is shallow-rooted and does not affect the unconformity U7. Inset: shows the profiles location on the eastern part of Area C.

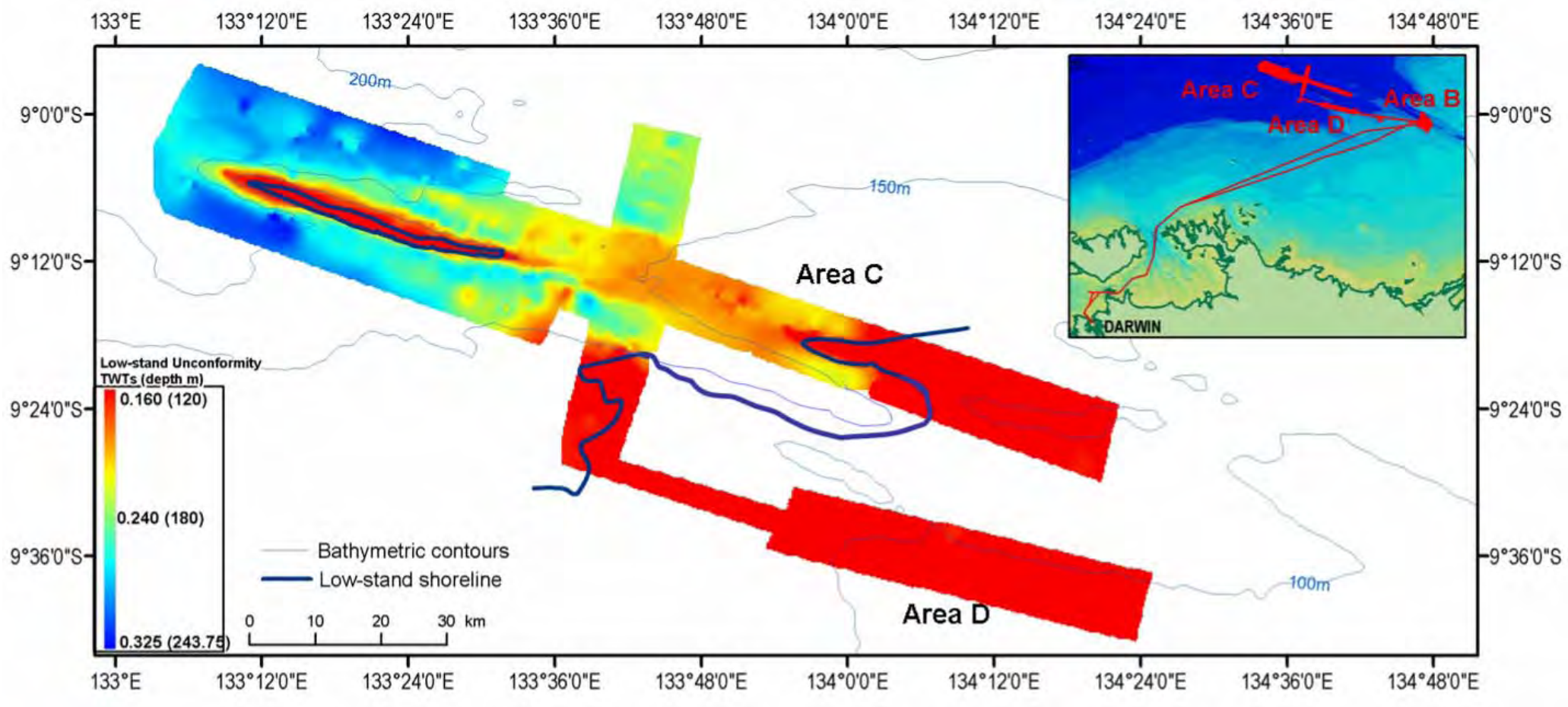

Figure 56 Grid showing the bathymetry at the last low-stand (corresponds to the unconformity U9, base of layer J). Blue line indicates the palaeo-shoreline during this period (estimated 120m = shoreline; refer to **Figure 3**). All of the strata within Area D were exposed during the last sea level low-stand.

3.8.2 Small-scale sea bed features

3.8.2.1 Lithified dunes

Lithified dunes are observed in Area C, on the eastern and western sides of the Eastern Bank and on the southern flank of Pillar Bank. These curvilinear dunes are up to 2 km long, less than 100 m wide and 2-6 m high. They are located on the top of the banks, oblique to the long axis of the banks (**Figures 57, 58 and 59**). The samples recovered over the lithified dunes indicate the surface is composed of calcareous sands and shelly gravel inhabited by burrowing organisms and soft corals (**Appendix 1 and 6**).

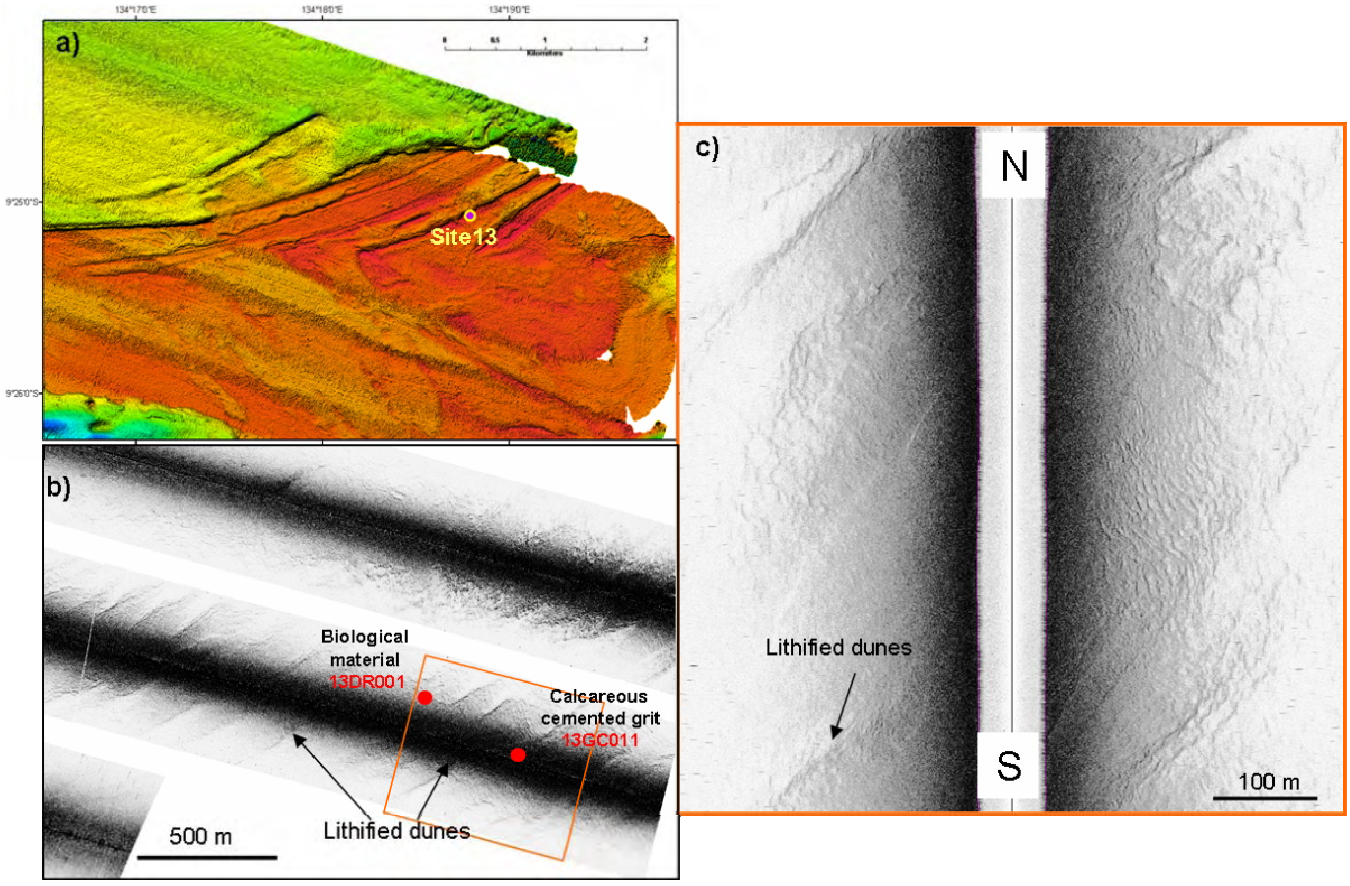

Figure 57 a) multibeam image compared to b) and c) Side-scan sonar images showing lithified dunes in the eastern part of Area C. Close to the ridges, bioclastic sand, calcareous cemented bioclastic grit were collected and corals, burrows and bioturbation were observed on video footage.

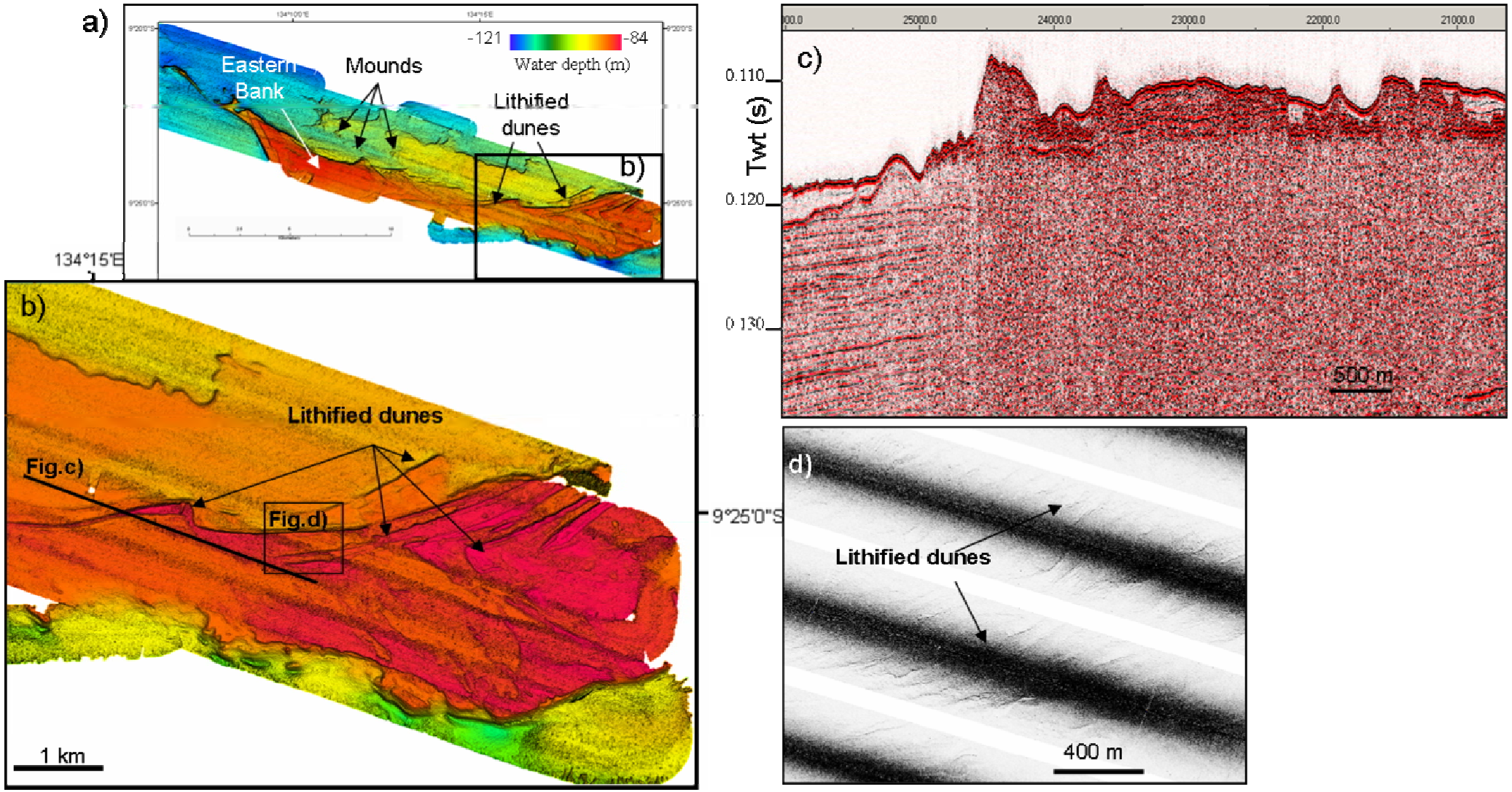

Figure 58 a) and b) show lithified dunes located on the eastern end of Eastern Bank in Area C. c) sub-bottom profile and d) side-scan sonar data over areas outlined in image b).

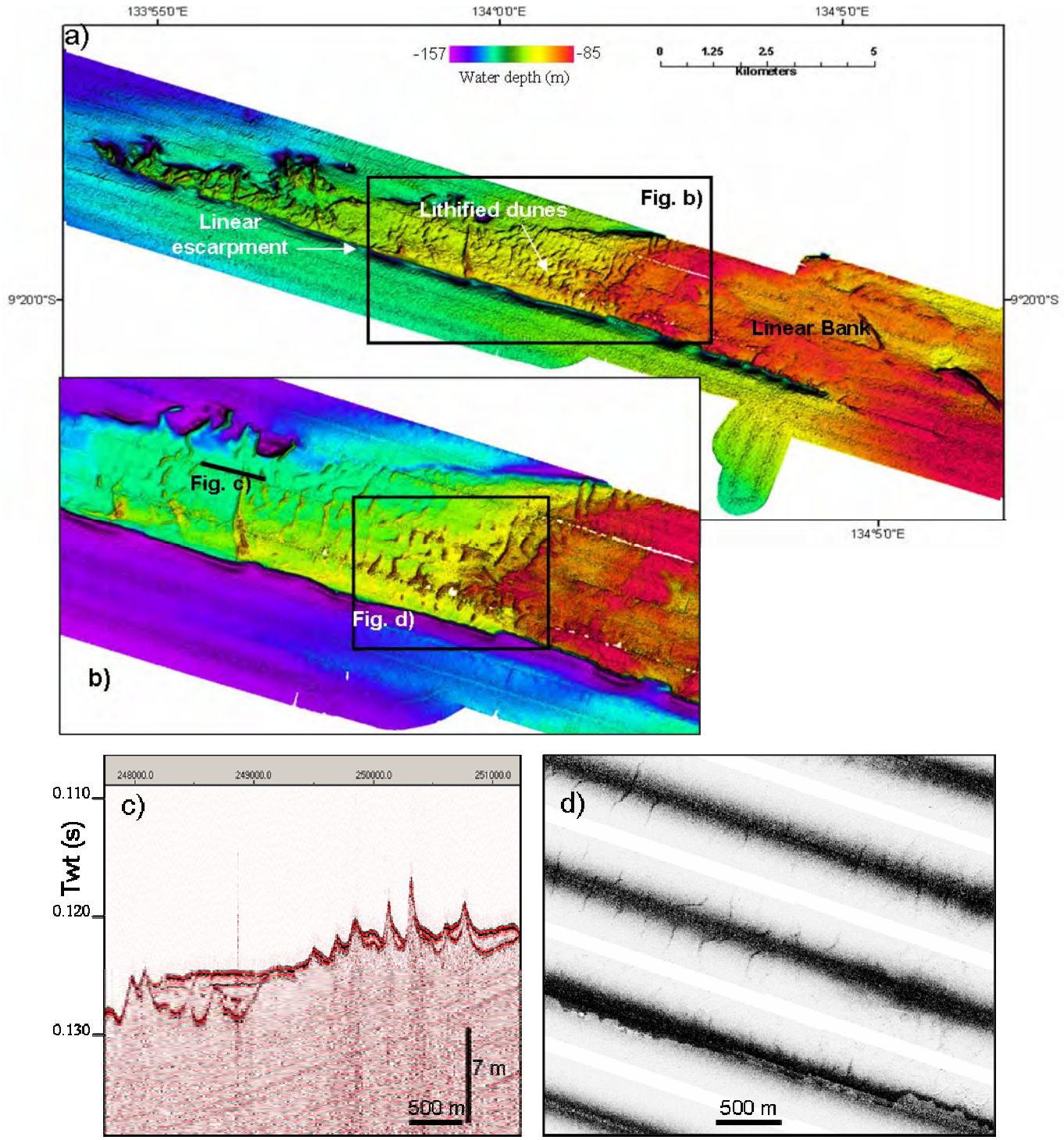

Figure 59 Lithified dunes located on Linear Bank in Area C (location on **Figure 7**), observed on a) and b) multibeam bathymetry, c) sub-bottom profile and d) side-scan sonar data

3.8.2.2 Mounds

Mounds are mostly observed in the central part of Area C (**Figure 60**), near the Eastern Bank (**Figure 61**), and also the north-western part of Area C, north of Pillar Bank (**Figure 50**).

On the basis of their sub-bottom profile character and side-scan back-scatter data, the mounds can be divided into two types, mud and carbonate. The carbonate mounds generally cause underlying signal attenuation in sub-bottom profiles and have a strong back-scatter side-scan sonar signal (**Figure 60**). Their sides are steeper and relief is often higher than mud mounds. Mud mounds form low-relief features observed on multibeam and side-scan sonar. Their sub-bottom profile character is often chaotic or transparent but they do not cause significant signal attenuation in underlying strata (**Figure 61**). The mud mounds appear to be the tops of diapiric structures that have pierced the sea bed.

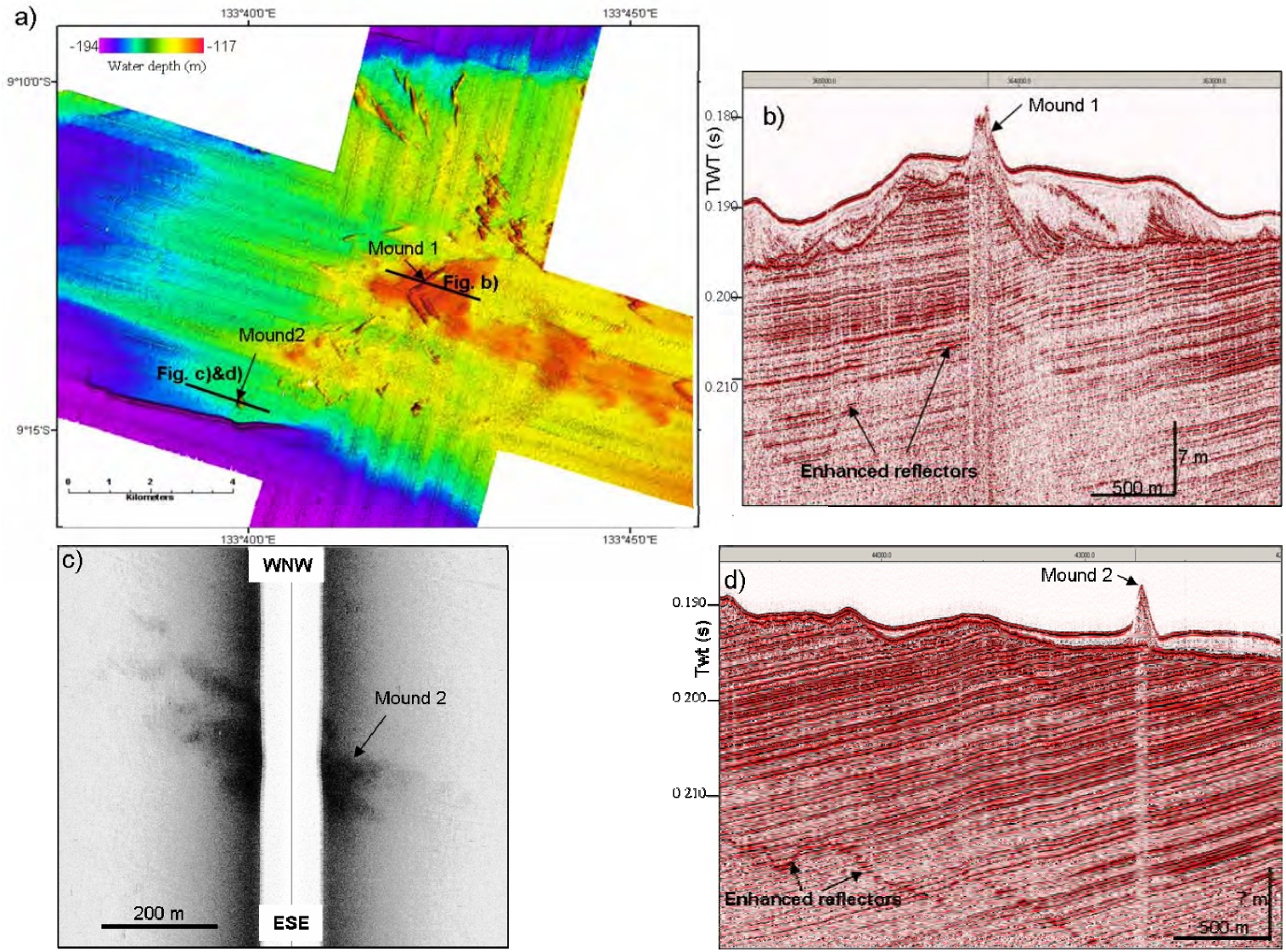

Figure 60 Several carbonate mounds are observed a) on multibeam bathymetry, in the central part of Area C; b) on sub-bottom profiler data, the seismic signal is attenuated beneath the 7m-high mound. Enhanced reflectors, cross-cutting the dipping stratigraphy, are observed in this area; c) on side-scan sonar data, the mound shows a strong back backscatter response suggesting a hard substrate.

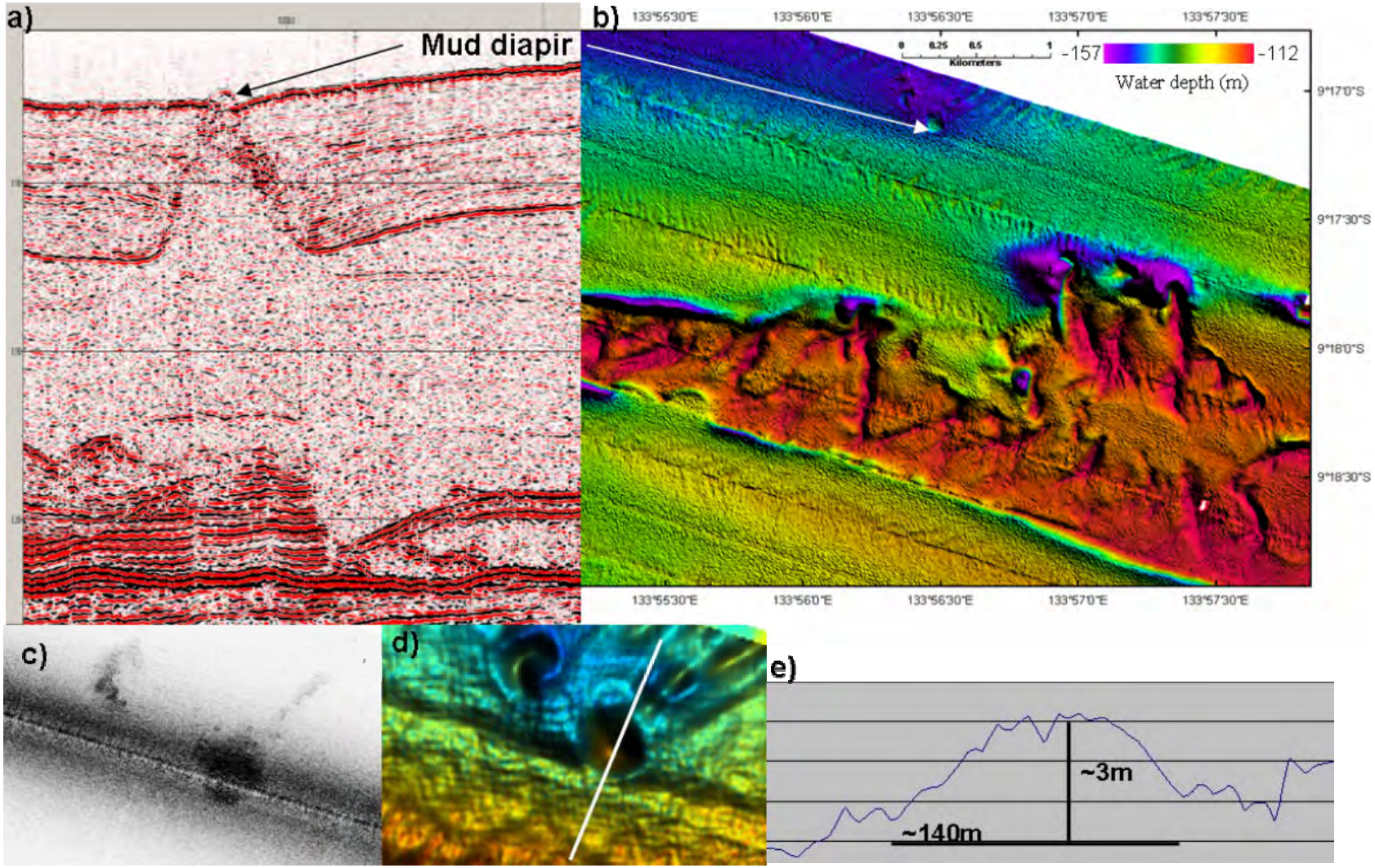

Figure 61 3 m-high mud mound located north of Linear Bank, in the eastern part of Area C, observed on a) sub-bottom profile C8, b) multibeam bathymetry and c) side-scan sonar data. d) enlargement of the multibeam bathymetry over the mound; white line shows the location of the profile e).

3.8.2.3 Pockmark fields

Pockmark fields are located in Areas B, C and D. Different densities of pockmarks are observed across the survey area (**Figure 62**):

1. High-density pockmarks (~350/km²) are mainly located in Area D;
2. Medium-density pockmarks (~150/km²) are found in the eastern part of Area C and Area B;
3. Low-density pockmarks (30/km²) are found in the western part of Area C.

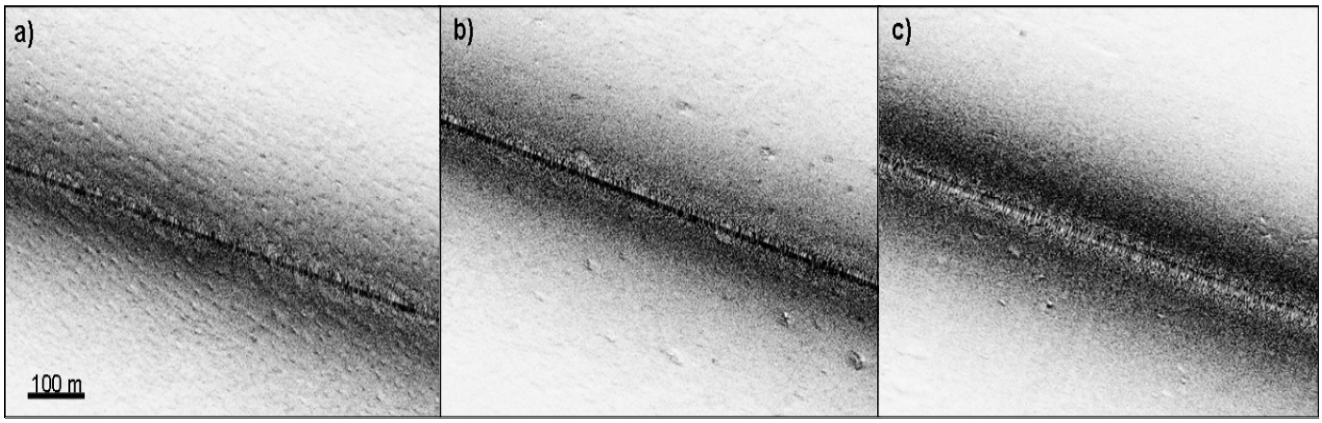

Figure 62 Side-scan sonar mosaics showing the varying pockmark densities in the surveyed areas: a) high-density pockmarks in Area D; b) medium-density pockmarks in Area C; c) low-density pockmarks in Area C.

In high-density pockmark fields (**Figure 63**), the sizes of individual pockmarks vary between 5-20 m long x 5-10 m across x <2 m deep. The pockmarks have formed in muddy Holocene sediments infilling palaeo-channels. High gas concentrations are associated with the high-density pockmark fields and this gas appears to be microbially generated, based on carbon isotope data and gas wetness (see **Section 3.7.1**). The microbial gas may be generated within Unit J. However, geophysical indicators of gas have also been identified below the palaeo-channels in sub-bottom profile data, suggesting that other gas sources may be involved in combination with gas generated *in situ* to form the pockmark fields (**Section 3.10**).

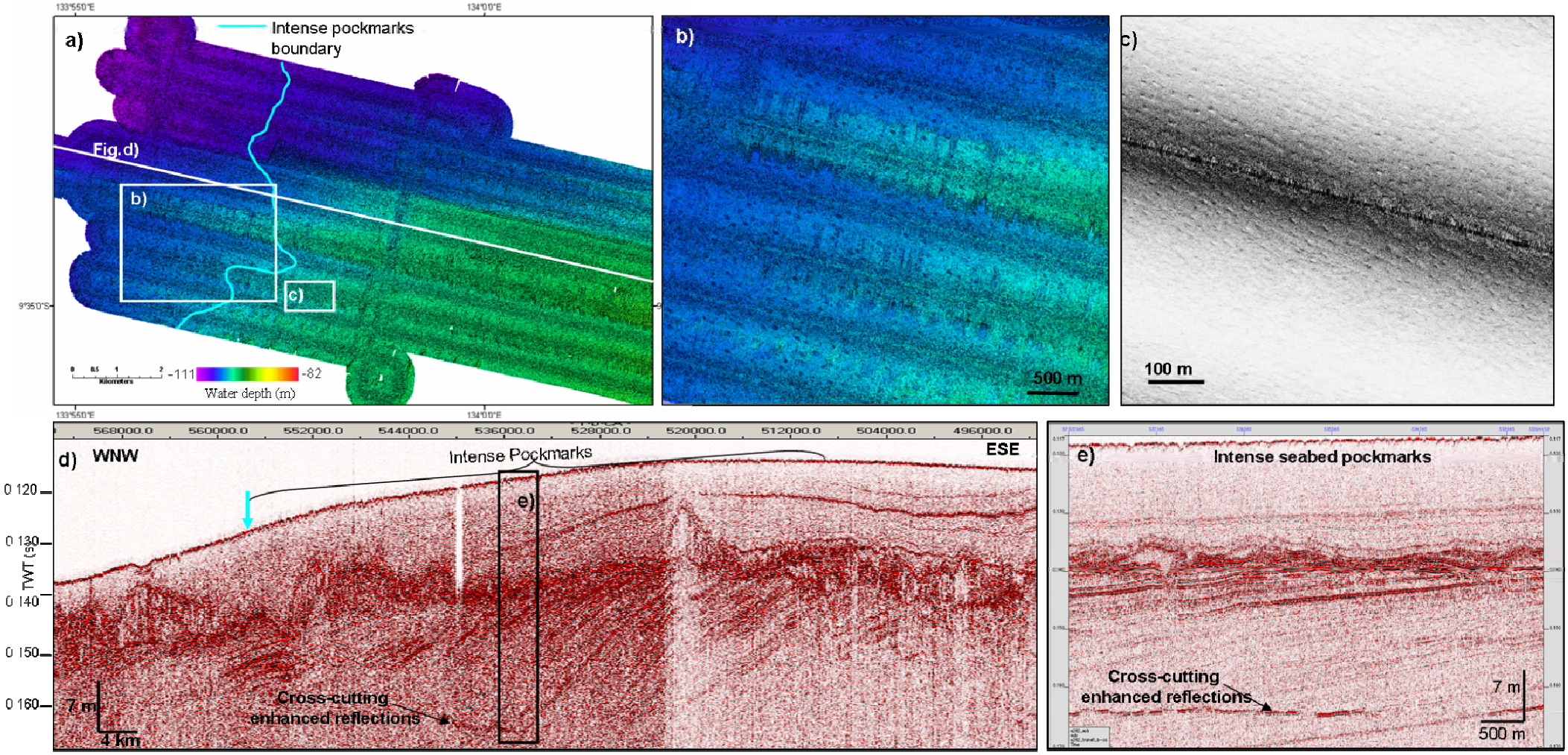

Figure 63 High-density pockmark field in Area D observed on a) and b) multibeam bathymetry, c) side-scan sonar, d) and e) sub-bottom profile data.

In medium-density pockmark fields (~150/km^2), the sizes of in individual pockmarks range between 15-35 m long x 10-15 m across x <2 m deep. They are often associated with palaeo-channels but the infilling sediments are generally not as muddy as in the areas of high-density pockmarks (**Figure 64**). Gas levels in sediments from these areas were not significantly higher than the background level. These low gas levels may be related to the coarse nature of the sediment or the cores not intersecting sediment with high pore gas levels.

In low-density pockmark fields (~30/km^2), the size of individual pockmarks ranges between 5-25 m long x 5 m across x <2 m deep. Sea bed samples did not contain gas concentrations above background levels and sediments were generally composed of coarser, bioclastic, muddy sand (**Figure 65**).

The density of pockmarks appears to be directly related to the nature of the sea bed sediment. Where sediments are muddier, pockmarks are smaller and more densely spaced. As the sediment grain size increases, based on core and grab samples, pockmarks become larger and less densely spaced. There is also a general correlation between the highest density pockmark fields and Holocene mud packages of Unit J which fill palaeo-channels. This second correlation is at least partly related to *in situ* generation of microbial gases.

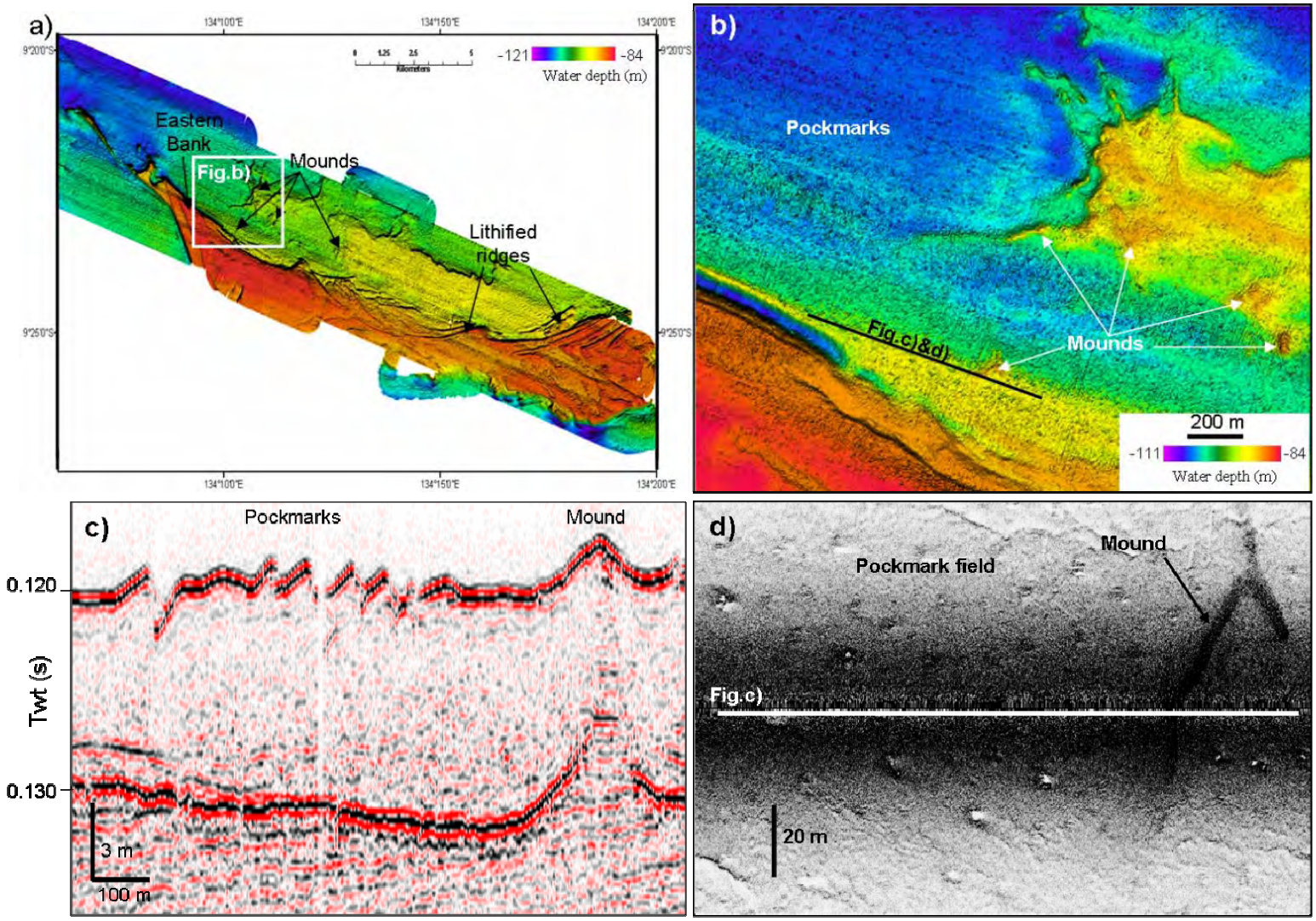

Figure 64 Medium-density pockmark field in the eastern part of Area C. a) Multibeam bathymetry showing the location of Figure b). b) enlarged multibeam image showing mounds and the pockmark field (each pockmark is 1-3 m deep and less than 20 m across). c) Sub-bottom profile over some pockmarks and a 3 m-high mound. d) Side-scan sonar image showing the pockmarks and the mound over the location of Figure c).

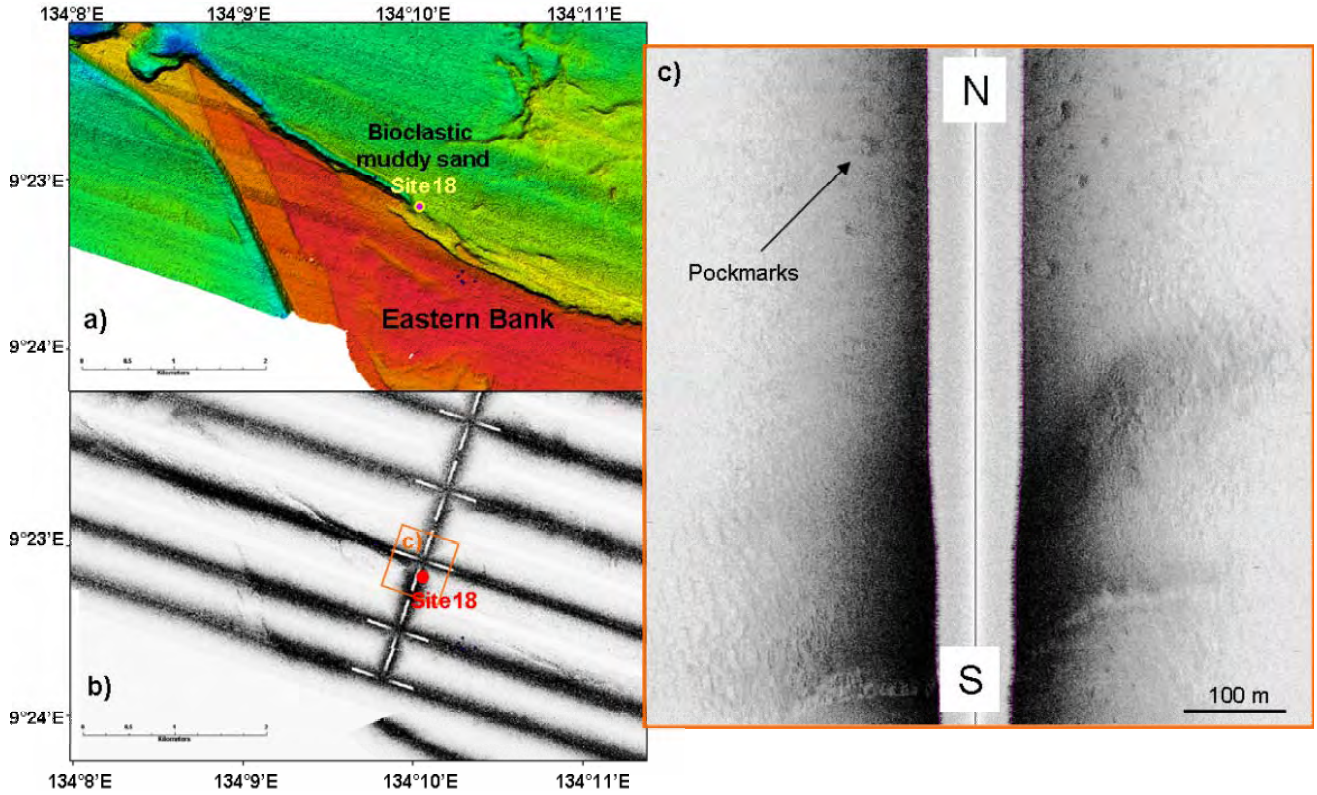

Figure 65 Low-density pockmark field (30/km²) at Site 18 (Area C) formed in coarse, muddy sand. Site location is indicated in a) the multibeam bathymetry map, located north of Eastern Bank, in the eastern part of Area C. b) and c) are side-scan sonar images showing the pockmarks.

3.9 HABITATS AND BIODIVERISITY

Several different types of sample techniques were used during the survey depending on the type of substrate, to maximise sample collection. For example, muddy substrate was sampled with the epi-benthic sled, rocky substrate was sampled using the rock dredge, and sandy substrate was sampled with the Smith-McIntyre grab.

The Smith-McIntyre grab recovered between 1 and 71 species at each sample station, the dredge recovered 2 – 54 and the species count from the sled samples ranged from 1 – 11. However, the substrate type is indicative of the species diversity irrespective of sample equipment used. The numbers of species types recovered per sample for each substrate type are shown in **Table 2**. The more poorly sorted the sediment sample was, the higher the species count. For example, muddy, sandy gravel species

counts ranged from 5 to 54, and the rocky substrates species counts ranged from 8 to 54. Higher diversity was generally found on substrates that included sandy gravels, shelly grit rocks and, poorly-sorted rocks.

Substrate type	**Number of species/sample**
Gravel	10 - 31
Gravelly mud	3
Mud	1 - 8
Muddy gravel	1 - 23
Muddy sand / sandy mud	2 - 24
Muddy sandy gravel / shelly grit	5 - 54
rocky	6 – 54

Table 2 The substrate type and corresponding species diversity recorded during Survey 282.

Across all sites there was low representation of epifaunal species (fixed or sessile) and nektonic/planktonic species were seen only sporadically and were often solitary. Areas of high biodiversity and abundance generally correlated with harder substrates. In these areas, sea whips and fans, soft corals, hydroids, crinoids and octocorals were frequently identified and also sessile benthos extended up to ~50cm in height.

The extensive areas of soft substrate commonly exhibited low-relief benthic communities which often covered less than 5% of the sea bed. Such areas were also often characterised by pockmark fields and the general uniformity of the environment. Bioturbation was evident in many of the sites with soft substrate, although visible biota was frequently sparse and/or lacking in diversity. Area D has had a uniformly muddy sea bed with some bioturbation and burrows. The samples here yielded only a few large specimens of biota.

Much of the western part of the survey area is below the oceanic mixed layer with strong currents (>40cm/s) below 100 metres depth. As a result, most hard substrates are inhabitated by filter-feeding mega-fauna, especially at the crests of ridges where the current is strongest, providing the best habitat for filter-feeders. Live stalked crinoids (a Palaeozoic relict group) were seen in the west of Area C. They were recorded on the benthic video and sampled in some of the dredges where individual stem sections were recovered.

The top of Pillar Bank was highly rugose with minimal fine sediment, whereas the sea bed to the north was composed of hemipelagic oozes. The deepest sample site, adjacent to the northern flank of Pillar Bank, recovered sandy sediment with shell gravel. Sampling at the shallow sites on the southern flank of Pillar Bank, recovered oyster shells, coral and bryozoan fragments. The sea bed surrounding Pillar Bank consisted of soft bioturbated sediments with few epifauna.

3.10 SUB-SURFACE CHARACTERISATION AND FLUID FLOW

3.10.1 Sub-bottom profile data

There are a range of features identified on sub-bottom profile data related to sub-surface structure and also indicators of fluid flow/shallow gas. These indicators can include: enhanced reflections, acoustic blanking, pockmarks, and a highly reflective sea bed. There are also possible carbonate structures, mud diapirs, and injectites, which may be related to gas expulsion or other fluid movement. This evidence of fluid flow is in addition to that provided by head space gas analysis of cores (**Section 3.7.1**). Examples of the various features identified within Survey 282 sub-bottom profile data are described below and their locations are given in **Figure 66**.

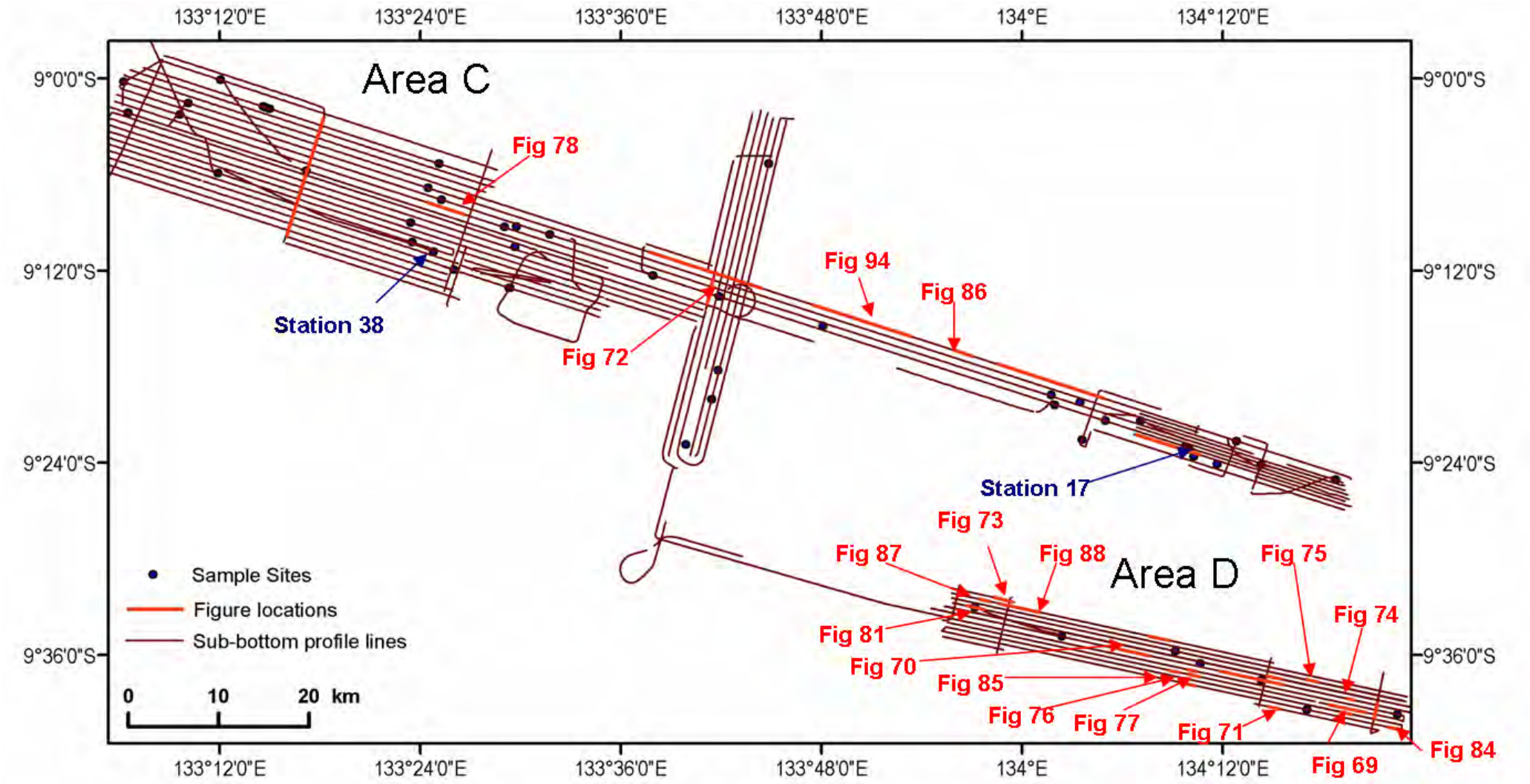

Figure 66: Location of figures showing shallow gas indicators.

The following terms are commonly used in the description of shallow gas indicators in high resolution seismic reflection profiles (Hovland *et al*., 1984; Judd and Hovland, 1992; Schroot and Schuttenhelm, 2003):

Enhanced reflections: coherent seismic reflections which have increased amplitude for part of their extent. High-amplitude reflections can have various causes, but when they are gas related they generally show a combination of high-amplitude, reverse-polarity and low-frequency.

Acoustic blanking: reflections are faint or absent and occur as a lowering of seismic frequency response, masking internal layering. Various explanations are possible; these include signal attenuation, over–pressured porewater, and the destruction of layering by migrating fluids (Judd and Hovland, *in press*).

Enhanced reflections can be a strong indication of the presence of gas due to the enhancement of the acoustic impedance contrast between gas-charged layers and adjacent gas-free layers, where pore spaces are filled by water (Hart and Hamilton, 1993). A reversal in reflection polarity (as in **Figure 67**) occurs in response to an acoustic impedance contrast where the overlying layer has a higher density / rigidity than the lower layer. This may be because the lower layer comprises softer sediment, or because its bulk density is reduced by the presence of gas rather than water in the pore spaces. In **Figure 68**, for example, the enhanced reflection is likely to be related to gas charge as indicated by the reverse-polarity of the reflection and the presence of overlying pockmarks. However, enhanced reflections can also be related to sedimentary features (e.g. changes from clastics to carbonates) or they could be seismic artefacts; the example in **Figure 69** is thought to be an artefact caused by the geometry of the reflectors and a variation in the strength of the returned signal as the

geometry changes across the feature. In this example, the horizontal reflector (at the crest of the undulation) returns more energy to the receiver located directly above than the inclined reflectors on the flanks of the undulation.

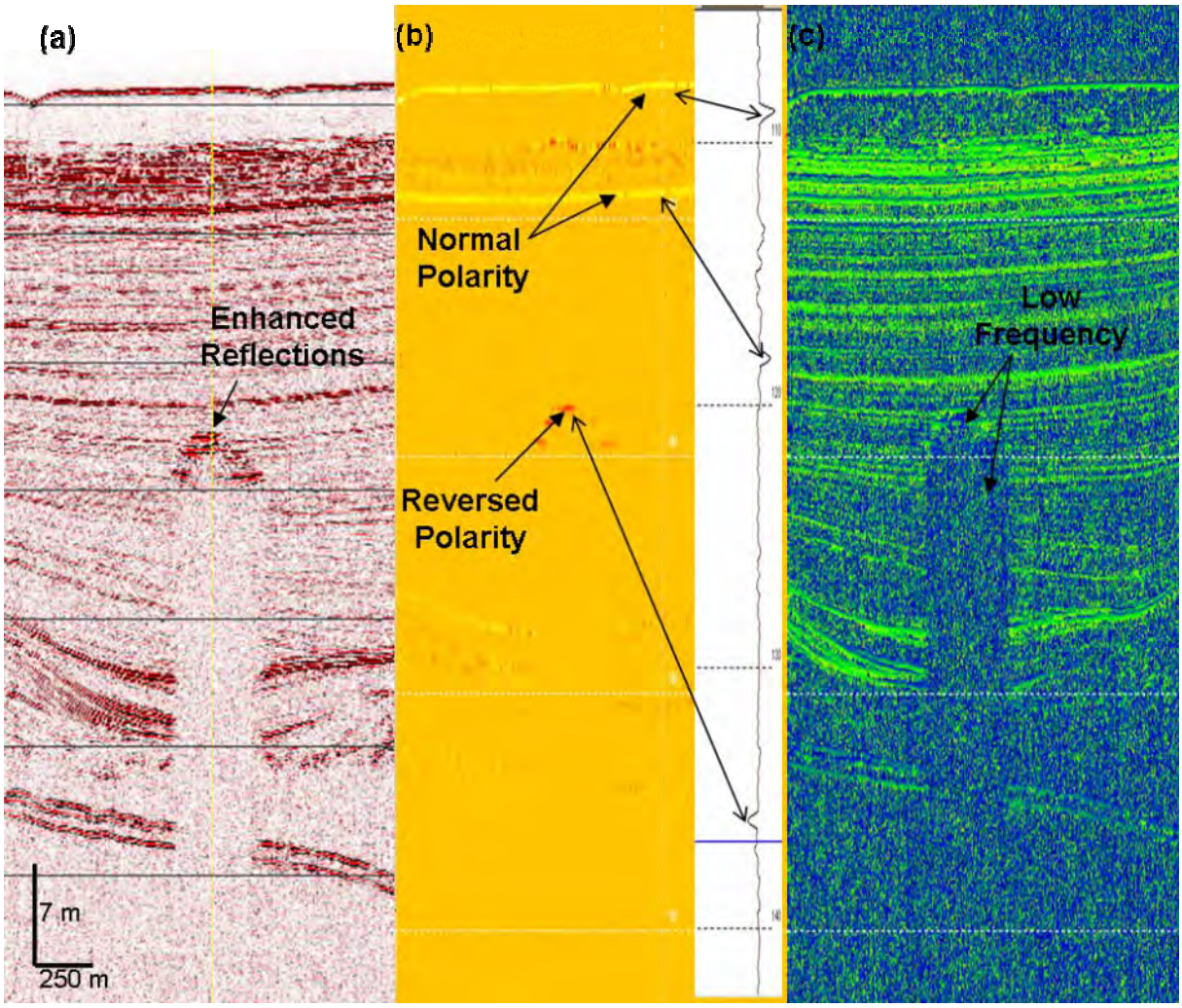

Figure 67 (a) Enhanced reflections within Unit I displayed in amplitude view. (b) Polarity domain displays normal polarity as yellow and reversed polarity as dark orange. (c) Frequency domain displays low frequency as dark blue. Note: the enhanced reflections with reversed polarity have low frequency signals and the underlying signal blanking also has a low frequency, possibly indicating vertical gas migration and trapping at the enhanced reflection surfaces. (Line S282_transit_b-ca)

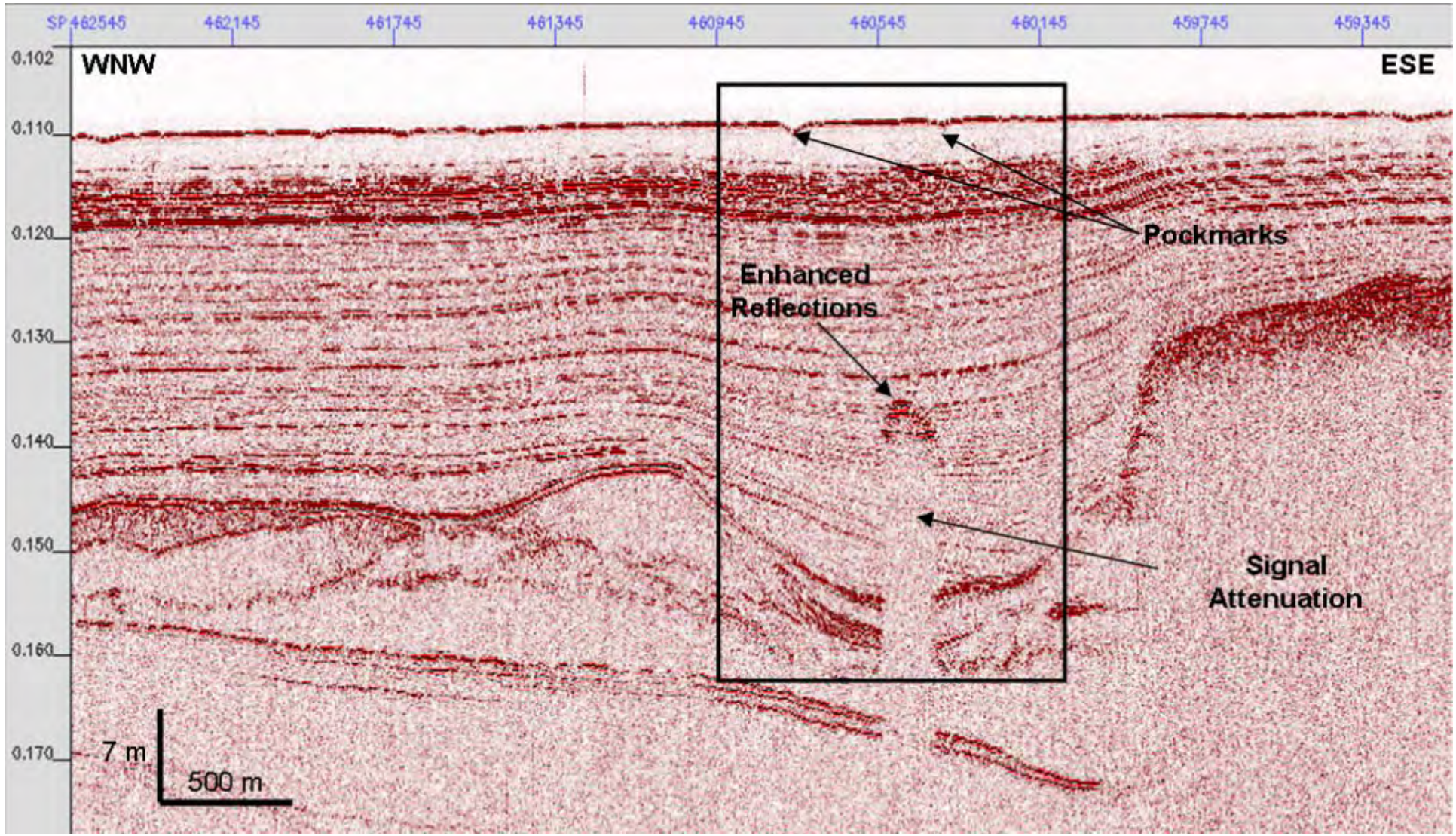

Figure 68 Enhanced reflections within Unit I with signal attenuation through the underlying units and pockmarks on the sea bed (Line S282_transit_b-ca). The area within the black rectangle is displayed in more detail in **Figure 67**.

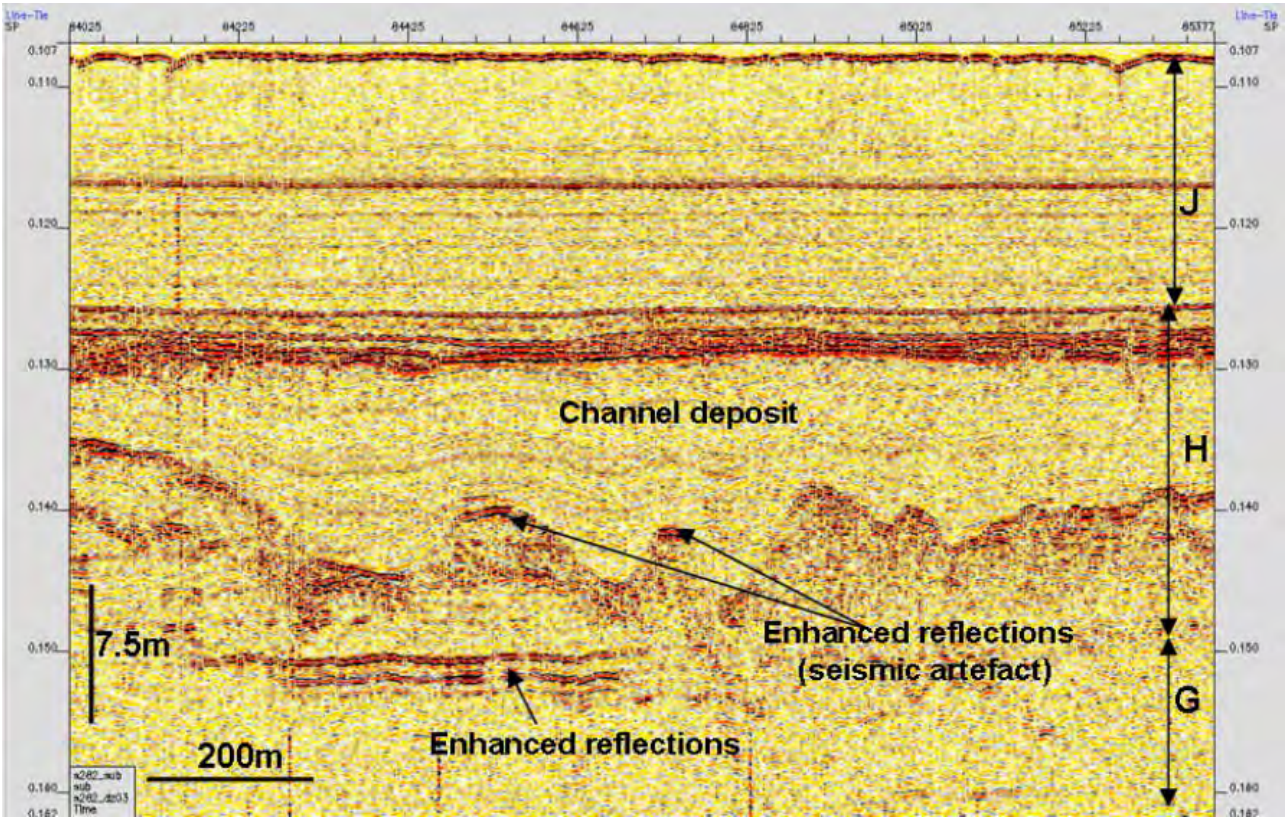

Figure 69 Enhanced reflections below channel of Unit H within Area D. Shows enhanced reflections (at about 0.14 ms) probably caused by a seismic geometry related to changing incidence angle of profile beam with reflector surface (Line S282_dz03).

In Unit G of Area d, enhanced reflections are present at two levels (indicated by yellow and pink arrows in **Figure 70**). The reflector indicated by the yellow arrow has anomalously high-amplitude over part of its length, and is conformable with the stratigraphy above and below. Examples such as this, which show high-amplitude, reverse-polarity and low-frequency, have been attributed by some authors (e.g. Judd and Hovland, 1992) to gas rising laterally and up-dip within relatively coarse sediment layers. In contrast, the sub-horizontal reflections at about 0.16 ms twt, indicated by the pink arrow (**Figure 70**), cut across the stratigraphy of Unit G. In detail, this cross-cutting reflector is composed of reversed polarity segments which step up and down through the stratigraphy of Unit G. This could be interpreted as representing gas exsolving from pore waters or possibly a diagenetic front formed below U7 during low stand exposure. The gas interpretation is favored because of

the low frequency and reversed polarity of these reflectors. A diagenetic front causing mineralization would most probably exhibit normal polarity and higher frequency, if it involved cementation.

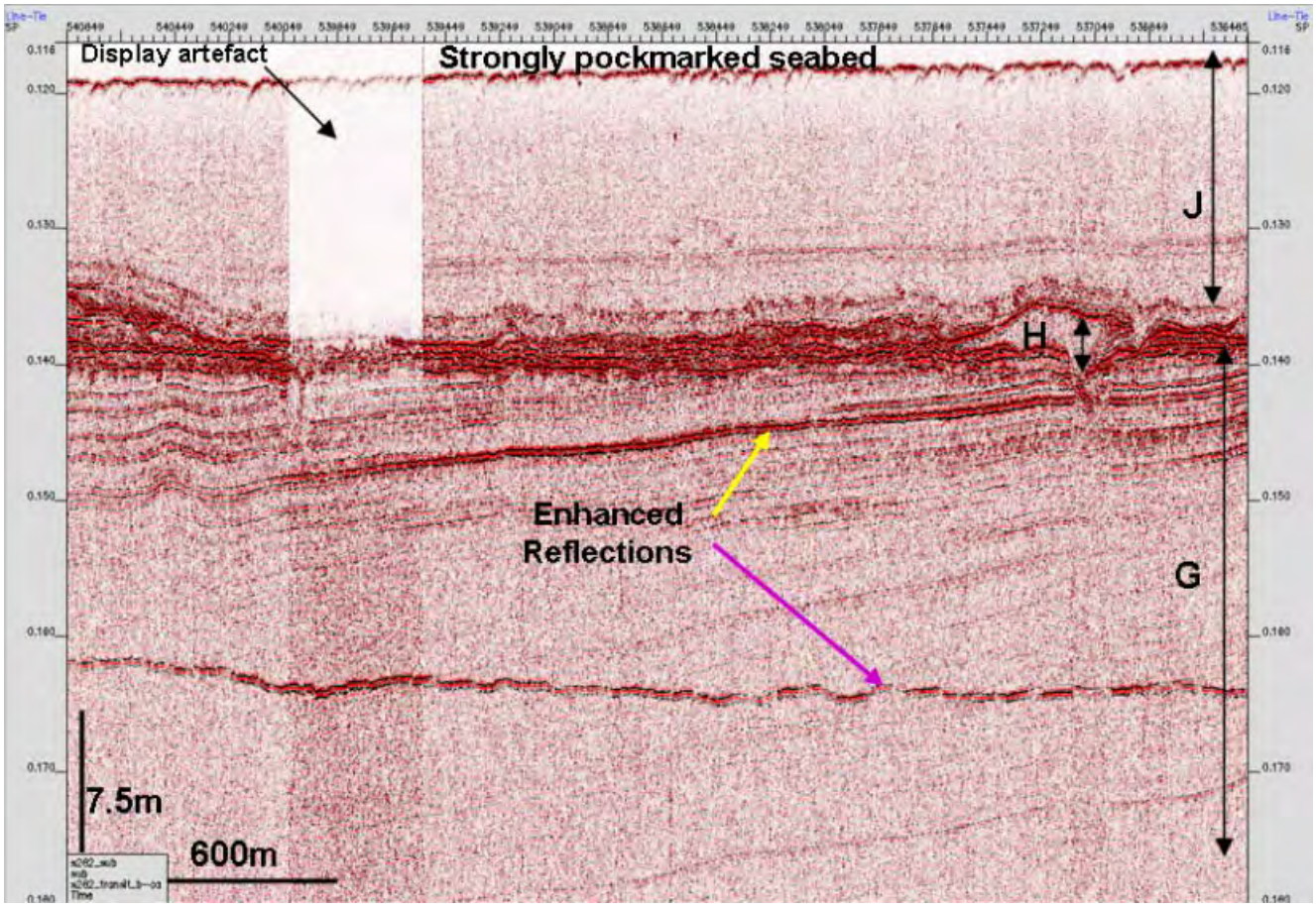

Figure 70 Two levels of enhanced reflections in Unit G that are characterised by reversed polarity (Line S282_transit_b_ca, Area D). Yellow: continuous reflection enhancements along individual inclined reflections within Unit G (implying lateral up-dip migration within relatively coarse layers). Purple: intermittent reflection enhancements cross-cutting the bedding of Unit G. This possibly indicates free gas accumulation at a common depth.

Figure 71 (from Area D) and **Figure 72** (Area C) show laterally-extensive, reverse-polarity enhanced reflections that step up and down between horizons. This suggests vertical gas migration, rather than lateral up-dip migration which would be conformable with the stratigraphy.

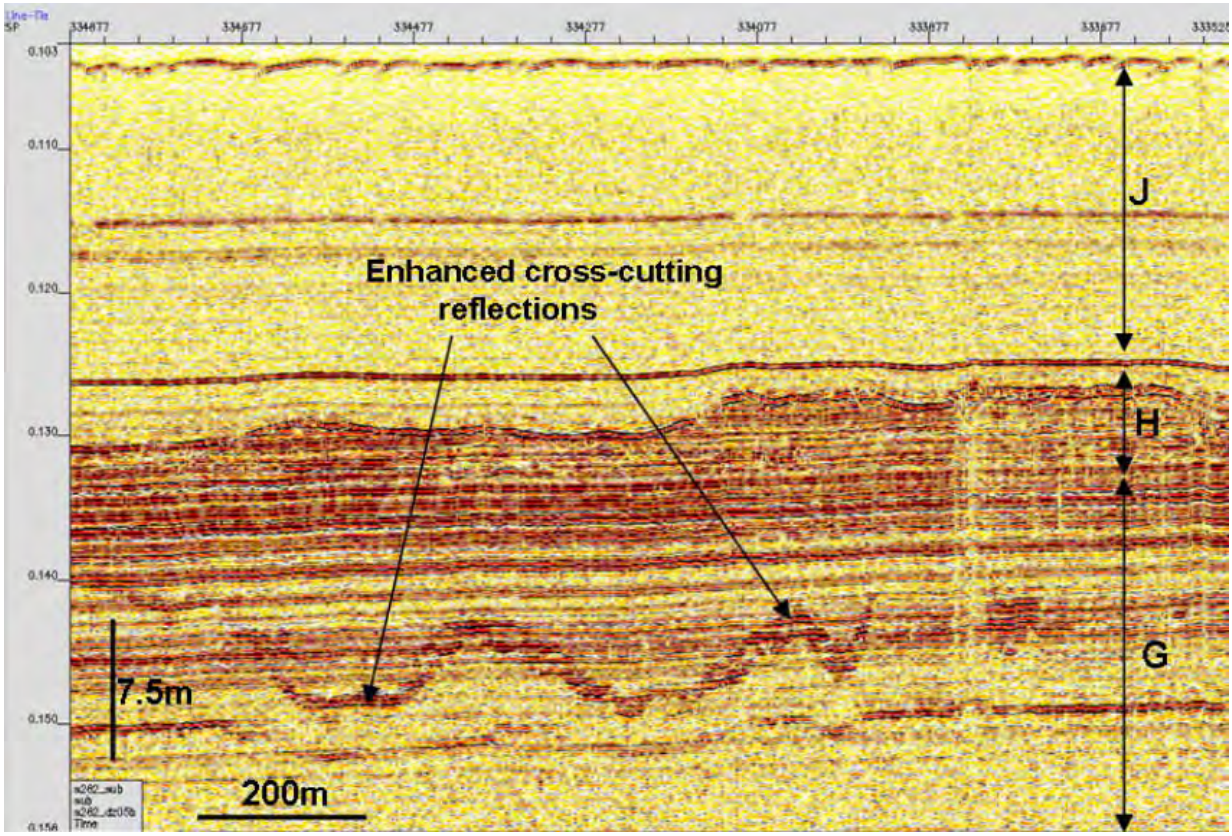

Figure 71 Enhanced reflections with reversed polarity in Area D. These cross-cutting enhanced reflections may indicate a free gas accumulation at depth (i.e. where gas exsolves from porewater) (Line S282_dz05b).

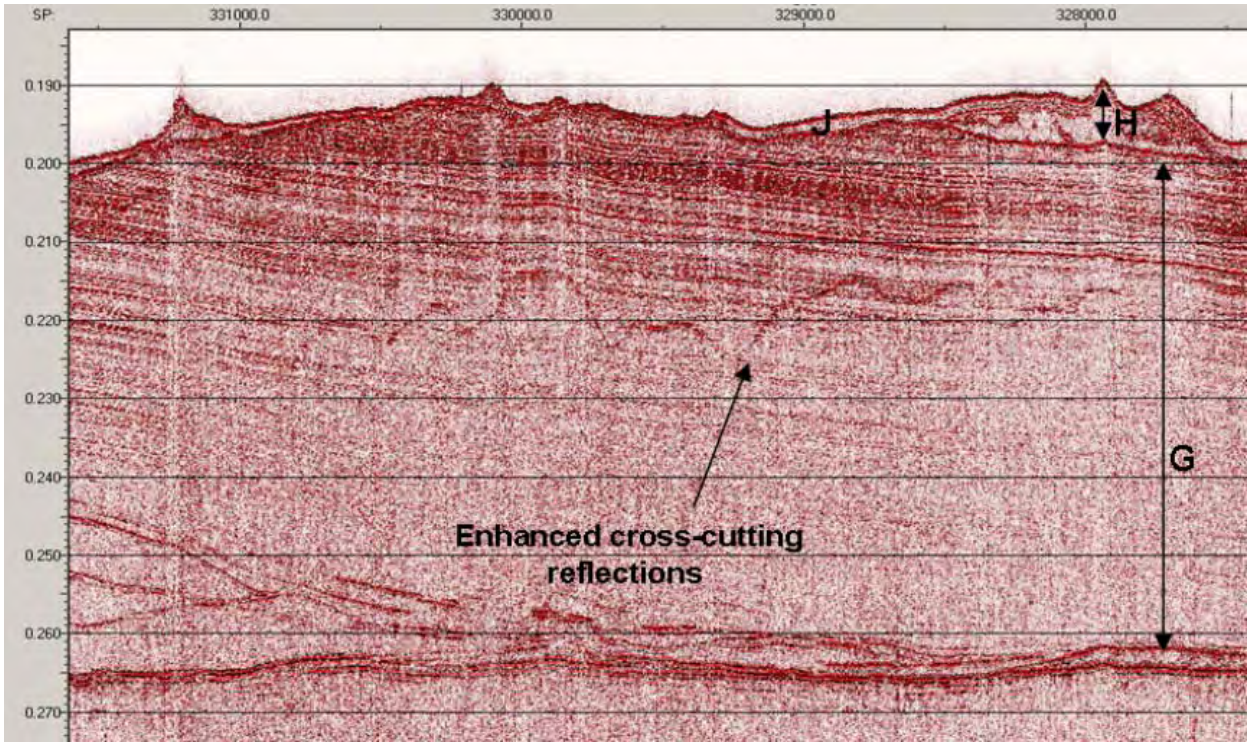

Figure 72 Enhanced reflections with reversed polarity cross-cutting the dipping stratigraphy of Unit G, in Area C. (Line S282_c16, Area C)

In some areas, reversed-polarity enhanced reflections are observed above the apex of the tidal sand ridges in Unit H. This juxtaposition, when associated with concentrations of sea bed pockmarks (**Figure 73**), suggests that gas has migrated into and through the sand body, escaping vertically from the apex and then accumulating in an overlying relatively coarse sediment layer before moving upwards to escape through the sea bed.

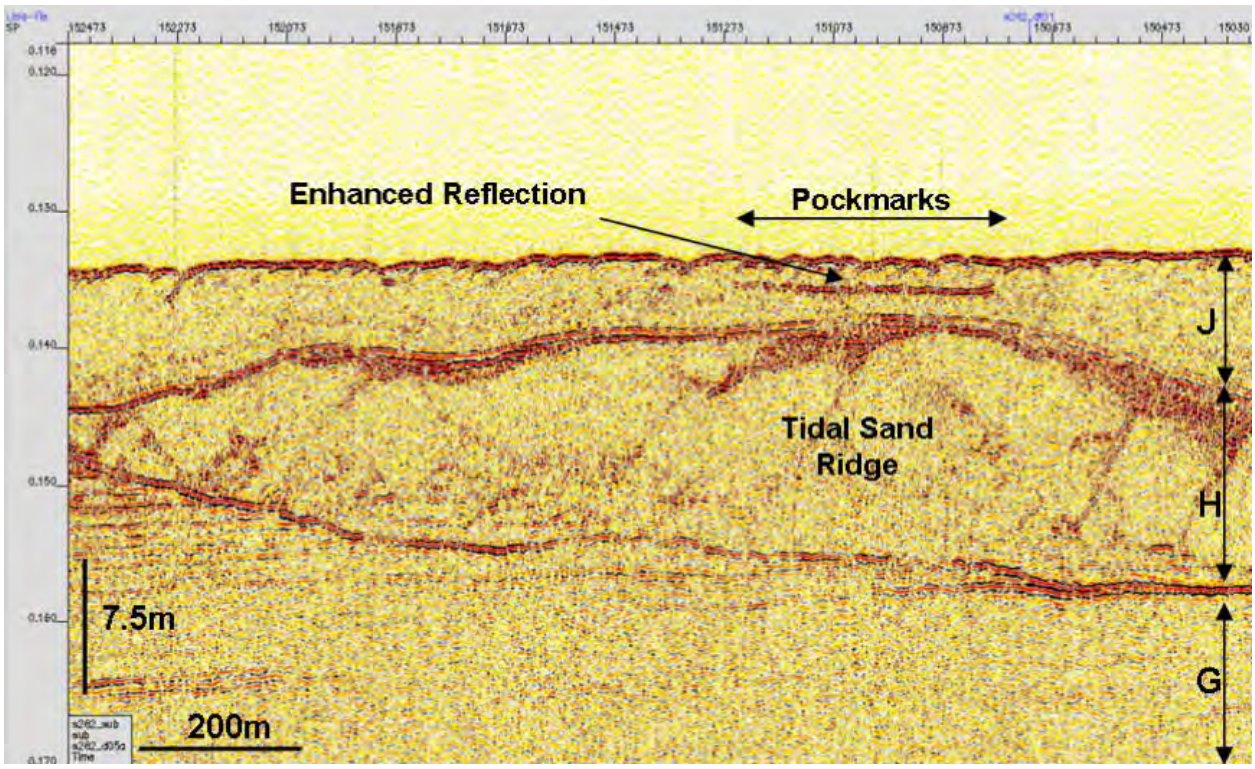

Figure 73 Tidal sand ridge with an enhanced reflector (reversed polarity) above the highest point (Line S282_d05a, Area D). This, together with the pockmarked sea bed above, is a possible indication of vertical gas migration in Unit J.

Acoustic Blanking that may be related to fluid or gas-charge is evident in Unit G in **Figure 74** and in Unit J in **Figure 75**. Signal attenuation caused by overlying high amplitude reflectors is also common and can be either related to the presence of hard layers (**Figure 76**) or to gas charging where the enhanced reflection displays reversed polarity (**Figure 77**). Hard layers (which are normal polarity) can cause signal attenuation and may include cemented sediments and carbonates, including

methane-derived authigenic carbonates. These carbonates may be an indication of palaeo-seepage, particularly where they are associated with underlying enhanced reflections and overlying pockmarks (**Figure 76**). On a larger scale carbonate cementation has been associated with active gas seepage in the Timor Sea (Rollet *et al*., 2006).

In Unit H in Area D, tidal sand ridges and channels are acoustically transparent. This character most likely indicates massive sand deposition with no significant bedding, rather than the presence of gas (**Figure 26a**).

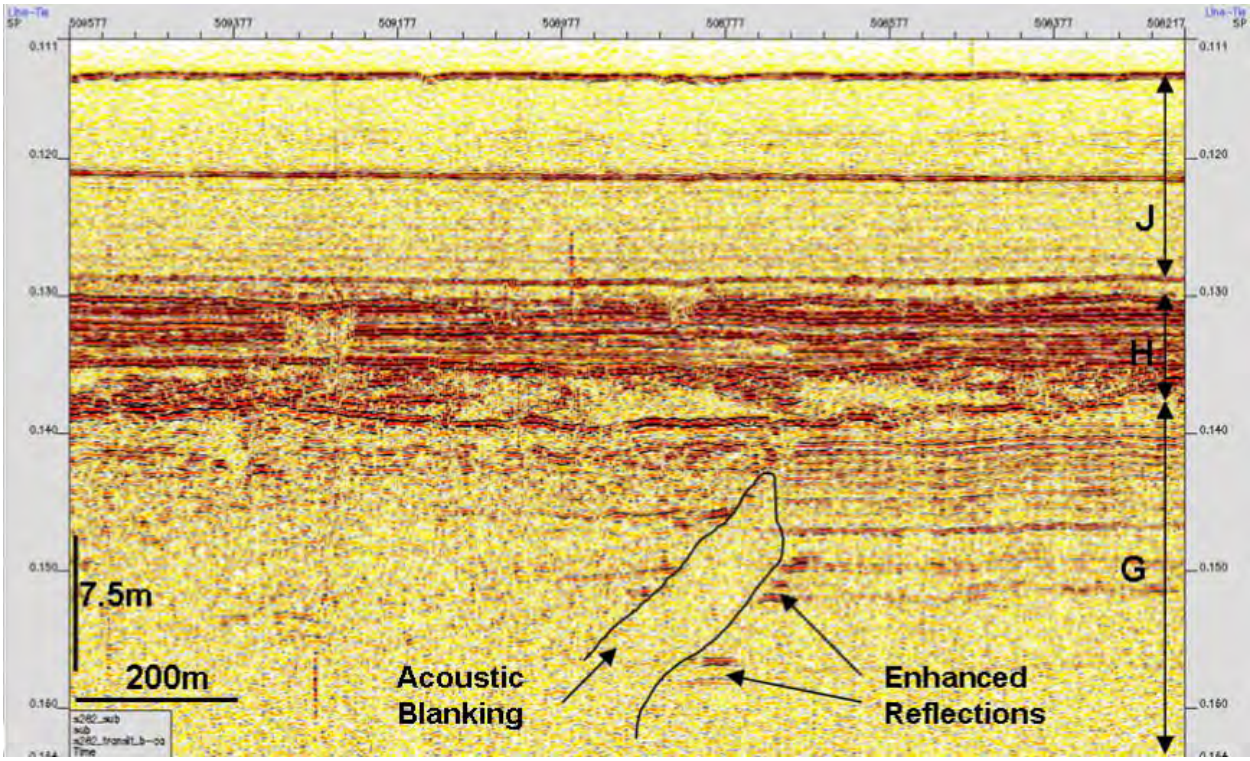

Figure 74 Acoustic blanking with enhanced reflectors on the edge of the blanking zone, probably related to fluid migration (Line S282_transit_b_ca, Area D). Note: this feature is not classed as a gas chimney because it is not vertical.

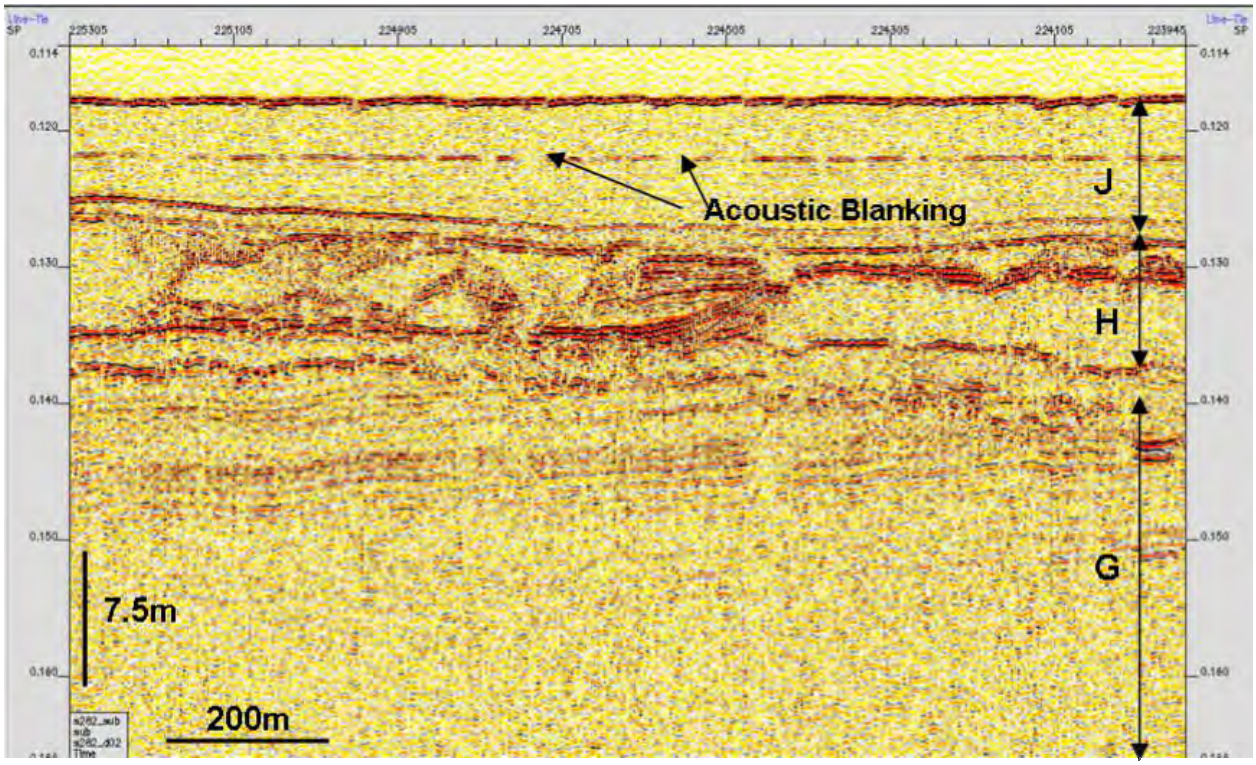

Figure 75 Acoustic blanking probably related to fluid migration in Units G, H and J (Line S282_d02, Area D).

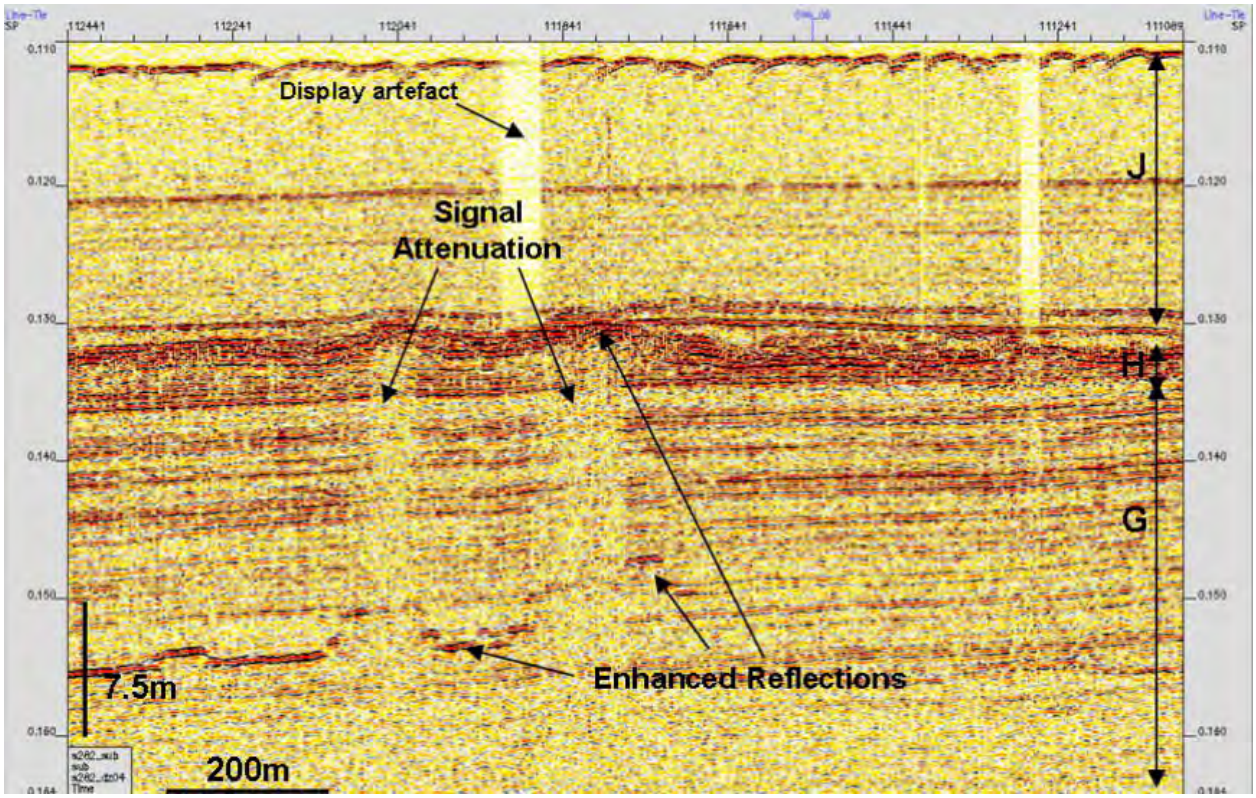

Figure 76 Signal attenuation below enhanced reflections. In this case there is no reverse polarity at the strong reflector, so the enhanced reflection indicates a hard layer, not gas. However, the hard layer might be methane-derived authigenic carbonate, which is supported by the evidence of possible gas migration in Unit G (Line S282_dz04, Area D).

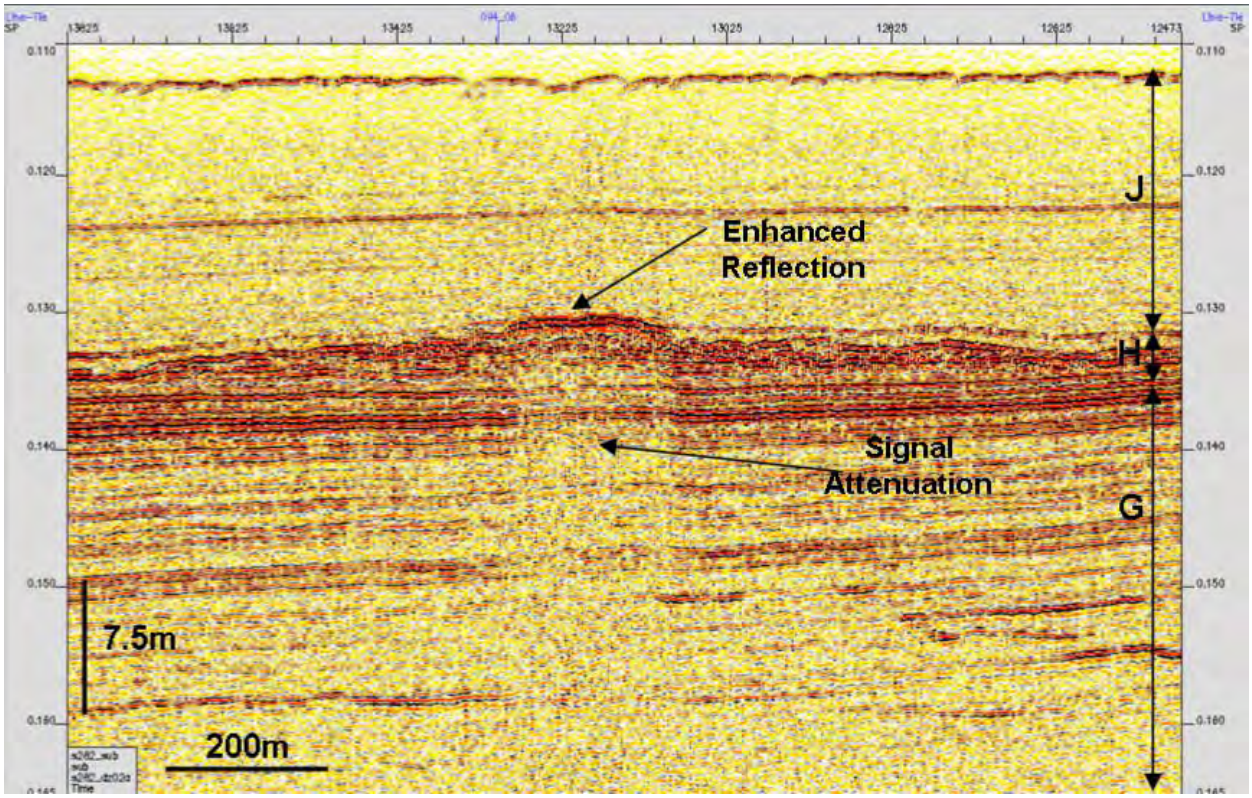

Figure 77 Enhanced reflection probably causing underlying signal attenuation (Line S282_dz02a, Area D).

Pockmarks are sea bed depressions formed by the movement of sea bed sediments by escaping fluids. Pockmarks vary in size depending on the nature of the sea bed sediments, and are generally between a few metres to a few hundred metres across, and from <1m to 20m deep (Judd and Hovland, 1992). Unit J in Areas C and D consists of fine muds, providing a suitable medium for pockmark formation. In the Arafura Survey area, pockmarks are generally present where Unit J is thick (>15 m) (**Figures 75 and 76**). Most pockmarks are small (5-35 m long x 5-15 m across x <2 m deep) and are observed in water depths of 85-220 m. The pockmarks are present in higher density in the western part of Area D as seen in the side-scan data (**Figure 80**) and also identified in the sub-bottom profile data (**Figure 81**). As outlined in Section 3.8.2.3, the density of pockmarks is correlated with grain size of the sediments and is also often correlated with mud filled palaeo-channels where *in situ* generation of gas is occurring (**Figures 78 and 79**).

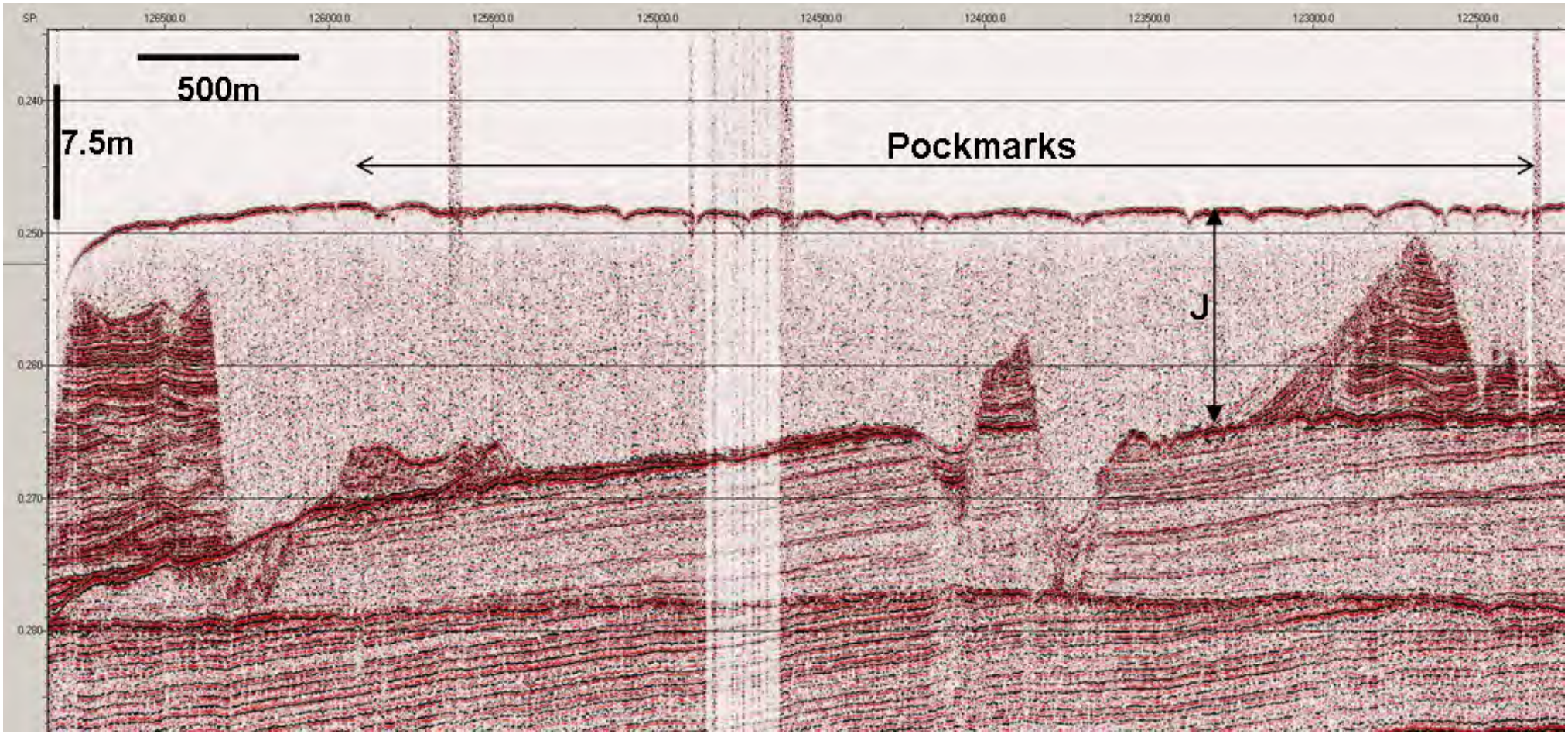

Figure 78 Pockmarks observed in Area C, above the thick Unit J (Line S282_C5).

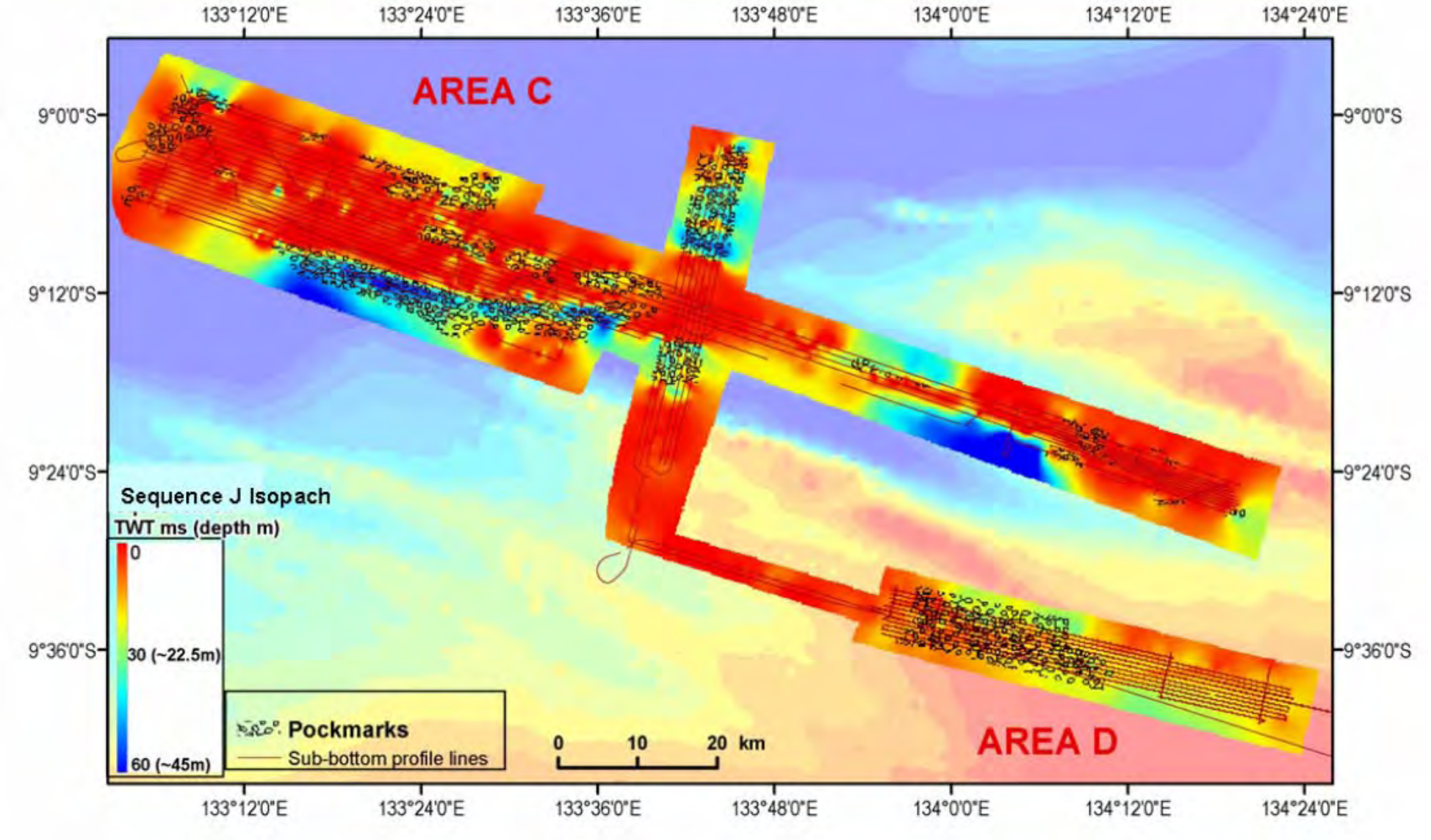

Figure 79 Isopach map of Unit J with areas of intense pockmarking displayed. Note the correlation between the thick Unit J and the pockmarks.

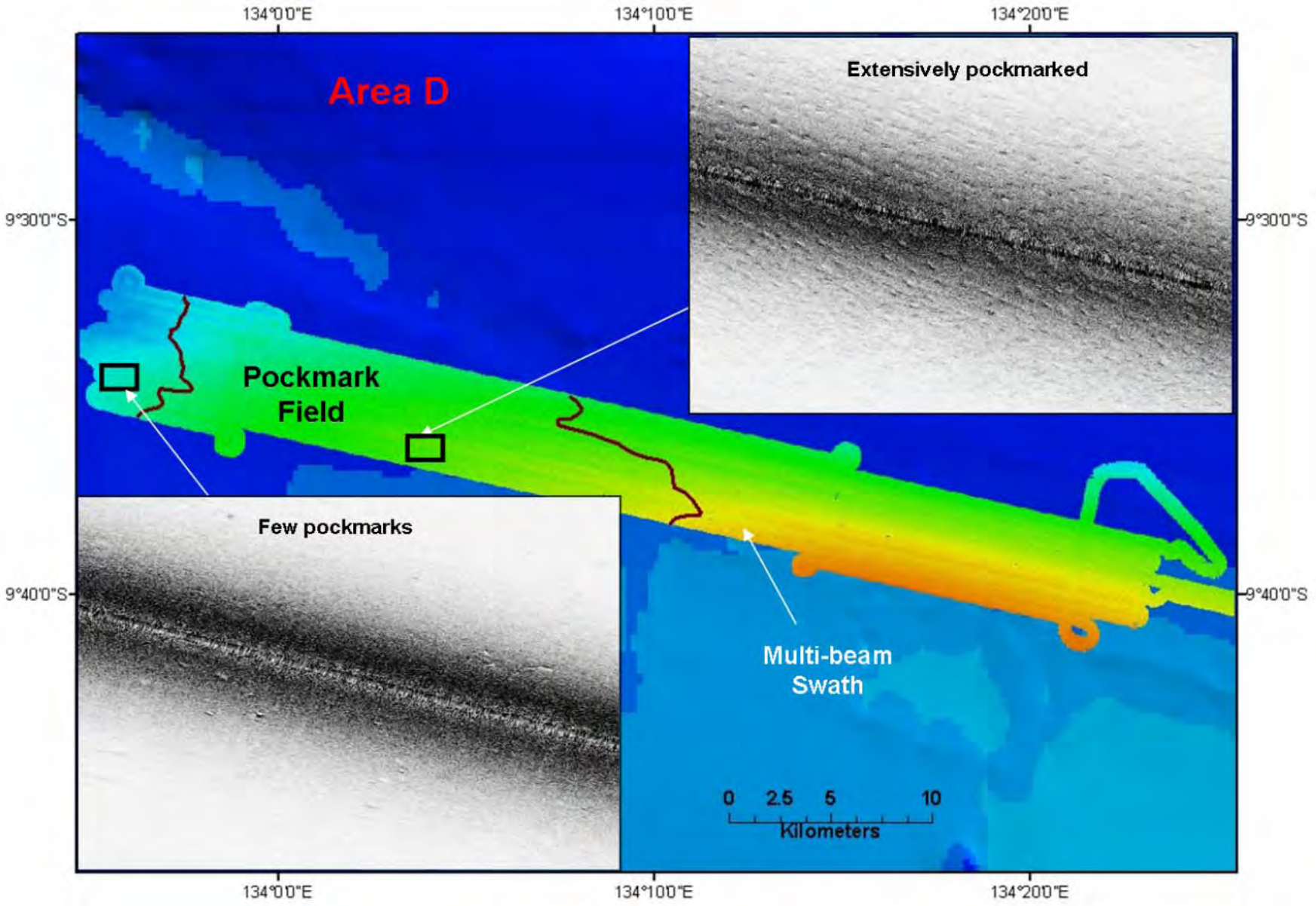

Figure 80 Side-scan sonar images showing the variation in pockmark density across Area D.

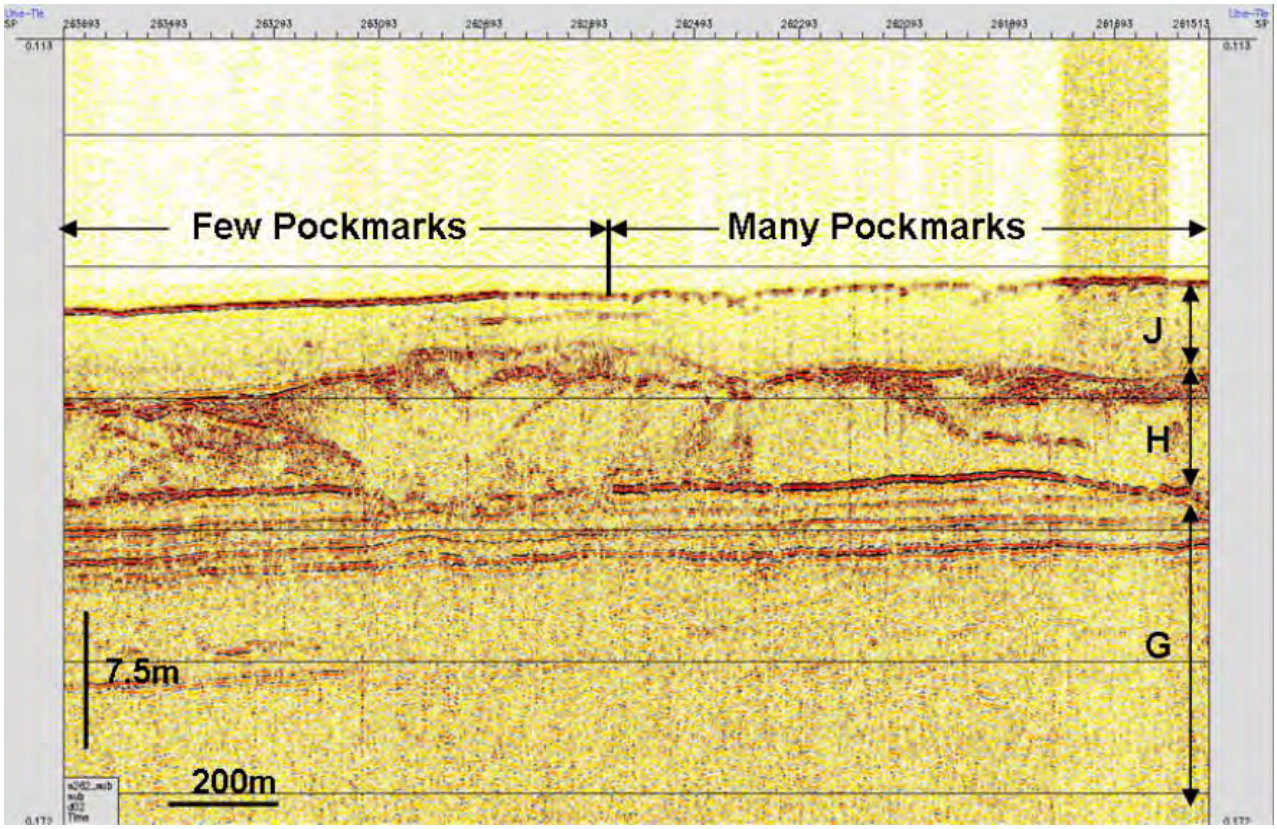

Figure 81 Pockmarks at sea bed. This sub-bottom Line S282_d02 shows western reduction in the areal density of pockmarks in Area D.

Highly reflective sea bed can arise from: cementation of the sea bed due to oxidation of hydrocarbons and precipitation of carbonate cements (Judd and Hovland, 1992; Rollet *et al*., 2006); from hard surfaces, such as rocky outcrop or carbonates; or from a higher than normal abundance of bottom dwelling animals and skeletal remains (Hovland, 1992). **Figure 82** displays the amplitude of the sea bed reflection in Area C. Areas of high reflectivity are generally related to hard surfaces, such as the tops of Pillar Bank and the Eastern Bank (**Figure 83**). The regions where there is evidence of fluid seepage (i.e. high and medium density pockmark fields) are generally correlated with areas of lower reflectivity, corresponding to a muddy sea bed substrate.

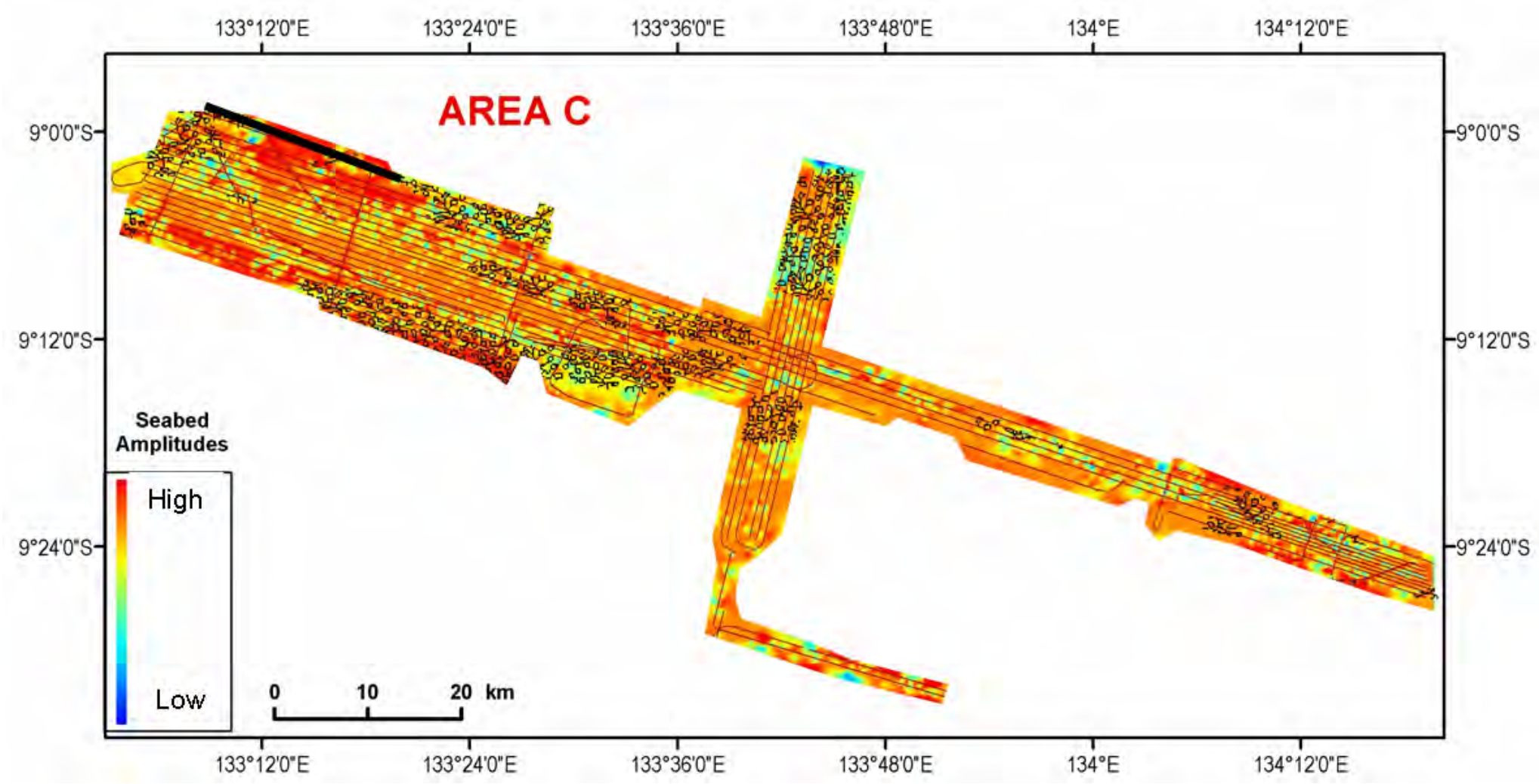

Figure 82 Sea bed reflection amplitude in Area C, with pockmarks marked in black (interpreted from side-scan sonar data). The NW end of Area C displays high amplitudes (shown in red) that are correlated with the underlying older and probably harder units outcropping at the sea bed (**Figure 83**).

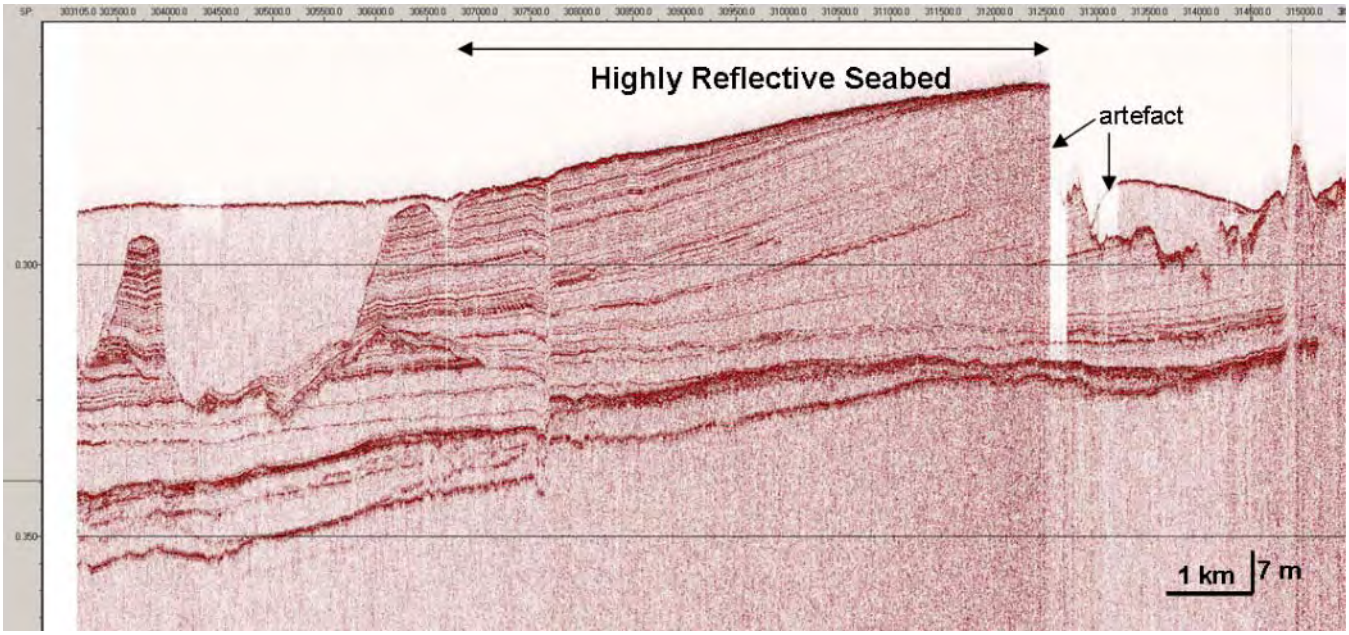

Figure 83 Sub-bottom profile line C14 across an area of highly reflective sea bed. Note, the region of high reflectivity is related to outcropping older and probably harder units (see location of black line **Figure 82**). Acquisition artefact is due to loss of automatic seabed tracking.

Carbonate structures in the Arafura Sea survey areas can be divided into four possible types – calcrete, beach rock, reefs or Methane-Derived Authigenic Carbonate (MDAC). If present, MDAC is direct evidence of gas seepage at the sea bed. The presence of carbonates may explain the sea bed hard-grounds (highly reflective sea bed, e.g. **Figures 82 and 83**) that may have formed during exposure of some terraces in Area C at LGM.

In Area D, there are two features that may be identified as palaeo-carbonate mounds (**Figure 84**) and a palaeo-carbonate crust (**Figure 85**). These features cause a loss of acoustic signal below, which is consistent with seismic imaging of carbonates. The high concentrations of CO_2 in cores collected from this survey area indirectly support the possibility of MDAC within sediments in Area D because the CO_2 had a $\delta^{13}C$ value of -32‰, indicating that it was derived from the oxidation of organic carbon

(recent organic matter or methane gas). The high levels of CO_2 within the sediments will directly effect carbonate precipitation.

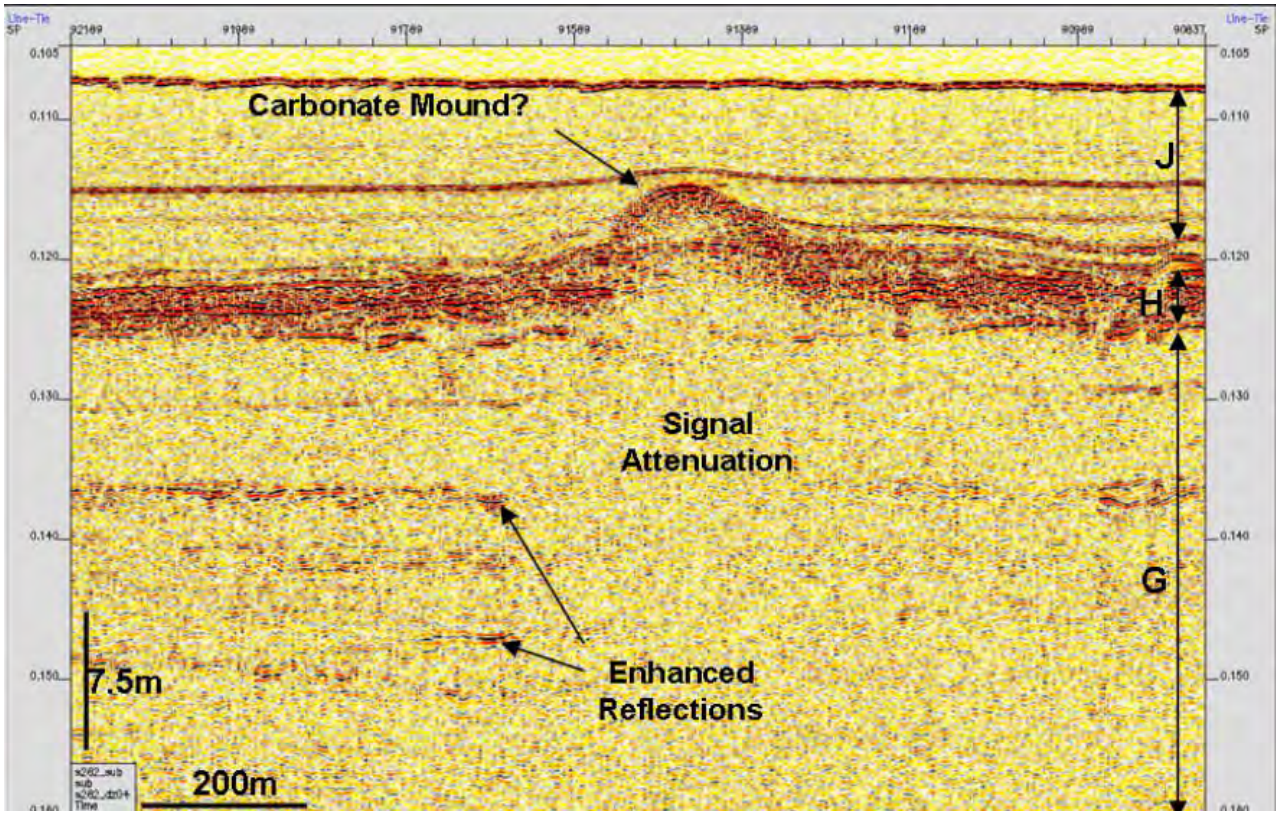

Figure 84 Possible buried-carbonate mound – the normal polarity, enhanced reflection at the top of the mound indicates a hard surface (Line S282_dz04). Enhanced reflections on the margin of the signal attenuation show reversed polarity, indicating possible gas migration coinciding with carbonate mound formation (possible palaeo-seepage feature). Note that Unit J onlaps the mound which suggests that it had positive relief at the time of deposition of Unit J.

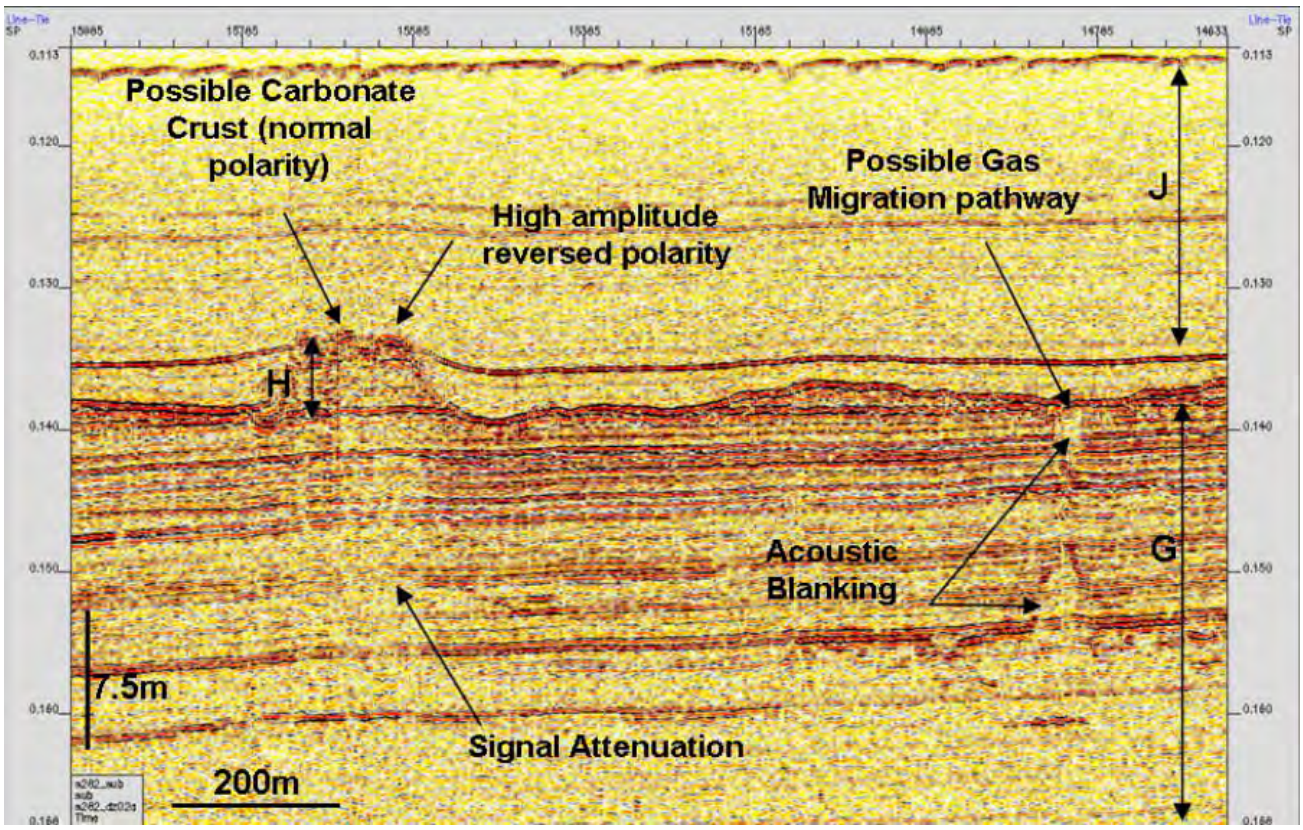

Figure 85 Signal attenuation below enhanced reflection possibly related to a carbonate crust (Line S282_dz02a). Part of the enhanced reflection shows reversed polarity which indicates the possible presence of gas. Note the draping near the base of Unit J over the feature, which suggests that it had positive relief at that time.

Mud Diapirs develop when buoyancy effects cause a body of plastically deforming, fine-grained sediment to pierce the overlying sediment. The plastic material can be either gas-charged or over-pressured clay or mud (Judd and Hovland, 1992). A feature which appears to be a mud diapir was observed in Unit J at the south-eastern end of Area C (**Figure 86**). This feature displays enhanced reflections on its flanks and an enhanced reflection deeper in Unit J that has reversed polarity. This could be an indication that the mud diapir is associated with gas migration. The bathymetry of the sea bed over the mud diapir indicates that the sub-bottom profile line (C8; **Figure 86a and b**) imaged the southern edge of a 3m-high and 140m-wide feature (**Figure 86c**). The multibeam bathymetric data indicate that this feature is one of several in this immediate area. Although salt is often a source of diapir formation, it is not a possible explanation for these structures in the Holocene sediments of the

Arafura Sea because there is no evidence for the formation of evaporates in the region at this time.

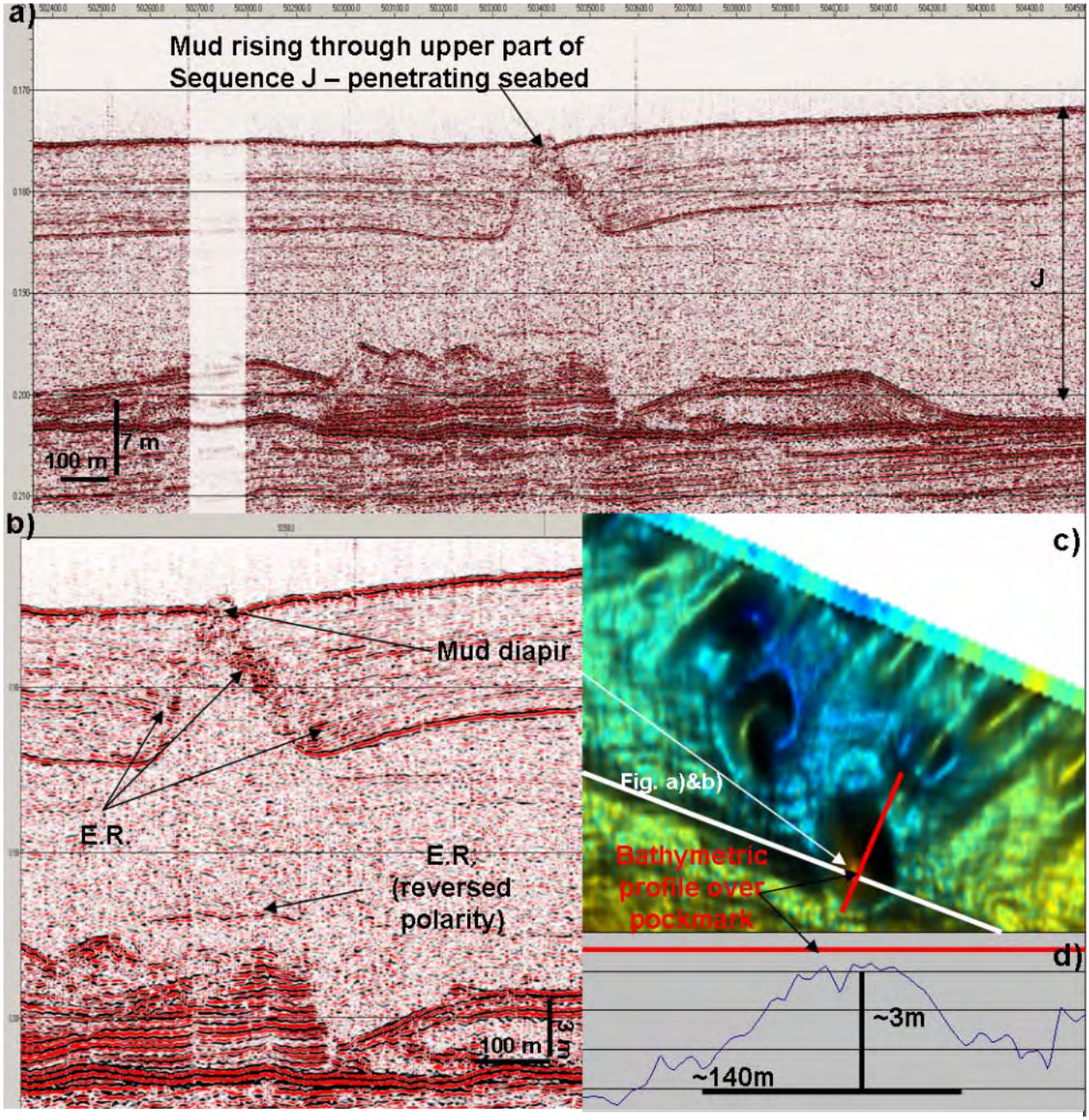

Figure 86 (a) Mud diapir/mound observed in Unit J (Line S282_C8, SE Area C). A depressional moat is observed at the base of the mud diapir due to sediment movement into the mound. (b) Enlargement of Line C8 with (c) corresponding bathymetric image and profile lines. The rising mud may be gas-charged due to enhanced reflections on the margins (polarity is inconclusive) and the underlying reversed polarity enhanced reflection. E.R. = Enhanced Reflection. Note the chaotic seismic character of the material recorded within this feature. d) Bathymetric profile over the diapir (location on Figure c).

Injectites are similar to mud diapirs, in that they also form when mobilised sediments penetrate overlying deposits, but are sand cored. Injectites form when sand is remobilised by sediment fluidisation (Hurst *et al*., 2002). Area D contains possible indications of injectites above Unit H (**Figures 87 and 88**).

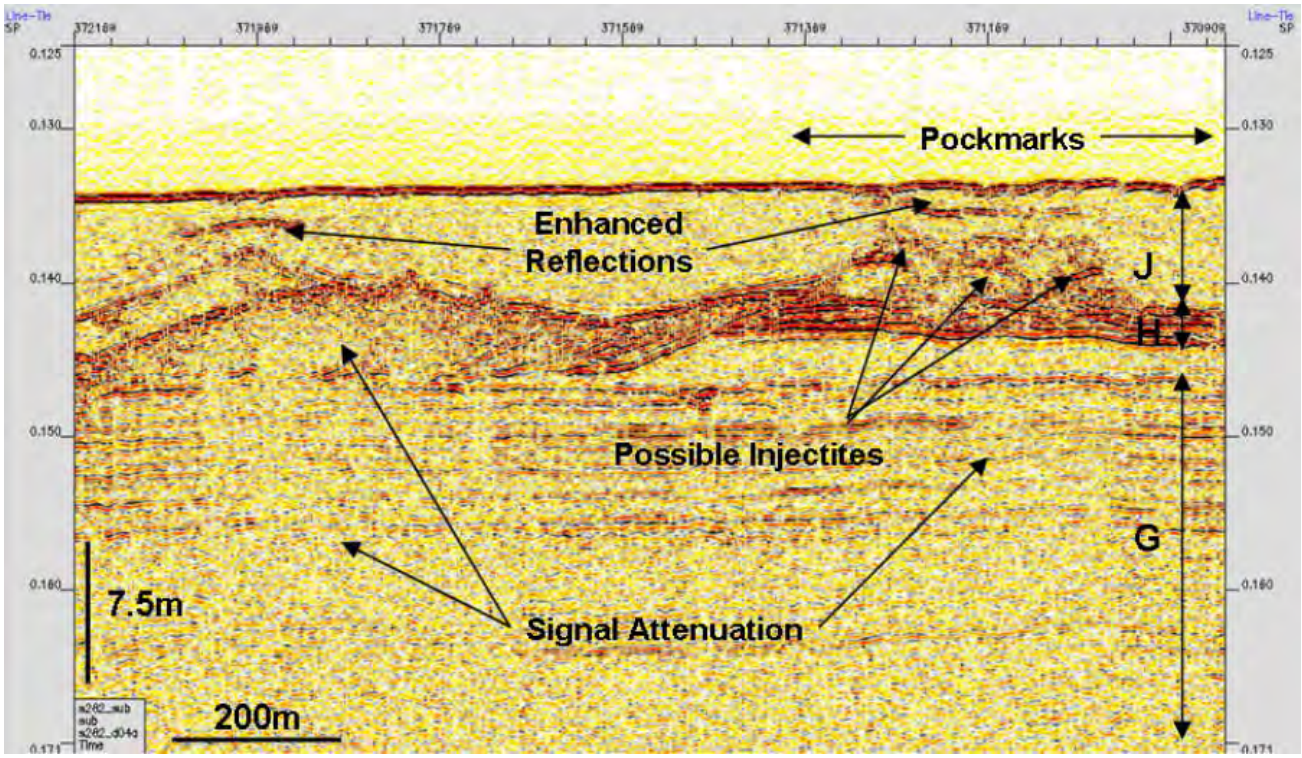

Figure 87 Acoustically transparent sand ridges with reversed polarity enhanced reflectors above the crests (Line S282_d04a). Possible injectites are present below the enhanced reflections giving further evidence of fluid migration.

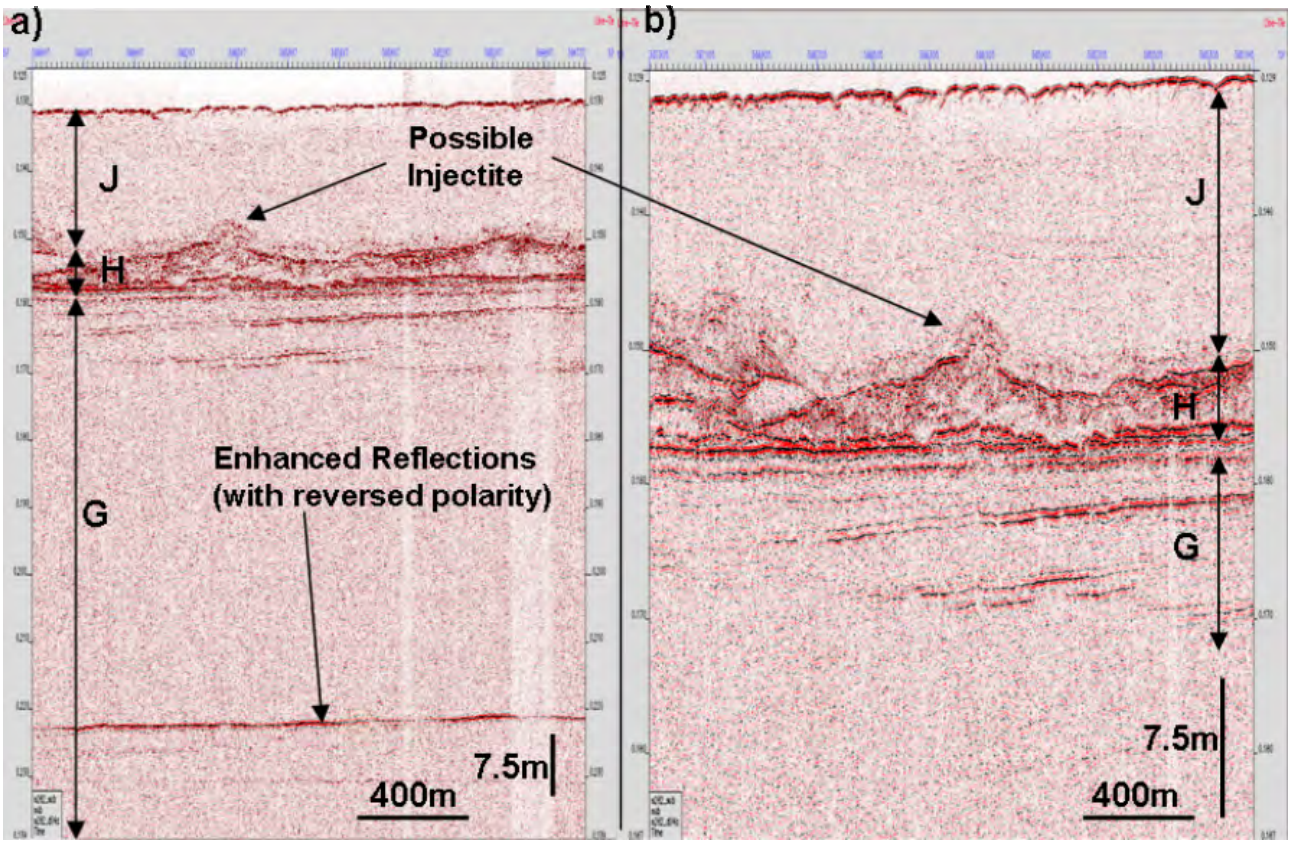

Figure 88 Interpreted injectite possibly related to fluid migration through massive sand bodies in Unit H (Line S282_d04a, Area D). Intermittent reflection enhancements along individual inclined reflections within Unit G imply lateral up-dip fluid migration within relatively coarse layers. Note that (b) is an enlargement of Figure (a).

3.10.2 Correlation with conventional seismic data

Evidence for gas saturation in the deeper (pre- and post- Money Shoal unconformity) sediments was assessed on conventional 2D seismic lines across Areas C and D (**Figure 89**). The areas of interpreted gas in these conventional seismic sections were then correlated with areas of possible shallow gas in the Survey 282 sub-bottom profile data and also with Synthetic Aperture Radar (SAR) anomalies, multibeam bathymetry and side-scan sonar data. In some instances, the survey data correlates with potential hydrocarbon migration pathways to the shallow sub-surface layers, either along faults or along unconformity surfaces. Gas that has migrated from deeper in the section may also be augmented by modern (post-LGM) microbial gas generated within Unit J (see **Section 3.7.1**).

Area D and the south-eastern end of Area C are located above a seismic poor quality data zone (PQDZ) observed in the conventional seismic data (**Figures 89 and 90**). The PQDZ is a well defined vertical zone underneath the major Money Shoal unconformity where the seismic facies is chaotic with variable amplitude (**Figure 90**). The reflection continuity observed on both sides of the zone is lost within the PQDZ. The zone is up to 130 km long and 75 km wide in the eastern part of the Arafura Sea. Its origin is uncertain. It could be due to a wide spread hard-ground on the Money Shoal unconformity preventing signal penetration underneath or it could result from a broad hydrocarbon leakage zone. The PQDZ is located beneath the base Money Shoal (Early Jurassic) unconformity, down to the bottom of the recorded section (**Figure 90**). Some faulting is observed within Area C, these faults are coincident with interpreted shallow gas based on sub-bottom and side-scan sonar data (enhanced reflectors with reverse polarity and pockmark fields) (**Figure 91**).

The correlation of interpreted gas indicators with the deep structure observed on the seismic lines shows that the deepest part of the Arafura Basin, in the northeast of the basin (eastern part of Line 106-10p1), coincides with the PQDZ, the presence of faults in the seismic data, and with reverse-polarity, low-frequency, enhanced reflectors and pockmark fields. Integration of these observations suggests that shallow gas interpreted in Areas C and D could be supplemented by deeper gas accumulations migrating to the sea bed either along faults or the major Money-Shoal unconformity.

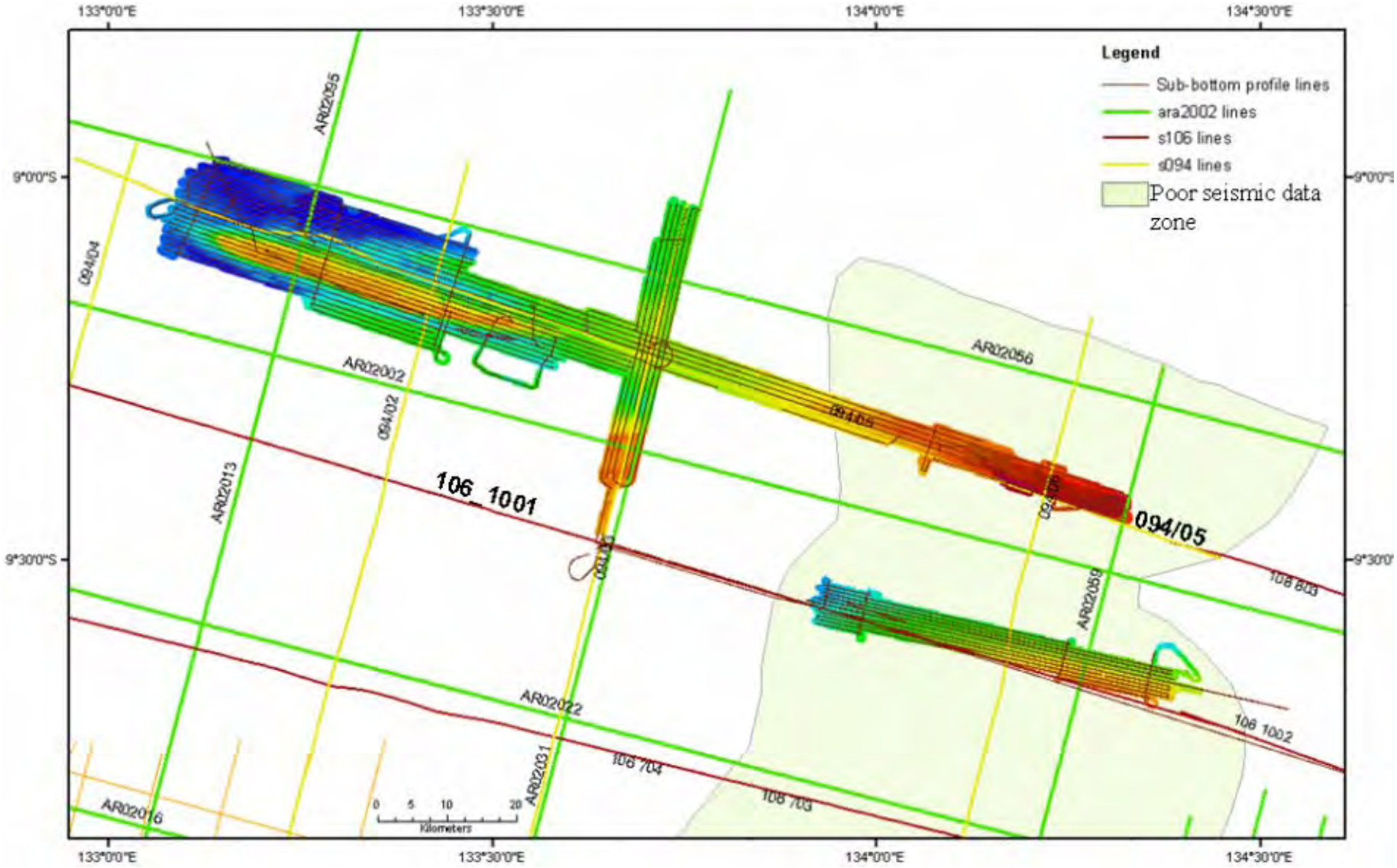

Figure 89 Location of deep seismic profiles (green, yellow and red lines) in the survey area, combined with sub-bottom profiles location (brown lines). The poor quality data zone (pale green polygon) is located over Area D and the eastern part of Area C.

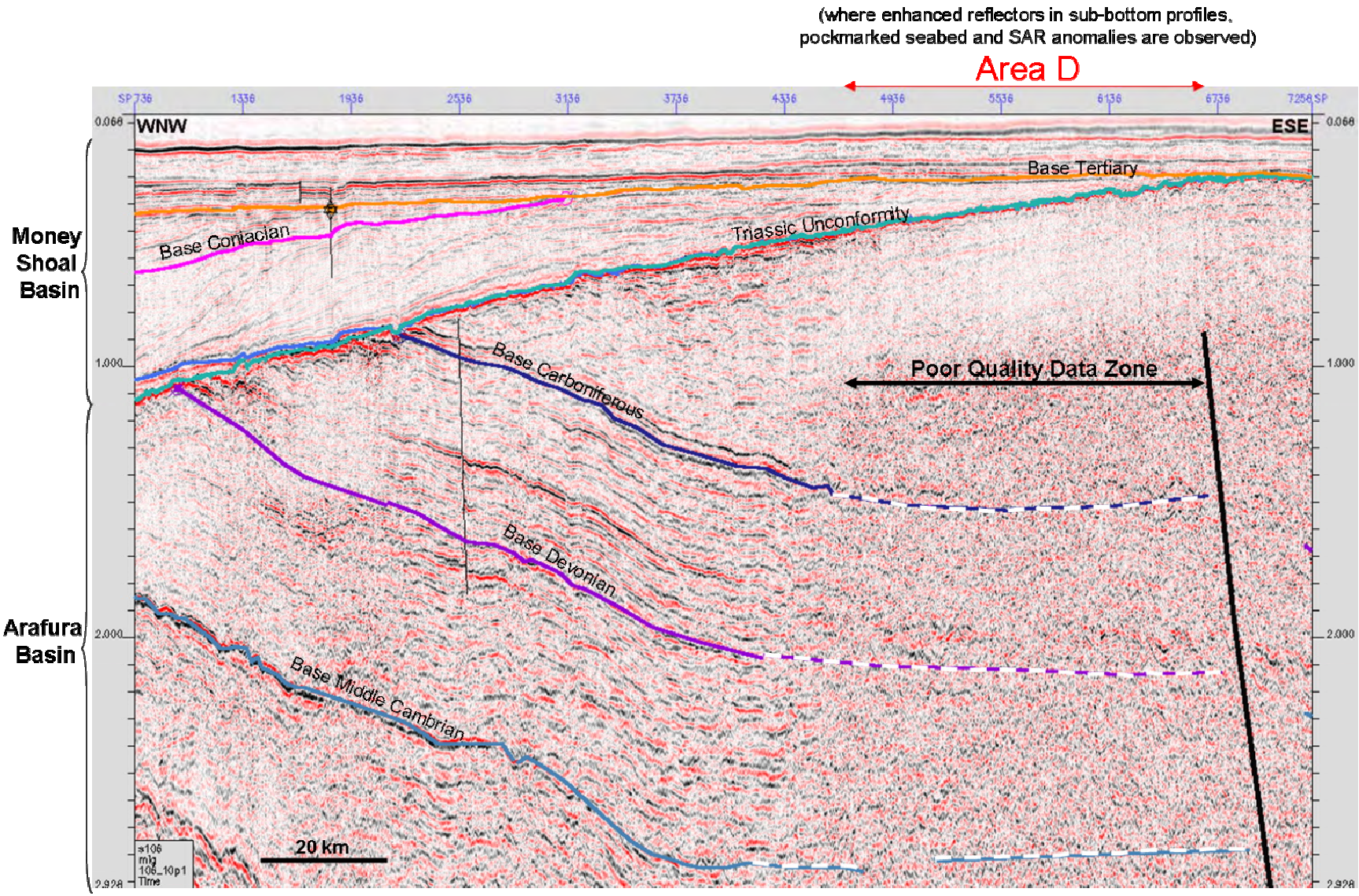

Figure 90 Conventional seismic Line 106_1001 over Area D showing the different geological units from the Precambrian to present. Note the chaotic seismic facies within the poor quality data zone located beneath the zone with evidence for shallow gas observed in Area D. This area correlates with enhanced reflections observed in the sub-bottom profiles, pockmarks on the sea bed and SAR anomalies.

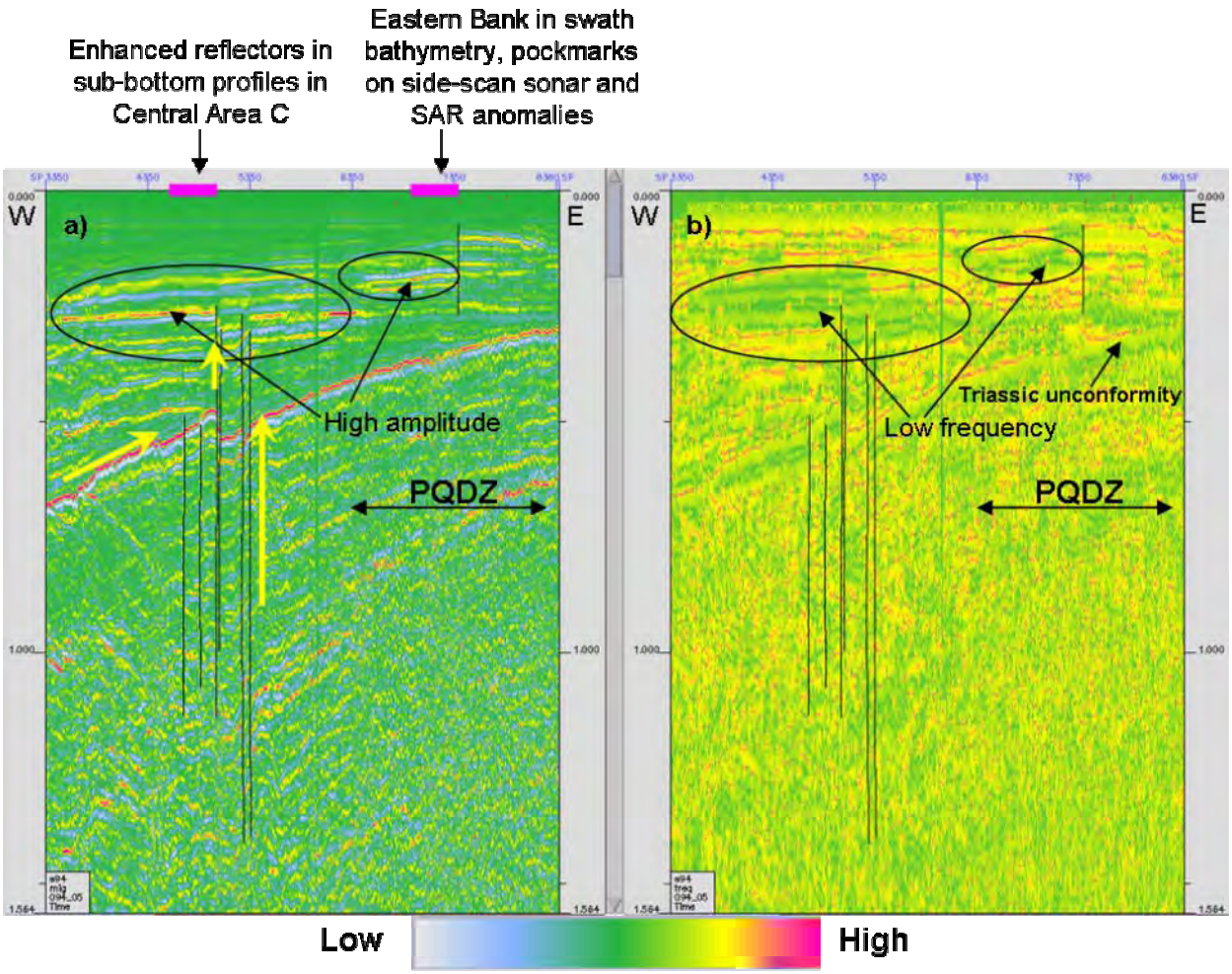

Figure 91 a) Amplitude display of Line 094/05 across Area C, from west to east. b) Same section in the frequency domain. The high-amplitude anomalies in pink in figure a) correlate with low frequencies in green in figure b) suggesting that gas may have migrated from depth. The reflectors underlie areas of interpreted shallow gas in sub-bottom profile data. In this case, gas probably migrated along the faults or the Triassic unconformity (marked by yellow arrows). PQDZ: Poor Quality Data Zone (see location **Figure 89**). Black vertical lines represent faults probably active during the Jurassic.

3.10.3 Summary of occurrence and distribution of gas indicators

Across the survey Areas C and D, a range of gas indicators have been described (**Section 3.10.1**). Their occurrence and expression appear to be related to the nature of the host facies. Unit J is composed of a sandy mud and intense pockmark fields are developed generally where this mud is thickest. The area density of pockmarks declines as sediment grain size increases. Unit J also has direct evidence for microbial methane generation based on the analysis of head space gas samples

(**Section 3.7.1**). However, there is not a simple one-to-one correlation between the palaeo-channels that contain the thickest Holocene mud packages and the high-density pockmark fields (**Figure 79**). There are areas where Unit J is thick that do not have pockmarks, notably in the eastern part of Area C, and also areas where the unit is thin but where high-density pockmarks occur, for example the western end of Area C (**Figure 79**). This suggests that *in situ* generation of microbial gas may not be the only factor responsible for fluid expulsion in Unit J.

Below Unit J, a range of possible gas indicators have been observed. Possible injectites have been interpreted within Area D (**Figures 87 and 88**). These may be dewatering features related to underlying sand bodies, but they could also be related to gas. The presence of reverse-polarity, enhanced reflections above the crests of these sand bodies and signal attenuation below (**Figures 69, 78 and 84**) suggests that over-pressure due to gas is a more likely reason for these injectites.

High-amplitude, reverse-polarity, low-frequency reflections are observed in Unit J, I, G, E and C within Areas C and D. These reflections display three different characteristics:

1. Within Unit J, these reflections are sub-horizontal and often co-occur with pockmarks at the sea bed and fluid movement features in the underlying units (**Figure 84**).
2. Dipping, bedding-conformable enhanced reflections with reverse-polarity and low-frequency are observed in Units I, G, E and C and are interpreted as evidence of gas migration (**Figure 70**).
3. Cross-cutting reflections are widely observed within Unit G in Areas C and D (**Figures 70, 71 and 72**). In detail, these reflections are low-frequency, reverse-polarity, and high-amplitude and step up and down through the stratigraphy of Unit G. These reflections are interpreted to be a gas front.

The presence of gas indicators beneath Unit J supports the interpretation that other sources of gas may also contribute to the formation of pockmark, not just the *in situ* generation of microbial gases that was documented during the survey (see **Section 3.7.1**). The widespread occurrence of cross-cutting reflections in Unit G may indicate that shallow gas is present over a large area. In some areas, dipping, bedding-conformable enhanced reflectors are observed in conjunction with an up-dip cross-cutting reflection (**Figure 70**). The development of the dipping, bedding-conformable enhanced reflections, with reverse-polarity and low-frequency in Units I, G, E and C suggests widespread gas migration through the upper 70 m of section studied using sub-bottom profile data. These progradational units are stacked in an apparently retrogradational pattern, with each prograding unit stepping back to the southeast. This overall stacking pattern and the internal progradational geometry create a potential migration pathway from northwest to southeast (**Figures 24 and 25**).

The wide-spread presence of gas indicators on a NW-SE trend is consistent with observations made in conventional seismic data across the survey area. The development of the PQDZ, outlined in *Section 3.10.2* and illustrated in **Figures 89 and 90**, correlates with the wide distribution of enhanced reflectors with reversed polarity and low-frequency in the sub-bottom profile data in both Areas C and D. Deeper faults (**Figure 92**) and associated gas indicators in conventional seismic data (**Figure 91**) have been mapped below survey areas where gas indicators are common in sub-bottom profile data. The possible NW-SE gas migration trend observed in sub-bottom profile data is consistent with the sedimentary dip of the Money Shoals Basin (**Figure 93**). The east to south-easterly dip of the Proterozoic-Palaeozoic section beneath the Triassic unconformity is favourable for the migration of hydrocarbons into the westerly dipping Money Shoal Basin reservoirs (**Figure 93**). The stratigraphy, structural architecture and petroleum systems of the Arafura Basin are covered in greater detail in Struckmeyer (2006).

3.11 POSSIBLE CONTROL OF SEA-BED FEATURES BY DEEPER STRUCTURAL ELEMENTS

Major faults and the depth to basement have been mapped using conventional seismic data by Struckmeyer (2006) (**Figure 92**). Accurate mapping of the faults across the region is limited by the spacing of the seismic grid and by data quality. Despite this limitation, several major Proterozoic faults are interpreted to underlie the survey area and their orientation appears to be similar to the orientation of some shallow faults mapped on sub-bottom profile (**Figure 94**). There is no direct connection between the Proterozoic faults and sea bed. While the major faults do not offset the Money Shoals unconformity, deformation zones above these faults are commonly the site of Early Jurassic extensional faulting. In some instances, minor Cainozoic extensional and contractional faulting also occurs (**Figures 91 and 93**). Therefore, it is possible that a deeper structural grain, provided by the first-order Proterozoic faults may be controlling the development of later faults up to the sea bed.

At a broad scale, it appears that there may be some correlation between the extent of some of the bathymetric features and the location of some of the Proterozoic faults (**Figure 92**). Shallow faults observed in the sub-bottom profile appear to be focused above the second-order Jurassic faults, which in turn are focused above the Proterozoic faults (**Figure 93**). We speculate that the structural grain developed at depth may influence some of the surface morphology. If the faults have been successively reactivated, as suggested here, then these interconnected faults could provide a fluid migration pathway from the deeper parts of the Arafura Basin up to the sea bed.

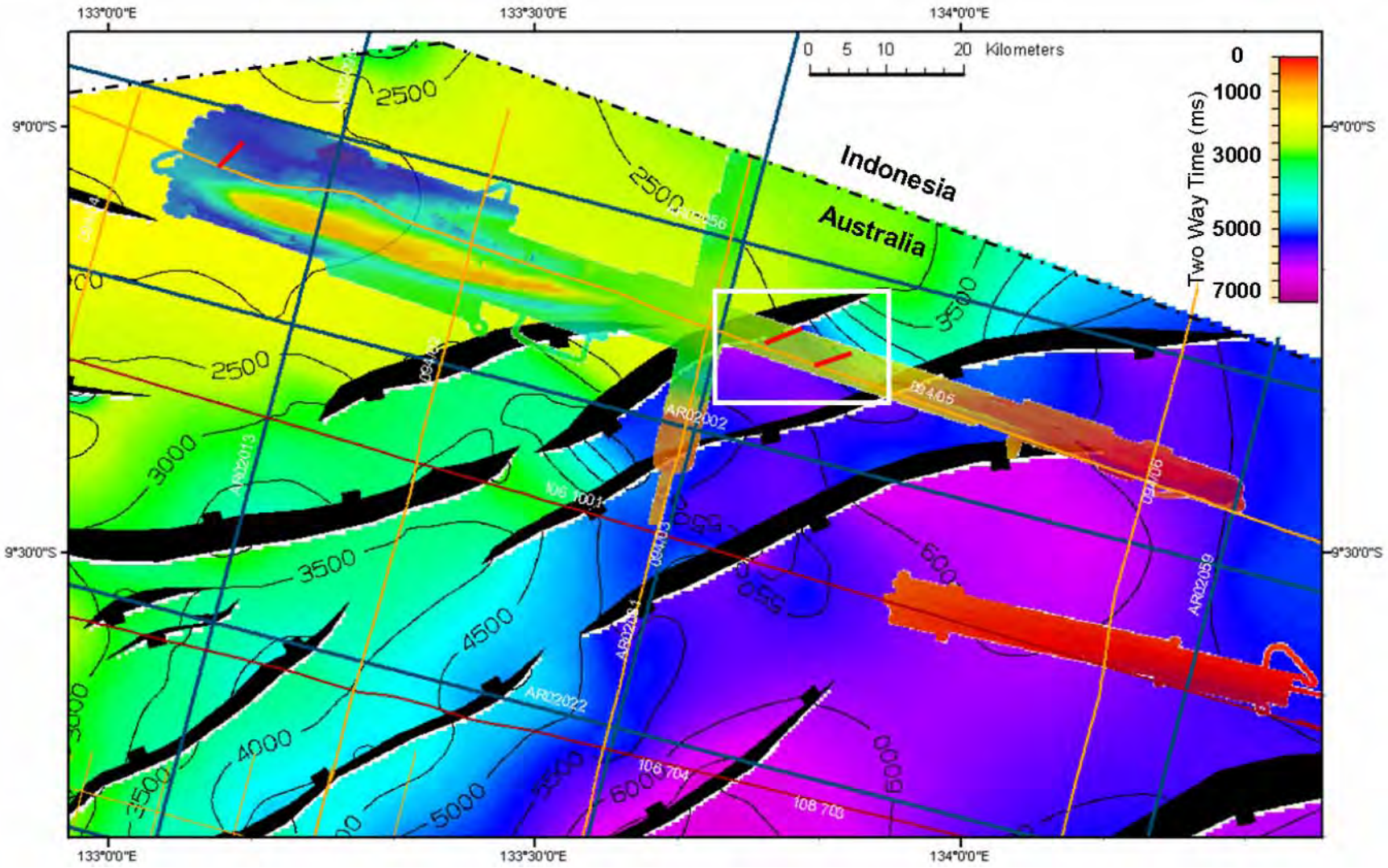

Figure 92: Multibeam bathymetry image in Areas C and D superimposed on the isochron structure map of the Base Wessel Group (Proterozoic). The major SW-NE Proterozoic faults are mapped in black. The recent faults observed on the sub-bottom profile data are shown in red. The white rectangle shows the location of **Figures 93 and 94**.

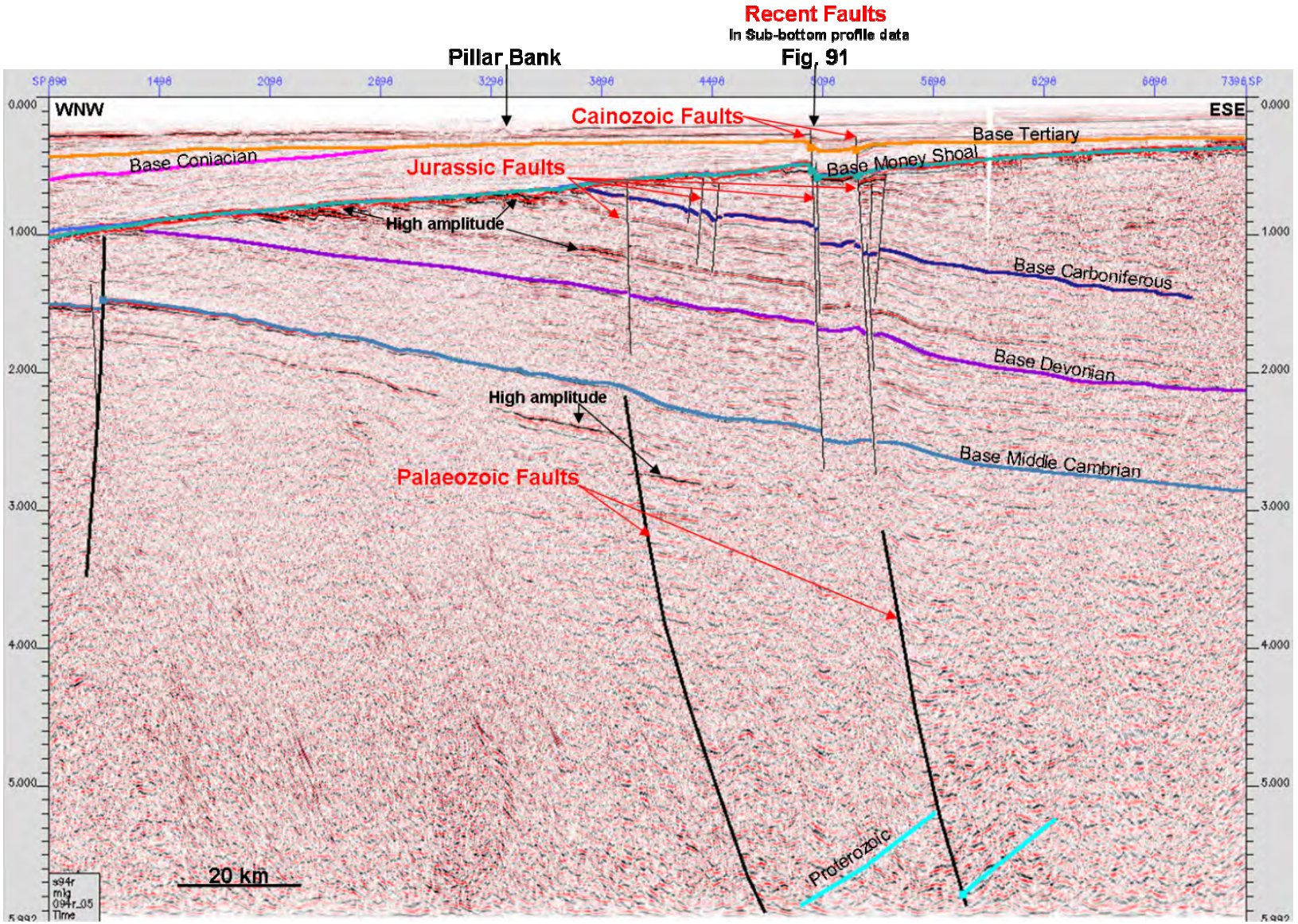

Figure 93 Conventional seismic Line 94r/05 (location in **Figures 89 and 92**) showing the superimposition of faults from the Palaeozoic, Jurassic, Cainozoic and Recent time (See **Figure 91**). These faults are potential vertical migration pathways from depth.

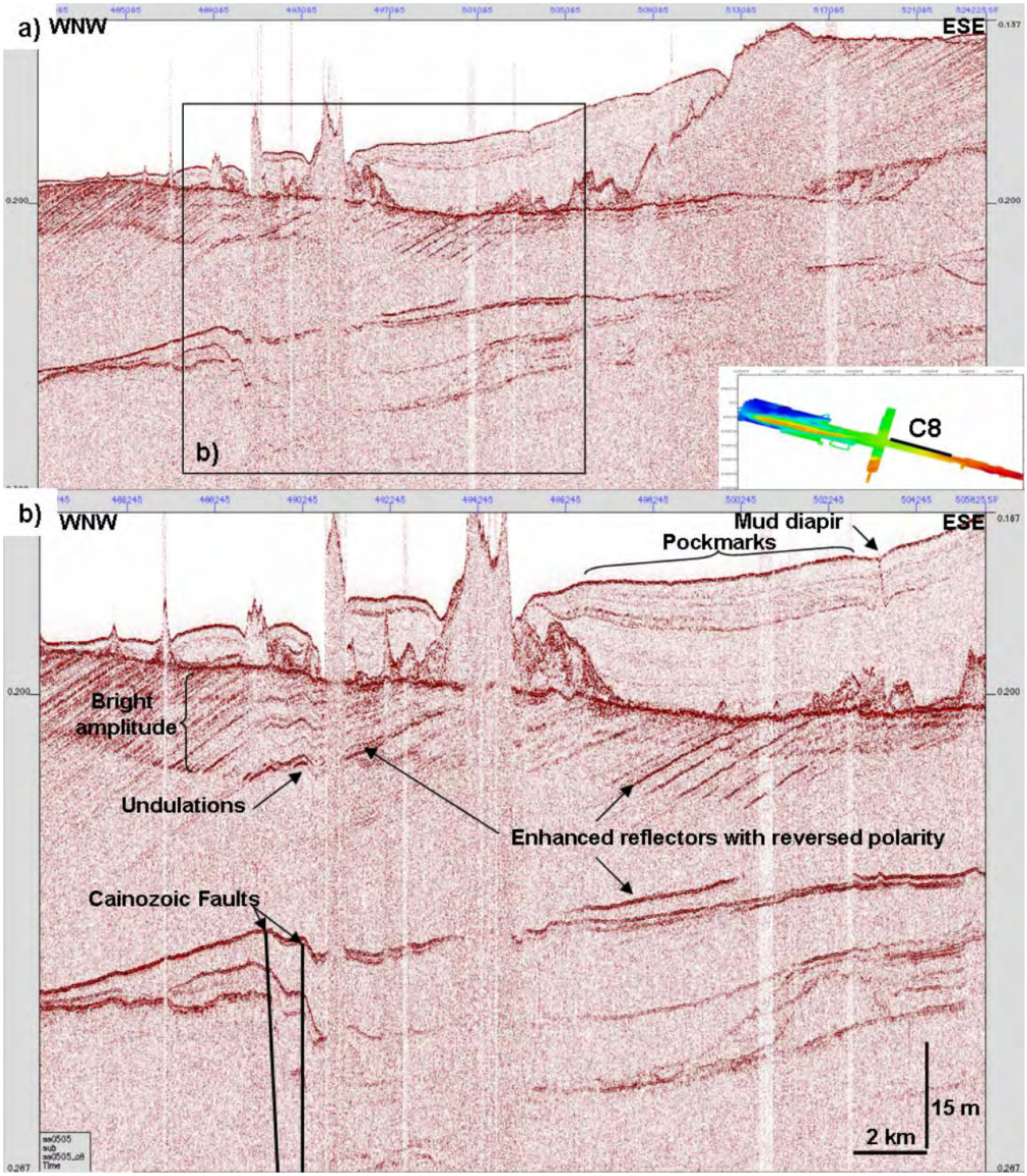

Figure 94 Sub-bottom profile C8 showing possible deformation or different compaction above Cainozoic faults maybe associated with the reactivation of pre-existing faults.

3.12 CORRELATION WITH SYNTHETIC APERTURE RADAR DATA

Area C and D were selected for surveying on the basis of geophysical anomalies in conventional seismic data and the presence of mapped hydrocarbon slicks interpreted in SAR data (INFOTERRA Global Seeps Database, see Chapter 6). During the survey, areas where SAR slicks had been interpreted were studied for active seepage using side-scan sonar and the 12 kHz echo-sounder. The presence of gas plumes caused by natural hydrocarbon seepage has previously been observed in Australian waters using these tools (Jones et al., 2005; Rollet et al., 2006). However, evidence of active seepage was not identified at any of the locations where SAR slicks had been mapped. However, seepage can be intermittent and the absence of active gas plumes during the survey does not rule out hydrocarbon release at these locations at other times. Significantly, there appears to be a strong correlation between the location of SAR slicks and pockmark fields in the survey Areas C and D (**Figure 95**).

Regionally, there is a grouping of SAR slicks which correlates with the PQDZ and a half graben mapped with conventional seismic data using the Proterozoic base Wessel Group as an isochron (Struckmeyer, 2006) (**Figure 96**). Some SAR slicks in this group also overlie a major fault and others appear to correlate with thinner parts of the basin fill (**Figure 96**). The conventional seismic data also exhibits a correlation with the edge of the interpreted regional seal. The sediments filling the half-graben are believed to include a Cambrian source rock developed in other parts of the basin (Struckmeyer, 2006).

The SAR slicks therefore appear to be related to sea bed features (pockmarks), major faults, and a half-graben containing a regional source rock and the edge of a regional seal. These relationships suggest that there is an active petroleum system within this half-graben and that natural hydrocarbon seepage does occur within survey Areas C and D.

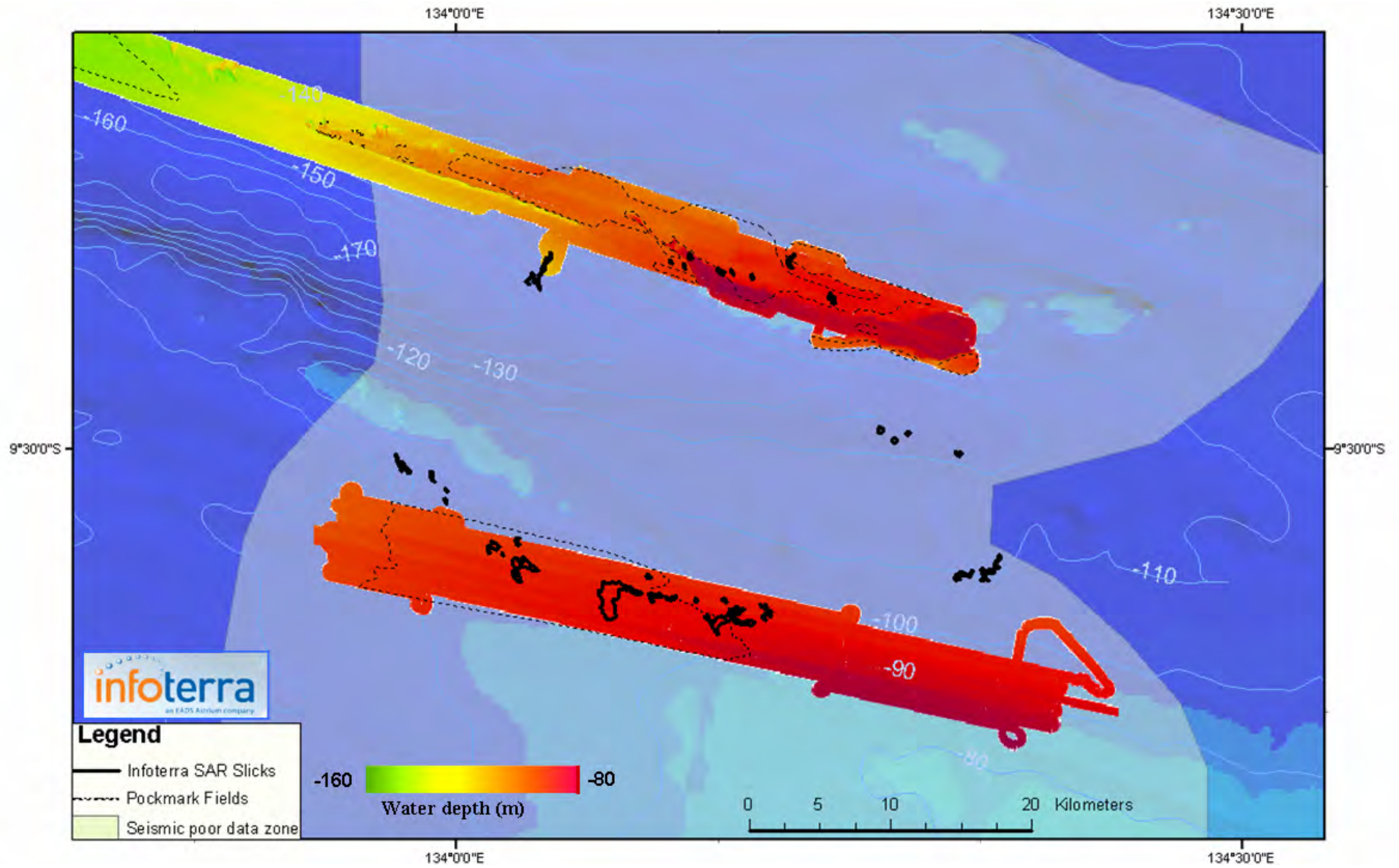

Figure 95 Multibeam bathymetry image in Areas C and D overlayed with pockmark fields interpreted on side-scan sonar data. The outlines of interpreted hydrocarbon slicks from SAR data (Infoterra) correlate with the pockmark field location. The poor quality data zone is also shown.

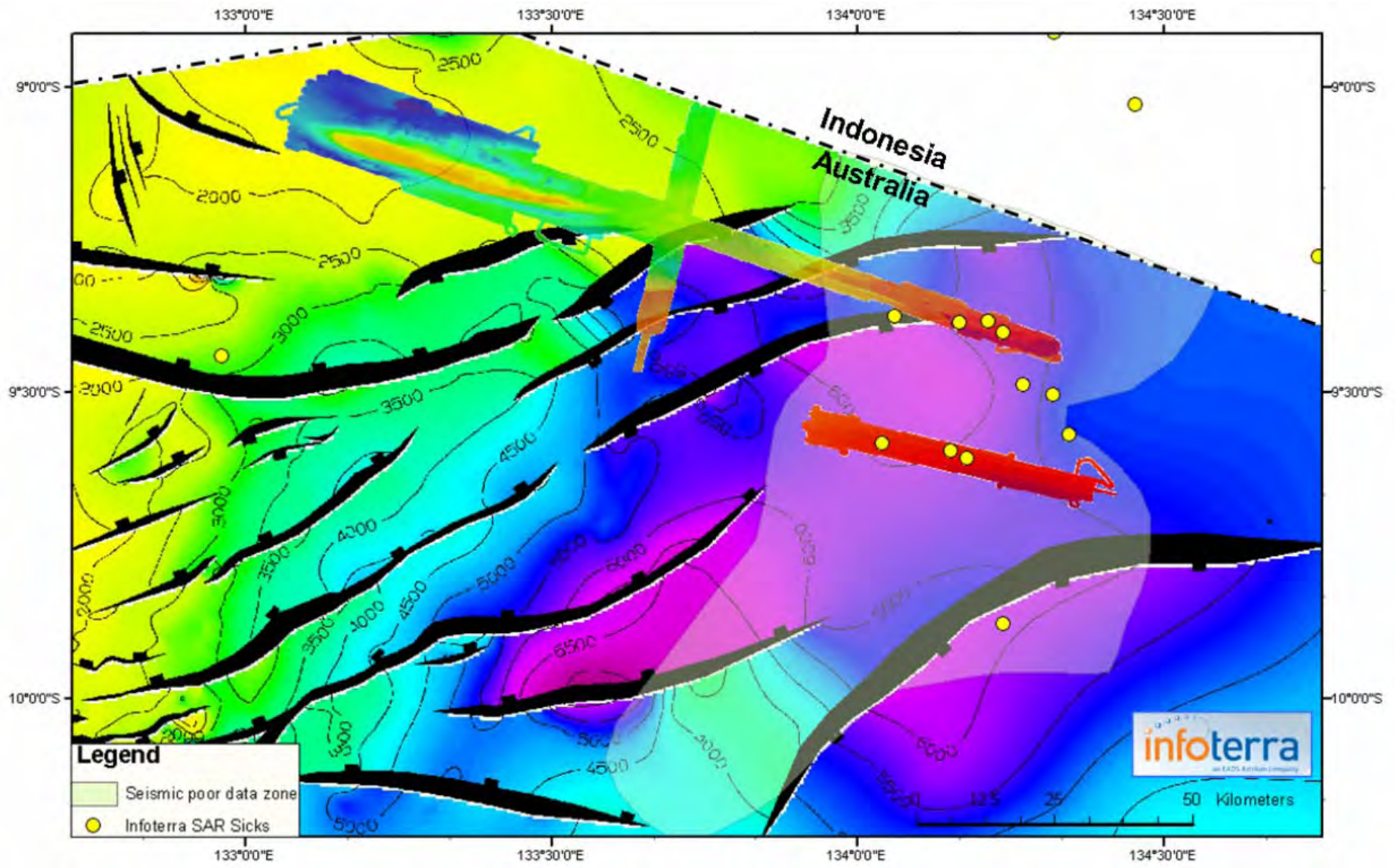

Figure 96 Isochron structure map of the Base Wessel Group (Proterozoic); major SW-NE Proterozoic faults are mapped in black. Interpreted SAR slicks appear to correlate with faults and half-graben. Note: poor quality data zone also appears to correlate with thickest sediment fill.

4. Conclusions

The Geoscience Australia Survey 282 had the following aims:

1. to identify and sample natural hydrocarbon seepage;
2. to improve our understanding of the petroleum resources in the Arafura Sea;
3. to document modern sedimentary/environmental settings of the Arafura Sea for bio-regionalization and regional marine planning

The acquisition of sub-bottom profile data, along with multibeam bathymetry, side-scan sonar and an associated sediment/benthos sampling program has provided a large quantity of new data within this region of northern Australia.

A wide variety of shallow gas indicators have been described, which can be correlated with features in conventional seismic and remotely-sensed satellite data (Synthetic Aperture Radar). Seepage across the region appears to be passive compared to the active gas seepage in the Timor Sea (Jones et al., 2005a,b; Rollet et al., 2006). For example, there no obvious gas plumes were observed in the water column during this Arafura survey. Consequently, the natural hydrocarbon seepage described in this report has been inferred from the geophysical data and the sea bed features observed during the survey. The range of fluid-expulsion sea bed features and sub-surface geophysical indicators for gas migration suggest both *in situ* generation of microbial gas in the Holocene mud of Unit J and shallow gas movement from older, deeper units. Therefore, integration of the new survey data with conventional seismic and remote sensing data suggests that the area north of the Goulburn Graben may be prospective for hydrocarbons.

The sea bed mapping and sampling phase of the survey has provided a much greater understanding of the spatial relationships of the sea bed, habitats and biota across the region. There is a strong correlation between substrate hardness and rugosity

and overall biodiversity. This is seen on the large, elongate Pillar Bank, where high diversity was observed due to the range of available habitats at different water depths and the confluence of shelf and deep sea waters. The third aim of the survey will be more specifically addressed by a more in-depth analysis of the benthos, to create a second biota-based report for the Department of the Environment and Heritage.

5. Availability of Survey Digital Data

Below is a list of survey data and products that can be requested for each data type. Data can be made available upon request, at cost of transfer. For further information on accessing digital data acquired during the survey contact: ausgeodata@ga.gov.au

Sub-bottom profile data was collected using a TOPAS PS 18 Parametric sub-bottom profiler. This data is in the raw form that can be read using Topas software and also in processed data in SEG-Y format.

Sub-bottom Profile Topas deliverables: ~80GB depending on format selected

1. Raw Topas internal format (no filtering or scaling) – requires Kongsberg Topas software to read but has the advantage of allowing data processing for specific attributes (amplitude, frequency and polarity).
2. Processed SEG-Y data – 32 bit IEEE format with filtering and time variant scaling applied

Multibeam data was collected using a Kongsberg Simrad EM 300 multibeam echo sounder with a nominal frequency of 30 kHz. This data was processed with Caris software.

EM300 Multibeam data deliverables: data volume ~5 to 50GB depending on format selected

1. Raw EM300 format data, which is an open-file format but has not been processed or despiked
2. Generic Sensor Format (GSF) with beam indexed amplitude; this is the reflectivity component of the multibeam. Note, this is fully processed and despiked data.
3. Caris HDCS format that contain all processed despiked data
4. X,Y,Z files as extracted from GSF data, which provides bathymetric at high resolution for use in a GIS. Note, these are fully processed and despiked data

Side-scan sonar data were collected using an Edge Tech 4200-FS tow fish operated mostly at 120 kHz. The original files are read within Edge Tech's acquisition software and were processed for towfish offset and mosaiced within Caris software.

Edge Tech side-scan deliverables: data volume ~300GB depending on format selected

1. Edge Tech internal acquisition format – needs operating software for Edge Tech side-scan sonar
2. XTF format files, this is a generic file format for side-scan data and can be uploaded into Caris or other processing/interpretation packages

6. Availability of INFOTERRA's Global Seeps Database

The synthetic aperture radar (SAR) surface slick data results used in this report are presented with the kind permission of INFOTERRA Ltd and are part of their commercial, non-exclusive, Global Seeps Database GIS project. Details of this project are available from www.infoterra.co.uk and by contacting Paul Chandler or Danny

Hughes at paul.chandler@infoterra-global.com and daniel.hughes@infoterra-global.com respectively.

7. Acknowledgements

We thank the crew and master of the RV *Southern Surveyor.* Alan Judd (U.K. Consultant on shallow gas and seepage) is thanked for his help and advice in the interpretation of shallow gas features. Rob Kirk (Tasmanian Consultant in sequence and seismic stratigraphy) is thanked for his assessment of the unit stratigraphy interpretation of some of the sub-bottom profile data. Fred Kroh and Anne Fleming, from Geoscience Australia, provided valuable help with attribute analysis and seismic processing. Infoterra Ltd are acknowledged for giving their kind permission to allow the publication of the slick data from their Global Seeps Database. Barry Bradshaw, Phil Symonds and Howard Stagg are thanked for comments and reviews. John Kennard and Andrew Jones are thanked for their discussions and advice during data analysis and write-up. Heike Struckmeyer, Jennie Totterdell and Karen Earl are thanked for their comments and advice on the structural setting and geological history of the Arafura Basin.

8. References

Abrams M.A., Francu E., Dahdah N.F., and Logan G.A., 2004. Surface Geochemistry Calibration Study Phase II: Laboratory Studies. Energy and Geoscince Institute at the University of Utah, *EGI Technical Report No. 2004-50501003.* Volumes I-III.

Boetius, A., Ravenschlag, K., Schubert, C.J., Rickert, D., Widdel, F., Gieseke, A., Amann, R., Jorgensen, B.B., Witte, U., and Pfannkuche, O., 2000. A marine microbial consortium apparently mediating anaerobic oxidation. *Nature* **407**, 623-626.

Boon, J. J., Rijpstra, W. I. C., De Lange, F., De Leeuw, J. W., Yoshioka, M., and Shimizu, Y., 1979. Black Sea sterol: a molecular fossil for dinoflagellate blooms. *Nature* **277**, 125-127.

Brassell, S. C., Brereton, R. G., Eglinton, G., Grimalt, J., Liebezeit, G., Marlowe, I. T., Pflaumann, U., and Sarnthein, M., 1986. Palaeoclimatic signals recognized by chemometric treatment of molecular stratigraphic data. *Organic Geochemistry* **10**, 649-660.

Brassell, S. C., Wardroper, A. M. K., Thomson, I. D., Maxwell, J. R., and Eglinton, G., 1981. Specific acyclic isoprenoids as biological markers of methanogenic bacteria in marine sediments. *Nature* **290**, 693-696.

Brocks, J.J., Pearson, A., 2005. Building the biomarker tree of life. In: Banfield, J., Nealson, K., Cervini-Silva., J. (Eds.), Reviews in Mineralogy and Geochemistry. 59. The Mineralogical Society of America., pp. 233-258.

Chappell, J. and Shackleton, N.J., 1986. Oxygen isotopes and sea level. *Nature*, **324**, 137-140.

Chivas A.R., Garcia A., van der Kaars S., Couapel M.J.J., Holt S., Reeves J.M., Wheeler D.J., Switzer A., Murray-Wallace C.V., Banerjee D., Price D.M., Wang, S.X., Pearson G., Edgar N.T., Beaufort L., De Deckker P., Lawson E. and Cecil C.B., 2001. Sea-level and environmental changes since the last interglacial in the Gulf of Carpentaria, Australia: an overview. *Quaternary International*, **83-85**, 19-46.

Conte, M.H., Volkman, J.K., and Eglinton, G., 1994. in The Haptophyte Algae, eds J. C. Green and B. S. C. Leadbeater. Clarendon Press, Oxford. 351-377pp

Eglinton, G. and Hamilton, R. J., 1967. Leaf epicutilar waxes. *Science* **156**, 1322-1324.

Emmel, F.J. and Curray, J.R., 1982. A submerged late Pleistocene delta and other features related to sea level changes in the Malacc Strait. *Marine Geology*, **47**, 197-216.

Farrington, J.W., Davis, A.C., Sulanowski, J., McCaffrey, M.A., McCarthy, M., Clifford, C. H., Dickinson, P., and Volkman, J.K., 1988. Biogeochemistry of lipids in surface sediments of the Peru Upwelling Area at 15˚S. *Organic Geochemistry* **13**, 607-617.

Ferreira, A.M., Miranda, A., Caetano, M., Baas, M., Vale, C., and Sinninghe Damsté, J.S., 2001. Formation of mid-chain alkane keto-ols by post-depositional oxidation of mid-chain diols in Mediterranean sapropels. *Organic Geochemistry* **32**, 271-276.

Gagosian, R.B., Smith, S.O., Lee, C., Farrington, J.W., and Frew, N.M. 1980 Steroid transformations in Recent marine sediments. *Physics and Chemistry of The Earth* **12**, 407-419.

Geoscience Australia Marine Database, MARS: http://www.ga.gov.au/oracle/mars/

Gelin, F., Volkman, J. K., Largeau, C., Derenne, S., Sinninghe Damsté, J. S., and De Leeuw, J. W., 1999. Distribution of aliphatic, nonhydrolyzable biopolymers in marine microalgae. *Organic Geochemistry* **30**, 147-159.

Haq, B.U., Hardenbolt, J., Vail, P.R., Wright, R.C., Stover, L.E., Baum, G., Loutit, T., Gombos, A., Davies, T., Pflum, C., Romine, K., Posamentier, H., Jan du Chene, R., 1986. Sea-level changes: an integrated approach. Eds. C.K. Wilgus, B.S. Hastings, C.G.St.C. Kendall, H.W. Posamentier, C.A. Ross, J.C. Van Wagoner, *Society of Economic Paleontologists and Mineralogists Special Publication*, **42**.

Hart, B.S., and Hamilton, T.S., 1993. High resolution acoustic mapping of shallow gas in unconsolidated sediments beneath the strait of Georgia, British Colombia. *Geo-Marine Letters,* **13**, 49-55.

Harvey, R.H., O'Hara, S.C.M., Eglinton, G., and Corner, E.D.S., 1989. The comparative fate of dinosterol and cholesterol in copepod feeding: Implications for a conservative molecular biomarker in the marine water column. *Organic Geochemistry* **14**, 635-641.

Herbert, T.D., 2003. in *Treatise on Geochemistry* Eds. Heinrich D. Holland and Karl K. Turekian, 391-432pp. Pergamon, Oxford.

Hinrichs, K.U., Hayes, J.M., Sylva, S.P., Brewer, P.G., and DeLong, E.F., 1999. Methane-consuming archaebacteria in marine sediments. *Nature* **398**, 802-805.

Hoefs, M.J.L., Rijpstra, W., Irene C., and Sinninghe Damste, J.S., 2002. The influence of oxic degradation on the sedimentary biomarker record I: evidence from Madeira Abyssal Plain turbidites. *Geochimica et Cosmochimica Acta* **66**, 2719-2735.

Hovland, M., Judd, A.G., and King, L.H. 1984. Characteristic features of pockmarks in the North Sea Floor and Scotian Shelf. *Sedimentology*, **31**, 471-480.

Hovland, M., 1992. Hydrocarbon Seeps in Northern Marine Waters – Their Occurrence and Effects. *Palaios*, **7,** 376-382.

Hurst, A., Cartwright, J, Duranti, D., Huuse, M., and Cronin, B., 2002. Sand Injectites: Controls on their Formation and Reservoir Character – an Assessment of Reserve Potential. *AAPG Annual Meeting* March 10-13, Houston, Texas.

James, N.P., Bone, Y., Kyser, T.K., Dix, G.R. and Collins, L.B., 2004. The importance of changing oceanography in controlling late Quaternary carbonate sedimentation on a high-energy, tropical, oceanic ramp: north-western Australia. *Sedimentology*, **51**, 1179-1205.

Judd, A.G., and Hovland, M., 1992. The evidence of shallow gas in marine sediments. *Continental Shelf Research*, **12**, 1081-1095.

Judd, A.G., and Hovland, M., 2006. Submarine Fluid Flow. Cambridge University Press. 300pp

Jones, H.A., 1971. Late Cenozoic forms on the Northwest Australian continental shelf. *Marine Geology*, **10**, 20-26.

Jongsma, D., 1970. Eustatic Sea Level Changes in the Arafura Sea. *Nature*, **228**, 150-151.

Jongsma, D., 1974. Marine Geology of the Arafura Sea. *BMR Journal of Australian Geology and Geophysics*, **Bulletin 157**.

Keep, M., and Moss, S., 2000. Basement reactivation and control of Neogene structures in the Outer Browse Basin, North West Shelf. *Exploration Geophysics* **31**, 424–432.

Killops, S. D. and Frewin, N. L., 1994. Triterpenoid diagenesis and cuticular preservation. *Organic Geochemistry* **21**, 1193-1209.

Lavering, I.H., 1993. Quaternary and modern environments of the Van Diemaen Rise, Timor Sea, and potential effects of additional petroleum exploration activity. *BMR Journal of Australian Geology and Geophysics*, **13**, 281-292.

Marlowe, I. T., Brassell, S. C., Eglinton, G., and Green, J. C., 1984. Long chain unsaturated ketones and esters in living algae and marine sediments. *Organic Geochemistry* **6**, 135-141.

McCaffrey, M.A., Farrington, J.W., and Repeta, D.J. 1991. The organic geochemistry of Peru margin surface sediments: II. Paleoenvironmental implications of hydrocarbon and alcohol profiles. *Geochimica et Cosmochimica Acta*, **55**, 483-498.

Metzger, P. and Casadevall, E. Lycopadiene, 1987. A tetraterpenoid hydrocarbon from new strains of the green alga Botryococcus braunii. *Tetrahedron Letters* **28**, 3931-3934.

Morris, R.J., Brassell, S.C., 1988. Long-chain alkanediols: biological markers for cyanobacterial contributions to sediments. *Lipids* **23**, 256-258.

Nott, J., and Roberts, R.G., 1996. Time and Process rates over the past 100 m.y.: A case for dramatically increased landscape denudation rates during the late Quaternary in northern Australia. *Geology*, **24**, 883-887.

Pancost, R.D., Bouloubassi, I., Aloisi, G., Sinninghe Damsté, J.S., and Scientific Party, the Medinaut Shipboard, 2001. Three series of non-isoprenoidal dialkyl glycerol diethers in cold-seep carbonate crusts. *Organic Geochemistry* **32**, 695-707.

Pancost, R. D., Hopmans, E. C., and Sinninghe Damsté, J. S., 2001. Archaeal lipids in Mediterranean cold seeps: molecular proxies for anaerobic methane oxidation. *Geochimica et Cosmochimica Acta*, **65**, 1611-1627.

Pancost, R.D. and Boot, C.S., 2004. The palaeoclimatic utility of terrestrial biomarkers in marine sediments. *Marine Chemistry*, **92**, 239-261.

Pelejero, C. and Calvo, E., 2003. The upper end of the UK'37 temperature calibration revisited. *Geochemistry Geophysics Geosystems*, **4**, 1014,

doi:10.1029/2002GC000431.

Plumb, K.A., and Roberts, H.G., 1992. The Geology of Arnhem Land, Northern Territory. *BMR Record* **1992/55**.

Reeburgh, W.S., 1996. Microbial growth on C1 compounds. Eds. Lidstrom, M. E., Tabita, F. R. Kluwer Academic Publishers, Andover, UK, 334-342pp.

Robinson, N., Eglinton, G., Brassell, S. C., and Cranwell, P. A., 1984. Dinoflagellate origin for sedimentary 4α-methylsteroids and 5α(H)-stanols. *Nature* 308, 439-442.

Rollet N., Logan G.A., Kennard J.M., O'Brien P., Jones A.T. and Sexton M., 2006. Characterisation and correlation of active hydrocarbon seepage using geophysical data sets: an example from the tropical, carbonate Yampi Shelf, Northwest Australia. *Marine and Petroleum Geology,* **23**, 145-164.

Schroot, B.M., and Schuttenhelm, R.T.E, 2003. Expressions of shallow gas in the Netherlands North Sea. *Netherlands Journal of Geosciences,* **82**, 91-105.

Scourse, J., Marret, F., Versteegh, G.J.M., Jansen, J. H. Fred, S.E., and van der Plicht, J., 2005. High-resolution last deglaciation record from the Congo fan reveals significance of mangrove pollen and biomarkers as indicators of shelf transgression. *Quaternary Research*, **64**, 57-69.

Sikes, E. L., Farrington, J. W., and Keigwin, L. D., 1991. Use of the alkenone unsaturation ratio U37k to determine past sea surface temperatures: core-top SST calibrations and methodology considerations. *Earth and Planetary Science Letters* **104**, 36-47.

Sinninghe Damsté, J.S., Rampen, S., Irene, W., Rijpstra, C., Abbas, B., Muyzer, G., and Schouten, S., 2003b. A diatomaceous origin for long-chain diols and mid-chain hydroxy methyl alkanoates widely occurring in quaternary marine sediments: indicators for high-nutrient conditions. *Geochimica et Cosmochimica Acta* **67**, 1339-1348.

Smallwood, B.J. and Wolff, G.A., 2000. Molecular characterisation of organic matter in sediments underlying the oxygen minimum zone at the Oman Margin, Arabian Sea. *Deep Sea Research Part II: Topical Studies in Oceanography* **47**, 353-375.

Struckmeyer, H.I.M. (compiler), 2006. in prep. — Petroleum geology of the Arafura Basin. Geoscience Australia Record.

Summons, R. E., Jahnke, L. L., Hope, J. M., and Logan, G. A. 1999. 2-methylhopanoids as biomarkers for cyanobacterial oxygenic biosynthesis. *Nature* **400**, 554-557.

Teixidor, P. and Grimalt, J.O. 1992 Gas chromatography determination of isoprenoid alkylglycerol diethers in archaebacterial cultures and environmental samples. *Journal of Chromatography* **607**, 253-259.

Thiel, V., Blumenberg, M., Hefter, J., Pape, T., Pomponi, S., Reed, J., Reitner, J., Worheide, G., and Michaelis, W., 2002. A chemical view of the most anicent metazoa- biomarker chemotaxonomy of hexactinellid sponges. *Naturwissenschaften* **89**, 60-66.

Veeh, H.H. and Veevers, J.J., 1970. Sea level at -175 m off the Great Barrier Reef 13,000 to 17,000 years BP. *Nature*, **226**, 536-537.

Veevers, J.J., 1971. Shallow stratigraphy and structure of the Australian continental margin beneath the Timor Sea. Marine *Geology*, **11**, 209-249.

Versteegh, G. J. M., Bosch, H. J., and De Leeuw, J. W., 1997. Potential palaeoenvironmental information of C24 to C36 mid-chain diols, keto-ols and mid-chain hydroxy fatty acids; a critical review. *Organic Geochemistry* **27**, 1-13.

Versteegh, G.J.M., Schefuss, E., Dupont, L., Marret, F., Sinninghe Damsté, J.S., and Jansen, J.H.F., 2004. Taraxerol and Rhizophora pollen as proxies for tracking past mangrove ecosystems. *Geochimica et Cosmochimica Acta*, **68**, 411-422.

Volkman, J.K., 1986. A review of sterol markers for marine and terrigenous organic matter. *Organic Geochemistry* **9**, 83-99.

Volkman, J.K., Barrett, S.M., Blackburn, S.I., Mansour, M.P., Sikes, E.L., and Gelin, F., 1998. Microalgal biomarkers: A review of recent research developments. *Organic Geochemistry* **29**, 1163-1179.

Volkman, J.K., Barrett, S.M., Dunstan, G.A., and Jeffrey, S. W., 1992. C30-C32 alkyl diols and unsaturated alcohols in microalgae of the class Eustigmatophyceae. *Organic Geochemistry*, **18**, 131-138.

Wakeham, S.G., 1987. Steroid geochemistry in the oxygen minimum zone of the eastern tropical North Pacific Ocean. *Geochimica et Cosmochimica Acta,* **51**, 3051-3069.

Wakeham, S.G., Freeman, K.H., Pease, T.K., and Hayes, J.M., 1993. A photoautotrophic source for lycopane in marine water columns. *Geochimica et Cosmochimica Acta*, **57**, 159-165.

Wilson, G.D.F, 2005. Arafura Sea Biology Survey. Report on the RV Southern Surveyor Expedition 05/2005. *Department of th Environment and Heritage*, pp1-17.

Woodroffe, C.D., 1993. Late quaternary evolution of coastal and lowland riverine plains of Southeast Asia and northern Australia: an overview. *Sedimentary Geology* **83**, 163-175.

Woodroffe, C.D., Thom, B. G., and Chappell, J., 1985. Development of widespread mangrove swamps in mid-Holocene times in northern Australia. *Nature* **317**, 711-713.

Yokoyama, Y., De Deckker, D., Lambeck, K., Johnston, P., Fifield, L.K., 2001. Sea-level at the Last Glacial Maximum: evidence from northwestern Australia to constrain ice volumes for oxygen isotope stage 2. *Palaeogeography, Palaeoclimatology, Palaeoecology*, **165**, 281-29.

Appendix 1 Sample location data N. Rollet

LAT	LONG	SAMPLEID	DATE	SAMPLE_TYPES	COMMENTS	SAMPLE_DESCRIPTION
-9.879633	135.365050	282/003GC001	04/05/2005	CORE GRAVITY	Sedimentology core	
-9.873967	135.317667	282/004GC002	04/05/2005	CORE GRAVITY	Sedimentology core	
-9.840583	135.268367	282/005GC003	04/05/2005	CORE GRAVITY	Sedimentology core	
-9.839500	135.348300	282/006GC004	04/05/2005	CORE GRAVITY	Sedimentology core	
-9.835550	135.296183	282/007GC005	04/05/2005	CORE GRAVITY	Sedimentology core	Terminated in sticky marine mud (calcareous)
-9.832550	135.327467	282/008GC006	04/05/2005	CORE GRAVITY	Sedimentology core	Terminated in very sticky calcareous muddy medium sand
-9.821517	135.326800	282/009GC007	04/05/2005	CORE GRAVITY	Sedimentology core	
-9.812733	135.256967	282/010GC008	05/05/2005	CORE GRAVITY	Sedimentology core	Terminated in very stiff calcareous muddy fine sand
-9.796500	135.282483	282/011GC009	05/05/2005	CORE GRAVITY	Sedimentology core	
-9.793650	135.277717	282/012GC010	05/05/2005	CORE GRAVITY	Sedimentology core	
-9.418000	134.313333	282/013GC011	10/05/2005	CORE GRAVITY	No Core. Only core cutter recovered	Calcareous cemented bioclastic grit on end of the core cutter, 2 layers: Munsell 10YR 6/8 (orange/yellow), and 10YR 6/2 (grey)
-9.402183	134.238183	282/014GC012	10/05/2005	CORE GRAVITY	Samples taken for geochem only. Only cc and kk kept.	
-9.402200	134.238117	282/014GC013	10/05/2005	CORE GRAVITY	Geochem samples only. Only cc kept. 6m barrel	
-9.402000	134.238000	282/014GC014	10/05/2005	CORE GRAVITY	Geochem samples only. Only cc kept. 6m barrel.	
-9.377300	134.213917	282/015GC015	10/05/2005	CORE GRAVITY	Part 3a (top) kept for stratigraphy, other samples are for geochemistry	
-9.377517	134.214250	282/015GC016	10/05/2005	CORE GRAVITY	Geochem samples only	
-9.377633	134.214200	282/015GC017	10/05/2005	CORE GRAVITY	Geochem samples only. Core catcher kept.	
-9.377833	134.214000	282/015GC018	10/05/2005	CORE GRAVITY	Geochem samples only. Core catcher kept.	
-9.401583	134.194800	282/016GC019	10/05/2005	CORE GRAVITY	No core. Only a bag of sediment.	Terminated in calcareous mud with halameda flakes, coral fragments up to 15cm in diameter in bottom of core barrel
-9.393333	134.171500	282/017GC021	10/05/2005	CORE GRAVITY	No core. Only a bag of sediment.	Muddy silty sand, 5Y/5/4 (Munsell), coarse grained, semi-lithified limestone (cc)
-9.393333	134.171500	282/017GC022	11/05/2005	CORE GRAVITY	Sedimentology core	
-9.392367	134.171533	282/017GC023	11/05/2005	CORE GRAVITY	Geochem samples only	
-9.392850	134.171183	282/017GC024	11/05/2005	CORE GRAVITY	Terminated in limestone	
-9.386167	134.167333	282/018GC025	11/05/2005	CORE GRAVITY	Geochem samples only	
-9.386167	134.167333	282/018GC026	11/05/2005	CORE GRAVITY	Sedimentology core	
-9.386167	134.167333	282/018GC027	11/05/2005	CORE GRAVITY	Geochem samples only	

-9.386167	134.167333	282/018GC028	11/05/2005	CORE GRAVITY	Geochem samples only	
-9.356500	134.082833	282/021GC029	11/05/2005	CORE GRAVITY	Sedimentology core	Terminated in stiff slightly dewatered clay, reducing H2S smell
-9.376167	134.060167	282/022GC030	11/05/2005	CORE GRAVITY	Geochem samples only	Very strong H2S smell in part 1B, mild in 2A
-9.376167	134.060333	282/022GC031	11/05/2005	CORE GRAVITY	Geochem samples only	Strong H2S smell
-9.376000	134.060333	282/022GC032	11/05/2005	CORE GRAVITY	Some sample lost on deck	
-9.376033	134.060350	282/022GC033	11/05/2005	CORE GRAVITY	Geochem samples only	
-9.339833	134.033000	282/024GC035	11/05/2005	CORE GRAVITY	Sedimentology core. 3m barrel.	
-9.329167	134.029167	282/025GC036	12/05/2005	CORE GRAVITY	No Core. Only a bag of sediment. Core probably fell over.	Muddy medium sandy with shelly gravel.
-9.329100	134.029217	282/025GC037	12/05/2005	CORE GRAVITY	No Core. Only a bag of sediment.	Terminated in muddy shelly gravel, hard bottom.
-9.258050	133.801700	282/026GC038	12/05/2005	CORE GRAVITY	Sedimentology core	
-9.258167	133.801667	282/026GC039	12/05/2005	CORE GRAVITY	Sedimentology core	
-9.381167	133.664667	282/027GC040	13/05/2005	CORE GRAVITY	Sedimentology core	
-9.334000	133.691167	282/028GC041	13/05/2005	CORE GRAVITY	Packed at top and bottom with foam pacers, sedimentology	Terminated in stiff shelly mud, large shell fragments
-9.303833	133.696833	282/029GC042	13/05/2005	CORE GRAVITY	Bomb u-bend broken on recovery, sedimentology core	Terminated in stiff calcareous mud
-9.227500	133.698333	282/030GC043	13/05/2005	CORE GRAVITY	Sedimentology core. Core catcher kept.	Terminated in stiff dewatered mud.
-9.227500	133.698333	282/030GC044	13/05/2005	CORE GRAVITY	Geochem samples only	
-9.227500	133.698333	282/030GC045	14/05/2005	CORE GRAVITY	Geochem samples only	Terminated in stiff sticky mud (dewatered)
-9.217500	133.698333	282/030GC046	14/05/2005	CORE GRAVITY	Geochem samples only	Terminated in stiff sticky mud,
-9.089500	133.747717	282/031GC047	14/05/2005	CORE GRAVITY	Buried to the top of the bomb, geochem samples only	Strong H2S smell
-9.089500	133.747700	282/031GC048	14/05/2005	CORE GRAVITY	Geochem samples only. Appriximately 3m penetration.	
-9.089483	133.746067	282/031GC049	14/05/2005	CORE GRAVITY	Sedimentology core	
-9.089500	133.747733	282/031GC050	14/05/2005	CORE GRAVITY	Geochem samples only	
-9.089500	133.747717	282/031GC051	14/05/2005	CORE GRAVITY	Geochem samples only	
-9.205433	133.632533	282/032GC052	14/05/2005	CORE GRAVITY	Sedimentology core	Terminated in stiff calcareous mud
-9.205467	133.632583	282/032GC053	14/05/2005	CORE GRAVITY	Sub-sampled for Geochem. Remaining sections kept for sedimentology	
-9.205467	133.632417	282/032GC054	14/05/2005	CORE GRAVITY	Sub-sampled for Geochem.	
-9.205500	133.632533	282/032GC055	14/05/2005	CORE GRAVITY	Sub-sampled for Geochem	
-9.205617	133.632483	282/032GC056	14/05/2005	CORE GRAVITY	Sub-sampled for Geochem	
-9.003917	133.104467	282/033GC057	16/05/2005	CORE GRAVITY	Sedimentology core	Terminated in indurated mst/sst of the underlying reflector.
-9.033800	133.104283	282/034GC058	16/05/2005	CORE GRAVITY	Sedimentology core	Terminated in sticky calcareous mud.
-9.033800	133.104250	282/034GC059	16/05/2005	CORE GRAVITY	Sub-sampled for Geochem	Terminated in sticky calcareous mud
-9.033900	133.104233	282/034GC060	16/05/2005	CORE GRAVITY	Sub-sampled for Geochem	Terminated in sticky calcareous mud
-9.033650	133.104150	282/034GC061	16/05/2005	CORE GRAVITY	Sub-sampled for Geochem	Terminated in dewatered sticky muddy sand

-9.033700	133.104000	282/034GC062	16/05/2005	CORE GRAVITY	Sub-sampled for Geochem	Terminated in dewatered sticky sandy mud
-9.026217	133.169000	282/035GC063	17/05/2005	CORE GRAVITY	Geochem samples only. 2.5 to 3 m penetration	
-9.026200	133.169017	282/035GC064	17/05/2005	CORE GRAVITY	Geochem samples only	
-9.026233	133.169033	282/035GC065	17/05/2005	CORE GRAVITY	Geochem samples only	
-9.037850	133.160467	282/036GC066	17/05/2005	CORE GRAVITY	Broke spanish fingers, mud very well compacted	
-9.037850	133.160417	282/036GC067	17/05/2005	CORE GRAVITY	Sedimentology core	
-9.098883	133.198500	282/037GC068	17/05/2005	CORE GRAVITY	Sedimentology core	Terminated in slightly muddy sand and gravel
-9.171033	133.392400	282/039GC069	17/05/2005	CORE GRAVITY	Cemented ridge on Pillar Bank; old beach ridge or sand bars	Terminated in compacted friable packstone, partially cemented
-9.150483	133.390617	282/040GC070	18/05/2005	CORE GRAVITY	Terminated in sticky muddy sand	
-9.126717	133.421350	282/041GC071	18/05/2005	CORE GRAVITY	Sedimentology core	
-9.089483	133.418283	282/043GC072	19/05/2005	CORE GRAVITY	Sedimentology core	Small amount of grit in CC, bioclastic shelly material, tubes and spines
-9.032083	133.250033	282/047GC073	20/05/2005	CORE GRAVITY	Sedimentology core	Terminated in partially de-watered sticky calcareous mud
-9.001767	133.201317	282/048GC074	20/05/2005	CORE GRAVITY	Geochem samples plus top section (2A) for sedimentology	
-9.002200	133.201150	282/048GC075	20/05/2005	CORE GRAVITY	Geochem samples plus top section (2A) for sedimentology	
-9.096583	133.286950	282/049GC076	20/05/2005	CORE GRAVITY	Sedimentology core	
-9.199750	133.433817	282/050GC080	21/05/2005	CORE GRAVITY	Geochem samples	
-9.199800	133.433617	282/050GC081	21/05/2005	CORE GRAVITY	Geochem samples only	
-9.199967	133.433783	282/050GC082	21/05/2005	CORE GRAVITY	Geochem samples Parts 1B, 2A. Also top Part 3 kept for sedimentology	
-9.218217	133.484883	282/051GC077	21/05/2005	CORE GRAVITY	Geochem samples Parts 1C, 2B. Sedimentology sample part 3	
-9.218167	133.488583	282/051GC078	21/05/2005	CORE GRAVITY	Geochem samples Parts 1C, 2B. Sedimentology sample part 3	
-9.218183	133.488600	282/051GC079	21/05/2005	CORE GRAVITY	Geochem samples Parts 1C, 2B. Sedimentology sample part 3	
-9.176183	133.494717	282/053GC083	21/05/2005	CORE GRAVITY	Core cutter only	Terminated in core cutter. Calcareous slightly muddy dewatered gravel.
-9.154867	133.484550	282/055GC084	21/05/2005	CORE GRAVITY	Sedimentology core	Terminated in unconsolidated dewatered calcareous sand and gravel, shell hash
-9.162450	133.529000	282/056GC085	21/05/2005	CORE GRAVITY	Sedimentology core	Terminated in sticky slightly dewatered calcareous sandy mud.
-9.550733	133.953100	282/057GC086	24/05/2005	CORE GRAVITY	Sedimentology core	
-9.580650	133.039550	282/058GC087	24/05/2005	CORE GRAVITY	Geochem core	
-9.581267	134.039683	282/058GC088	24/05/2005	CORE GRAVITY	Geochem core	
-9.580650	134.039550	282/058GC089	24/05/2005	CORE GRAVITY	Sedimentology core	

-9.580750	134.039717	282/058GC090	24/05/2005	CORE GRAVITY	Geochem core	
-9.595783	134.153083	282/059GC091	24/05/2005	CORE GRAVITY	Geochem samples plus top 0.33m kept for sedimentology	Terminated in sticky calcareous mud, 5Y 5/4, mild H2S smell
-9.595717	134.153417	282/059GC092	24/05/2005	CORE GRAVITY	Geochem samples	Terminated in sticky calcareous mud, 5Y5/4, moderate H2S smell
-9.595767	134.153417	282/059GC093	24/05/2005	CORE GRAVITY	Geochem samples, control tin and disrupter taken, cc and	Terminated in sticky calcareous mud, 5Y 5/4
-9.609033	134.178300	282/060GC094	24/05/2005	CORE GRAVITY	Sedimentology core	Terminated in sticky calcareous mud, 5Y 4/4, mild H2S smell
-9.608967	134.178467	282/060GC095	24/05/2005	CORE GRAVITY	Geochem samples	Terminated in sticky calcareous mud, 5Y 4/4, mild H2S smell
-9.609183	134.178183	282/060GC096	24/05/2005	CORE GRAVITY	Geochem samples	Terminated in sticky calcareous mud, 5Y 5/4, mild H2S smell
-9.609350	134.178383	282/060GC097	24/05/2005	CORE GRAVITY	Geochem samples	Terminated in sticky calcareous mud, 5 Y 5/4, mild H2S smell
-9.626083	134.238683	282/061GC098	25/05/2005	CORE GRAVITY	Geochem samples only	Terminated in calcareous gravelly mud, very shelly, 5Y 4/4, mild H2S smell
-9.626067	134.238683	282/061GC099	25/05/2005	CORE GRAVITY	Geochem samples only	Terminated in calcareous gravelly mud (shelly), 5Y 4/4, mild H2S smell
-9.626317	134.239067	282/061GC100	25/05/2005	CORE GRAVITY	Geochem samples only	Terminated in gravelly mud (calcareous), 5Y 5/4, mild H2S smell
-9.656533	134.284467	282/062GC101	25/05/2005	CORE GRAVITY	Sedimentology core. No core catcher or core cutter. 6m core barrel	
-9.661483	134.374700	282/063GC102	25/05/2005	CORE GRAVITY	Sedimentology core	
-9.739717	135.265867	282/064GC103	25/05/2005	CORE GRAVITY	Sedimentology core	Terminated in calcareous muddy fine sand
-9.916833	134.500667	282/001BS001	01/05/2005	DREDGE BENTHIC	A - bulk sediment ,B - 300 microns sieve of bulk. ADCP Site	Mud with calcareous particles. Munsell colour; Gley 1/5 SGY
-9.799117	135.367067	282/002BS002	02/05/2005	DREDGE BENTHIC	A - bulk sediment, B - sieved 300 micron of bulk for biology	
-9.833917	135.295667	282/007BS003	04/05/2005	DREDGE BENTHIC		
-9.377667	134.214500	282/015BS004	10/05/2005	DREDGE BENTHIC	A - bulk	
-9.094017	133.746433	282/031BS005	14/05/2005	DREDGE BENTHIC	A - bulk, B - biology, no grab at site due to soft mud	Mud
-9.205517	133.648383	282/032BS006	14/05/2005	DREDGE BENTHIC	Sample filtered for biota	
-9.030567	133.105667	282/034BS007	17/05/2005	DREDGE BENTHIC	A - bulk, B - biology	Calcareous mud (poorly sorted).
-9.032133	133.160900	282/036BS008	17/05/2005	DREDGE BENTHIC	Mud appears to have been winowed out during retrieval.	Mud with minor winowed shell grit
-9.030633	133.250250	282/047BS009	20/05/2005	DREDGE BENTHIC	A (bulk) and B (biology) samples	Calcareous slightly sandy mud
-9.199950	133.435150	282/050BS011	21/05/2005	DREDGE BENTHIC	A (bulk) and B (biology) samples	Calcareous poorly sorted sandy mud.
-9.219167	133.490200	282/051BS010	21/05/2005	DREDGE BENTHIC	A - bulk. Winnowed mud	Heavily winnowed very soft mud
-9.162117	133.532633	282/056BS012	22/05/2005	DREDGE BENTHIC	A sediment sample	Calcareous poorly sorted mud.
-9.548717	133.951350	282/057BS013	24/05/2005	DREDGE BENTHIC	A - bulk, B- biology samples	Sandy mud.
-9.610467	134.182533	282/060BS014	24/05/2005	DREDGE BENTHIC		
-9.661683	134.374267	282/063BS015	25/05/2005	DREDGE BENTHIC	A - bulk sample, B -biology	Mud
-9.377167	133.662000	282/027DR008	13/05/2005	DREDGE CHAIN BAG	No Bulk or Biology sample. Fine mesh bag in chain bag to catch small material	Mud, shells, 2 fragments retained. Bored and encrusted mollusc and coral fragments.
-9.180533	133.413700	282/038DR009	17/05/2005	DREDGE CHAIN BAG	Dredge up benched escarpment. Samples A1-A5	Large fragments of limestone, strongly cemented, coarse grained and fine-medium grained types.
-9.116967	133.412083	282/042DR011	18/05/2005	DREDGE CHAIN BAG	A - bulk sample, note no sample A3 or A4.	80% mud, 10% shell hash, 10% rocks
-9.088533	133.416483	282/043DR012	19/05/2005	DREDGE CHAIN BAG	Hooked up dredge and damaged lip of dredge collar.	
-9.030167	133.245333	282/045DR014	19/05/2005	DREDGE CHAIN BAG	Dredge used to attain sediment sample	terrigenous mudstone, weathered, lithified. A6 3 Tonna gastropod mould. A4 semi -lithified firm mudstone, highly burrowed, weathered (worm and bivalve

-9.176083	133.496067	282/053DR015	21/05/2005	DREDGE CHAIN BAG		75% loose limestone fragments plus mud. Type A1 calcareous mudstone. Type A2 bivalve/oyster shells. Type A3 coral/bryozoans. Type A4 coarse limestone.
-9.415550	134.310317	282/013DR001	10/05/2005	DREDGE DIAMANTINA	A - bulk sediment, B - biological sample	Dredge mostly biological material.
-9.386100	134.168700	282/018DR002	11/05/2005	DREDGE DIAMANTINA	A - bulk sample	Muddy bioclastic sand.
-9.381833	134.164000	282/019DR003	11/05/2005	DREDGE DIAMANTINA	A - bulk sediment, B and D - biological sample	Muddy sand.
-9.353167	134.118667	282/020DR004	11/05/2005	DREDGE DIAMANTINA	A - bulk sediment, D - biology sample	Bioclastic muddy sand.
-9.356333	134.119333	282/020DR005	11/05/2005	DREDGE DIAMANTINA	A - bulk, B - biology sample, C - coral rock fragments	mixture of muds and biological components
-9.349350	134.057617	282/023DR006	11/05/2005	DREDGE DIAMANTINA		solitary corals, indurated limestone, worm tubes, weathered, vesicles, many chunks up to 25 cm in diameter, well developed weathering rinds, staghorn
-9.328667	134.029167	282/025DR007	12/05/2005	DREDGE DIAMANTINA	A - bulk, B - biology, C - coral fragments, D - biological sample	
-9.179683	133.412400	282/038DR010	17/05/2005	DREDGE DIAMANTINA	A - bulk sample	
-9.028267	133.242433	282/044DR013	19/05/2005	DREDGE DIAMANTINA		Large slab of mudstone (Type A2), subrounded bored and weathered cobbles of mudstone (Type A3), bivalve and oyster shells (Type A1). No mud (winnowed out).
-9.799867	135.366683	282/002GR001	02/05/2005	GRAB SMITH MCINTYRE	A - bulk sample, B - biological sample. Bruce Site	Mostly forams and molluscs. Moderately sorted calcareous slightly muddy medium to fine sand, SGY 10/1 (Munsell)
-9.799767	135.366783	282/002GR002	02/05/2005	GRAB SMITH MCINTYRE	Grab taken for biological sampling 300 micron sieve used	Moderately sorted calcareous slightly muddy, medium to fine sand
-9.799767	135.383283	282/002GR003	02/05/2005	GRAB SMITH MCINTYRE	Grab taken for biological sampling 300 micron sieve used	Moderately sorted, calcareous, slightly muddy, medium to fine sand
-9.799883	135.367100	282/002GR085	26/05/2005	GRAB SMITH MCINTYRE	A -bulk and B - biology	moderately sorted calcareous muddy fine sand, 5Y 5/3, sand fraction mollusc fragments and well sorted
-9.799883	135.367100	282/002GR086	26/05/2005	GRAB SMITH MCINTYRE	B - biology sample	
-9.879333	135.364733	282/003GR004	04/05/2005	GRAB SMITH MCINTYRE	A - bagged bulk sediment	Sandy mud.
-9.879367	135.364850	282/003GR005	04/05/2005	GRAB SMITH MCINTYRE	B - biological sample	Sandy mud.
-9.841100	135.268317	282/005GR006	04/05/2005	GRAB SMITH MCINTYRE	A - bulk sediment	Muddy sand.
-9.841167	135.268317	282/005GR007	04/05/2005	GRAB SMITH MCINTYRE	B - Biology sample.	Muddy sand.
-9.839350	135.348400	282/006GR008	04/05/2005	GRAB SMITH MCINTYRE	A - Bulk sample (GA), B - biological sample.	Mostly forams and mollusc fragments. Calareous poorly sorted muddy fine sand.
-9.839267	135.348133	282/006GR009	04/05/2005	GRAB SMITH MCINTYRE	B - Biological sample	
-9.835300	135.296033	282/007GR010	04/05/2005	GRAB SMITH MCINTYRE	A - bulk sediment sample. B - sieved 300 micron of bulk	Calcareous poorly sorted muddy fine sand, minor amounts of gravel, mollusc and foram fragments, some organic matter.
-9.835433	135.296100	282/007GR011	04/05/2005	GRAB SMITH MCINTYRE	B - biological sample	Calcareous poorly sorted muddy fine sand, minor amounts of gravel, mollusc and foram fragments, some organic matter.
-9.832533	135.327300	282/008GR012	04/05/2005	GRAB SMITH MCINTYRE	A - Bulk sediment	Poorly sorted calcareous muddy fine sand, some calcareous gravel clasts, mostly mollusc and foram fragments, organic material
-9.832217	135.327600	282/008GR013	04/05/2005	GRAB SMITH MCINTYRE	B - biological sample, 300 micron sieve. D - biological,	Poorly sorted calcareous muddy fine sand, some calcareous gravel clasts, mostly mollusc and foram fragments, organic material

-9.821317	135.326367	282/009GR014	04/05/2005	GRAB SMITH MCINTYRE	A (bulk sediment) and B (biological, sieved 300 microns)	
-9.821567	135.326650	282/009GR015	04/05/2005	GRAB SMITH MCINTYRE	B - biological sample only, sieved 300 microns. D - biolo	Poorly sorted calcareous muddy medium sand, Munsell 5Y 4/2. Mostly mollusc and foram fragments, some organic fragments
-9.811850	135.223667	282/010GR016	05/05/2005	GRAB SMITH MCINTYRE	A (bulk) and B (biology) samples taken	Sandy mud.
-9.812900	135.256867	282/010GR017	05/05/2005	GRAB SMITH MCINTYRE	B - biological sample, 300 micron sieve. D - biological s	
-9.796133	135.282250	282/011GR018	05/05/2005	GRAB SMITH MCINTYRE	biology sample (B and D), bulk sample (A)	Muddy sand.
-9.793500	135.277267	282/012GR019	05/05/2005	GRAB SMITH MCINTYRE	A (bulk), B (biology, 300 micron sieve), D (biology, 5mm	Muddy sand.
-9.417867	134.313067	282/013GR020	10/05/2005	GRAB SMITH MCINTYRE	A - bulk sediment, D - biology	Sandy bioclastic, 5Y5/2 (Munsell).
-9.418017	134.312983	282/013GR021	10/05/2005	GRAB SMITH MCINTYRE	B - biological sample, 300 micron sieved. D - biological	Bioclastic sand.
-9.402317	134.238183	282/014GR022	10/05/2005	GRAB SMITH MCINTYRE	A - bulk sediment sample, D - biological	Muddy silt.
-9.402350	134.237800	282/014GR023	10/05/2005	GRAB SMITH MCINTYRE	B and D - biological sample only	
-9.377183	134.213567	282/015GR024	10/05/2005	GRAB SMITH MCINTYRE	A - bulk sediment sample	Sandy mud.
-9.377167	134.213833	282/015GR025	10/05/2005	GRAB SMITH MCINTYRE	B and D - biological sample	Sandy mud.
-9.401667	134.194333	282/016GR026	10/05/2005	GRAB SMITH MCINTYRE	A - bulk sediment sample, B and D - biology	Poorly sorted calcareous muddy fine to medium sand, sand gravel, carbonate clasts, molluscs and form fragments, fresh to intermediate presentation
-9.401617	134.194583	282/016GR027	10/05/2005	GRAB SMITH MCINTYRE	B and D- biological sample	
-9.393333	134.172833	282/017GR028	10/05/2005	GRAB SMITH MCINTYRE	A - bulk sediment, B and D - biology	Poorly sorted, calcareous, muddy, medium sand and gravel, Munsell 5Y5/4, mostly molluscs and foram fragments, very sloppy
-9.393500	134.171667	282/017GR029	10/05/2005	GRAB SMITH MCINTYRE	B and D - biological samples	Poorly sorted, calcareous, muddy, medium sand and gravel, Munsell 5Y5/4, mostly molluscs and foram fragments, very sloppy
-9.386183	134.167383	282/018GR030	11/05/2005	GRAB SMITH MCINTYRE	A - bulk sediment sample, D - biology	Bioclastic muddy sand, GLEY 1 4/10Y (Munsell)
-9.386167	134.167333	282/018GR031	11/05/2005	GRAB SMITH MCINTYRE	B and D - biological sample	Bioclastic muddy sand, GLEY 1 4/10Y (Munsell)
-9.383167	134.163000	282/019GR032	11/05/2005	GRAB SMITH MCINTYRE	A - bulk sediment sample, D - biology	Muddy sand with bioclasts, 5Y 5/2(Munsell)
-9.383167	134.163000	282/019GR033	11/05/2005	GRAB SMITH MCINTYRE	B and D - biological sample	
-9.356167	134.118133	282/020GR034	11/05/2005	GRAB SMITH MCINTYRE	A - bulk sediment sample	Long white spine, a few crusty bits
-9.356167	134.118100	282/020GR035	11/05/2005	GRAB SMITH MCINTYRE	B and D - biology sample	
-9.356333	134.082833	282/021GR036	11/05/2005	GRAB SMITH MCINTYRE	A - bulk sediment	Sandy mud.
-9.356333	134.083167	282/021GR037	11/05/2005	GRAB SMITH MCINTYRE	B - biological	Sandy mud.
-9.375783	134.059750	282/022GR038	11/05/2005	GRAB SMITH MCINTYRE	A - bulk sediment	Calcareous sandy mud (poorly sorted) and very fine sand grains, very sloppy
-9.376000	134.060000	282/022GR039	11/05/2005	GRAB SMITH MCINTYRE	B - biological	Calcareous sandy mud (poorly sorted) and very fine sand grains, very sloppy

-9.348983	134.057400	282/023GR040	11/05/2005	GRAB SMITH MCINTYRE	A - bulk sediment, B - biological	Large boulder, indurated limestone, well developed weathering rind, burrows filled with mud.
-9.348967	134.057417	282/023GR041	11/05/2005	GRAB SMITH MCINTYRE	A - bulk sediment, B - biological, D - >5mm biological	Poorly sorted calcareous gravelly mud, 5Y 5/4 (Munsell), very sloppy
-9.347333	134.058000	282/023GR042	11/05/2005	GRAB SMITH MCINTYRE	B - biology sample, 300 micron sieve	
-9.339867	134.032950	282/024GR043	11/05/2005	GRAB SMITH MCINTYRE	A - bulk sediment, B - biological sample	Poorly sorted calcareous mud, no sand grains or gravel clasts
-9.339867	134.032933	282/024GR044	11/05/2005	GRAB SMITH MCINTYRE	B - biology sample, 300 micron sieve	
-9.329100	134.029233	282/025GR045	12/05/2005	GRAB SMITH MCINTYRE	A - bulk, B - biology	Poorly sorted calcareous muddy medium sand
-9.224733	133.801700	282/026GR046	12/05/2005	GRAB SMITH MCINTYRE	A - bulk, B - biology	Mud
-9.381167	133.664667	282/027GR047	13/05/2005	GRAB SMITH MCINTYRE	A - bulk sample, D - biology	Muddy sand.
-9.381167	133.664833	282/027GR048	13/05/2005	GRAB SMITH MCINTYRE	B - bulk sediment, sample collected for biological specim	Muddy sand.
-9.333817	133.690867	282/028GR049	13/05/2005	GRAB SMITH MCINTYRE	A - bulk sample. B and D - Sample collected for biologica	Very poorly-sorted calcareous sandy mud (with some gravel); gravel clasts are all calcareous, mostly mollusc fragments with fresh to intermediate preservation
-9.333783	133.690867	282/028GR050	13/05/2005	GRAB SMITH MCINTYRE	B and D - Sample collected for biological specimens	
-9.303750	133.696750	282/029GR051	13/05/2005	GRAB SMITH MCINTYRE	A - Bulk sample. B - Sample collected for biological spec	Poorly sorted slightly gravelly mud, very sloppy
-9.303500	133.697000	282/029GR052	13/05/2005	GRAB SMITH MCINTYRE	B and D- Sample collected for biological specimens	
-9.227333	133.698333	282/030GR053	13/05/2005	GRAB SMITH MCINTYRE	A - Bulk sample. B and D - Sample collected for biology	Poorly sorted calcareous slightly sandy mud. Sandy grains of forams, mollusc fragments. Very sloppy
-9.227500	133.698333	282/030GR054	13/05/2005	GRAB SMITH MCINTYRE	B and D Biology Sample	
-9.033717	133.104050	282/034GR055	16/05/2005	GRAB SMITH MCINTYRE	No sample in grab jaws. Small sample recovered from grab	Calcareous Mud. Few sand grains, very unconsolidated
-9.098733	133.198183	282/037GR056	17/05/2005	GRAB SMITH MCINTYRE	A - bulk sediment, B and D - biological sample	Calcareus slightly muddy coarse sand and gravel, very poorly sorted. Sand and gravel fractions mostly mollusc fragments. 5Y5/4 (Munsell)
-9.098750	133.198283	282/037GR057	17/05/2005	GRAB SMITH MCINTYRE	B and D - biological sample	Calcareous slightly muddy coarse sand and gravel, very poorly sorted. Sand and gravel fractions mostly mollusc fragments.
-9.179617	133.413583	282/038GR058	17/05/2005	GRAB SMITH MCINTYRE	B - Biology sample	Minor biota only
-9.179517	133.413583	282/038GR059	17/05/2005	GRAB SMITH MCINTYRE	A - bulk sediment sample. B and D - Biology sample	Calcareous poorly sorted slightly muddy sandy gravel. Sand fraction is coarse grained. Gravel and sand carboanate fragments, maybe some lithics and te rrigenous sand.
-9.179567	133.413667	282/038GR060	17/05/2005	GRAB SMITH MCINTYRE	B and D - Biology sample	
-9.170850	133.392250	282/039GR061	17/05/2005	GRAB SMITH MCINTYRE	A - bulk sediment sample. B - Biology sample	Calcareous poorly sorted muddy coarse sand. Gravel and sand fraction calcareous (inderterminate preservation).
-9.171067	133.392283	282/039GR062	17/05/2005	GRAB SMITH MCINTYRE	B - biology sample	Calcareous poorly sorted muddy coarse sand. Gravel and sand fraction calcareous (inderterminate preservation).
-9.150467	133.390833	282/040GR063	18/05/2005	GRAB SMITH MCINTYRE	A - bulk sediment, B - biology	Calcareous, muddy medium sand, sponge spicules

-9.150100	133.390817	282/040GR064	18/05/2005	GRAB SMITH MCINTYRE	B - biology sample	Calcareous, muddy medium sand, sponge spicules.
-9.126417	133.421450	282/041GR065	18/05/2005	GRAB SMITH MCINTYRE	A - bulk sediment sample, D- biology	
-9.126450	133.421483	282/041GR066	18/05/2005	GRAB SMITH MCINTYRE	B - biology sample	Mud. 5Y 5/2 (Munsell).
-9.114183	133.408000	282/042GR067	18/05/2005	GRAB SMITH MCINTYRE	A - bulk sediment, only 1/10 full, small sample taken	Shell grit.
-9.089633	133.418433	282/043GR068	19/05/2005	GRAB SMITH MCINTYRE	A - bulk sample, D - biology	Bioclastic muddy grit.
-9.089417	133.418167	282/043GR069	19/05/2005	GRAB SMITH MCINTYRE	B and D - biology sample	Bioclastic muddy grit.
-9.029633	133.243200	282/044GR070	19/05/2005	GRAB SMITH MCINTYRE	A - bulk sediment, B - biology	Calcareous muddy gravel (A1), and cobbles (A2). Cobbles of very hard ?terrigenous mudstone, bored, encrusted and weathered.
-9.029517	133.243433	282/044GR071	19/05/2005	GRAB SMITH MCINTYRE	B - Biology	
-9.030100	133.244683	282/045GR072	19/05/2005	GRAB SMITH MCINTYRE	Sample B taken for biology. Grab broken, weld snapped during depolyment	
-9.002033	133.200967	282/048GR073	20/05/2005	GRAB SMITH MCINTYRE	A - bulk sample, D - biology	Bioclastic muddy sand.
-9.001833	133.200917	282/048GR074	20/05/2005	GRAB SMITH MCINTYRE	B - biology sample, 300 micron sieve, D - biology	Coarse bioclastic muddy sand.
-9.096333	133.286783	282/049GR075	20/05/2005	GRAB SMITH MCINTYRE	A - bulk sample	Coarse bioclastic muddy sand.
-9.096450	133.286717	282/049GR076	20/05/2005	GRAB SMITH MCINTYRE	A - bulk sample. Rock in teeth of grab.	Rock shows a slight weathering profile from a rusty brown on the outside to a grey in the centre. Sedimentary rock a carbonaceous marl.
-9.096367	133.286583	282/049GR077	20/05/2005	GRAB SMITH MCINTYRE	A - bulk sample (2 rock types). Rock in teeth plus sandy	A1 sedimentary limestone, highly bored and soft sediment infilled in the borings. Other sample is only bored on the exposed surface, also has soft wor m tubes and some algae. A2 sedimentary rock. Cobble of marl limestone no sign of boring cobbel is ~8cm
-9.096383	133.286800	282/049GR078	20/05/2005	GRAB SMITH MCINTYRE	B - biology, 300 micron sieve	Bioclastic sandy mud.
-9.175817	133.494517	282/053GR079	21/05/2005	GRAB SMITH MCINTYRE	A - bulk sample, B- biology sample	Calcareous muddy gravel.
-9.175667	133.494533	282/053GR080	21/05/2005	GRAB SMITH MCINTYRE	A - bulk sample, B- biology sample	Calcareous muddy gravel.
-9.154317	133.484100	282/055GR081	21/05/2005	GRAB SMITH MCINTYRE	A - bulk sample, B and D- biology sample	Poorly sorted calcareous gravelly mud, with cobble of coarse limestone. 5Y5/4 (Munsell).
-9.626317	134.239100	282/061GR082	25/05/2005	GRAB SMITH MCINTYRE	A - Bulk sediment sample. B - Biology sample	Calcareous mud (very unconsolidated)
-9.738617	135.265617	282/064GR083	25/05/2005	GRAB SMITH MCINTYRE	A - Bulk sediment sample. B - Biology sample	Poorly sorted calcareous muddy fine sand. Sand fraction mostly foram and mollusc fragments.
-9.738600	135.265783	282/064GR084	25/05/2005	GRAB SMITH MCINTYRE	B - biology sample	
-9.799433	135.368083	282/002CAM001	02/05/2005	UNDER WATER CAMERA	relatively barren, 15 minutes recovery. Bruce Site DV tape =1, VHS tape =1	Pink fish, irregular sand waves, no biota visible on sea bed.
-9.799883	135.367083	282/002CAM062	26/05/2005	UNDER WATER CAMERA	moderate to poor visibility DV tape = 60; VHS tape = 7	Sandy substrate, rippled, 2 fish, red fish, burrow, fish in water column (1:53), red fish (1:58 - bright white/light blue object in water column, look ed anthroprogenic)
0.000000	0.000000	282/003CAM002	04/05/2005	UNDER WATER CAMERA	Get navigation from VHS tape. DV tape = 2; VHS tape = 1	

-9.873850	135.317233	282/004CAM003	04/05/2005	UNDER WATER CAMERA	DV tape = 3; VHS tape = 1	Bottom seems soft, many burrows, seafloor heavily bioturbated.
-9.840633	135.268750	282/005CAM004	04/05/2005	UNDER WATER CAMERA	see overlay for navigation (VHS tape). Parked camera in w	Solitary coral, fewer and bigger burrows (10-20 cm), particles moving across field of vision, soft coral or anenome, large burrow ejecting sediment, l ots of thin tubes laying on substrate
-9.838567	135.338567	282/006CAM005	04/05/2005	UNDER WATER CAMERA	DV tape = 5; VHS tape = 1	Relatively sparse biota - some infaunal biota, burrows, silty sandy surface, small undulations in sea bed (small ripples)
-9.834667	135.296367	282/007CAM006	04/05/2005	UNDER WATER CAMERA	DV tape = 6; VHS tape = 1	Scallops, burrows, sponge?, sea pens.
-9.831333	135.326333	282/008CAM007	04/05/2005	UNDER WATER CAMERA	relatively sparse biota DV tape = 7; VHS tape = 1	Rubbly at start with shells and hydroid, sea pen, worm tube, fish, more sea pens/whips, bottom sitting fish, octocoral, small sand ripples, burrows.
-9.821750	135.326850	282/009CAM008	04/05/2005	UNDER WATER CAMERA	relatively sparse biota DV tape = 8; VHS tape = 1	Murky sediment in suspension at beginning, current ripples, sandy, irregular ripples, sea pen, flat fish (flounder), small octacoral colony, red objec t (unknown), yellow sponge
-9.813033	135.256600	282/010CAM009	05/05/2005	UNDER WATER CAMERA	DV tape = 9; VHS tape = 1	Fish, sea whip (octacoral), burrows, frequent ripples (poorly defined), sparse burrows and biota on silty undulated sand
-9.797450	135.733633	282/011CAM010	05/05/2005	UNDER WATER CAMERA	DV tape = 10; VHS tape = 1	Rippled sandy bed, swail infill of ripples spread ~20cm 2/3cm height. Bioturbated burrows apparent but lower density compared to other sites, worm bur rows expelling sand. One dead shell. Little apparent life in sand.
-9.422333	134.312233	282/013CAM011	10/05/2005	UNDER WATER CAMERA	DV tape = 11; VHS tape = 1	octocorals, sea whips (some Junieella type), seafans, crinoid on sea fan, soft coral, burrows, fenestrate bryozoan clumps, low sponge clumps, crinoids , anemone (Dofleina armata)
-9.401833	134.237267	282/014CAM012	10/05/2005	UNDER WATER CAMERA	minimal life forms observed, apparently quite barren. DV tape = 12, VHS tape = 1	Very soft muddy substrate, some mounds, fecal pellets rolling around
-9.376683	134.211900	282/015CAM013	10/05/2005	UNDER WATER CAMERA	DV tape = 13; VHS tape = 1	silty bottom, heavily bioturbated, fish, mounds
-9.403617	134.195967	282/016CAM014	10/05/2005	UNDER WATER CAMERA	DV tape = 14; VHS tape = 1	possible diffuse hydroids, octocorals and possible antipatherians, small fans fish, bioturbated bottom, sea whips, stick octocorals, no ripples, barr en silty sand, bioturbated
-9.392750	134.170983	282/017CAM015	10/05/2005	UNDER WATER CAMERA	DV tape = 15; VHS tape = 1	sea whips, fish, minimal current, black coral, sponges, fans, sub-crops of biota, intermittant hard grounds, extensive sand areas, silty sand
-9.384617	134.164667	282/018CAM016	11/05/2005	UNDER WATER CAMERA	DV tape = 16, VHS tape = 2	Spiral tip white sea whips, seawhips, sea fans, crinoids, octocorals, spiral antipatherians, soft corals, outcrops, crevices, large fish, sponge vase, small stripped wrasse, scorpenoid, some large fans, some dense aggregations of octocorals, nidalid soft
-9.383267	134.162900	282/019CAM017	11/05/2005	UNDER WATER CAMERA	DV tape = 17; VHS tape = 2	initial intermittent sparse biota, isolated octocoral, small sea whips and sea fans, soft patches, bioturbated, extensive sandy mud areas with fecal pellets and some burrows
-9.356000	134.125000	282/020CAM018	11/05/2005	UNDER WATER CAMERA	DV tape = 18; VHS tape = 2	rocky bottom, sea whips, octocorals, dense population, silty slope, on rocky slope orange encrustations, sea whips, echinoid, gorgonian/octocoral gard en, soft coral, blue octocoral, sponges, barket star
-9.356500	134.083150	282/021CAM019	11/05/2005	UNDER WATER CAMERA	Very limited effective footage DV tape = 19; VHS tape = 2	Turbidity high, soft bottom, occasional burrows, visibility very poor, mud substrate.
-9.376100	134.059533	282/022CAM020	11/05/2005	UNDER WATER CAMERA	DV tape = 20; VHS tape = 2	Very turbid, poor visability, soft floculant sediment, bioturbated burrows, many burrows, large depression

-9.347333	134.058000	282/023CAM021	11/05/2005	UNDER WATER CAMERA	DV tape = 21; VHS tape = 2	soft bottom, turbid water, poor visibility, sea whip, octocoral, very sparse biota, gergonian, black coral, shrimp, patches of soft and firmer substra te, crinoid, sandy mud and muddy sand
-9.339833	134.033000	282/024CAM022	12/05/2005	UNDER WATER CAMERA	DV tape = 22; VHS tape = 2	Very turbid, poor visibility, muddy substrate, bioturbated, isolated rock near end, strong current
-9.329167	134.029167	282/025CAM023	12/05/2005	UNDER WATER CAMERA	DV tape = 23; VHS tape = 2	Bioturbated, faecal pellets, burrows, turbid water, poor visibility, sea whips, gorgonians, sponge, hardgrounds, soft coral, fish, some barren patches , feather star, soft corals, flat fish and sea bed.
-9.258167	133.801500	282/026CAM024	12/05/2005	UNDER WATER CAMERA	DV tape = 24; VHS tape = 2	Four fish, flat sea floor, soft bioturbated burrowed sediment with assorted fish (few in number).
-9.381217	133.664350	282/027CAM025	13/05/2005	UNDER WATER CAMERA	DV tape = 25; VHS tape = 2	Small fish (gobies and demersal), small swimming crustaceans (shrimps), bioturbation, no ripples, detritus, faecel pellets
-9.333667	133.690833	282/028CAM026	13/05/2005	UNDER WATER CAMERA	CAM did not focus - redeployed at same site as CAM027 DV	Poor visibility, soft muddy substrate, bioturbated
-9.334667	133.690833	282/028CAM027	13/05/2005	UNDER WATER CAMERA	CAM027 repeat run of CAM026 DV tape = 26; VHS tape = 3	Jelly fish, fish, burrows, flat substrate, sandy mud. ?Hydroids, sponge or shell. At 120m depth firm substrate, burrows. Turbidity increases at depth. Sparse biota at depth.
-9.304783	133.696767	282/029CAM028	13/05/2005	UNDER WATER CAMERA	DV tape = 27; VHS tape = 3	Very turbid, poor visibility. Burrowed muddy substrate, sparse biota. Sparse hardgrounds, with attached yellow sponge. ?Hydroid, sea fan, sea whip, ?o ctacoral.
-9.227300	133.697000	282/030CAM029	14/05/2005	UNDER WATER CAMERA	DV tape = 28; VHS tape = 3	Bioturbated mud, relatively featureless.Tubular sponges, sea whips, low fans, seapen, gorgonians, bryozoan clumps, soft corals (Netheid type), fish
-9.089250	133.747700	282/031CAM030	14/05/2005	UNDER WATER CAMERA	DV tape = 29; VHS tape = 3	Hit into soft sediment, visibility poor, shallow depression, soft coral, bioturbated, surface with many small burrows, large open burrows.
-9.205533	133.632517	282/032CAM031	14/05/2005	UNDER WATER CAMERA	WRONG LABEL ON CLOCK - written as 282/032CAM032 when shou	Heavily burrowed, soft bottom, flat, muddy, sparse biota, fish, stripey fish on seabed, sponges, soft corals
-9.033433	133.104083	282/034CAM033	16/05/2005	UNDER WATER CAMERA	DV tape = 31; VHS tape = 4	large, steep hole; fish; undulating, burrowed seabed with large burrows/holes; very muddy and unconsolidated; very turbid; low visibility
-9.026233	133.168783	282/035CAM034	17/05/2005	UNDER WATER CAMERA	DV tape = 32; VHS tape = 4	Bioturbated sea floor, sandy mud. Holes are up to 5cm across. 08:54:50 on tape: edge of large hole (pock mark?).
-9.037633	133.159700	282/036CAM035	17/05/2005	UNDER WATER CAMERA	DV tape = 33; VHS tape = 4	Bioturbated sediments, high density of particulate matter in the water column. Camera went in a hole and a large decapod (>6cm) was observed at 11:33: 00 mins into the tape.
-9.099100	133.198633	282/037CAM036	17/05/2005	UNDER WATER CAMERA	DV tape = 34; VHS tape = 4	Relatively flat sandy bottom, shelly sand, no burrows. Large fish (snappers), hard flat sand. Faecal pellets,anemones (white and black), fallen octoco ral, crinoid, red fish, silver fish, small ground fish with gobles, sea whip/octocoral
-9.179733	133.413633	282/038CAM037	17/05/2005	UNDER WATER CAMERA	DV tape = 35; VHS tape = 4	Good biota cover, low height biota, minimal loose sediment, firm substrate. Small bushy octacorals and seafans with crinoids, seawhips, small fish, bl ack coral. Bedrock. Black crinoids,anenome, octacorals, red octacoral. Escarpment at 135m
-9.171483	133.392417	282/039CAM038	17/05/2005	UNDER WATER CAMERA	DV tape = 36; VHS tape = 4	Hard sandy calcareous substrate, pavement-like. Negligible current, good visibility. Shell debris, soft bryozoans and hydroids, seawhip, seafan, octac orals, anemones, crinoids, antipatherys (bushy and flat forms), large black coral, sponges, fish

-9.150417	133.390967	282/040CAM039	18/05/2005	UNDER WATER CAMERA	DV tape = 37; VHS tape = 4	Flat, sand, reasonably hard, crinoids, some bioturbation, feeding mounds - worms or enteropneusts, hemichordates, white anemme, small silver fish, sea urchin, low dome, other anemones, cerianthid anemonem sponges, orange bottom fish, small bottom fish
-9.127267	133.422167	282/041CAM040	18/05/2005	UNDER WATER CAMERA	DV tape = 38; VHS tape = 4	Worm tubes, soft sediment, 15 cm across hole, mollusc on substrate, fish resting on bottom.
-9.116067	133.408733	282/042CAM041	18/05/2005	UNDER WATER CAMERA	DV tape = 39; VHS tape = 4	Bioturbated floor, muddy/sandy bottom, blade/octa corals, sponges, crustaceans, solitary corals, sea whips/fans, crinoid
-9.088650	133.416717	282/043CAM042	19/05/2005	UNDER WATER CAMERA	DV tape = 40; VHS tape = 4	mounded soft sediments, bioturbated, rocky hard surface at 13:19, sponges, black coral, sea anenomes, crinoids, large sea fan, wobbegong shark, lots o f particulates in water, octacoral, hard substrate, sea whip, red fish, solitary coral, squirrel fish,
-9.031050	133.244233	282/044CAM043	19/05/2005	UNDER WATER CAMERA	VHS tape ran out, Part 1 on VHS 4 and Part 2 on VHS 5 DV	Rocky and rubbly substrate, flaggy bedded rocks, subcrop and exposures. Murky water, visibility OK. Patches and veneer of muddy sediment. Crinoids w hite anemones, large snapper, sponge, burrowed sediment patches, brown fish, red crinoid. Sparse biota.
-9.030200	133.244933	282/045CAM044	19/05/2005	UNDER WATER CAMERA	DV tape = 42; VHS tape = 5	Rocky substrate with veneer and patches of muddy sediment. Sponges, red fish (?squirrel), spring from Grab, red star fish, white sponges, ?hexanelid s ponge, yellow sponge. Sparse biota.
-9.030700	133.245883	282/046CAM045	19/05/2005	UNDER WATER CAMERA	Increasing amount of soft muddy sediment during drift. DV tape = 43; VHS tape = 5	Rubbly substrate with sparse patches of very unconsolidated fine sediment. Rocky outcrops and subcrops. Thin sediment veneer; white sponge, yellow spo nge, stalked crinoid, black coral (spiral form), bryozoan, white starfish, sea fan, small fish, anaemon
-9.031917	133.249600	282/047CAM046	20/05/2005	UNDER WATER CAMERA	DV tape = 44; VHS tape = 5	lots of fish, soft sediment, bioturbation, some feeding depressions, mounds, pockmarks, red crinoid?, large burrows, crab running across bottom?, large rock or possible hole - core site?
-9.003600	133.202117	282/048CAM047	20/05/2005	UNDER WATER CAMERA		Bioturbated soft sediments, light brown fish (5:22:40), big hole/large burrow (5:25), fish in hole (5:29), sea urchin
-9.096350	133.286717	282/049CAM048	20/05/2005	UNDER WATER CAMERA	DV tape = 46; VHS tape = 6	Hard substrate, echinoderm, sponges, crinoids, sea anemones, bioturbated bottom, stork crinoid, scattered boulders on hard substrate, 9:47:30 - stork crinoid, water column particulates, sea whip, black coral, 9:49 - increasing density of sea floor biota
-9.198683	133.430567	282/050CAM049	21/05/2005	UNDER WATER CAMERA	DV tape = 47; VHS tape = 6	Jelly fish and many smaller similar biota on the way down. Some phenomena in water seen on echo sounder.
-9.217550	133.486200	282/052CAM050	21/05/2005	UNDER WATER CAMERA	DV tape = 48; VHS tape = 6	Jelly fish in water at 22m water depth, decrease in abundance at 36m water depth. 100m - biota in water column. Bioturbated muddy substrate. Fish, spa rs biota, benthic fish, hole on LHS (04:26), squirrel fish?, ridge (04:31:10), large depression. On ret
-9.175683	133.494500	282/053CAM051 A	21/05/2005	UNDER WATER CAMERA	Run A downslope (followed by Run B upslope) DV tape = 49; VHS tape = 6	Hard substrate, abudant biota. Antipatherians, crinoids, sponges, anemones fish, gorgonians, seafans, large fenestrate bryozoans, sea whips, ?coral (stag horn form), red crinoid, small red fish. Sub-crop drop-off (sounder 160m, 17:49) rocky ledges
-9.176200	133.497000	282/053CAM051 B	21/05/2005	UNDER WATER CAMERA	Run B upslope (preceeded by Run A downslope) DV tape = 49; VHS tape = 6	Soft muddy substrate at 156m. Bioturbated, red fish in burrow, sparse biota. Rocky ledges at 160m (18:18), white sponge, ?barnacles, sea whip, crinoid , cliff ledge. Top of drop off at 136m (18:20), patchy to abundant biota, sea fan, hexactinellid sponge
-9.154133	133.496300	282/054CAM052	21/05/2005	UNDER WATER CAMERA	missed base of slope DV tape = 50; VHS tape = 6	Soft muddy substrate with rocky patches. Sponges, bushy seafans, crinoids. Drop of to 214m (20:39), rocky ledge, fish, sponges, octacorals. (20:45) So ft muddy substrate, bioturbated, very sparse biota.

-9.162517	133.529400	282/056CAM053	22/05/2005	UNDER WATER CAMERA	DV tape = 51; VHS tape = 6	Soft muddy substrate, bioturbated, poor visibility. Sparse biota, ?core hole (00:26:20), fish, red biota, ?feeding marks, fish on RHS, burrows (00:33: 36).
-9.550800	133.952900	282/057CAM054	24/05/2005	UNDER WATER CAMERA	DV tape = 52; VHS tape = 6	9:15:40 - fish, fairly featureless muddy bottom, a little bioturbation (09:19:50)
-9.580733	134.039583	282/058CAM055	24/05/2005	UNDER WATER CAMERA	camera sinks directly into soft bottom. DV tape = 53; VHS tape = 6	Very soft sediments
-9.595433	134.152067	282/059CAM056	24/05/2005	UNDER WATER CAMERA	DV tape = 54; VHS tape = 6	Small fish in water column (distinct signal on echosounder), visibility very poor, very muddy, sparse biota, rare biota on the surface, soft sticky mud, burrows, recorded fish on way down
-9.608617	134.179000	282/060CAM057	24/05/2005	UNDER WATER CAMERA	Very bad footage, mud stuck on lens DV tape = 55; VHS tape = 6	Very poor visibility, sticky mud, unconsolidated material, few burrows/sparse biota
-9.626067	134.238900	282/061CAM058	25/05/2005	UNDER WATER CAMERA	generally very poor visibility DV tape = 56; VHS tape = 6	Very poor visibility, soft mud, sparse biota, some burrows
-9.655967	134.282917	282/062CAM059	25/05/2005	UNDER WATER CAMERA	DV tape = 57; VHS tape = 6	Very soft muddy bottom, water off bottom Very cloudy/murky, b ~ 5m, water clarity to 70m Very good, little penetration to 65m.
-9.661333	134.373283	282/063CAM060	25/05/2005	UNDER WATER CAMERA	DV tape = 58; VHS tape = 7	photic zone down to 80m, very soft muddy bottom, water very murky
-9.739350	135.265083	282/064CAM061	25/05/2005	UNDER WATER CAMERA	DV tape = 59; VHS tape = 7	Sandy substrate, small fish near bottom. Burrows, very sparse biota, ?ripples. Small fish, red object (LHS 18:37), ?crab (18:40).

Appendix 2

Water and Suspended Sediment Samples

L. Sbaffi

1.1. Water samples processing

During Survey 282, a total of 54 water samples were collected from 24 different sites across the Arafura Sea. The CTD Seabird SBE911 Plus, took water samples at each site at 1m from the surface and 1m from the sea floor. Water depths ranged from 74m in the south-eastern part of the surveyed area to 226m in the north-western sector (Figure 1). Two stations, 282/50CTD18 and 282/51CTD19, were sampled at the additional depths of 140, 165 and 170 m.

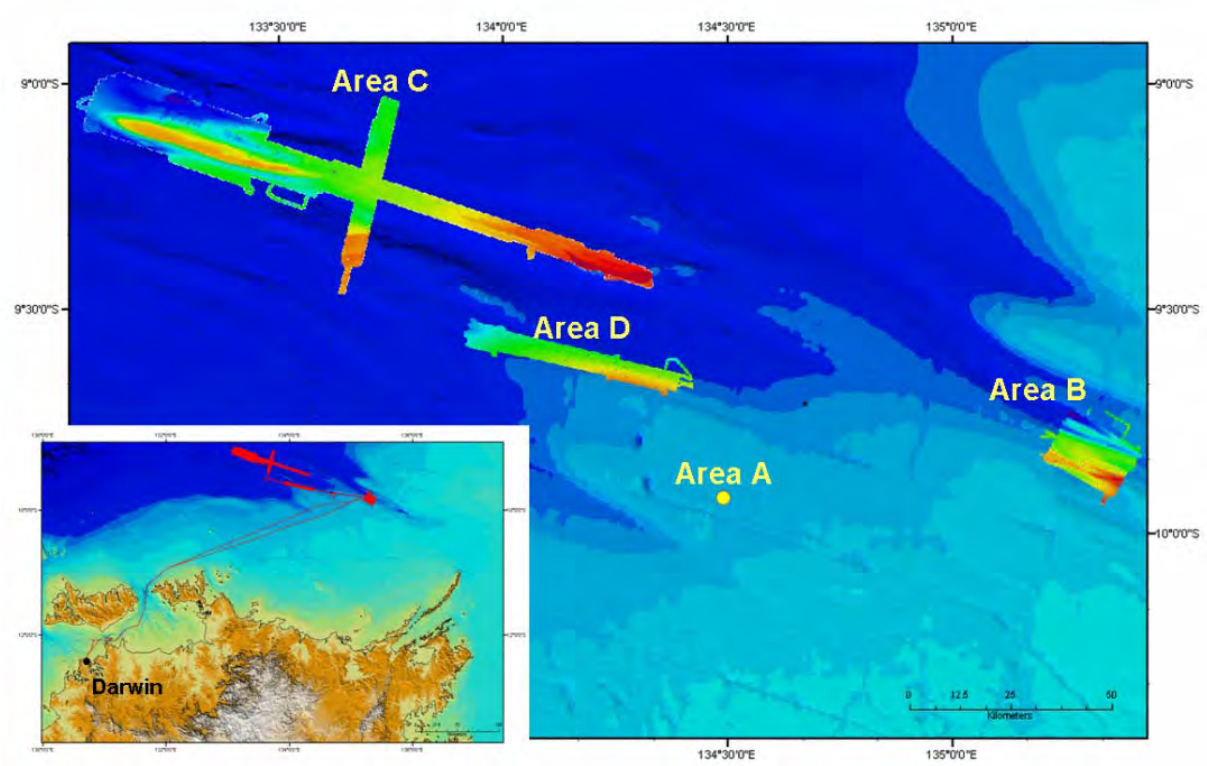

Figure 1: Multibeam bathymetry over the surveyed areas A, B, C and D on the Northern Arafura Platform. Insert: ship track of GA survey S282.

Water samples were collected using the ship's CTD rosette and 2.5 ltr Niskin bottles. One litre of sea water was filtered through pre-weighted 45µm mesh glass membranes using a vacuum system on board the vessel. The filter papers were then stored in a dry

freezer and, on return to the Geoscience Australia's laboratory, were oven dried at 60˚C and re-weighted to ±0.0001g to obtain the weight of suspended sediments. Suspended sediment concentrations (SSCs) were finally calculated from these weights. The details were entered into Geoscience Australia's Marine Sediment Database (MARS). http://www.ga.gov.au/oracle/mars/

All samples were subsequently visually inspected using a standard binocular microscope to provide an assessment of the type and nature of the particles in suspension.

1.2. Suspended sediment concentration

Near-bed SSCs (Figure 2.a) range from 2mg/l to 26.9mg/l (average of 8.65mg/l). About 52% of the samples are above the average value and a general overview indicates a pattern of decreasing concentrations from the SE to the deeper NW region of the study area (Figure 1).

A more detailed observation of the samples using the light microscope, indicates that three filter papers with very high SSCs (024CTD007, 026CTD008 and 063CTD022) are located in the central surveyed area and are particularly rich in silt rather than in organic particles.

At the surface (Figure 2.b), sediment concentrations attain an average value of 6 mg/l, with a minimum of 2mg/l and a maximum of 8.7mg/l, over three times smaller than the near-bed samples. About 70% of the samples present a SSC above the average but there is no obvious pattern in the distribution of such concentrations as 'heavy' samples are found throughout the study area.

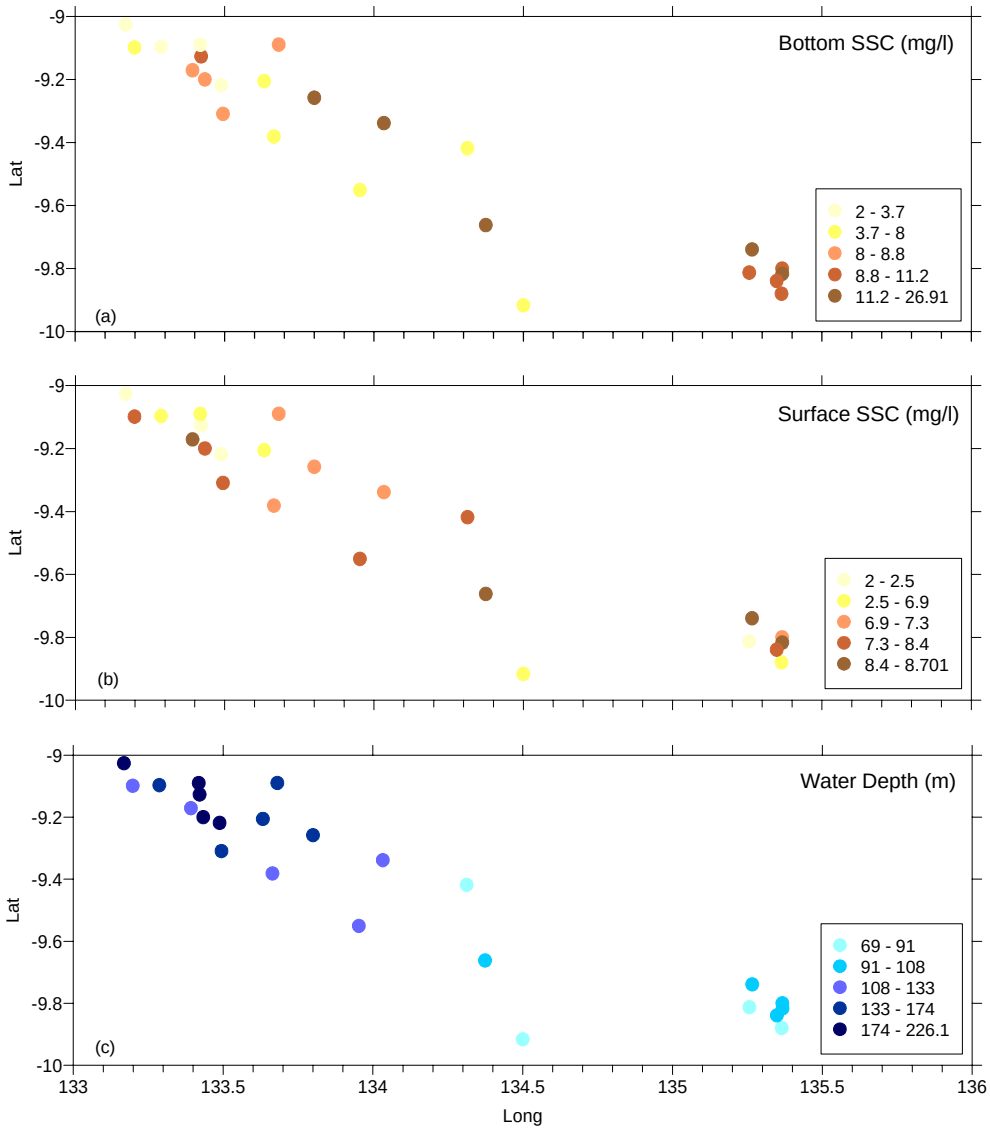

Figure 2. (a) Suspended sediment concentrations of near-bottom samples; (b) suspended sediment concentrations of surface samples; (c) water depths of the near-bottom water samples.

1.3. Composition of the filter papers

1.3.1. Surface samples

There are very low concentrations of suspended material on filter papers used to collect material from surface water samples. The largest component of these low weight papers are diatom spicules. Few centric diatoms specimens have been observed in samples 013CTD006, 024CTD007 and 026CTD008. Very few forms (~5 - 6 specimens in each sample) of juvenile planktonic foraminifera, mainly *Globigerinoides* spp., have also been observed in most samples, particularly the distal ones in the north-western sector of the survey area. The same samples also present a

small number of brown filaments which are identified as algae. On the other hand, few specimens of copepods, around 4 to 8 in each sample, have been recognised in most of the samples in the central and south-eastern part of the survey. Most of the copepods in the samples belong to the *Euchaeta* family and small brown wool-like particles have been identified as copepods fecal pellets. Most of the filter papers also present a few dinoflagellates specimens (1-3 per sample) of, generally belonging to the *Ceratium* family. As a general trend, the biological content of the water samples decreases from the more distal sites towards the southern sites. The mineralogical content of the samples is also very low, with small particles of quartz, biotite and manganese (the inorganic fraction represents ~2/3% of the total composition of the samples).

1.3.2. Near-bottom samples

The major biological groups recorded in these samples are, in order of decreasing abundance: diatoms spicules, benthic foraminifera, centric diatoms, copepods and gastropods. In terms of biological abundance and diversity, the whole survey area could be divided into three sub-areas (Figure 3).

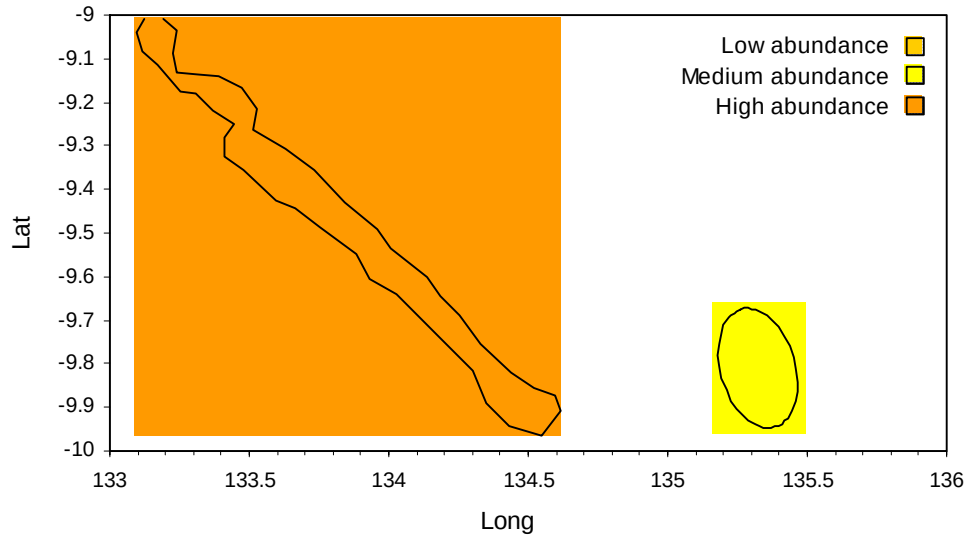

Figure 3. Distribution of the biological abundances in the water samples showing three distinct sectors in the surveyed area.

1) The south-eastern area is characterised by medium abundances with an average of 10 to 15 juvenile benthic foraminifera and 2-3 centric diatoms in each sample. The presence of copepods is here limited to an average of 1-2 specimens/sample, all of the *Euchaeta* family.
2) The more northern samples located in the central and north-western areas present a very low biological content, limited to an average of 9-11 benthic foraminifera and 5-8 copepods per sample. Some of these samples are particularly rich in mud and inorganic content, such as manganese and quartz fragments.
3) The southern samples located in the central and north western areas are the richest and most diversified of the whole surveyed area. While visual observations of gastropods and planktonic foraminifera have been made, diatoms spicules are the predominant group. The presence of benthic foraminifera is limited to about 5-6 specimens/sample and copepods are mostly absent.

Overall, the size fraction of the material deposited on the near-bottom filter papers is smaller than that from the surface samples. The exceptions being the deeper, northern locations. The inorganic content is also higher at depth, although is very difficult, due to the very small size of the filter papers, identify the nature of the mineral grains observed. As an average visual value, about 70-80% of the near-bottom samples are composed of inorganic particles.

Future work

Future work includes XRD (X-Ray Diffraction) and dot-mapping analyses on a selection of the deep sea samples and several surface ones to determine the exact composition of the inorganic fraction. It is also anticipated that a select range of grab samples will be analysed and the results will be compared with those of the filter papers to identify near bottom currents affecting sediment transport.

Appendix 3

Meteorology and Oceanography

M. Hemer

Meteorology

Methods

The RV Southern Surveyor has on an on board meteorological log which records Atmospheric temperature, relative humidity, mean and gusting wind speeds and direction, and atmospheric pressure. These logs are available electronically post-survey from the National Facility website.

Results

Figure 1 displays the meteorological conditions for the 28 day survey period. It should be noted that the meteorological conditions are recorded on the vessel, and consequently contain both spatial and temporal variability. For the purposes of this report, spatial variability is ignored. Data is recorded every 10 seconds, however for this report, it has been re-sampled at hourly intervals. The record commences at 0119 30-Apr-2005 GMT (Julian Day 119.056), and continues until 2130 27-May-2005 GMT (Julian Day 146.90).

Wind direction recorded by the on-board ships log is erroneous. Station forms typically indicate a wind-direction from the ESE, whereas the ships log suggest wind are typically from the N. Given the time of year, the Trade wind season is expected to bring winds from the SE in the Arafura Sea region. Wind speed ranged from 10-30 knots for the entire period of the survey. Maximum wind speed of 32 knots was recorded on Julian Day 121. A second period of increased wind speeds occurs between Julian Day 140-145 (Table 1).

Air Temperature exhibits a diurnal signal with magnitude of approximately 4.0˚C. A strong diurnal signal is also observed in the atmospheric pressure, with magnitude of

approximately 4 hPa. Similarly, the humidity displays a diurnal signal of magnitude of approximately 5 %.

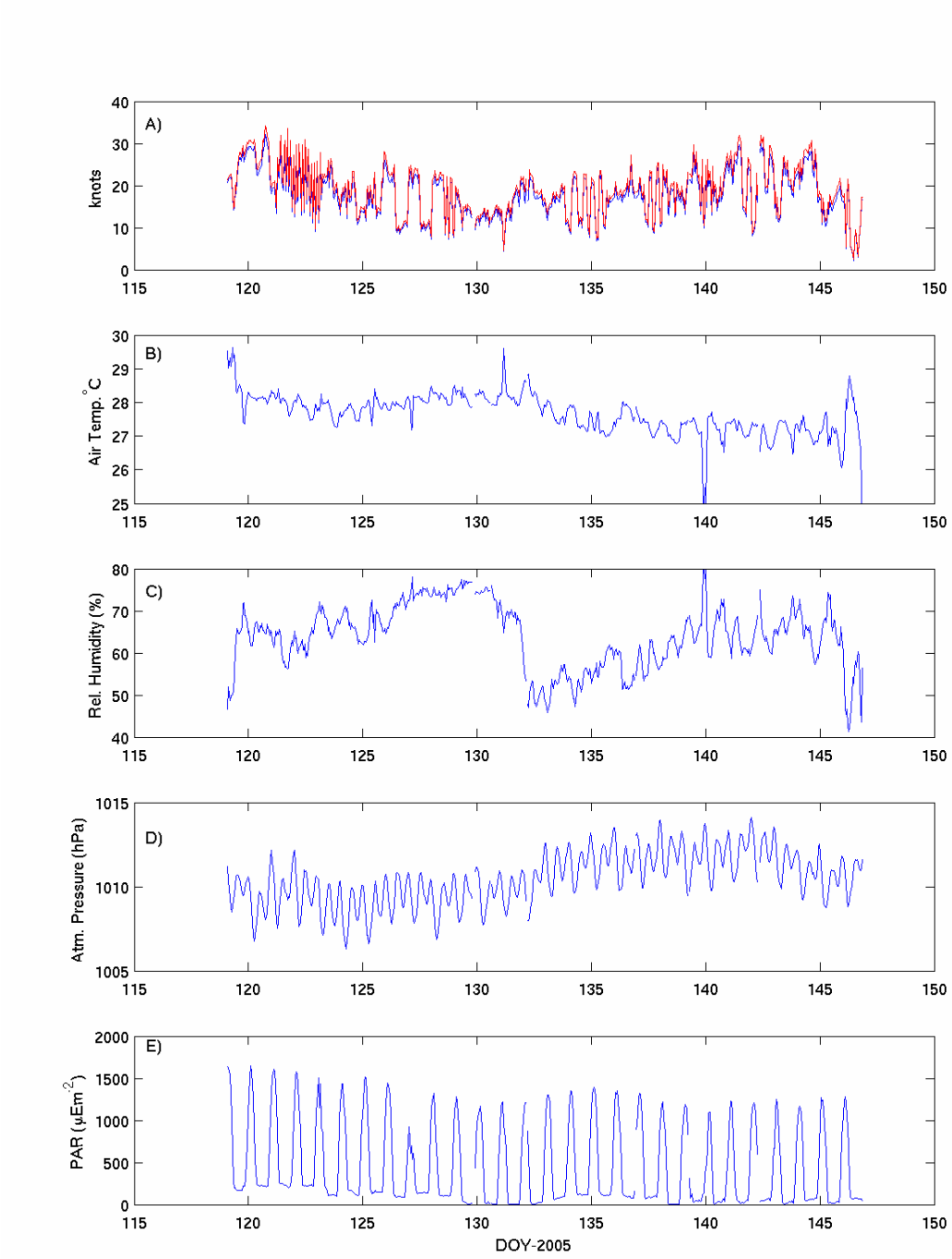

Figure 1. Time-series of raw meteorological data from the FRV Southern Surveyor for the period of survey 282. a) wind speed. b) air temperature, c) Relative humidity, d) Atmospheric pressure, and e) PAR – light sensor.

First Record GMT (2005)	Last Record GMT (2005)	Sampling Interval	Wind Spd Mean Wind Spd Std Wind Spd Max	Temp Min Temp Mean Temp Max	Pres Min Pres Mean Pres Max	Humidity Min Humidity Mean Humidity Max	PAR Min PAR Mean PAR Max
0119 30-Apr 2005	2130 27-May 2005	Hourly	17.95 kts 5.61 32.05	23.54°C 27.66 29.63	1006.3 hPa 1010.5 1014.1	41.31 % 63.86 82.47	5.9 uE/m2 446.0 1651.0

Table 1. Raw meteorological statistics from underway data obtained from FRV Southern Surveyor for the period of Surveys 282. This data is stored within Geoscience Australia in \\Diamond\smac\1\smac\research_cruises\S282\UNDERWAY

Oceanography.

Underway data.

The RV southern surveyor log records surface salinity, temperature and fluorescence at the location of the vessel for the period of deployment using the Southern Surveyor on-board thermosalinograph. Initial processing and calibration of the data were carried out by CSIRO marine and atmospheric research technicians.

The data from each of the Water Temp, Salinity and Fluorescence properties contain considerable spatial and temporal variability (Table 2, Figure 2, 3, 4). On transit to and from the study region, water temperature varied considerable, with maximum temperatures recorded during the outward transit, and minimum water temperatures recorded on the return transit. A cooling trend is observed for the entire period of the survey.

Salinity shows strong temporal variability in Area B (Figure 3). Minimum salinity values were recorded in Area B at the beginning of the survey. On return to Area B to collect the oceanographic mooring, salinities were approximately 1.5 PSU greater in Area B than at the beginning of the survey.

A peak in Fluorescence occurred during Julian Day 129, which drops away sharply. The record suggests that an instrumental check may have occurred at the end of the peak, however no record has been made of this (Figure 4).

First Record GMT (2005)	Last Record GMT (2005)	Sampling Interval	Water Temp Min Water Temp Mean Water Temp Max	Salinity Min Salinity Mean Salinity Max	Fluorescence Min Fluorescence Mean Fluorescence Max
0119 30-Apr 2005	2130 27-May 2005	Hourly	27.46°C 28.44 29.86	32.45 PSU 33.79 34.70	0.022 0.14 1.14

Table 2. Raw thermosalinograph statistics from underway data obtained from FRV Southern Surveyor for the period of Survey 282.

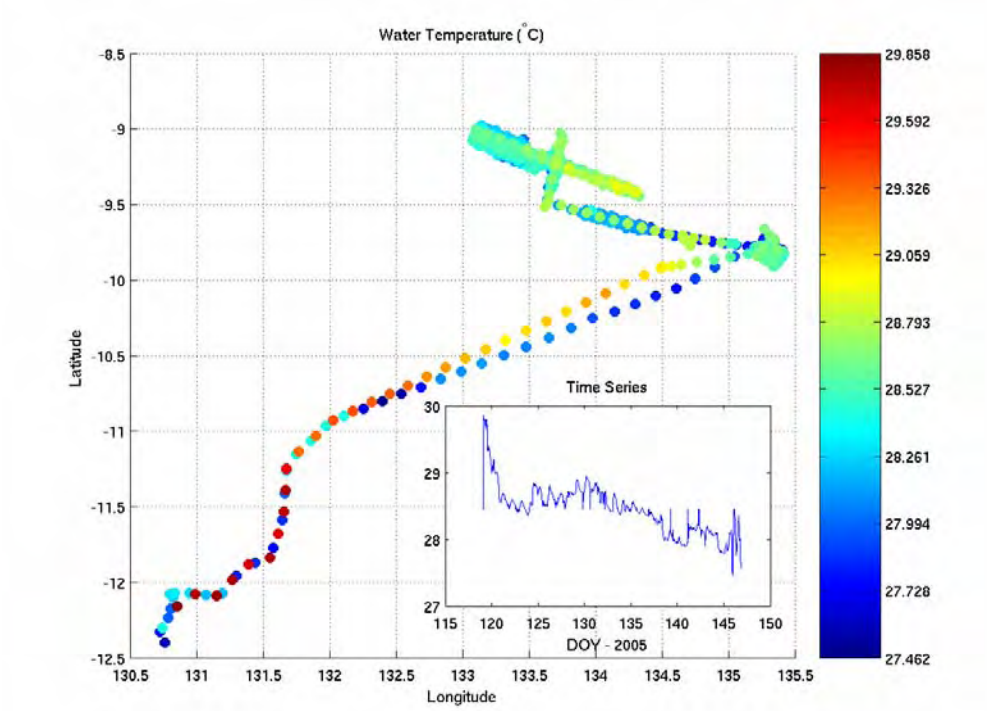

Figure 2. Spatial and temporal variability of surface water temperature as measured by the thermosalinograph and recorded by the UNDERWAY ships log.

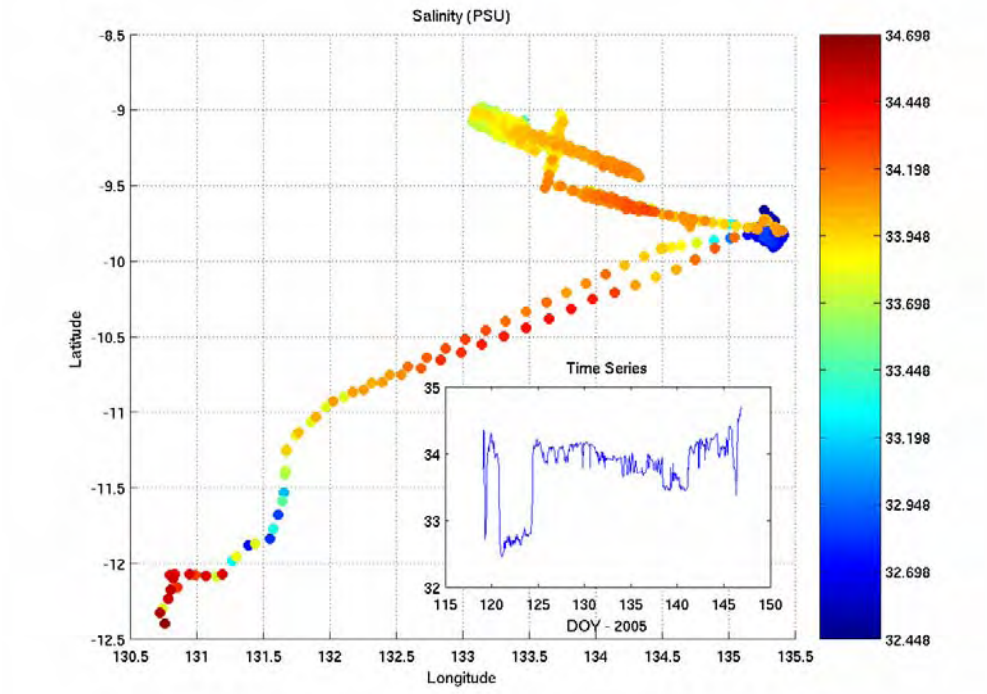

Figure 3. Spatial and temporal variability of surface salinity as measured by the thermosalinograph and recorded by the UNDERWAY ships log.

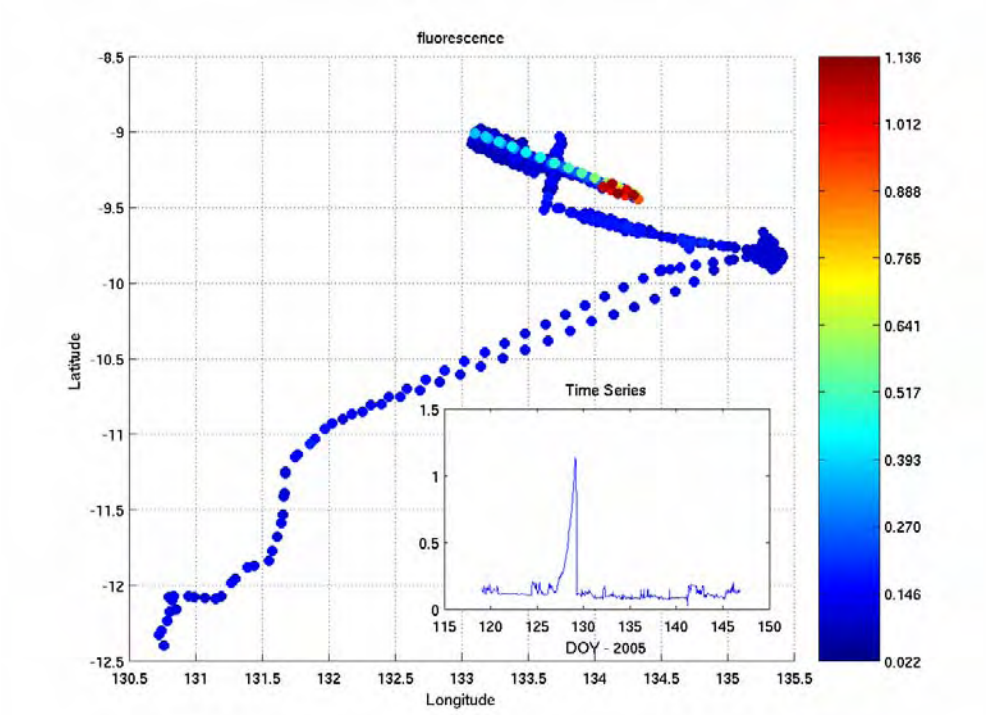

Figure 4. Spatial and temporal variability of surface fluorescence as recorded by the UNDERWAY ships log.

CTD Profiles

The Southern Surveyor has a Seabird SBE911 CTD aboard. 29 CTD deployments were carried out during the survey. 5 deployments were thermosalinograph calibration deployments, the remaining 24 deployments occurring on survey stations as listed in Table 3. Initial processing and calibration of the data were carried out by CSIRO marine and atmospheric research technicians. CSIRO CTD deployment numbering differs to GA sequencing. The GA CTD deployment and the corresponding CSIRO CTD deployments are listed in Table 3. The locations of the CTD deployments are shown in Figure 5.

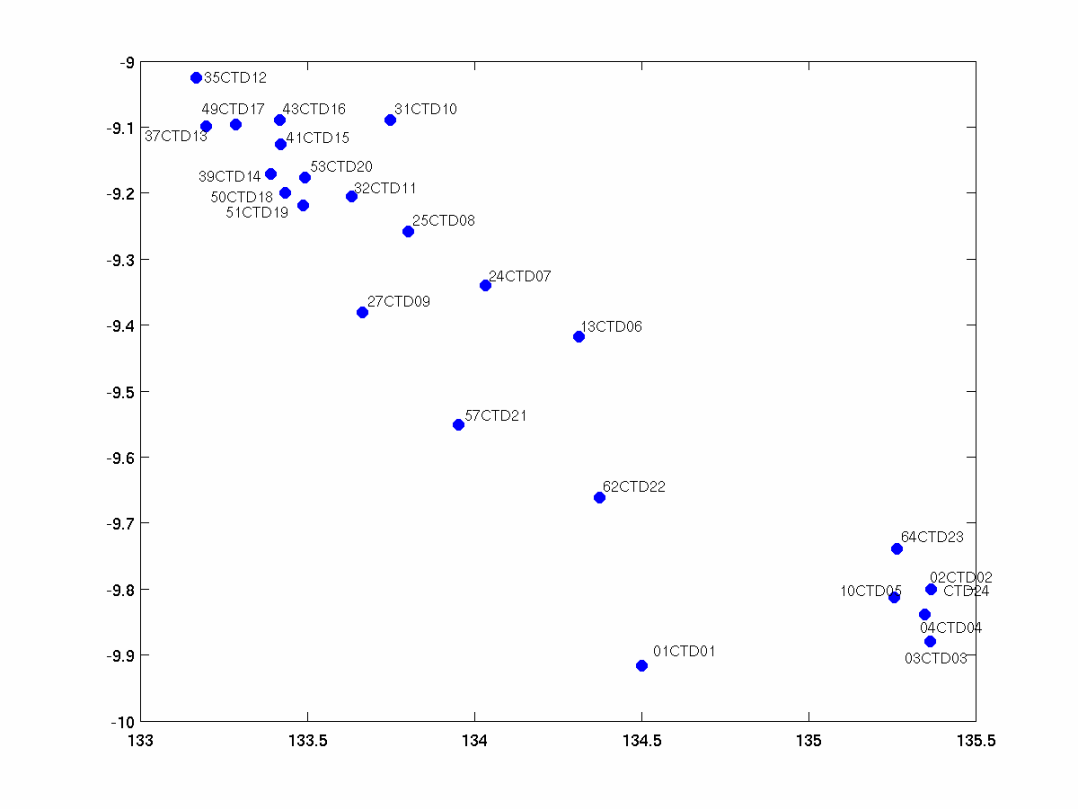

Figure 5. Location of stations at which CTD profiles were taken during Survey 282.

GA Seq. No.	CSIRO Seq. No.
01CTD01	1
02CTD02	2
03CTD03	6
04CTD04	7
10CTD05	8
13CTD06	9
24CTD07	10
25CTD08	11
27CTD09	13
31CTD10	14
32CTD11	15
35CTD12	16
37CTD13	17
39CTD14	18
41CTD15	19
43CTD16	20
49CTD17	21
50CTD18	22
51CTD19	23
53CTD20	24
57CTD21	25
62CTD22	26
64CTD23	27
02CTD24	28

Table 3. List of CTD deployments, and GA and CSIRO sequence numbers.

List of CTD deployments

The Seabird SBE911 CTD was configured to measure profiles of salinity, temperature, turbidity, and PAR light through the water column. Figures 6-9 display all profiles of salinity, temperature, Transmission, and PAR light as indicators of turbidity respectively.

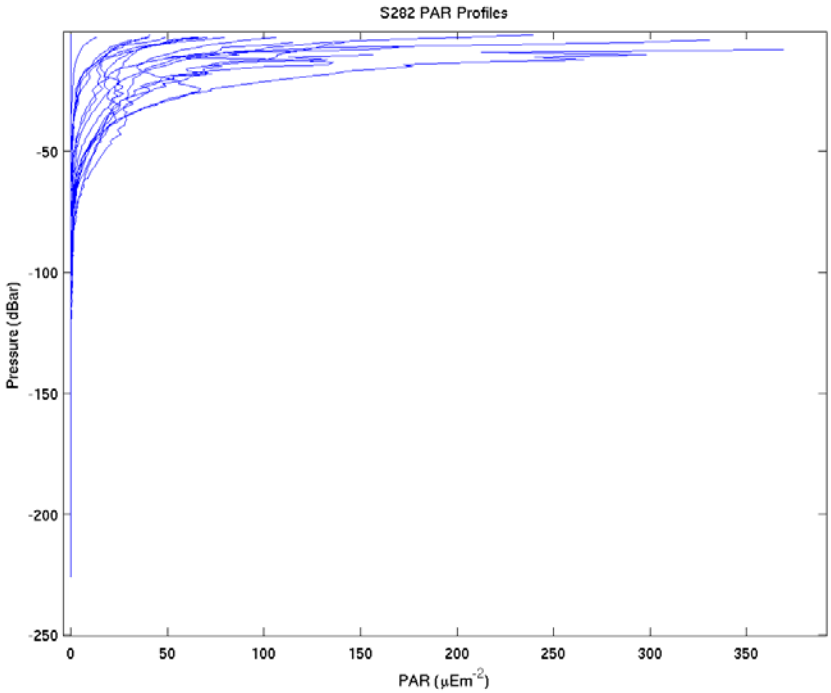

Figure 6. Salinity profiles from all CTD deployments during Survey 282.

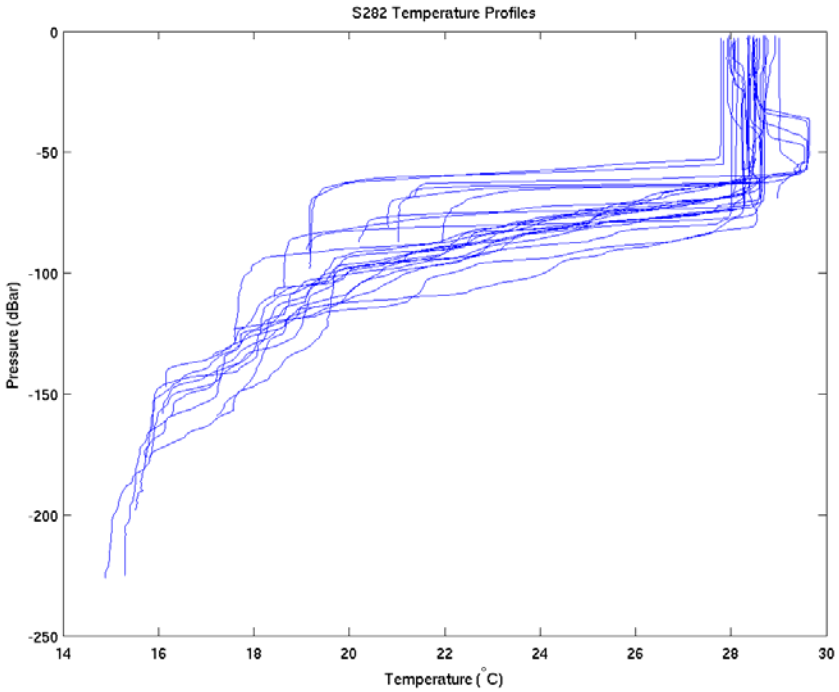

Figure 7. Temperature profiles from all CTD deployments during Survey 282.

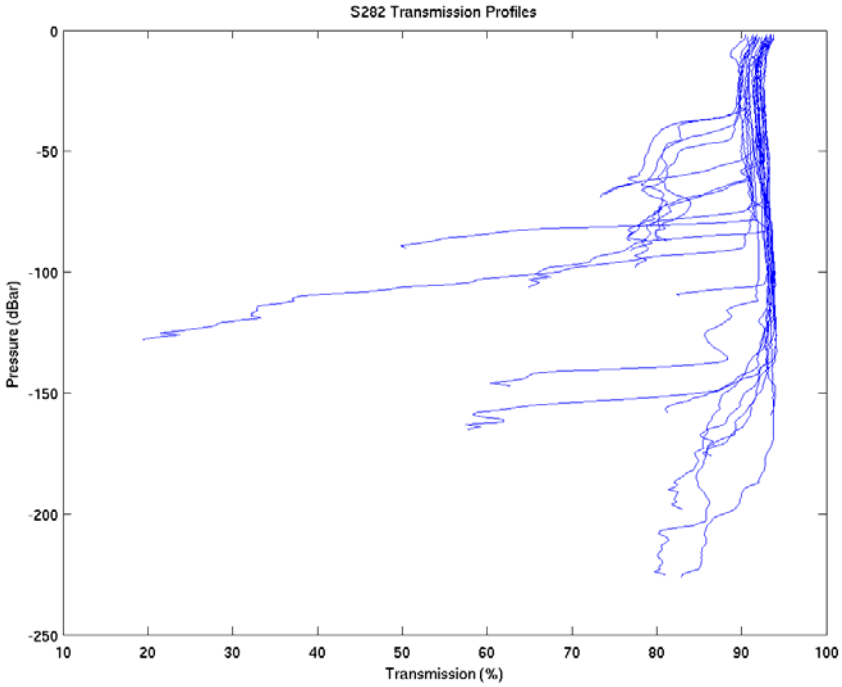

Figure 8. Transmission profiles from all CTD deployments during Survey 282.

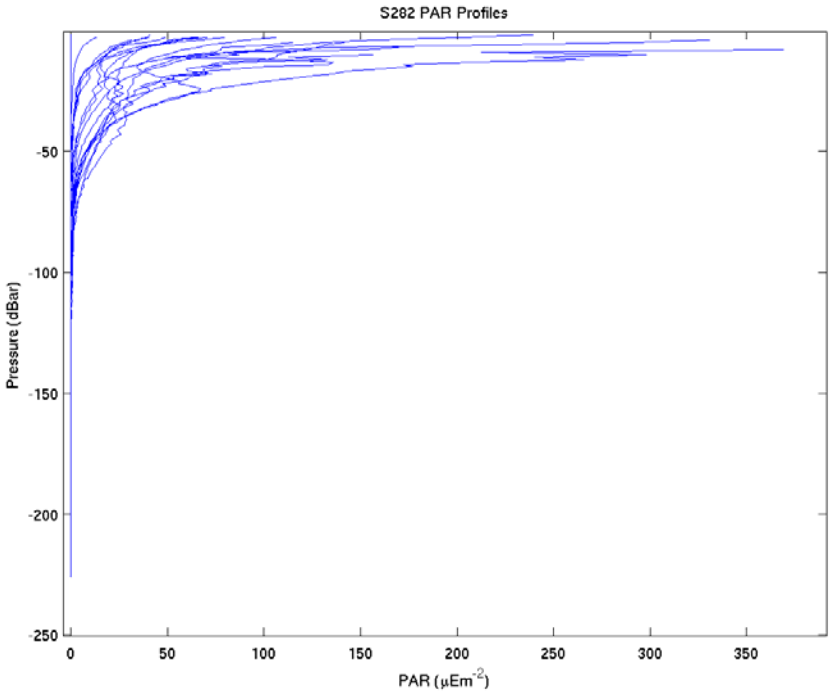

Figure 9. PAR profiles from all CTD deployments during Survey 282.

The surface mixed layer is observed to have variable salinity. Lowest surface salinities are observed in Area B (consistent with the Underway thermosalinograph data). Minimum salinities of approximately 32.5 PSU are observed in this region. Below approximately 100m water depth, salinity is greatest with values of approximately 34.6.

The surface mixed layer has relatively consistent temperatures of approximately 28 °C. In Area B (Stns 02, 03, 04 and 10), a warm plume is observed between approximately 40 and 60m depth, with maximum temperatures of the survey recorded of approximately 29.5 °C. The mixed layer depth shows variation from approximately 25m to approximately 80m. Coolest temperatures are observed near the seafloor at the deepest stations, with minimum temperatures of approximately 15 °C recorded.

The mid-water column warm plume observed in Area B near the beginning of the survey (profiles 02-05) is not observed in Area B near the end of the survey (profiles 23-24), indicating that the warm plume is intermittent. In the latter profiles, the surface mixed layer extends to approximately 60m depth (i.e., the lower depth limit of the warm plume).

The PAR profiles indicate that no light reaches beyond 80m water depth. Transmission is typically high in the surface mixed layer. Minimum Transmission values of less than 20% are recorded in the near bed layer. Transmission drops sharply in the near-bed layer, suggesting the presence of suspended material near to the seabed.

The salinity-temperature plot (Figure 10) displays all data from all CTD profiles during the survey.

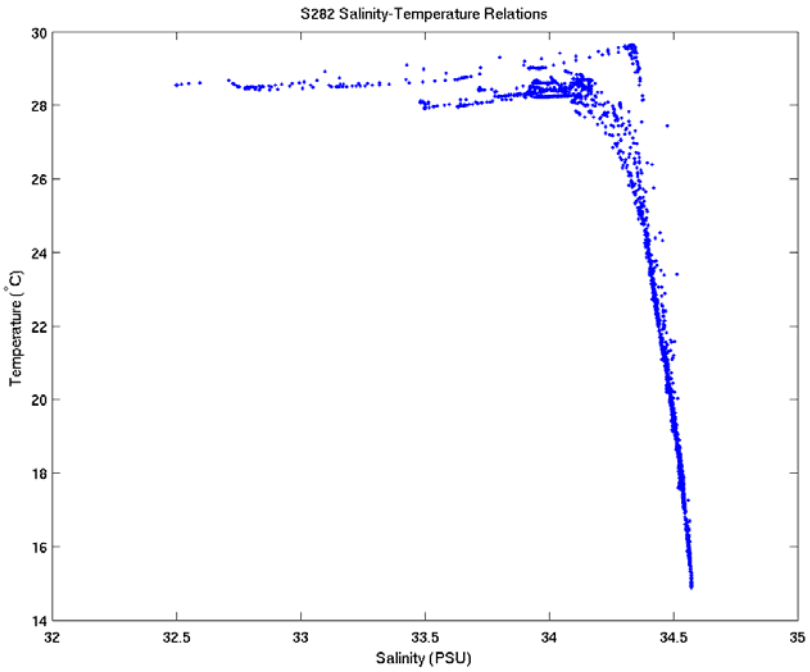

Figure 10. Salinity Temperature relation for all data from all CTD deployments during Survey 282.

Three water masses are identified. A warm and fresh water mass (A), a warm saline water mass (B), and a cool saline water mass (C). A brief interpretation of the origins of each water mass follows:

1. Water Mass A is expected to be formed during the Monsoon season, with high rainfall and runoff from Irian Jaya. Monsoon winds push this water mass South-Eastwards into the Gulf of Carpentaria, and when the Trades winds commence, the water mass is pushed North-Westwards , effectively increasing the area over

which this water mass is found. A similar water mass was described by Rochford (1966).

2. Water Mass B is identified as the warm plume observed in mid water depths in Area B. This is warm saline water which has been overlain by fresher less dense water formed during the preceding Monsoon season. The high temperatures and salinities of water mass B are typical of a water mass formed by evaporation.

3. Water Mass C, as the most dense, cool and saline water mass originates in the deeper waters found down the slope, in the north-west of the study region. The influence of this water mass is observed near the seabed in Area B, having mixed with the overlying water.

Figures 11 - 13 show an interpolated cross-shelf transect, which passes north-westwards from stn03 through CTD profiles (03CTD03, 04CTD04, 10CTD05, 13TCTD06, 24CTD07, 25CTD08, 32CTD11, 53CTD20, 41CTD15, 49CTD17, 35CTD12). Density was calculated using the CSIRO MatLAB seawater Library (CSIRO, 2005) from the Salinity, Temperature and Pressure data, using the sw_dens routine.

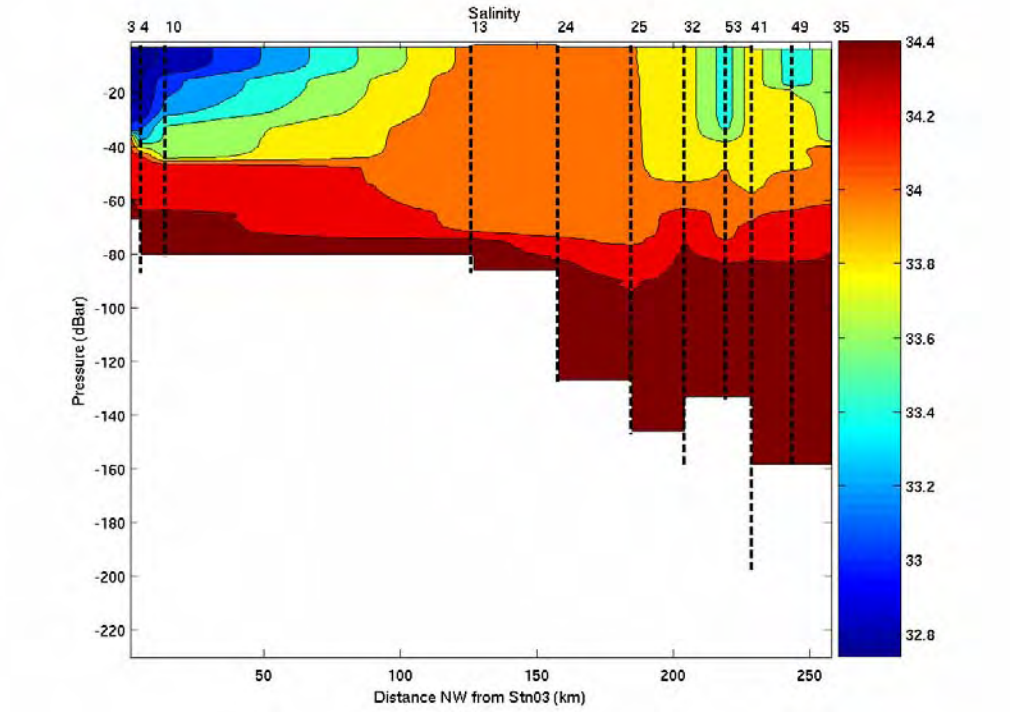

Figure 11. SE-NW Transect of Salinity during Survey 282.

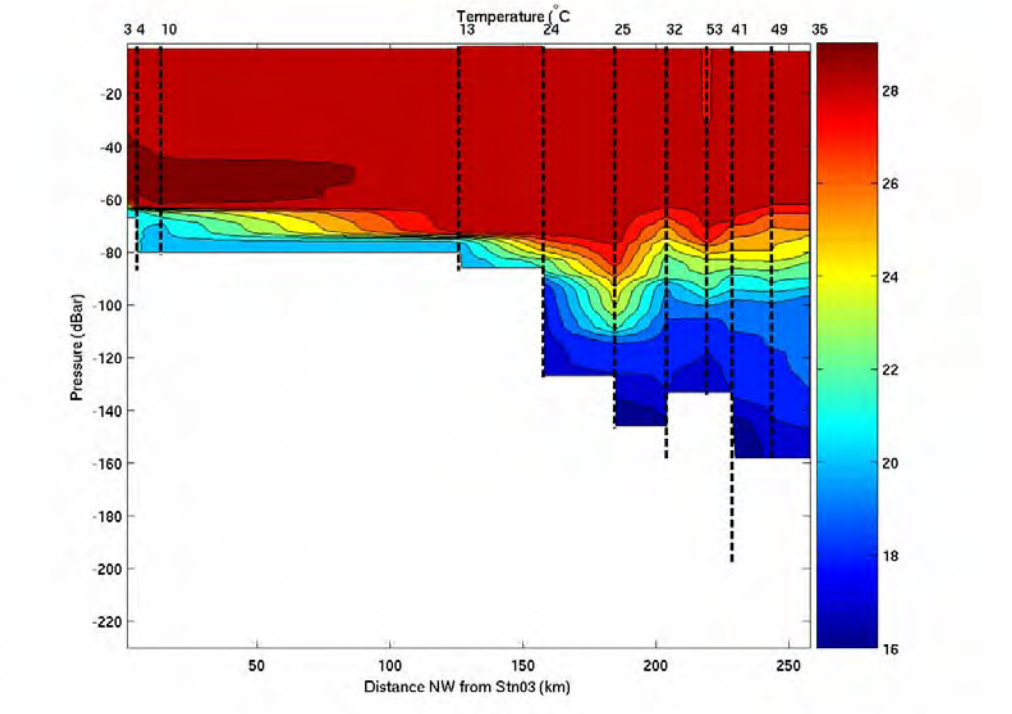

Figure 12. SE-NW Transect of Temperature during Survey 282.

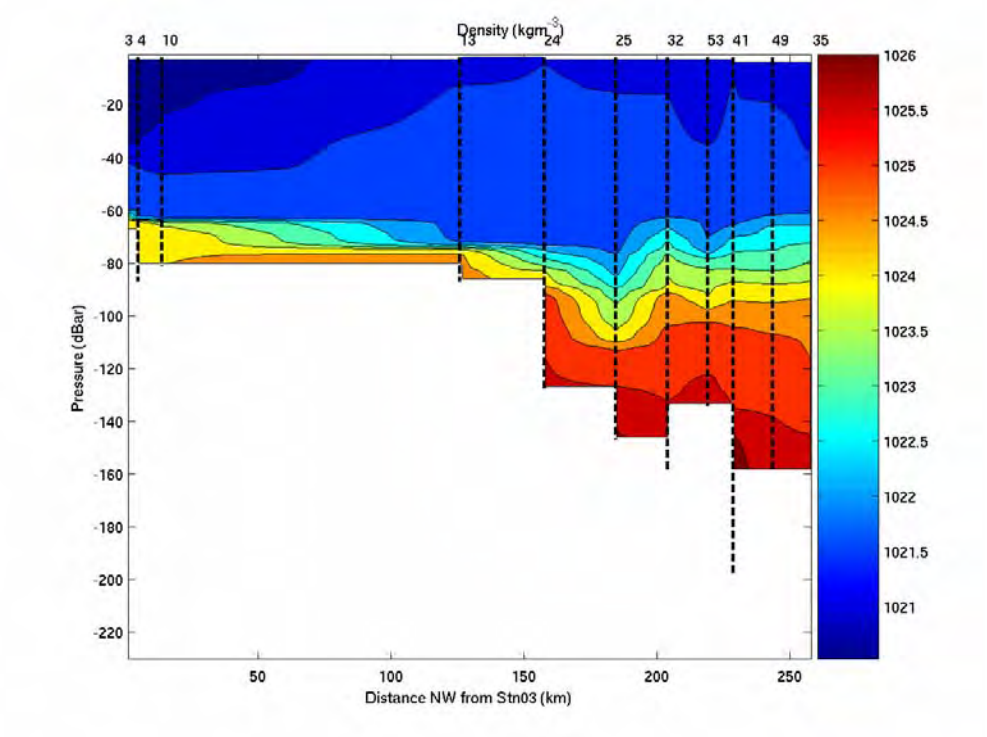

Figure 13. SE-NW Transect of Water Density during Survey 282.

The fresh, low density water is constrained to the surface layer in the south-east region. A strong pycnocline (brought about by the strong thermocline) is evident in this region at approximately 60m water depth. The pycnocline (thermocline) is less strong in the deeper waters to the north-west, and is centred around 80m water depth. Aside from the warm plume in the south-east, the upper 60m of the water column over the whole study region is relatively uniform at approximately 28 °C.

Salinity displays greater variability in the surface layer. A surface salinity maxima is observed at stations 13, 24 and 25, with salinities of approximately 34.2. To the south-east, the fresh surface waters of Area B are located, and to the north-west, slightly fresher (salinity 33.5) surface waters are found. Maximum salinities of approximately 34.5 are observed at all stations, with the depth of occurrence increasing with distance north-westwards.

Oceanographic Mooring Data

The hydrodynamic conditions were recorded with an oceanographic mooring designed to measure localised currents on the shelf edge at Station 002. A second mooring was to be deployed but was abandoned on survey due to difficulties with the Acoustic Release. The mooring consisted of the Geoscience Australia instrument frame, BRUCE (Benthic Research frame for Underwater sediment Concentration Experiments). BRUCE was deployed in Area B at location 9° 48.014' S, 135° 22.000' E in 92.0 m water depth. The mooring was complete at 0409 2/05/2005 GMT.

BRUCE comprised a 300 kg weighted steel frame equipped with:

- A Nortek^{TM} Vector Acoustic Doppler Velocimeter (ADV #N4103). This instrument was positioned to sample at 100 cm above the base of the benthic frame. The vector uses acoustic sampling techniques to measure flow in a remote sampling volume (Nortek, 2000). The instrument was programmed to burst sample every hour for 8 minutes at 8 Hz to record at turbulent time scales. This instrument logs vector components of velocity (east, north and up), pressure and temperature internally to be downloaded on recovery. The Nortek vector (ADV #N4103) contains 82 MB of internal memory (~$2x10^6$ samples).
- Two Benthos^{TM} optical backscatter sensors, positioned to sample at 100 cm (OBS #897) and 27 cm (OBS #2167) above the base of the benthic frame. The OBS instruments measure suspended sediment concentration in the water column. These instruments were powered by, sampled at the same rate as, and logged to, the Nortek Vector as “analog inputs” on the Advanced Tab of the Deployment Planning dialog box.

Mooring Stn2BRUCE commenced logging of data on the Nortek Vector at 06:00 02/05/2005 GMT (Julian Day 121.25). The first reading of the instrument after the mooring was complete occurs at 06:00 02/05/2005 (Julian Day 121.25). The last reading to occur before recovery occurred at 22:30 25/05/2005 (JD 144.94). All recordings after this time have also been deleted. The total record length is 23.6875 days.
On deployment, two grab samples (282/002GR02 and 282/002GR03), a CTD station (282/002CTD02), and a camera station (282/002CAM01) were also collected. The mooring was left for the period of the survey to be recovered on the return leg to Darwin.

The BRUCE Mooring 282/Stn2BRUCE was recovered at 2348 25/05/2005 GMT. Data were successfully retrieved from the Nortek Vector. The mooring had only minor biofouling.

After data were downloaded from the instruments and converted to a readable format, they were carefully checked for instrument malfunctions and then edited. Data processing was carried out using Matlab. The beginning and end of each data series were truncated and outliers deleted. Short data gaps have typically been left as gaps, having been filled with 'NaN' values where applicable. Data were carefully checked at each stage of processing. After editing, the basic version of the data file includes variables recorded at the basic sampling interval, and a low-pass filtered data file created from the basic version. The low-pass filter essentially removes all fluctuations of periods less than 33 hours. Low-pass filtered data were sub-sampled every 6 hours. Raw statistics have been calculated for each variable recorded on each mooring. These include minimum, maximum, mean and standard deviation values of each variable during the entire deployment of each mooring.

Statistics for each of the currents recorded by the Nortek at Stn2 during the entire deployment are displayed in Table 4.

East minimum	East mean	East maximum	East Std Dev.
-30.17	-6.57	35.27	15.33
North minimum	North mean	North maximum	North Std Dev.
-29.43	-3.64	18.85	10.70
	Speed mean	Speed maximum	Speed Std
	18.24	41.66	8.50

Table 4. Stn2BRUCE: Raw current meter statistics. All statistics are in cm/s.

Sea Level

A pressure record is recorded by each of the instruments listed here:
- the Nortek Vector. Sea-level is recorded in 'm' above the instrument.

A classical harmonic tidal analysis has been carried out on the sea-level record obtained from each instrument of a mooring using the T_TIDE package in MATLAB (Pawlowicz et al., 2002) and compared. The results of the analysis for the four largest constituents (M2, S2, K1, O1) are presented in the following section.

To determine the nature of the tides at each mooring location, the 'form ratio', F = (K1+O1)/(M2+S2), a measure of the signature based on the relative magnitudes of their main diurnal and semi-diurnal constituents (Pond & Pickard, 2000), has been calculated.

F = 0 to 0.25: semi-diurnal tides.
F = 0.25 to 1.5: mixed, mainly semi-diurnal tides.
F = 1.5 to 3.0: mixed, mainly diurnal tides.
F > 3.0: Diurnal tides.

At Stn2BRUCE, pressure is recorded by the Nortek. A time-series plot of sea-level recorded by the Nortek is shown in Figure14.

Table 5 presents the results of the tidal analysis of the sea-level record for the four largest constituents (M2, S2, O1, K1).

Tide	Frequency (cph)	Amplitude (m)	Amp. Error (m)	Phase (degrees)	Ph. Error (degrees)
01	0.0387307	0.3642	0.056	242.64	8.32
K1	0.0417807	0.3411	0.056	259.89	9.47
M2	0.0805114	0.5866	0.077	275.94	7.31
S2	0.0833333	0.2008	0.077	323.45	21.36

Table 5. Results from the classical harmonic analysis. Record Length 25.00 days. Start time is 26/02/05 18:00:00. Mean water depth from record is 95.0 m. Phase is with respect to Greenwich Mean Time.

The form ratio, F, calculated at Stn2BRUCE is equal to 0.895, indicating that tides are mixed, mainly semi-diurnal at the site.

Significant constituents calculated within the tidal analysis, where amplitude of a tidal constituent is greater than the calculated error in amplitude for that constituent, are predominantly in the diurnal and semi-diurnal bands (~0.04 and ~0.08 cph respectively) (Figure. 14). Some higher frequency constituents are also significant. Tidal phase, presented in Figure 14C) show that the significant constituents generally have small phase errors. The residual time-series after removal of the tidal signal has low amplitudes, indicating that the sea surface signal is almost entirely driven by tidal effects.

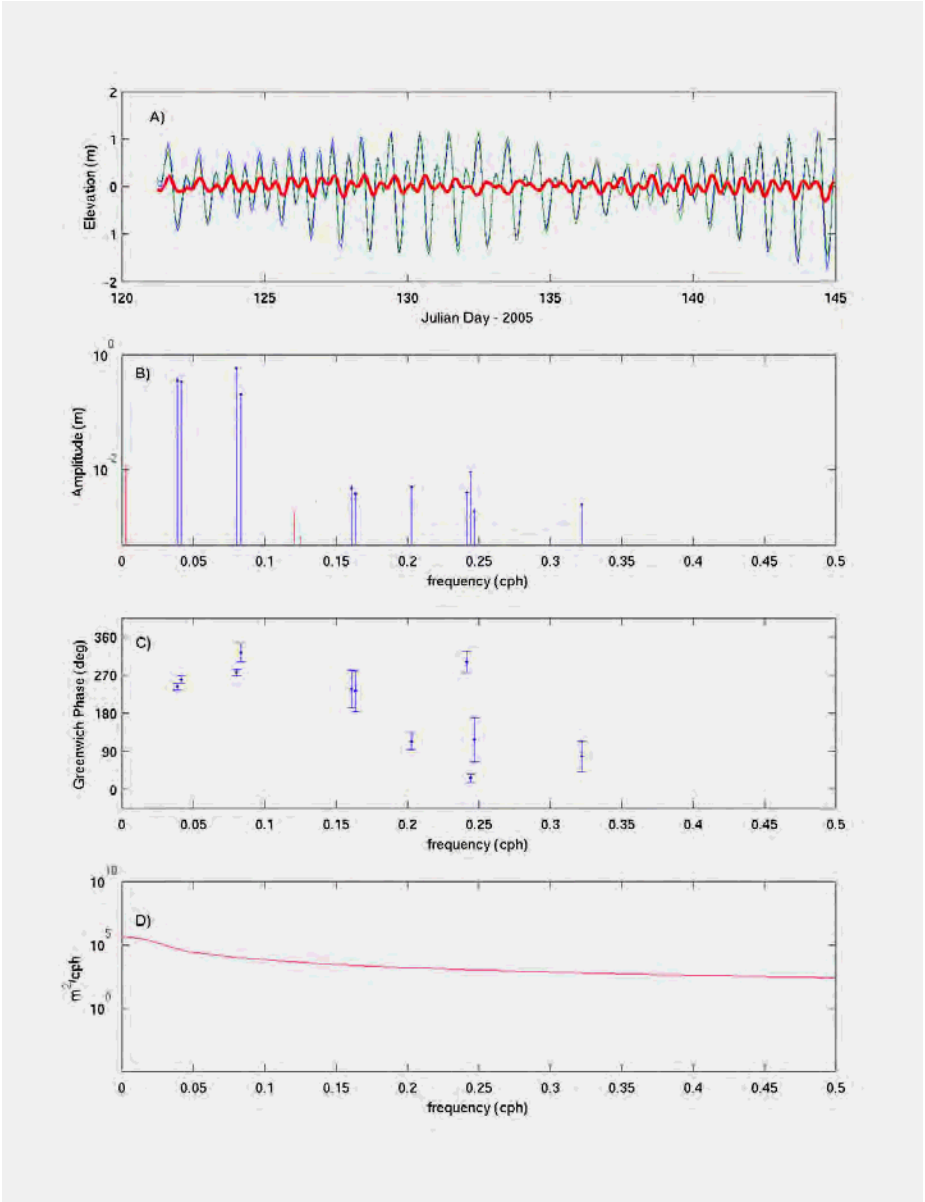

Figure 14. Results of classical harmonic analysis of pressure data from Stn2BRUCE. A) Blue line is Raw Time Series referenced to the mean level in the record, Green line is Tidal prediction from analysis

referenced to the mean, Red line is residual time series after removal of the tidal signal; B) Amplitude of all analysed components with 95% significance level (green dashed line). Note frequency dependence. Significant constituents (amp>amp_err) are marked with a solid circle; C) Phase of significant constituents with 95% confidence interval; D) Spectral Estimates before and after removal of tidal energy. Blue-line is energy of original time-series, red-line is non-tidal energy.

Waves.

In 95 m water depth, the depth attenuation results in the wave signal, in this instance, to be too small to be quantified using the PUV method using the BRUCE data.

Currents

Given our interest is in sea-bed processes, currents were measured at a height of 1 m above the seabed.

At each current meter mooring, the following analyses have been carried out on the near-bed currents:

1. Progressive vector plots, and determination of the mean residual current during the deployment.
2. Time series plots, to provide an overview of the observations and to determine the mean absolute current speeds during the deployment.
3. Principal axes for both the basic 10-min processed data and the low-passed currents were computed for the entire record and by month. Major and minor axes, orientation, and ellipticity were computed from the east (u) and north (v) current components as:

$$\text{major axis} = [0.5\ (UU + VV) + R] / n\}^{(1/2)}$$
$$\text{minor axis} = [0\ 5\ (UU + VV) - R] / n\}^{(1/2)}$$
$$\text{orientation} = 90° - 0.5\ \tan\text{-}1\ [2\ UV / (UU - VV)]$$
$$\text{ellipticity} = 1 - (\text{minor axis} / \text{major axis})$$

where

$$UV = \text{Sum}(u*v) - n*U*V$$

$$UU = \text{Sum}(u*u) - n*U*U$$
$$VV = \text{Sum}(v*v) - n*V*V$$
$$R = [\ (0.5\ (UU - VV)\ )^2 + (UV)^2\ ]^{(1/2)}$$

and U and V are the means of the east and north velocity components, respectively. Sum means sum over the entire data set of n valves. The orientation is measured clockwise from true north. 0° is true north, and 90° is east.

4. Scatter plots of the basic processed data and the low-passed currents (subsampled to be 6-hourly) to visually show the distribution of the current speed and direction. Superimposed on the scatter plots are the mean vector current over the entire deployment, and the principal axes of the currents, shown as an ellipse.
5. A tidal analysis of the currents. The following procedure has been followed to determine tidal ellipses of each current record.

    - Read in horizontal velocity time series (u,v)
    - Remove means from both u and v.
    - Determine amplitude and phase of each tidal constituent for u and v components separately using T_TIDE software (Pawlowicz et al., 2000).
    - For each constituent, use the fit amplitudes to construct tidal ellipse parameters using 'tidal_ellipse' package (Xu, 2002) in MATLAB. This provides estimates of:
        - the semi-major axis (or maximum current velocity),
        - ellipse eccentricity (the ratio of semi-minor to semi-major axis). A negative value indicates that the ellipse is traversed in a clockwise direction,
        - Ellipse inclination, or angle between east (x-) and semi-major axis, and
        - Phase, the angle that the oppositely rotating circular components must traverse from their initial positions for them to meet.

1. A progressive vector plot for each of the bed currents, and that at the top of the water column are shown in Figures 15. Note that missing data does not contribute to calculated displacement.

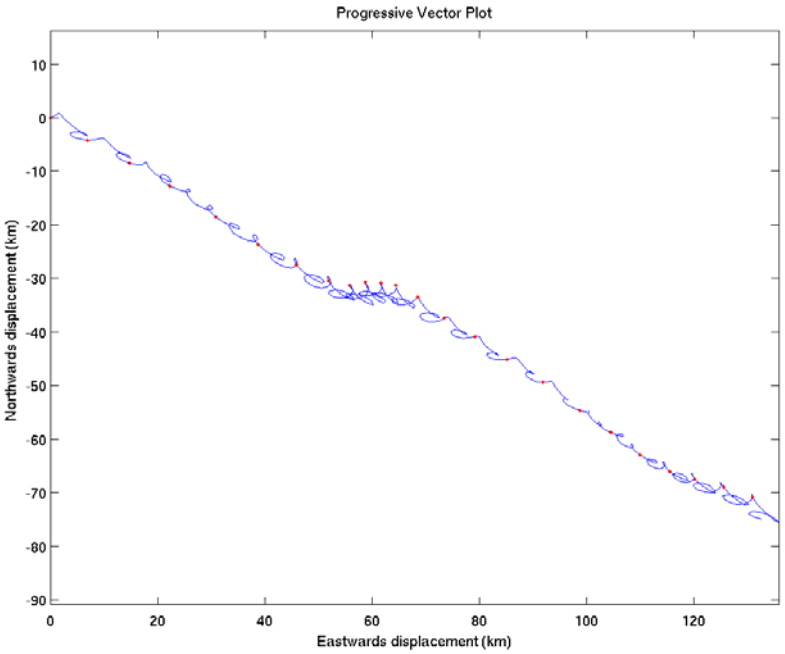

Figure 15. Stn2BRUCE current meter progressive vector plot obtained from data recorded. The origin of the plot corresponds to the location of the Stn2BRUCE mooring. Dots indicate the beginning of each 24 hour period.

2. A time series of current meter data are shown in Figure 16.

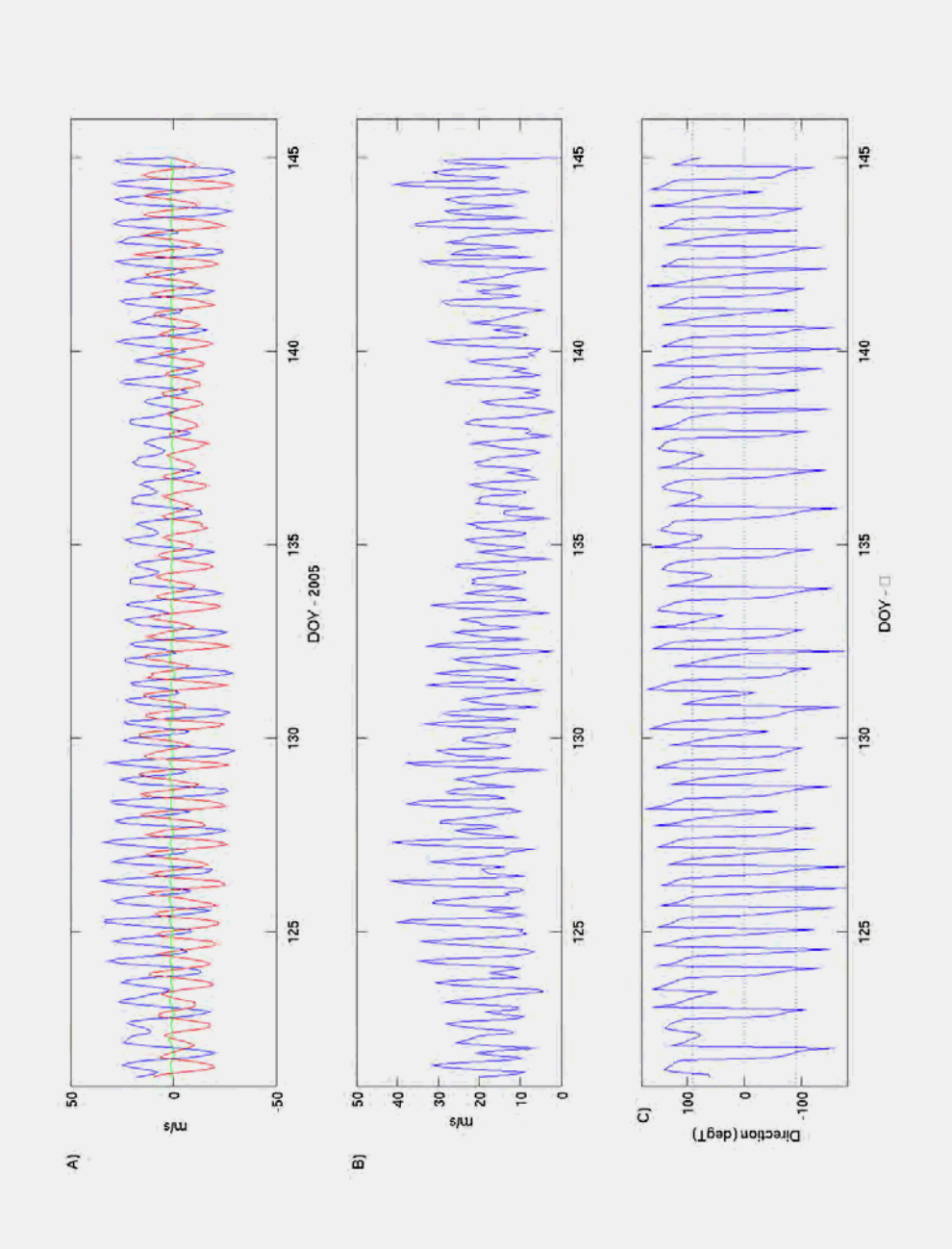

Figure 16. Stn2BRUCE current meter time-series obtained from data. A) Time series of East (Blue), North (Red), and Up (Green) velocity components B) Time series of absolute current speed, C) Time series of current direction.

Time series of low-pass filtered current meter data stn2BRUCE are show in Figure 17.

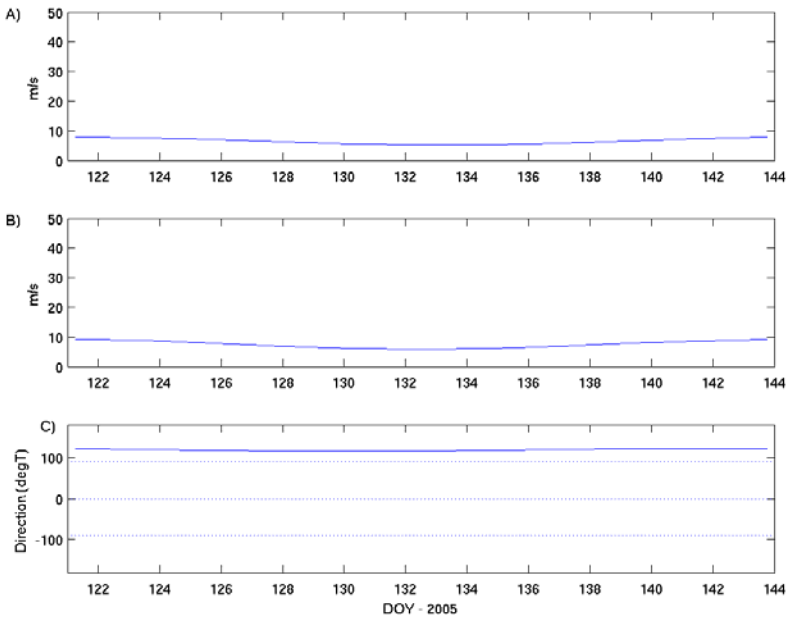

Figure 17. Stn2BRUCE Low-Pass Filtered current meter time-series obtained from data recorded. A) Time series of East (Blue), North (Red), and Up (Green) velocity components B) Time series of absolute current speed, C) Time series of current direction.

3. Table 6 displays the principal axes for both the processed data and the low-passed currents for currents recorded at 1 mab.

	1.0 mab
Major-	16.82
Minor -	8.06
Orient -	-61.68
Ellip	0.5207
Major – LP	1.32
Minor – LP	0.19
Orient – LP	-51.14
Ellip – LP	0.8561

Table 6. Stn2BRUCE. Principal axes of currents for currents at sea-bed and sea 'surface'. LP, indicates from Low Pass filtered record.

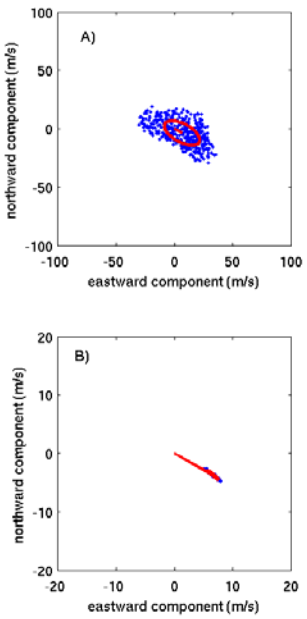

Figure 18. Stn2BRUCE scatter plots with the mean current vector (origin zero), and the ellipse of the principal axes of currents superimposed. The ellipse is centred upon the mean current vector: A) displays scatter plots of the basic 90-min processed current data from 1 mab; B) displays scatter plots of the low-pass filtered current data from 1 mab.

4. Tidal ellipse parameters for the four major constituents (M2, S2, K1, O1) are listed in Table 7 for the Stn2BRUCE Mooring. The ellipses are plotted for the four major constituents (M2, S2, K1, O1) in Figure 19. Red indicates that the ellipses are travelled clockwise.

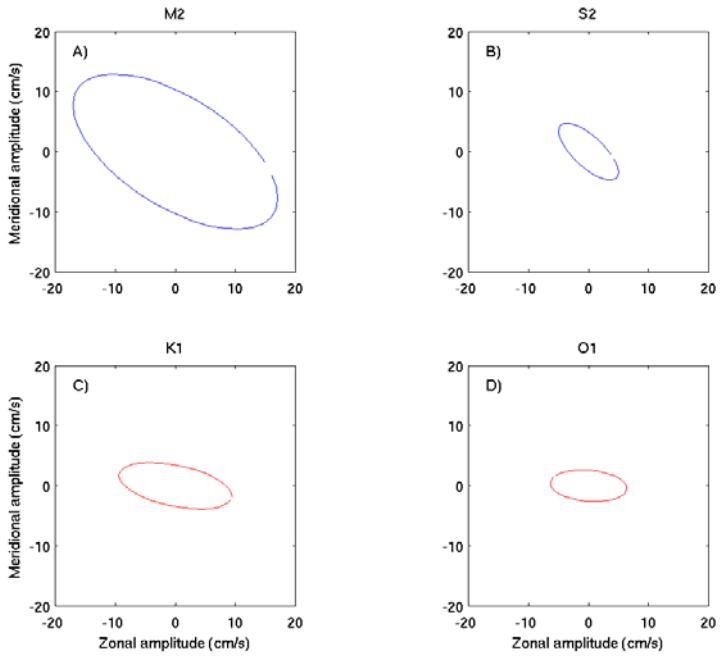

Figure 19. Tidal ellipses for the four main tidal constituents: A) M2, B) S2, C) K1 and D) O1. Red indicates that the ellipses are travelled clockwise.

Constituent	Semi-major Axis (cm/s)	Eccentricity	Inclination (degrees)	Phase (degrees)
M2	19.36	0.472	147.57	134.41
S2	6.39	0.395	137.07	118.25
K1	9.56	-0.358	168.37	171.94
O1	6.34	-0.412	175.27	329.98

Table 7. Stn2BRUCE. Tidal Ellipse parameters of bed and surface currents from Mooring Stn2BRUCE.

Bedload Transport Estimates

Five methods have been used to estimate bedload transport at the site. These include:

a) Bagnold's bedload equation, modified by Gadd et al. (1978)
$q = (\beta/\rho_s)(u_{100}-u_{cr})^3$,

where q is the volume rate of sediment transport per unit wi°Trueh of bed [m^2/s], β has a value of 1.73, as used in the SE°TRUERANS96 model, outlined in Li and Amos. (2001). The critical velocity for the initiation of bedload transport u_{cr} is

obtained from $\tau_{cr} = 0.5\rho f_{cs} u_{cr}^2$, and u_{100} is the current speed measured 100cm above the bed.

b) The Engelund-Hansen (1967) total load equation. For continental shelf conditions, this equation is modified to (Li and Amos, 2001):

$$q = 0.05 u_{100}^2 \rho^2 u_*^3 / D(\Delta\rho g)^2,$$

where $\Delta\rho = \rho_s - \rho$, and ρ_s is the density of the sediment (For quartz 2650 kgm-3), and ρ is the density of seawater. u* is the skin-friction shear velocity.

c) The Einstein-Brown bedload equation (Brown, 1950). This equation can be written in the form (Li and Amos., 2001)

$$q = 40 W_s D(\rho/\Delta\rho g D)^3 u^{*5} |u^*|,$$

where Ws is the settling velocity.

d) Yalin bedload equation (Yalin, 1963).

$$q = 0.635 D u^* [(\tau^* - (1/a)\ln(1 + a\tau^*)],$$

where $\tau^* = (\tau_b - \tau_{cr})/\tau_{cr}$, is the normalised shear stress and a is equal to $2.45(\rho/\rho_s)^{0.4}(\tau_{cr}/\Delta\rho g D)^{0.5}$.

e) Bagnold's bedload equation as modified by Hardisty (1983)

$$q = k1(u_{100}^2 - u_{cr}^2)\, u_{100},$$

u_{cr} is the critical threshold velocity defined in this instance as

$$u_{cr}\, r = 1.226(100D)^{1.29}$$

as outlined by Miller et al. (1977). K1 is a function of sediment grain size (D) such that:

$$k1 = (1/6.6\ (1000D)^{1.23}\ \text{kg m}^{-4}\ \text{s}^2$$

It is this bedload transport equation which has been used in all previous Geoscience Australia cruise reports, so is included here for completeness.

For consistency with previous cruise reports, the above estimates of q in units [m2/s] must be multiplied by $1/(10\rho_s)$ to express bedload transport in units g/cm/s.

Grain-size data at each site was unavailable at the time of writing, so a mean grain size, D of 0.0005 m (0.5 mm) has been assumed.

Vector Stick plots of Bedload Transport estimates are presented (Table 8 and Figure 20) to enable an overview of the main stage of tide at which bedload is important.

	Bagnold (Gadd et al., 1978)	Engelund-Hansen	Einstein-Brown	Yalin	Bagnold (Hardisty, 1983)
Q – Ave. (10^{-5} g $cm^{-1}s^{-1}$)	0.496	87.13	11.89	443.16	0.0
Q - total (10^{3} g cm^{-1})	0.010	1.26	0.184	2.27	0.000
Dirn (º True)	126.3	125.9	126.6	111.8	NA

Table 8 displays the calculated total bedload and direction at Stn2BRUCE for the entire deployment using each of the defined formulations.

Vector stick plots are plotted for bedload for each method in Figure 20.

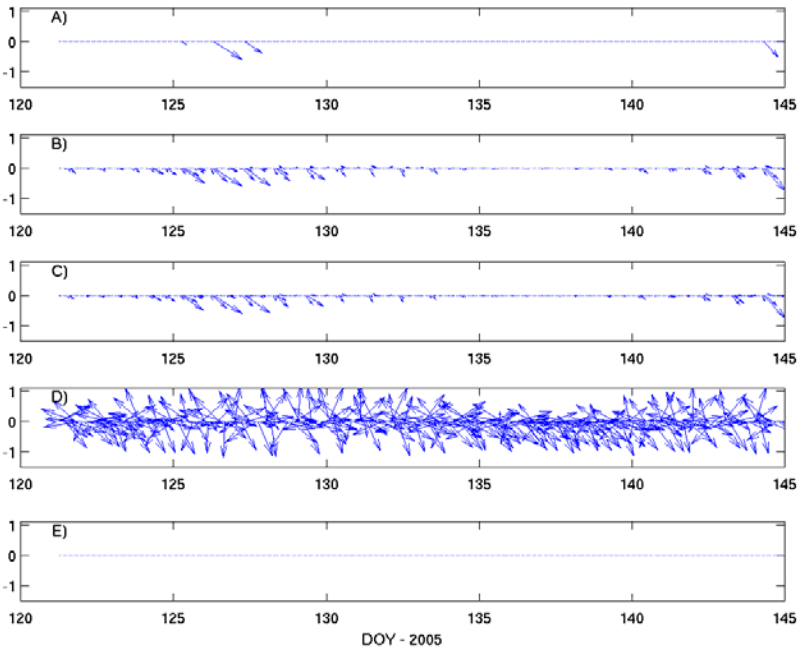

Figure 20. Vector stick plots of bedload transport at Stn2BRUCE, as calculated using a) Bagnold (Gadd et al., 1978), b) Engelund Hansen, c) Einstein-Brown, d) Yalin, e) Bagnold (Hardisty, 1983).

Discussion

The deployment covered a period of approximately 23 days. At the time of deployment (Julian Day 121), neap tides were approaching, and occurred on Julian Day 124. Spring tides occurred on Julian Day 130 approximately during the middle of the deployment. Neap tide conditions were experienced on Julian Day 139, and spring tide conditions were present at the time of instrument recovery (Julian Day 145). Tides are mixed-semidiurnal at the deployment site, consistent with Easton (1970).

Maximum tidal current speeds of 41.66 cm/s 120 °True were experienced during Julian Day 126 on a flood tide. Flood tide currents were directed to the ESE (~120 °True), and ebb currents were directed WNW (~300 °True). The bedload transport calculations indicate that flood tide current speeds had a greater net effect, with integrated bedload transport using 4 of the 5 bedload transport formulae indicating transport direction to the ESE.

The four main constituents M2, S2, O1, and K1 tidal ellipses are all oriented similarly (inclination approximately 150 degrees). Eccentricity is similar for each of the constituents, with the major axis 2-3 times the magnitude of the minor axis (eccentricity ~ 0.4). The diurnal tides display an anticlockwise orientation to the ellipses, and the semi-diurnal tides display a clockwise orientation.

The progressive vector plot, and the low-pass filtered time-series, indicate that the residual currents consist of a steady ESE current of speed of approximately 7.5 cm/s. The residual current is of similar magnitude to the tidal current speeds. Net water displacement during the deployment was to the ESE, and the total displacement was approximately 150 km. The ESE residual current is directed upslope along the axis of the submarine channel in which BRUCE was deployed. This direction is opposite to surface wind forcing.

References

Agrawal, Y.C., and Pottsmith, H. C. (2000) Instruments for particles size and settling velocity observations in sediment transport. Marine Geology, 168, 89-114.

Brown, C.B. (1950) In Rouse, H (Ed.), Engineering Hydraulics. Wiley, New York, 1039pp.

CSIRO (2005) The CSIRO MatLAB Seawater Library. http://www.marine.csiro.au/~morgan/seawater.

Engelund, F., and Hansen, E. (1967) A monograph on sediment transport in alluvial streams. Teknisk Vorlag, Copenhagen, Denmark, 62pp.

Gadd, P. E., Lavelle, J. W., and Swift, D.J. P. (1978) Estimates of sand transport on the New York Shelf using near-bottom current-meter observations. Journal of Sedimentary Petrology 48, 239-252.

Hardisty, J. (1983) An assessment and calibration of formulations for Bagnold's bedoad equation. Journal of Sedimentary Petrology, 53, 1007-1010.

Li, M.Z., and Amos, C. L. (2001) SE°TRUERANS96: the upgraded and better calibrated sediment-transport model for continental shelves. Computers and Geosciences, 27, 619-645.

Miller, M.C., McCave, I.N. and Komar, P.D. (1977) Threshold of sediment motion under unidirectional currents. Sedimentology, 24, 507-527.

Nortek, 2000. Vector Operations Manual, 1 November 2000. http://www.nortek-as.com

Pawlowicz, R., Beardsley, B. amd Lentz, S. (2002) Classical tidal harmonic analysis including error estimates in MATLAB using T_TIDE. Computers and Geosciences, 28, 929-937.

Pond, S. and G. L. Pickard (2000) Introductory Dynamical Oceanography, 2nd Edition. Butterworth Heinemann, Oxford. 329pp.

Rochford (1966) Some hydrological features of the Eastern Arafura Sea and the Gulf of Carpentaria in Auguest 1964. *Australian Journal of Marine and Freshwater Research.* 17, 31-60.

Xu, Z. (2002) Ellipse Parameters Conversion and Velocity Profiles for Tidal Currents in Matlab. Maurice-Lamontagne Institute, Ocean Science Division, Fisheries and Ocean Canada. 24pp.

Yalin, M.S. (1963) An expression for bedload transportation. Journal of Hydraulics Division, Proceedings ASCE 90 (HY5), 105-119.

Appendix 4

Radiometric Dates and Core Logs

K. Glenn

A total of 101 gravity cores were recovered during the survey. Forty three sediment cores were collected during the survey for stratigraphic purposes. Five gravity cores, acquired during the survey, were selected for radiometric dating, three from Area B, and one each from Areas C and D. Each core was sub-sampled and 30 of these samples were processed and the detailed results reported in this appendix.

The core logs, core photos, texture and composition information and Multi Sensor Logs (MSL) are presented in this appendix. The core logs contain the physical property data (Bulk Density, P-wave Velocity, magnetic susceptibility, Fractional Porosity), texture and composition information, visual log (including digital images and x-ray radiographs) and comments on specific sedimentological features.

Further analysis of these cores is forth coming and will be presented in the associated report from this survey (K Glenn, et al. 2006)

Appendix 4
Radiomentirc Dates Core material from Survey 282 K. Glenn

Sample ID	Location	Location	material dated	Core #	depth (cm)	Area	Sediment Munsell colour	d13C	Radiocarbon Age	uncorrected age	error	corrected age		corrected error	d14C	D14C	Percent Modern
1682777	-9.8395	135.3483	treated foram/shell mixture	GC 04	0.5	B		0.3	5082 ± 30 BP	5082	30	4712	6084	78	444.7 ± 2.1	472 ± 2	52.76 ± 0.2
1682779	-9.8395	135.3483	treated foram/shell mixture	GC 04	35.5	B		0.4	3844 ± 30 BP	3844	30	3474	6084	78	352 ± 2.4	384.5 ± 2.3	16.55 ± 0.23
1682782	-9.8395	135.3483	treated foram/shell mixture	GC 04	75.5	B		0.6	12041 ± 40 BP	12041	40	11671	6784	82.36504113	766.3 ± 1.2 ‰	778.1 ± 1.1 ‰	22.19 ± 0.11
1682783	-9.8395	135.3483	treated shell	GC 04	101	B		-0.9	8574 ± 30 BP	8574	30	8204	6084	78	-641.3 ± 1.4 ‰	-658.4 ± 1.4 ‰	34.16 ± 0.14
1682786	-9.8395	135.3483	Treated Sediment - TOC	GC 04	135	B	5Y 6/1	-20.2	14313 ± 60 BP	14313	60	13943	8784	93.72299611	-831.2 ± 1.3 ‰	-832.8 ± 1.2 ‰	16.72 ± 0.12
1682787	-9.8395	135.3483	Treated Sediment - TOC	GC 04	162	B	5Y 5/1	-19.5	14457 ± 55 BP	14457	55	14087	8209	90.60353194	-833.9 ± 1.1 ‰	-835.8 ± 1.1 ‰	16.42 ± 0.11
1682789	-9.8395	135.3483	Treated Sediment - TOC	GC 04	199	B	5Y 5/1	-20.2	14548 ± 60 BP	14548	60	14178	8784	93.72299611	-836 ± 1.2 ‰	-837.6 ± 1.2 ‰	16.24 ± 0.12
1682791	-9.8395	135.3483	Treated Sediment	GC 04	234.5	B	5Y 5/1	-19.3	14272 ± 70 BP	14272	70	13902	10084	100.4191217	-830 ± 1.4 ‰	-831.9 ± 1.4 ‰	16.81 ± 0.14
1682793	-9.8395	135.3483	Treated Sediment	GC 04	272.5	B	5Y 5/1	-20.5	14175 ± 55 BP	14175	55	13805	8209	90.60353194	-828.3 ± 1.1 ‰	-829.9 ± 1.1 ‰	17.01 ± 0.11
1682825	-9.0338	133.1043	Treated Sediment	GC 058	1.5	C	5Y 5/2	-20.2	1307 ± 35 BP	1307	35	937	6409	80.05623024	-147.6 ± 3.5 ‰	-155.9 ± 3.5 ‰	84.41 ± 0.35
1682827	-9.0338	133.1043	Treated Sediment	GC 058	39.5	C	5Y 5/2	-19.7	1965 ± 40 BP	1965	40	1595	6784	82.36504113	-213.8 ± 3.7 ‰	-222.3 ± 3.7 ‰	77.77 ± 0.37
1682830	-9.0338	133.1043	Treated Sediment	GC 058	99.5	C	5Y 5/2	-19.9	2841 ± 30 BP	2841	30	2471	6084	78	-295.3 ± 2.6 ‰	-302.6 ± 2.6 ‰	69.74 ± 0.26
1682832	-9.0338	133.1043	Treated Sediment	GC 058	139.5	C	5Y 5/2	-20	3348 ± 30 BP	3348	30	2978	6084	78	-338.6 ± 2.4 ‰	-345.3 ± 2.4 ‰	65.47 ± 0.24
1682835	-9.0338	133.1043	Treated Sediment	GC 058	199.5	C	5Y 6/2	-20.6	4840 ± 35 BP	4840	35	4470	6409	80.05623024	-451.4 ± 2.2 ‰	-456.3 ± 2.2 ‰	54.37 ± 0.22
1682843	-9.1625	133.529	Treated Sediment	GC 85	1.5	C	5Y 6/2	-20.5	1109 ± 30 BP	1109	30	739	6084	78	-126.8 ± 3.2 ‰	-134.8 ± 3.1 ‰	86.52 ± 0.31
1682846	-9.1625	133.529	Treated Sediment	GC 85	49.5	C	5Y6/2	-20.2	1825 ± 30 BP	1825	30	1455	6084	78	-200.8 ± 3 ‰	-208.6 ± 3 ‰	79.14 ± 0.3
1682849	-9.1625	133.529	Treated Sediment	GC 85	109.5	C	5Y 6/2	-20.1	2557 ± 30 BP	2557	30	2187	6084	78	-270.2 ± 2.6 ‰	-277.5 ± 2.6 ‰	72.25 ± 0.26
1682851	-9.1625	133.529	TOC	GC 85	149.5	C	5Y 4/2	-20.1	2878 ± 30 BP	2878	30	2508	6084	78	-298.8 ± 2.6 ‰	-305.8 ± 2.6 ‰	69.42 ± 0.26
1682854	-9.1625	133.529	TOC	GC 85	207.5	C	5Y 5/2	-20	3501 ± 35 BP	3501	35	3131	6409	80.05623024	-351 ± 2.6 ‰	-357.7 ± 2.6 ‰	64.23 ± 0.26
1682855	-9.5507	133.9531	TOC	GC 86	0.5	D	5Y 5/2	-9.5	7847 ± 30 BP	7847	30	7477	6084	78	-614.1 ± 1.6 ‰	-626.1 ± 1.5 ‰	37.39 ± 0.15
1682856	-9.5507	133.9531	TOC	GC 86	30.5	D	5Y 5/1	-11.4	7831 ± 30 BP	7831	30	7461	6084	78	-614.8 ± 1.5 ‰	-625.3 ± 1.5 ‰	37.47 ± 0.15
1682861	-9.5507	133.9531	treated shell	GC 86	119.5	D		1.7	11040 ± 40 BP	11040	40	10670	6784	82.36504113	-734.7 ± 1.4 ‰	-748.7 ± 1.3 ‰	25.13 ± 0.13
1682872	-9.7397	135.2659	treated foram/shell mixture	GC 103	0.5	B		0.5	3291 ± 30 BP	3291	30	2921	6084	78	305.7 ± 2.7 ‰	340.6 ± 2.6 ‰	65.94 ± 0.26
1682874	-9.7397	135.2659	treated foram/shell mixture	GC 103	23.5	B		0.3	6847 ± 30 BP	6847	30	6477	6084	78	554.2 ± 1.8	576.5 ± 1.7	42.35 ± 0.17
1682877	-9.7397	135.2659	treated foram/shell mixture	GC 103	48.5	B		0.7	22105 ± 90 BP	22105	90	21735	13284	115.2562363	933.2 ± 0.8	936.6 ± 0.7	6.34 ± 0.07
1682878	-9.7397	135.2659	treated foram/shell mixture	GC 103	86.5	B		0.6	15543 ± 55 BP	15543	55	15173	8209	90.60353194	-848.9 ± 1.1 ‰	-856.5 ± 1 ‰	14.35 ± 0.1
1682880	-9.7397	135.2659	TOC	GC 103	97.5	B	1.5/1 Gley	-18.8	13925 ± 55 BP	13925	55	13555	8209	90.60353194	-822.3 ± 1.2 ‰	-824.5 ± 1.2 ‰	17.55 ± 0.12
1682881	-9.7397	135.2659	treated shell	GC 103	103.5	B		-5.1	21543 ± 85 BP	21543	85	21173	12409	111.3956911	929.2 ± 0.8 ‰	-932 ± 0.7 ‰	6.8 ± 0.07
1682882	-9.7397	135.2659	treated foram/shell mixture	GC 103	119.5	B		1.2	35140 ± 350 BP	35140	350	34770	127684	357.3289801	-986.8 ± 0.6 ‰	-987.5 ± 0.6 ‰	1.25 ± 0.06
1682884	-9.7397	135.2659	TOC	GC 103	138.5	B	5Y 5/1	-0.4	30270 ± 280 BP	30270	280	29900	83584	289.108976	-975.9 ± 0.8 ‰	-977.1 ± 0.8 ‰	2.29 ± 0.08

Core: 282/006GC004 **Location:** Area B, Arafura Shelf **Total Length (m):** 2.8

Latitude: -9°50.370 **Longitude:** 135°20.898 **Recovery Date:** 04-05-05 **Water Depth (m):** 87

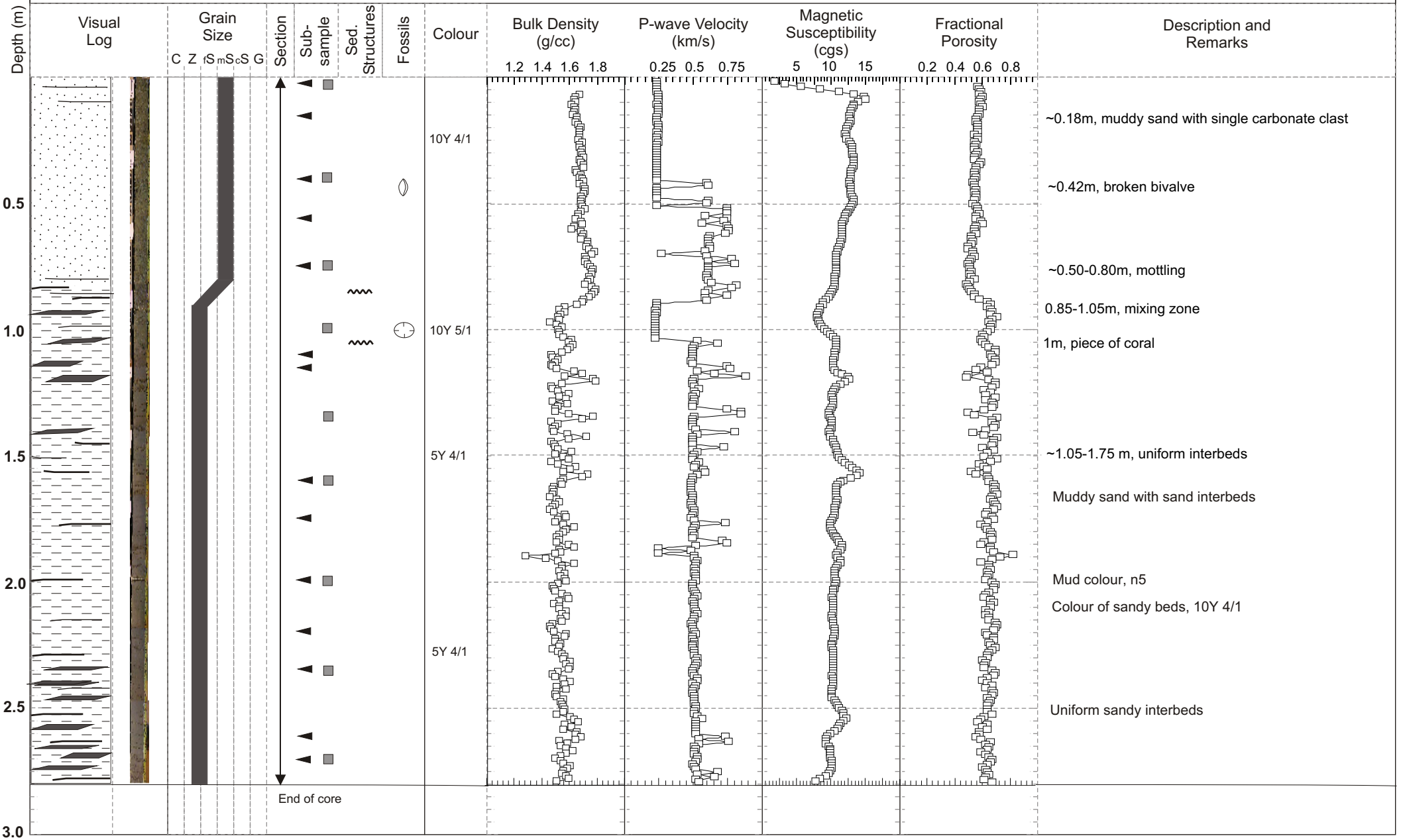

Core: 282/064GC103 **Location:** Area B, Arafura Sea **Total Length (m):** 1.4

Latitude: -9°44.383 **Longitude:** 135°15.952 **Recovery Date:** 25-05-05 **Water Depth (m):** 102

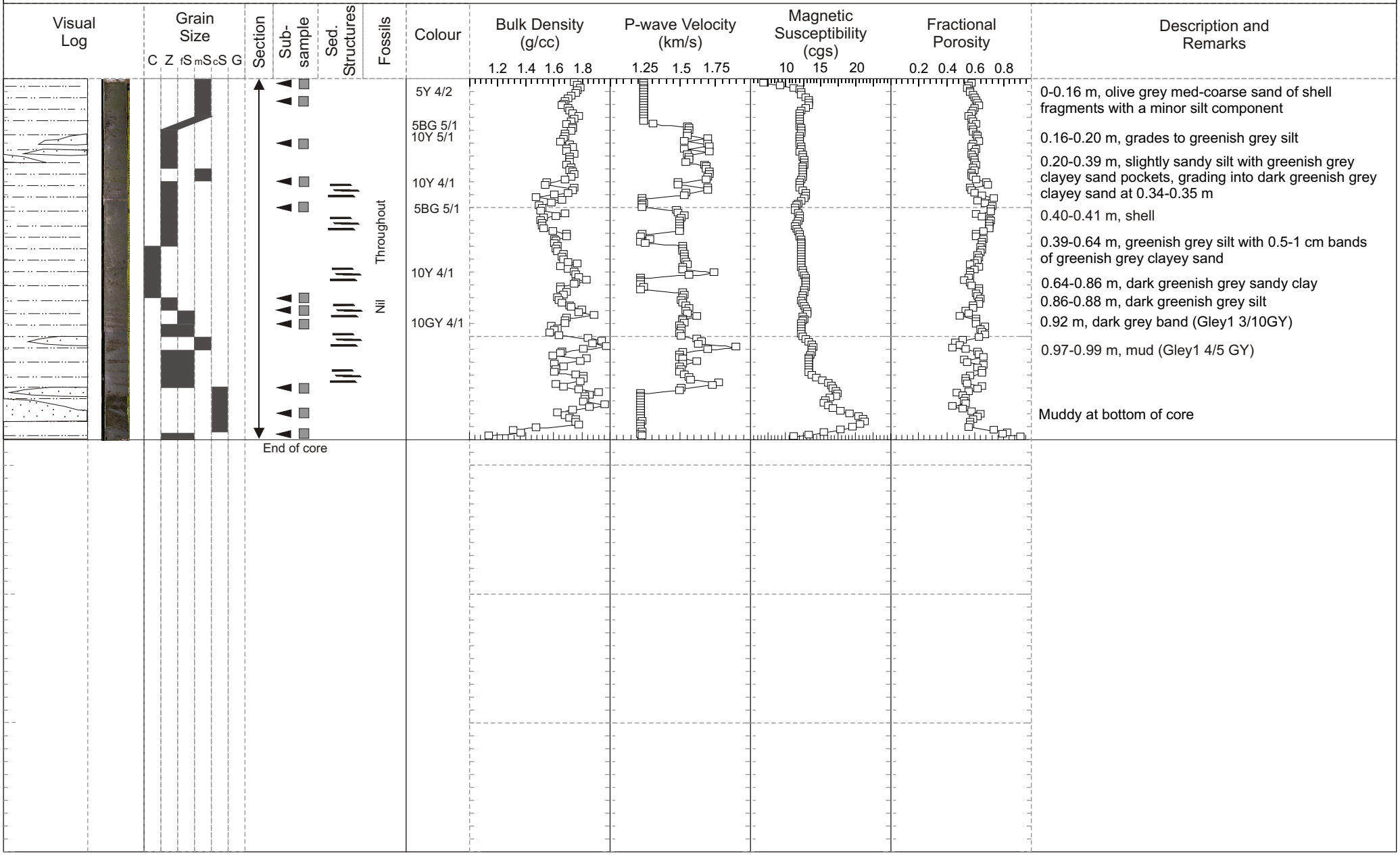

Core: 282/024GC035 **Location:** Area C, Arafura Sea **Total Length (m):** 2.4

Latitude: -9°20.390 **Longitude:** 134°01.980 **Recovery Date:** 11-05-05 **Water Depth (m):** 131

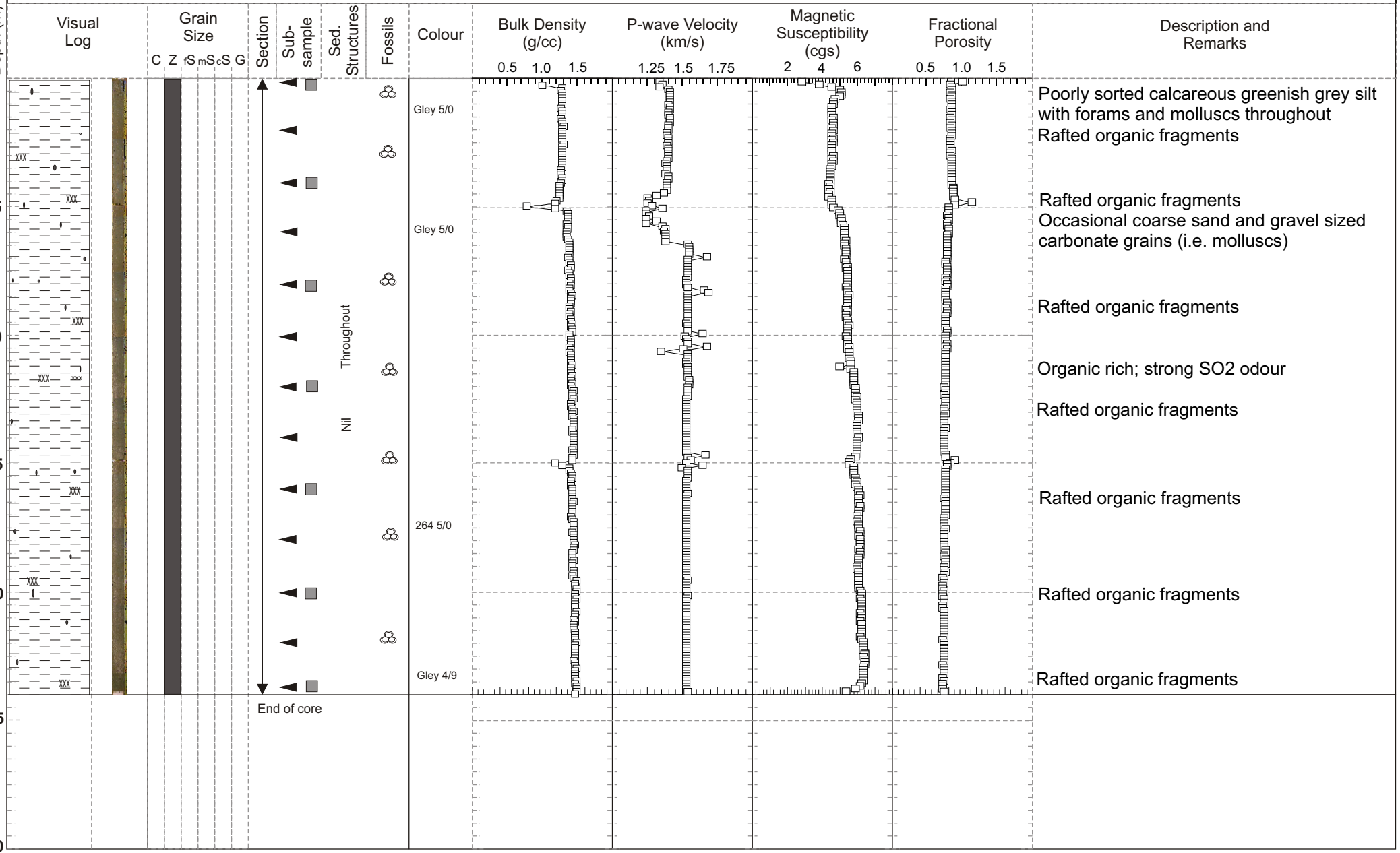

Core: 282/027GC040 **Location:** Area C, Arafura Sea **Total Length (m):** 0.50

Latitude: -9°22.88 **Longitude:** 133°39.89 **Recovery Date:** 13-05-05 **Water Depth (m):** 112

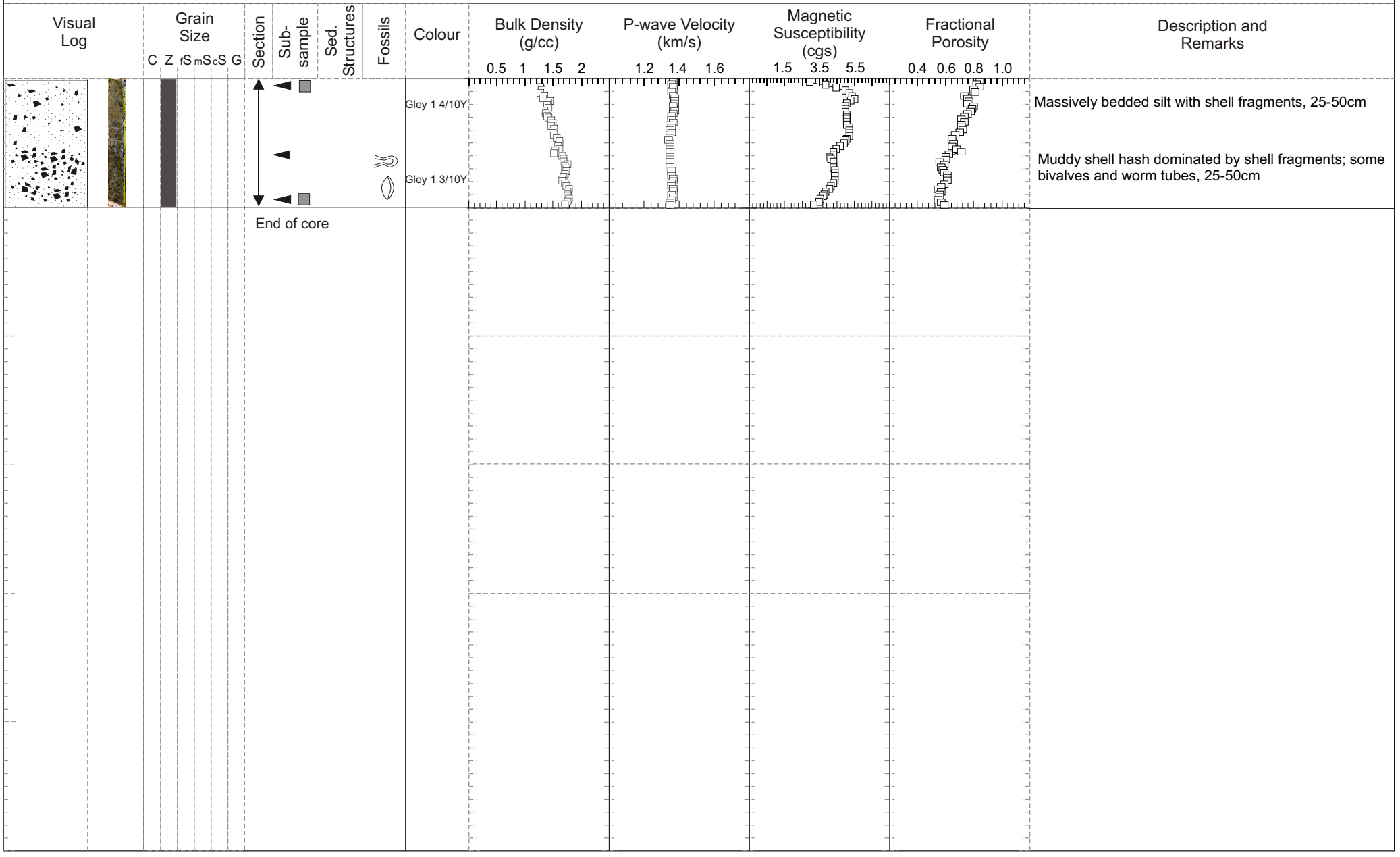

Core: 282/026GC038 **Location:** Arafura Sea **Total Length (m):** 2.22

Latitude: -9°15.483 **Longitude:** 133°48.102 **Recovery Date:** 12-05-05 **Water Depth (m):** 147

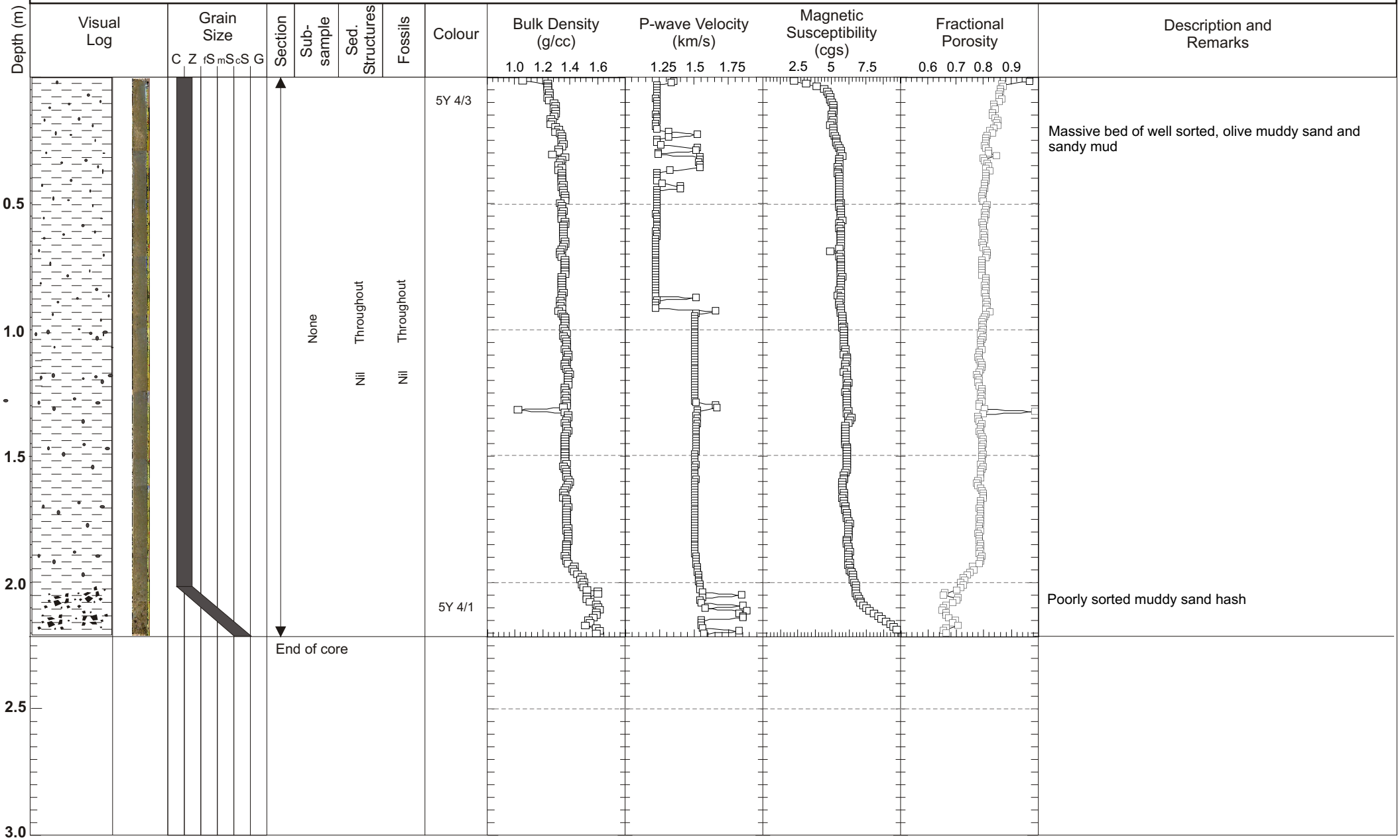

Core: 282/034GC058 **Location:** Area C, Arafura Sea **Total Length (m):** 2.4

Latitude: -9°02.028 **Longitude:** 133°06.257 **Recovery Date:** 16-05-05 **Water Depth (m):** 212

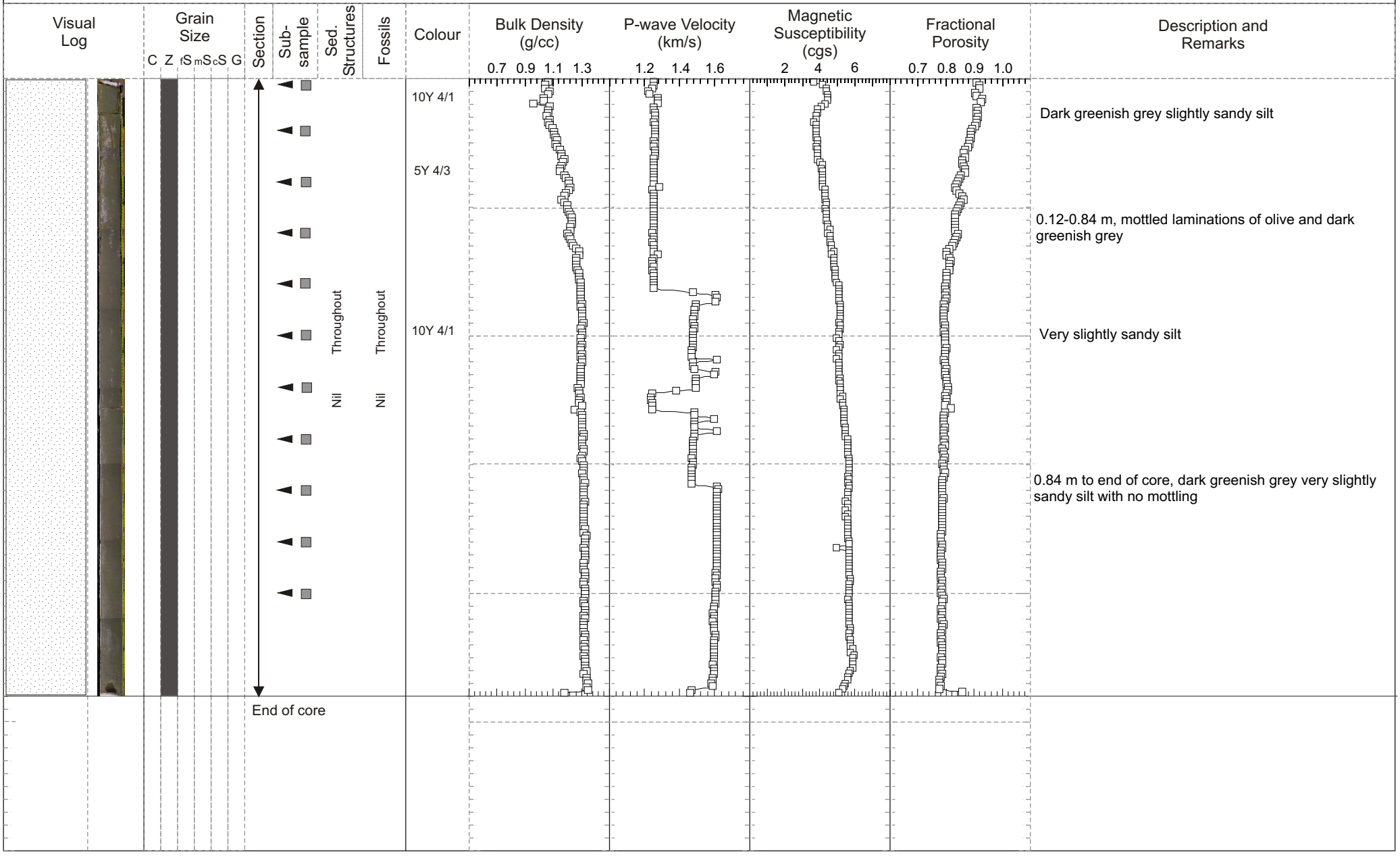

Core: 282/033GC057 **Location:** Area C, Arafura Sea **Total Length (m):** 0.22

Latitude: -9°00.235 **Longitude:** 133°06.268 **Recovery Date:** 16-05-05 **Water Depth (m):** 214

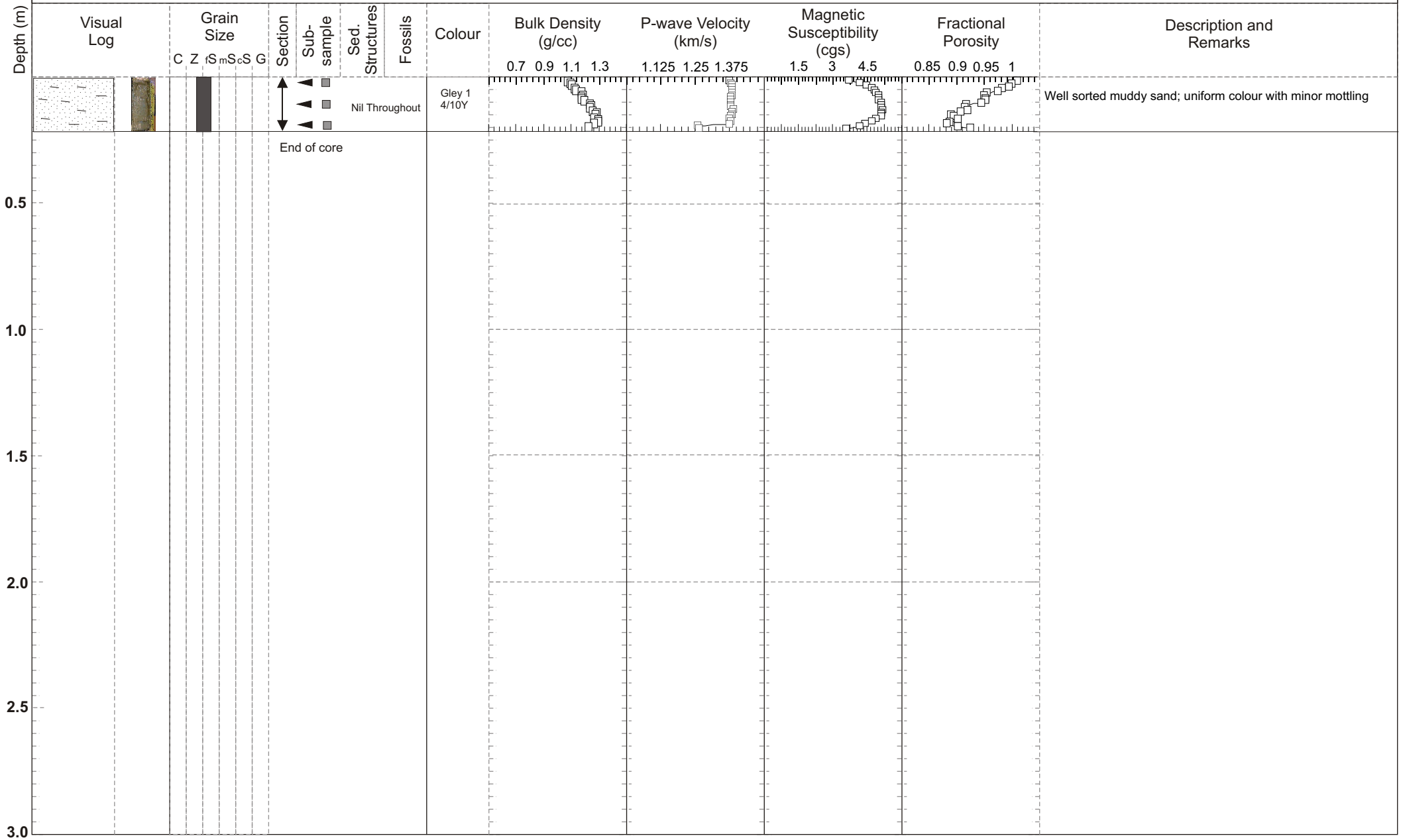

Core: 282/029GC042 **Location:** Area C, Arafura Sea **Total Length (m):** 0.75

Latitude: -9°18.230 **Longitude:** 133°41.810 **Recovery Date:** 13-05-05 **Water Depth (m):** 187

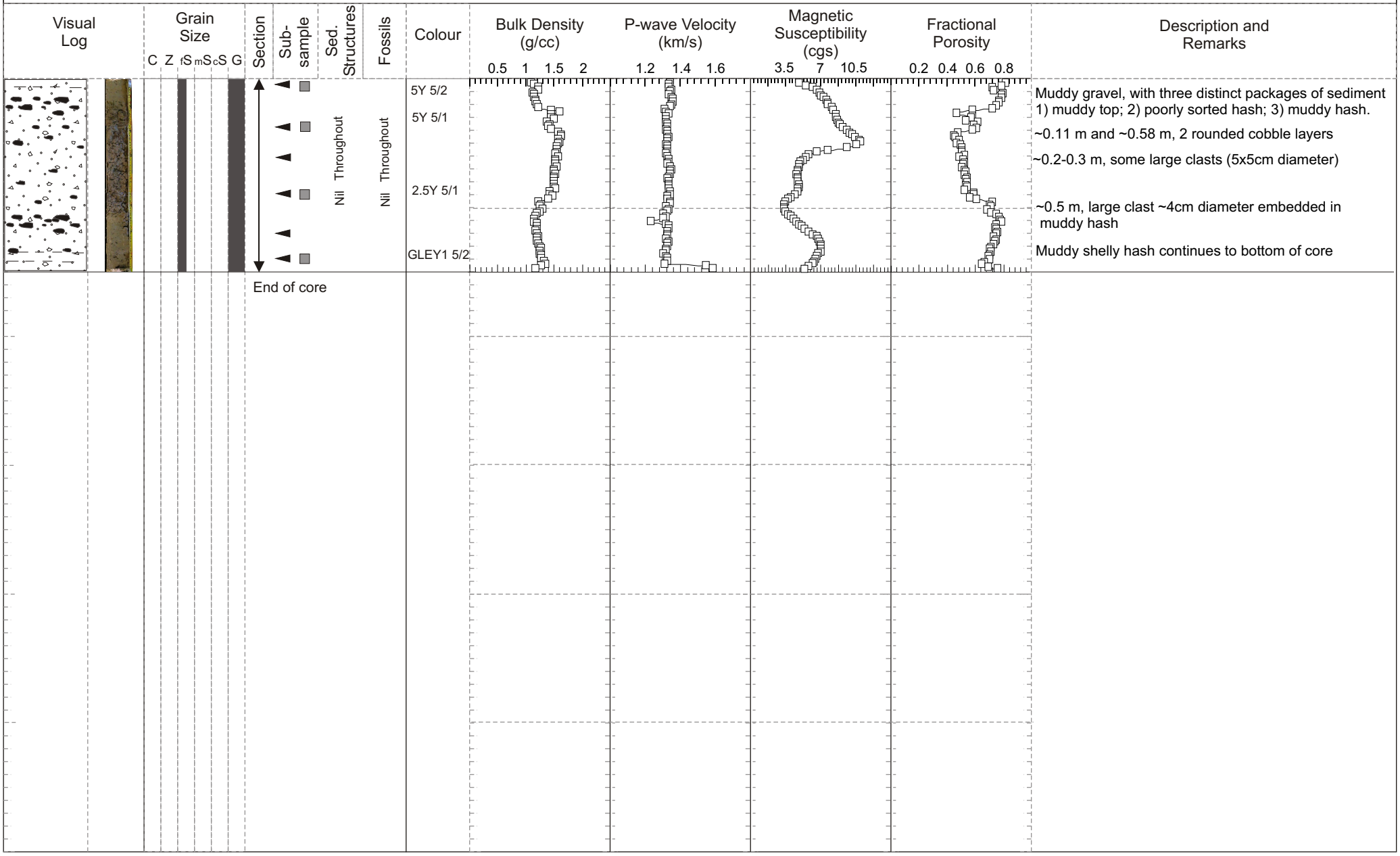

Appendix 5 Video descriptions of the seafloor for Survey 282

K. Glenn and L. Twyford

SAMPLE ID	Area #	ACQUIRED	SAMPLE NO	start lat	start long	end lat	end long	COMMENTS	wd start	wd end	substrate	sample description
282/002CAM001	B	02-May-05	1668023	-9.7994	135.3681	-9.797333	135.36625	relatively barren, 15 minutes recovery. Bruce Site DV tape = 1; VHS tape = 1	92	92	unconsolidated	unconsolidated muddy sand sub parallel ripples ~2cm height 5 - 10 cm long. Faecal pellets, Pink fish, irregular sand waves, no biota visible on sea bed. Marine snow and isolated 10 - 15cm high sea whips.
282/002CAM062	B	26-May-05	1668024	-9.7999	135.3671	-9.7989	135.37138	moderate to poor visibility DV tape = 60; VHS tape = 7	92.8	92.8	unconsolidated	Unconsolidated substrate firms to a sandy substrate in places, devoid of benthos, multidirectional ripples ~1cm wave height, with darker sediment in swales (biogenic faecal pellets and organic matter(?). No bioturbidation and limited vis. 2 fish, red fish, burrow, fish in water column (1:53), red fish (1:58 - bright white/light blue object in water column, looked anthropogenic)
282/003CAM002	B	04-May-05	1668095					Get navigation from VHS tape. DV tape = 2; VHS tape = 1				no footage
282/004CAM003	B	04-May-05	1668025	-9.8739	135.3172	-9.873883	135.3176	DV tape = 3; VHS tape = 1	77	77	unconsolidated	Bottom seems soft, sandy muddy, many burrows, seafloor bioturbated worm holes on otherwise featureless sea floor.
282/005CAM004	B	04-May-05	1666764	-9.8406	135.2688			see overlay for navigation (VHS tape). Parked camera in water column to let it come straight. DV tape = 4; VHS tape = 1			unconsolidated	Solitary coral, muddy sand unconsolidated lightly bioturbated with fewer and bigger burrows (10-20 cm), particles moving across field of vision, soft coral or anemone, large burrow ejecting sediment, lots of thin tubes laying on substrate Occasional red fish some shell and biogenic detritus throughout the sediments.
282/006CAM005	B	04-May-05	1668026	-9.8386	135.3386	-9.837617	135.34817	DV tape = 5; VHS tape = 1	86.4	86.4	unconsolidated	Marine Snow, subtle sea floor features, unconsolidated muddy sand. Relatively sparse biota - some infaunal biota, burrows, silty sandy surface, small undulations in sea bed (small ripples) small wormholes, water and seds ejected from the wormholes as camera lands on the substrate.

282/007CAM006	B	04-May-05	1668027	-9.8347	135.2964	-9.832917	135.29468	DV tape = 6; VHS tape = 1	81	81	soft	Soft bioturbated muddy sand substrate. Frequent fish sighted absence of benthos flora, suspended and particulate matter close to the sea floor, sparse sea whips. Low visibility faecal pellets on sea floor small scale ripple marks, Unconsolidated sediment Scallops, burrows, sponge?,
282/008CAM007	B	04-May-05	1668028	-9.8313	135.3263	-9.828167	135.32333	relatively sparse biota DV tape = 7; VHS tape = 1	84	84	soft	Particulate matter in the lower water column, similar sea floor characteristics to previous site. Small burrows (bioturbation) low ripples (1cm wave height) and are unidirectional semi parallel. fine grained organic debris near the fish resting on the sea floor. Rubbly at start with shells and hydroid, worm tube, sea pens / whip, octocoral, .
282/009CAM008	B	04-May-05	1668029	-9.8218	135.3269	-9.816883	135.32495	relatively sparse biota DV tape = 8; VHS tape = 1	84	84	soft	suspended sediment at sea floor, Muddy sand, small scale bioturbation yet also areas where no bioturbidation is evident. Murky sediment in suspension at beginning, current ripples are non and unidirectional, sandy, irregular ripples, sea pen, flat fish (flounder), small octacoral colony, red object (unknown), yellow sponge
282/010CAM009	B	05-May-05	1668030	-9.813	135.2566	-9.810167	135.25687	DV tape = 9; VHS tape = 1	81	81	unconsolidated	Suspended matter in the water column, Fish, sea whip (octacoral), burrows, frequent low key ripples (poorly defined), sparse biota and low profile small scale bioturbated mounds
282/011CAM010	B	05-May-05	1668031	-9.7975	135.7336	-9.795583	135.28328	DV tape = 10; VHS tape = 1	84	84	unconsolidated	Suspended particulate matter, unidirectional Rippled sandy bed (2cm in height 15cm wave length, swale infill of ripples spread ~20cm 2/3cm height. Bioturbated burrows apparent but lower density compared to other sites, worm burrows expelling sand. Little apparent life in / on sand, current heading forward, camera at angle when stopped on bottom (4:54). 4:56 dead shell, 5:00 large burrows, 5:01 burrow expelling sediment, 5:06 start up

282/013CAM011	C	10-May-05	1668032	-9.4223	134.3122	-9.415317	134.31007	DV tape = 11; VHS tape = 1	87	87	firm substrate	Firmer substrate than other sites so far, Bioturbated and planar, sessile benthos >20cm. octocorals, sea whips (some Junieella type), sea fans, crinoid on sea fan, Crinoids excellent specimens, soft coral, burrows, fenestrate bryozoan clumps, low sponge clumps, crinoids , anemone (Dofleina armata) diversity and density of coverage varies across the transect.
282/014CAM012	C	10-May-05	1668033	-9.4018	134.2373	-9.401733	134.23753	minimal life forms observed, apparently quite barren. DV tape = 12; VHS tape = 1	95.5	95.5	unconsolidated substrate	suspended particulate mater close to the sea floor, Very soft muddy substrate, some mounds, faecal pellets rolling around in the current
282/015CAM013	C	10-May-05	1668034	-9.3767	134.2119	-9.3779	134.21507	DV tape = 13; VHS tape = 1	105	105	unconsolidated	particulate matter in water column, limited vis, soft sandy sand-silty bottom, medium bioturbated in places scattered mounds and burrows (from shrimp?), 10 - 15 cm fish, no sessile benthos.
282/016CAM014	C	10-May-05	1668035	-9.4036	134.196	-9.4019	134.19597	DV tape = 14; VHS tape = 1	87	87	firm substrate	Firm substrate with muddy sand low visibility deiod of benthos very flat sea floor small patches of diffuse hydroids, octocorals and possible antipatherians, small fans, fish, bioturbated bottom, isolated stalked soft corals (?) sea whips, stick octocorals, no ripples, barren silty sand,
282/017CAM015	C	10-May-05	1668036	-9.3928	134.171	-9.3888	134.17227	DV tape = 15; VHS tape = 1	88	88	unconsolidated	Very soft unconsolidated substrate, sea whips, small fish, minimal current, black coral, sponges, fans, sub-crops of biota, intermittent hard grounds, extensive sand areas, silty sand a section of the transect travels over a large depression (camera scrapes up the side) 02:21:42 circular (0.5 - 1m diameter) sharp sides of possible fluid escape structure.
282/018CAM016	C	11-May-05	1668037	-9.3846	134.1647	-9.386433	134.1673	dredge at this site probably full of mud prior to reaching the increasing biodiversity of rock edge, several cracks in rock 20 cm deep and wide. DV tape = 16; VHS tape = 2	96	96	firm substrate	Excellent site for biodiversity!! minor marine snow. Spiral tip white sea whips, sea whips, sea fans, crinoids, octocorals, spiral antipatherians, soft corals, outcrops, crevices, large fish, sponge vase, small stripped wrasse, scorpaenoid, some large fans, some dense aggregations of octocorals, nidalid soft coral, bryozoans - fenestrate, ellisellid finger fan large, black coral (white polyps, straight branches), small pink fish sand/mud, sparse sea whips. species up to 40 cm height.

282/019CAM017	C	11-May-05	1668038	-9.3833	134.1629	-9.3807	134.1647	DV tape = 17; VHS tape = 2	108	108	unconsolidated	Soft unconsolidated surficial muddy sand drape over a firmer substrate. Fine particulate matter in water column. Low benthic cover <5%. initial intermittent sparse biota, isolated octocoral, small sea whips and sea fans, soft patches, bioturbated, environmental changes with an extensive sandy mud area with faecal pellets and some burrows
282/020CAM018	C	11-May-05	1668039	-9.356	134.125	-9.354833	134.118	DV tape = 18; VHS tape = 2	101	101	rocky substrate	Apparent bedding noted in outcrop. Covered with a high range of benthos. Medium vis. rocky bottom, sea whips, octocorals, dense population, silty slope, on rocky slope orange encrustations, sea whips, echinoid, fish gorgonian/octocoral garden, soft coral, blue octocoral, sponges, basket star Benthos up to 50cm in height. High relief topography Adjacent sea floor has broken biogenic material sea urchins fish in rock crevices benthos coverage <15%
282/021CAM019	C	11-May-05	1668040	-9.3565	134.0832	-9.353483	134.08015	Very limited effective footage DV tape = 19; VHS tape = 2			unconsolidated	Turbidity high, soft bottom, occasional burrows, visibility very poor, mud substrate. Lone Octocoral (?).
282/022CAM020	C	11-May-05	1668041	-9.3761	134.0595	-9.374183	134.0568	DV tape = 20; VHS tape = 2	123	123	unconsolidated	Marine snow. Very turbid, poor visibility, soft flocculant sediment, small bioturbated burrows, some areas of many burrows and mounds, large depression and smooth surface.
282/023CAM021	C	11-May-05	1668042	-9.3473	134.058	-9.349333	134.05717	DV tape = 21; VHS tape = 2			unconsolidated to firm	Marine snow. Soft muddy sand bottom, turbid water, poor visibility, sea whip, octocoral, very sparse biota, gorgonian, black coral up to 10 cm in height. shrimp, patches of soft and firmer substrate , crinoid, sandy mud and muddy sand
282/024CAM022	C	12-May-05	1668043	-9.3398	134.033	-9.338167	134.03517	DV tape = 22; VHS tape = 2	131	131	unconsolidated	Very turbid, poor visibility, muddy substrate, bioturbated, isolated rock near end, strong current
282/025CAM023	C	12-May-05	1668044	-9.3292	134.0292	-9.3245	134.0303	DV tape = 23; VHS tape = 2	111	111	Muddy sand with some hardgrounds	particulate suspended matter in water column Bioturbated, faecal pellets, burrows, turbid water, poor visibility, scattered unidentified sessile benthos sea whips, gorgonians, sponge, hardgrounds, soft coral, fish, some barren patches , feather star, soft corals, flat fish and sea bed.

282/026CAM024	C	12-May-05	1668045	-9.2582	133.8015	-9.256067	133.8022	DV tape = 24; VHS tape = 2	145	145	soft unconsolidated	Four fish, flat sea floor, soft bioturbated burrowed sediment with assorted fish (few in number). small drifts of faecal matter
282/027CAM025	C	13-May-05	1668046	-9.3812	133.6644	-9.3785	133.66277	DV tape = 25; VHS tape = 2	112	112	unconsolidated	Small fish (gobies and demersal), small swimming crustaceans (shrimps), soft bioturbated burrowed sediment bioturbation, no ripples, detritus, faecal pellets
282/028CAM026	C	13-May-05	1668047	-9.3337	133.6908	-9.3315	133.69017	CAM did not focus - redeployed at same site as CAM027 DV tape = 26; VHS tape = 3	117	140	unconsolidated, soft sediment	Poor visibility, soft muddy substrate, sea flor scattered with faecal pellets, minor shell frags, bioturbated
282/028CAM027	C	13-May-05	1668048	-9.3347	133.6908	-9.3305	133.68983	CAM027 repeat run of CAM026 DV tape = 26; VHS tape = 3	117	141	unconsolidated. sandy mud	small jelly fish (<5cm), fish (<5cm), burrows, flat substrate, sandy mud. Biota very limited, ?Hydroid, shell frags. At 120m depth firm substrate, burrows. Turbidity increases at depth. Very sparse biota at depth.
282/029CAM028	C	13-May-05	1668049	-9.3048	133.6968	-9.303833	133.70217	DV tape = 27; VHS tape = 3	187	176	varied for soft seds to hard substrate across the transect	Very turbid, poor visibility. Burrowed soft unconsolidated muddy substrate with drifts of faecal pellets / organic matter., sparse biota. occasional patchy hardgrounds across the transect some with yellow sponge. ?Hydroid, sea fan, sea whip, ?octacoral on hardgrounds
282/030CAM029	C	14-May-05	1668050	-9.2273	133.697	-9.2248	133.70057	DV tape = 28; VHS tape = 3	151	151	soft unconsolidated sandy mud	Bioturbated mud, relatively featureless, limited bioturbidation. Tubular sponges, multiple species, sea whips, low fans, sea pen, gorgonians, bryozoan clumps, soft corals (Netheid type), fish
282/031CAM030	C	14-May-05	1668051	-9.0893	133.7477	-9.093833	133.74638	DV tape = 29; VHS tape = 3	166	166	soft unconsolidated sandy mud	very soft sediment, visibility V. poor, shallow depression, soft coral, bioturbated, surface with many small burrows, large open burrow.
282/032CAM031	C	14-May-05	1668052	-9.2055	133.6325	-9.207217	133.636	WRONG LABEL ON CLOCK - written as 282/032CAM032 when should be 282/032CAM031. Very turbid, low visibility. DV tape = 30; VHS tape = 3	158	156	unconsolidated	Heavily burrowed, soft bottom, flat, muddy, sparse biota, fish, stripy fish on seabed, sponges, soft corals

282/034CAM033	C	16-May-05	1668053	-9.0334	133.1041	-9.0302	133.10533	DV tape = 31; VHS tape = 4	209	210	unconsolidated	better visibility than other sites, large, steep seep hole; 10cm fish; undulating, burrowed seabed with multiple large burrows/holes 00:14:08 on the tape; very muddy and unconsolidated;
282/035CAM034	C	17-May-05	1668054	-9.0262	133.1688	-9.023467	133.16377	start recording 8.42.30. At 08.54.50 edge of hole is this an edge of a pock mark? DV tape = 32; VHS tape = 4	226	226	V Soft unconsolidated	Bioturbated sea floor, sandy mud. particulate matter in the water column. Burrow and mounds, holes are up to 5cm across. A range in morphologies of the holes08:54:50 on tape: edge of large hole (pock mark?). Textured surface of the seep scarp cohesive lumps of sandy mud.
282/036CAM035	C	17-May-05	1668055	-9.0376	133.1597	-9.036033	133.15997	DV tape = 33; VHS tape = 4	219	219	V Soft unconsolidated	Bioturbated sandy sand sediments across a smooth sea floor, high density of particulate matter in the water column. Frequent mounds and burrows, variation in the morphology of the 'holes' Camera went in a hole and a large decapod (>6cm) was observed at 11:33: 00 mins into the tape.
282/037CAM036	C	17-May-05	1668056	-9.0991	133.1986	-9.095867	133.19867	DV tape = 34; VHS tape = 4	125	125	muddy sand with some semi consolidated gravel substrates	Relatively flat sandy bottom, shelly sand, no burrows. Large fish (snappers), hard flat sand. Faecal pellets, anemones (white and black), fallen octocoral, crinoid, red fish, silver fish, small ground fish with gobles, sea whip/octocoral, small bushy octocorals, larger debris (possibly sub crop), anti pathanian, sea whips lying flat, rock + crinoid, possible urchins sand, tufts on seabed are possibly soft bryozoans and hydroids, reworked oyster shells (shallow lagoonal types, last lowstand). variation in the nature of the substrate across the transect with some areas of cobbles up to 10cm
282/038CAM037	C	17-May-05	1668057	-9.1797	133.4136	-9.181217	133.41345	DV tape = 35; VHS tape = 4	129	170	highly rugose lithified pavements / escarpment	Good biota cover, low height biota, minimal loose sediment, firm substrate. Small bushy octocorals and sea fans with crinoids, sea whips, small fish, black coral. Bedrock. Black crinoids, anemone, octocorals, red octacoral. cover = ~20%. Escarpment at 135m - slight changes in overall benthos in deeper water, hard substrate/ encrusted cobbles with corals / sponges across the out cropping pavement.

282/039CAM038	C	17-May-05	1668058	-9.1715	133.3924	-9.168417	133.39295	DV tape = 36; VHS tape = 4	124	124	hard sandy substrate	extensive hard, flat sandy calcareous burrowed substrate, pavement-like, littered with cobbles. Negligible current, good visibility. Shell debris, soft bryozoans and occasional hydroids, sea whip, sea fan, octocorals orals, anemones, crinoids, antipatherys (bushy and flat forms), large black coral, sponges, fish, bottom fish, rubble, blue sea fan, octocoral with crinoids. Some bioturbation in places. 00:00:20 good display of species succession / diversity crinoids soft corals sea whips sponges < 1% coverage.
282/040CAM039	C	18-May-05	1668059	-9.1504	133.391	-9.147883	133.39073	DV tape = 37; VHS tape = 4	142	142	lithified	Flat, reasonably featureless lithified sandy sea floor, crinoids, some bioturbation, feeding mounds - worms or enteropneusts, hemichordates, white anemone small silver fish, sea urchin, low dome, other anemones, cerianthid anemone sponges, orange bottom fish, small bottom fish, goby?, sea whip, sand ripples on soft sediment (<10cm wave length; <5cm high approx.). 00:53:06 unidentified organism of interest stalked anemone / soft corals (?) ripples continuos parallel small scale (2-3 cm height) 02:00:07 bidirectional
282/041CAM040	C	18-May-05	1668060	-9.1273	133.4222	-9.124933	133.42168	DV tape = 38; VHS tape = 4	199	199	unconsolidated	Soft sea floor with suspended sediments bioturbated Worm tubes, soft sediment, 15 cm across hole, mollusc on substrate, fish resting on bottom. Low vis, flat no ripples.
282/042CAM041	C	18-May-05	1668061	-9.1161	133.4087	-9.11435	133.40752	DV tape = 39; VHS tape = 4	208	208	unconsolidated / lithified cracked pavements	Soft unconsolidated sea floor with faecal pellets slightly bioturbated, muddy/sandy bottom, at 06:36:52 substrate changes abruptly form muddy sand to lithified outcropping pavements w/crevices=ices encrusting benthos including soft corals blade/octa corals, sponges, crustaceans, fenestrate bryozoans, solitary corals, sea whips/fans, crinoid, at 06:41:50 sea whips and sea fans .. benthos specimens are taller.

282/043CAM042	C	19-May-05	1668062	-9.0887	133.4167	-9.0903	133.4196	DV tape = 40; VHS tape = 4	214	214	unconsolidated	suspended sediment, soft sandy mud substrate scattering of faecal pellets rounded mounds smooth sea floor with mounded soft sediments, bioturbated. Rocky hard surface at 13:19, lithified outcropping strata, sponges, black coral, sea anemones, crinoids, large sea fan, wobbegong shark (?), lots of particulates in water, octacoral, sea whip, red fish, solitary coral, squirrel fish, brachiopod, sea urchin, storked crinoid 13:20:05 large striped fish on edge of abrupt change in bathymetry. Bottom drop off abrupt on a hard lithified substrate lightly covered with marine snow. 13:25:30 sea urchins bryozoans stalked crinoids.
282/044CAM043	C	19-May-05	1668063	-9.0311	133.2442	-9.0291	133.2438	VHS tape ran out, Part 1 on VHS 4 and Part 2 on VHS 5 DV tape = 41; VHS tape = 4+5	216	216		Rocky and rubbly substrate, flaggy bedded rocks, sub crop and exposures. Murky water, visibility OK. Patches and veneer of muddy sediment. Crinoids, w white anemones, large snapper, sponge, burrowed sediment patches, brown fish, red crinoid. Sparse biota.
282/045CAM044	C	19-May-05	1668064	-9.0302	133.2449	-9.029833	133.24388	DV tape = 42; VHS tape = 5	227	227	Rocky	Rocky substrate with marine snow veneer and patches of muddy sediment. Sponges, red fish (?squirrel), also the spring from broken SM Grab, red star fish, octocorals, anemone, white sponges, ?hexanelid sponge, yellow sponge. Sparse biota.
282/046CAM045	C	19-May-05	1668065	-9.0307	133.2459	-9.026917	133.24523	Increasing amount of soft muddy sediment during drift. DV tape = 43; VHS tape = 5	237	224	rubbly	Rubbly cobbled substrate with light cover of fine sediment sparse patches of very unconsolidated fine sediment. Rocky outcrops and sub crops. Thin sediment veneer; white sponge, yellow sponge, stalked crinoid, black coral (spiral form), bryozoan, white starfish, sea fan, small fish, small sponge (3cm) anemone all isolated specimens.

282/047CAM046	C	20-May-05	1668066	-9.0319	133.2496	-9.02855	133.2499	Approximately 8 mins of water column footage in middle of tape due to long layback. Ship speed at this time >2 knots. Only half of the footage is on t he VHS tape because it ran out during camera run. DV tape = 44; VHS tape = 5	233	233	unconsolidated	Marine snow med vis. lots of fish, soft sediment, bioturbation, burrows- mounds, pockmarks, red crinoid?, large burrows, crab running across bottom?, hole 15 cm across and ~ 5cm deep.
282/048CAM047	C	20-May-05	1668067	-9.0036	133.2021	-9.000283	133.20087		222	222	unconsolidated	Bioturbated soft muddy sediments, scattered low relief mounds, mostly smooth and flat and uniform, light brown fish (5:22:40), big hole/large burrow ~25 cm (5:25), fish in hole (5:29), sea urchin
282/049CAM048	C	20-May-05	1668068	-9.0964	133.2867	-9.093617	133.28145	DV tape = 46; VHS tape = 6	162	162	hard substrate	Hard substrate, limited vis, echinoderm, sponges, crinoids, sea anemones, bioturbated bottom, stork crinoid, <5% coverage, scattered boulders on hard substrate encrusted with algae and soft sediments, 9:47:30 - stork crinoid, water column particulates, sea whip, black coral, 10 cm height, 9:49 - increasing density of sea floor biota, octacoral/bryozoan. sporadic coverage along transect.
282/050CAM049	C	21-May-05	1668069	-9.1987	133.4306	-9.2015	133.43633	Soft substrate, poor visibility, fairly flat soft substrate, some large burrows @02:22:30 large fish? Several small fish, 02:224:58 ?Scallop fish, spar biota, pock mark at 02:28:35. sponge? (2:29) fish, rubble or large mud clasts (02:33) side of pock mar DV tape = 47; VHS tape = 6	178	178	very soft unconsolidated	Low visibility, v.soft unconsolidated substrate, slight undulations, hollows and rises possible escape structures. Sea floor features subdued due to all covered by soft sediments. later in the transect there are low profile 50 cm wave length parallel ripples some small semi circular pitted sections (15cm <=>) Jelly fish and many smaller similar biota on the way down. Some phenomena in water seen on echo sounder.

282/052CAM050	C	21-May-05	1668070	-9.2176	133.4862	-9.218983	133.49098	DV tape = 48; VHS tape = 6	168	168	unconsolidated	Jelly fish in water at 22m water depth, 2-3 cm in size decrease in abundance at 36m water depth. 100m - biota in water column. Bioturbated muddy substrate. very flat surface large scale (m's) depressions on the seafloor with sharp sides no sessile benthos faecal pellets / organic matter scattered across the sea floor. all features draped with soft sandy sediments. Fish, sparse biota, benthic fish, hole on LHS (04:26), squirrel fish?, ridge (04:31:10), large depression. On retrieval, a lot of particulate material up to 70m , 25-20m jellyfish again.
282/053CAM051A	C	21-May-05	1668071	-9.1757	133.4945	-9.1765	133.49752	Run A downslope (followed by Run B upslope) DV tape = 49; VHS tape = 6	136	150	Hard substrate	The video travels down an escarpment along the sea floor and up and escarpment . it shows a hard substrate, semi lithified muddy sandy gravel, abundant biota ~10% coverage. Antipatherians, crinoids, sponges, anemones, fish, gorgonians, sea fans, large fenestrate bryozoans, sea whips, up to 20cm tall, coral (stag horn form), red crinoid, small red fish. Sub-crop drop-off (sounder 160m, 17:49) rocky ledges, sea whip, less abundant biota at depth, deeper sea floor is flat with minor bioturbation mounds and burrows. crinoid, abundant particulate matter in water, poor visibility. Soft muddy substrate (17:51 160m on sounder), bioturbated, ? sea fan, sparse biota, sting ray (17:54).
282/053CAM051B	C	21-May-05	1668072	-9.1762	133.497	-9.1752	133.4928	Run B upslope (preceded by Run A downslope) DV tape = 49; VHS tape = 6	155	136	unconsolidated	Soft muddy substrate at 156m. Bioturbated, red fish in burrow, sparse biota. Rocky ledges at 160m (18:18), white sponge, ?barnacles, sea whip, crinoid , cliff ledge. Top of drop off at 136m (18:20), patchy to abundant biota, sea fan, hexactinellid sponge, crinoids, ?octocorals, echinoid, sea fans.

282/054CAM052	C	21-May-05	1668073	-9.1541	133.4963	-9.1551	133.50223	Footage reasonable, too much layback since ship travelling too fast. Eventually ship slowed down but missed base of slope. DV tape = 50; VHS tape = 6	182	214	unconsolidated	Soft muddy substrate with rocky patches. Sponges, bushy sea fans, crinoids up to 20cm in height with 10 - 15% coverage. Drop of to 214m (20:39), rocky ledge, fish, sponges, octocorals. (20:45) Soft muddy substrate, minimal bioturbation, very sparse biota yet some apparent fluid escape features (m's in diameter) .
282/056CAM053	C	22-May-05	1668074	-9.1625	133.5294	-9.163	133.53338	DV tape = 51; VHS tape = 6	183	183	unconsolidated	Soft muddy substrate, bioturbated, poor visibility. Sparse biota, ?core hole (00:26:20), fish, red biota, ?feeding marks, fish on RHS, small scale burrows and mounds (00:33: 36). Fluid escape features (?) devoid of sessile benthos.
282/057CAM054	D	24-May-05	1668075	-9.5508	133.9529	-9.549717	133.95188	DV tape = 52; VHS tape = 6			unconsolidated	Very low visibility due to suspended sediment , Sandy sand very soft and unconsolidated9:15:40 - fish, fairly featureless muddy bottom, a little bioturbation (09:19:50) drifts of faecal pellets.
282/058CAM055	D	24-May-05	1668076	-9.5807	134.0396	-9.582917	134.0432	camera sinks directly into soft bottom; relatively clear to 90 m WD then low visibility. Video all the way up particulates in entire water column. DV tape = 53; VHS tape = 6	99	99	unconsolidated	Very soft sediments unconsolidated sandy muddy almost no visibility
282/059CAM056	D	24-May-05	1668077	-9.5954	134.1521	-9.5964	134.1558	echo sounder image of fish recorded and put in station folder DV tape = 54; VHS tape = 6	96.4	96.4	unconsolidated	High productivity in the top of the water column. Small fish in water column (distinct signal on echo sounder), visibility very poor, very muddy, unconsolidated substrate, sparse biota, rare biota on the surface, soft sticky mud, burrows
282/060CAM057	D	24-May-05	1668078	-9.6086	134.179	-9.60955	134.1807	Very bad footage, could not see the sea bed, mud stuck to lens most of the time DV tape = 55; VHS tape = 6	95.6	95.6	unconsolidated	Very poor visibility, sticky mud, unconsolidated material, few burrows/sparse biota

282/061CAM058	D	25-May-05	1668079	-9.6261	134.2389	-9.626367	134.2431	Very limited amount of footage, generally very poor visual and footage DV tape = 56; VHS tape = 6	93	93	unconsolidated	Very poor visibility, soft mud, sparse biota, some burrows
282/062CAM059	D	25-May-05	1668080	-9.656	134.2829	-9.657717	134.28558	DV tape = 57; VHS tape = 6	86	86	unconsolidated	Very soft muddy bottom, water off bottom Very cloudy/murky, b ~ 5m, water clarity to 70m Very good, little penetration to 65m.
282/063CAM060	D	25-May-05	1668081	-9.6613	134.3733	-9.662967	134.37605	DV tape = 58; VHS tape = 7	91	91	unconsolidated	photic zone down to 80m, very soft muddy bottom, water very murky
282/064CAM061		25-May-05	1668082	-9.7394	135.2651	-9.741033	135.25148	DV tape = 59; VHS tape = 7	103	103	unconsolidated yet firm in places	very limited vis due to marine snow. Sandy substrate, multiple small fish (~5cm) near sea floor Burrows / mounds with relief up to 2 cm , Small fish, red object (LHS 18:37), ?crab (18:40). No sessile benthos.

Appendix 6 (A) Biological samples collected during Survey 282 K. Gowlett-Holmes

Cruise#	Station#	Gear	Access#	CAAB #	Phylum code	Family Code	Species Code	Phylum Text	Higher Taxon Text	Family Text	Genus Text	Species Text	Cor
SS0505-GA282	001	BS001B	001BS001-001	28911801	28	911	801	Crustacea	Brachyura	Portunidae	Portunus	sp. 1	pho
SS0505-GA282	001	BS001B	001BS001-002	22000801	22	0	801	Annelida	Polychaeta	unidentified	unidentified	sp. 1	pho
SS0505-GA282	001	BS001B	001BS001-003	25160801	25	160	801	Echinodermata	Ophiuroidea	unidentified	unidentified	sp. 1	pho
SS0505-GA282	001	BS001B	001BS001-004	28105801	28	105	801	Crustacea	Tanaidacea	unidentified	unidentified	sp. 1	pho
SS0505-GA282	001	BS001B	001BS001-005	28400801	28	400	801	Crustacea	Amphipoda Gammaridea	unidentified	unidentified	sp. 1	pho
SS0505-GA282	001	BS001B	001BS001-006	23207801	23	207	801	Mollusca	Bivalvia	Nuculanidae	unidentified	sp. 1	pho
SS0505-GA282	001	BS001B	001BS001-007	24202801	24	202	801	Mollusca	Gastropoda	Buccinidae Fasciolariinae	unidentified	sp. 1	pho
SS0505-GA282	001	BS001B	001BS001-008	22000802	22	0	802	Annelida	Polychaeta	unidentified	unidentified	sp. 2	pho
SS0505-GA282	001	BS001B	001BS001-009	99901007	99	901	7					coarse sample bulk	
SS0505-GA282	001	BS001B	001BS001-010	99901005	99	901	5					fine sample bulk	
SS0505-GA282	001	BS001B	001BS001-011	99901008	99	901	8					seived sample bulk	
SS0505-GA282	001	BS001B	001BS001-012	99901006	99	901	6					medium sample bulk	
SS0505-GA282	002	GR001B	002GR001B-001	28803801	28	803	801	Crustacea	Thalassinidea	Callianassidae	unidentified	sp. 1	pho
SS0505-GA282	002	GR001B	002GR001B-002	11328801	11	328	801	Cnidaria	Scleractinia	Flabellidae	Flabellum	sp. 1	pho
SS0505-GA282	002	GR001B	002GR001B-003	99901005	99	901	5					fine sample bulk	
SS0505-GA282	002	GR001B	002GR001B-004	99901007	99	901	7					coarse sample bulk	
SS0505-GA282	002	GR001B	002GR001B-005	23410801	23	410	801	Mollusca	Bivalvia	Thraciidae	unidentified	sp. 1	pho
SS0505-GA282	002	GR002B	002GR002B-001	11328801	11	328	801	Cnidaria	Scleractinia	Flabellidae	Flabellum	sp. 1	
SS0505-GA282	002	GR002B	002GR002B-002	99901005	99	901	5					fine sample bulk	
SS0505-GA282	002	GR002B	002GR002B-003	11314801	11	314	801	Cnidaria	Scleractinia	Caryophylliidae	unidentified	sp. 1	pho
SS0505-GA282	002	GR002B	002GR002B-004	11077801	11	77	801	Cnidaria	Hydrozoa	Stylasteridae	unidentified	sp. 1	pho
SS0505-GA282	002	GR003B	002GR003B-001	37065801	37	65	801	Chordata	Pisces	Nettastomatidae	unidentified	sp. 1	pho
SS0505-GA282	002	GR003B	002GR003B-002	99901005	99	901	5					fine sample bulk	
SS0505-GA282	002	BS002B	002BS002-001	28803801	28	803	801	Crustacea	Thalassinidea	Callianassidae	unidentified	sp. 1	
SS0505-GA282	002	BS002B	002BS002-002	28805801	28	805	801	Crustacea	Thalassinidea	Upogebiidae	unidentified	sp. 1	pho
SS0505-GA282	002	BS002B	002BS002-003	28865801	28	865	801	Crustacea	Brachyura	Raninidae	unidentified	sp. 1	pho
SS0505-GA282	002	BS002B	002BS002-004	99901005	99	901	5					fine sample bulk	
SS0505-GA282	002	BS002B	002BS002-005	99901003	99	901	3					debris-shells	
SS0505-GA282	003	GR004B	003GR004B-001	25176801	25	176	801	Echinodermata	Ophiuroidea	Ophiuridae	unidentified	sp. 1	pho
SS0505-GA282	003	GR004B	003GR004B-002	28865801	28	865	801	Crustacea	Brachyura	Raninidae	unidentified	sp. 1	pho
SS0505-GA282	003	GR004B	003GR004B-003	11328801	11	328	801	Cnidaria	Scleractinia	Flabellidae	Flabellum	sp. 1	pho
SS0505-GA282	003	GR004B	003GR004B-004	11077801	11	77	801	Cnidaria	Hydrozoa	Stylasteridae	unidentified	sp. 1	pho
SS0505-GA282	003	GR005B	003GR005B-001	25176801	25	176	801	Echinodermata	Ophiuroidea	Ophiuridae	unidentified	sp. 1	
SS0505-GA282	003	GR004B	003GR005B-002	28805802	28	805	802	Crustacea	Thalassinidea	Upogebiidae	unidentified	sp. 2	pho
SS0505-GA282	003	GR005B	003GR005B-003	28805802	28	805	802	Crustacea	Thalassinidea	Upogebiidae	unidentified	sp. 2	mal
SS0505-GA282	003	GR004B	003GR005B-004	99901005	99	901	5					fine sample bulk	
SS0505-GA282	005	GR006B	005GR006B-001	28030801	28	30	801	Crustacea	Stomatopoda	unidentified	unidentified	sp. 1	pho
SS0505-GA282	005	GR006B	005GR006B-002	28803801	28	803	801	Crustacea	Thalassinidea	Callianassidae	unidentified	sp. 1	pho
SS0505-GA282	005	GR006B	005GR006B-003	11001801	11	1	801	Cnidaria	Hydrozoa	unidentified	unidentified	sp. 1	pho
SS0505-GA282	005	GR007B	005GR007B-001	99901005	99	901	5					fine sample bulk	
SS0505-GA282	005	GR007B	005GR007B-002	37428801	37	428	801	Chordata	Pisces	Gobiidae	unidentified	sp. 1	pho
SS0505-GA282	005	GR007B	005GR007B-003	22000801	22	0	801	Annelida	Polychaeta	unidentified	unidentified	sp. 1	pho
SS0505-GA282	005	GR007B	005GR007B-004	25191801	25	191	801	Echinodermata	Ophiuroidea	Amphiuridae	unidentified	sp. 1	pho
SS0505-GA282	006	GR008B	006GR008B-001	28803801	28	803	801	Crustacea	Thalassinidea	Callianassidae	unidentified	sp. 1	
SS0505-GA282	006	GR008B	006GR008B-002	22000000	22	0	0	Annelida	Polychaeta	unidentified	unidentified	unidentified	
SS0505-GA282	006	GR009B	006GR009B-001	28030802	28	30	802	Crustacea	Stomatopoda	unidentified	unidentified	sp. 2	pho
SS0505-GA282	006	GR009B	006GR009B-002	28803801	28	803	801	Crustacea	Thalassinidea	Callianassidae	unidentified	sp. 1	
SS0505-GA282	006	GR009B	006GR009B-003	28765801	28	765	801	Crustacea	Caridea	Alpheidae	unidentified	sp. 1	pho
SS0505-GA282	006	GR009B	006GR009B-004	99901005	99	901	5					fine sample bulk	
SS0505-GA282	006	GR009B	006GR009B-005	24220801	24	220	801	Mollusca	Gastropoda	Turridae	unidentified	sp. 1	pho
SS0505-GA282	006	GR009B	006GR009B-006	11229801	11	229	801	Cnidaria	Actinaria	unidentified	unidentified	sp. 1	pho
SS0505-GA282	007	GR010B	007GR010B-001	28030803	28	30	803	Crustacea	Stomatopoda	unidentified	unidentified	sp. 3	pho
SS0505-GA282	007	GR010B	007GR010B-002	28865801	28	865	801	Crustacea	Brachyura	Raninidae	unidentified	sp. 1	
SS0505-GA282	007	GR010B	007GR010B-003	22000000	22	0	0	Annelida	Polychaeta	unidentified	unidentified	unidentified	
SS0505-GA282	007	GR011B	007GR011B-001	99901005	99	901	5					fine sample bulk	
SS0505-GA282	007	GR011B	007GR011B-002	22000803	22	0	803	Annelida	Polychaeta	unidentified	unidentified	sp. 3	pho
SS0505-GA282	007	GR011B	007GR011B-003	28803803	28	803	803	Crustacea	Thalassinidea	Callianassidae	unidentified	sp. 3	pho
SS0505-GA282	007	GR011B	007GR011B-004	28803802	28	803	802	Crustacea	Thalassinidea	Callianassidae	unidentified	sp. 2	pho
SS0505-GA282	007	GR011B	007GR011B-005	11314801	11	314	801	Cnidaria	Scleractinia	Caryophylliidae	unidentified	sp. 1	pho
SS0505-GA282	007	BS003B	007BS003-001	99901005	99	901	5					fine sample bulk	
SS0505-GA282	007	BS003B	007BS003-002	37000801	37	0	801	Chordata	Pisces	unidentified	unidentified	sp. 1	pho
SS0505-GA282	007	BS003B	007BS003-003	37065801	37	65	801	Chordata	Pisces	Nettastomatidae	unidentified	sp. 1	

SS0505-GA282	007	BS003B	007BS003-004	28711801	28	711	801	Crustacea	Penaeoidea	Penaeidae	unidentified	sp. 1	pho
SS0505-GA282	007	BS003B	007BS003-005	22062801	22	62	801	Annelida	Polychaeta	Polynoidae	unidentified	sp. 1	pho
SS0505-GA282	007	BS003B	007BS003-006	28220801	28	220	801	Crustacea	Isopoda	Cirolanidae	unidentified	sp. 1	pho
SS0505-GA282	007	BS003B	007BS003-007	28205801	28	205	801	Crustacea	Isopoda	Anthuridae	unidentified	sp. 1	pho
SS0505-GA282	007	BS003B	007BS003-008	22000000	22	0	0	Annelida	Polychaeta	unidentified	unidentified	unidentified	
SS0505-GA282	007	BS003B	007BS003-009	23355801	23	355	801	Mollusca	Bivalvia	Tellinidae	unidentified	sp. 1	pho
SS0505-GA282	007	BS003B	007BS003-010	25191801	25	191	801	Echinodermata	Ophiuroidea	Amphiuridae	unidentified	sp. 1	
SS0505-GA282	007	BS003B	007BS003-011	28803802	28	803	802	Crustacea	Thalassinidea	Callianassidae	unidentified	sp. 2	
SS0505-GA282	007	BS003B	007BS003-012	28105802	28	105	802	Crustacea	Tanaidacea	unidentified	unidentified	sp. 2	pho
SS0505-GA282	007	BS003B	007BS003-013	25191802	25	191	802	Echinodermata	Ophiuroidea	Amphiuridae	unidentified	sp. 2	pho
SS0505-GA282	007	BS003B	007BS003-014	25160802	25	160	802	Echinodermata	Ophiuroidea	unidentified	unidentified	sp. 2	pho
SS0505-GA282	007	BS003B	007BS003-015	99901008	99	901	8					seived sample bulk	
SS0505-GA282	007	BS003B	007BS003-016	99901003	99	901	3					debris-shells	
SS0505-GA282	008	GR012B	008GR012B-001	11173801	11	173	801	Cnidaria	Alcyonacea	unidentified	unidentified	sp. 1	pho
SS0505-GA282	008	GR012B	008GR012B-002	11314802	11	314	802	Cnidaria	Scleractinia	Caryophylliidae	unidentified	sp. 2	pho
SS0505-GA282	008	GR012B	008GR012B-003	99901008	99	901	8					seived sample bulk	
SS0505-GA282	008	GR012B	008GR012B-004	20325801	20	325	801	Bryozoa	Cheilostomata	Quadricellariidae	Nellia	sp. 1	pho
SS0505-GA282	008	GR012B	008GR012B-005	20300801	20	300	801	Bryozoa	Cheilostomata	Porinidae	Porina	vertebralis	pho
SS0505-GA282	008	GR013B	008GR013B-001	23499801	23	499	801	Mollusca	Scaphopoda	unidentified	unidentified	sp. 1	pho
SS0505-GA282	008	GR013B	008GR013B-002	99901005	99	901	5					fine sample bulk	
SS0505-GA282	009	GR014B	009GR014B-001	24221801	24	221	801	Mollusca	Gastropoda	Terebridae	unidentified	sp. 1	pho
SS0505-GA282	009	GR014B	009GR014B-002	99901008	99	901	8					seived sample bulk	
SS0505-GA282	009	GR015B	009GR015B-001	99901005	99	901	5					fine sample bulk	
SS0505-GA282	009	GR015B	009GR015B-002	17001801	17	1	801	Sipuncula		Sipunculidae	Sipunculus	sp. 1	pho
SS0505-GA282	009	GR015B	009GR015B-003	11314801	11	314	801	Cnidaria	Scleractinia	Caryophylliidae	unidentified	sp. 1	
SS0505-GA282	010	GR016B	010GR016B-001	22000801	22	0	801	Annelida	Polychaeta	unidentified	unidentified	sp. 1	pho
SS0505-GA282	010	GR017B	010GR017B-001	99901005	99	901	5					fine sample bulk	
SS0505-GA282	010	GR017B	010GR017B-002	37428802	37	428	802	Chordata	Pisces	Gobiidae	unidentified	sp. 2	pho
SS0505-GA282	010	GR017B	010GR017B-003	28220802	28	220	802	Crustacea	Isopoda	Cirolanidae	unidentified	sp. 2	pho
SS0505-GA282	010	GR017B	010GR017B-004	28803000	28	803	0	Crustacea	Thalassinidea	Callianassidae	unidentified	unidentified	
SS0505-GA282	011	GR018B	011GR018B-001	99901005	99	901	5					fine sample bulk	
SS0505-GA282	011	GR018B	011GR018B-002	25191803	25	191	803	Echinodermata	Ophiuroidea	Amphiuridae	unidentified	sp. 3	pho
SS0505-GA282	011	GR018B	011GR018B-003	22000000	22	0	0	Annelida	Polychaeta	unidentified	unidentified	unidentified	
SS0505-GA282	012	GR019B	012GR019B-001	99901005	99	901	5					fine sample bulk	
SS0505-GA282	012	GR019B	012GR019B-002	17000801	17	0	801	Sipuncula		unidentified	unidentified	sp. 1	pho
SS0505-GA282	012	GR019B	012GR019B-003	28803000	28	803	0	Crustacea	Thalassinidea	Callianassidae	unidentified	unidentified	
SS0505-GA282	013	GR020B	013GR020B-001	28880801	28	880	801	Crustacea	Brachyura	Majidae	unidentified	sp. 1	pho
SS0505-GA282	013	GR020B	013GR020B-002	22000000	22	0	0	Annelida	Polychaeta	unidentified	unidentified	unidentified	
SS0505-GA282	013	GR021B	013GR021B-001	37428803	37	428	803	Chordata	Pisces	Gobiidae	unidentified	sp. 3	pho
SS0505-GA282	013	GR021B	013GR021B-002	99901005	99	901	5					fine sample bulk	
SS0505-GA282	013	DR001B	013DR001B-001	25001801	25	1	801	Echinodermata	Crinoidea	unidentified	unidentified	sp. 1	pho
SS0505-GA282	013	DR001B	013DR001B-002	25171801	25	171	801	Echinodermata	Ophiuroidea	Gorgonocephalidae	unidentified	sp. 1	pho
SS0505-GA282	013	DR001B	013DR001B-003	11196801	11	196	801	Cnidaria	Alcyonacea	Plexauridae	unidentified	sp. 1	pho
SS0505-GA282	013	DR001B	013DR001B-004	25160000	25	160	0	Echinodermata	Ophiuroidea	unidentified	unidentified	unidentified	
SS0505-GA282	013	DR001B	013DR001B-005	11173802	11	173	802	Cnidaria	Alcyonacea	unidentified	unidentified	sp. 2	pho
SS0505-GA282	013	DR001B	013DR001B-006	11173803	11	173	803	Cnidaria	Alcyonacea	unidentified	unidentified	sp. 3	pho
SS0505-GA282	013	DR001B	013DR001B-007	25039801	25	39	801	Echinodermata	Crinoidea	Colobometridae	unidentified	sp. 1	pho
SS0505-GA282	013	DR001B	013DR001B-008	25039802	25	39	802	Echinodermata	Crinoidea	Colobometridae	unidentified	sp. 2	pho
SS0505-GA282	013	DR001B	013DR001B-009	25039803	25	39	803	Echinodermata	Crinoidea	Colobometridae	unidentified	sp. 3	pho
SS0505-GA282	013	DR001B	013DR001B-010	11191801	11	191	801	Cnidaria	Alcyonacea	Nephtheidae	unidentified	sp. 1	pho
SS0505-GA282	013	DR001B	013DR001B-011	25192801	25	192	801	Echinodermata	Ophiuroidea	Ophiotrichidae	Ophiothrix	sp. 1	pho
SS0505-GA282	013	DR001B	013DR001B-012	11192801	11	192	801	Cnidaria	Alcyonacea	Nidaliidae	unidentified	sp. 1	pho
SS0505-GA282	013	DR001B	013DR001B-013	28840004	28	840	4	Crustacea	Anomura	Galatheidae	Allogalathea	elegans	pho
SS0505-GA282	013	DR001B	013DR001B-014	11173804	11	173	804	Cnidaria	Alcyonacea	unidentified	unidentified	sp. 4	pho
SS0505-GA282	013	DR001B	013DR001B-015	11173805	11	173	804	Cnidaria	Alcyonacea	unidentified	unidentified	sp. 5	pho
SS0505-GA282	013	DR001B	013DR001B-016	20487801	20	487	801	Bryozoa	Cheilostomata	Phidoloporidae	Triphyllozoon	sp. 1	pho
SS0505-GA282	013	DR001B	013DR001B-017	11160801	11	160	801	Cnidaria	Antipatharia	unidentified	unidentified	sp. 1	pho
SS0505-GA282	013	DR001B	013DR001B-018	11173806	11	173	806	Cnidaria	Alcyonacea	unidentified	unidentified	sp. 6	pho
SS0505-GA282	013	DR001B	013DR001B-019	99901005	99	901	5					fine sample bulk	
SS0505-GA282	013	DR001B	013DR001B-020	11173807	11	173	807	Cnidaria	Alcyonacea	unidentified	unidentified	sp. 7	pho
SS0505-GA282	013	DR001B	013DR001B-021	11173809	11	173	809	Cnidaria	Alcyonacea	unidentified	unidentified	sp. 9	pho
SS0505-GA282	013	DR001B	013DR001B-022	11173808	11	173	808	Cnidaria	Alcyonacea	unidentified	unidentified	sp. 8	pho
SS0505-GA282	013	DR001B	013DR001B-023	11173811	11	173	811	Cnidaria	Alcyonacea	unidentified	unidentified	sp. 11	pho
SS0505-GA282	013	DR001B	013DR001B-024	11173810	11	173	810	Cnidaria	Alcyonacea	unidentified	unidentified	sp. 10	pho
SS0505-GA282	013	DR001B	013DR001B-025	11173812	11	173	812	Cnidaria	Alcyonacea	unidentified	unidentified	sp. 12	pho

SS0505-GA282	013	DR001B	013DR001B-026	10180801	10	180	801	Porifera	Demospongiae	unidentified	unidentified	sp. 1	pho
SS0505-GA282	013	DR001B	013DR001B-027	11173813	11	173	813	Cnidaria	Alcyonacea	unidentified	unidentified	sp. 13	pho
SS0505-GA282	013	DR001B	013DR001B-028	11173814	11	173	814	Cnidaria	Alcyonacea	unidentified	unidentified	sp. 14	pho
SS0505-GA282	013	DR001B	013DR001B-029	11173815	11	173	815	Cnidaria	Alcyonacea	unidentified	unidentified	sp. 15	pho
SS0505-GA282	013	DR001B	013DR001B-030	11173000	11	173	0	Cnidaria	Alcyonacea	unidentified	unidentified	unidentified	
SS0505-GA282	013	DR001B	013DR001B-031	11196803	11	196	803	Cnidaria	Alcyonacea	Plexauridae	unidentified	sp. 3	pho
SS0505-GA282	013	DR001B	013DR001B-032	11196802	11	196	802	Cnidaria	Alcyonacea	Plexauridae	unidentified	sp. 2	pho
SS0505-GA282	013	DR001B	013DR001B-033	19150801	19	150	801	Brachiopoda	Articulata	unidentified	unidentified	sp. 1	pho
SS0505-GA282	013	DR001B	013DR001B-034	11190801	11	190	801	Cnidaria	Alcyonacea	Melithaeidae	unidentified	sp. 1	pho
SS0505-GA282	013	DR001B	013DR001B-035	11173822	11	173	822	Cnidaria	Alcyonacea	unidentified	unidentified	sp. 22	pho
SS0505-GA282	013	DR001B	013DR001B-036	11173821	11	173	821	Cnidaria	Alcyonacea	unidentified	unidentified	sp. 21	pho
SS0505-GA282	013	DR001B	013DR001B-037	11173819	11	173	819	Cnidaria	Alcyonacea	unidentified	unidentified	sp. 19	pho
SS0505-GA282	013	DR001B	013DR001B-038	11173820	11	173	820	Cnidaria	Alcyonacea	unidentified	unidentified	sp. 20	pho
SS0505-GA282	013	DR001B	013DR001B-039	11173818	11	173	818	Cnidaria	Alcyonacea	unidentified	unidentified	sp. 18	pho
SS0505-GA282	013	DR001B	013DR001B-040	11173817	11	173	817	Cnidaria	Alcyonacea	unidentified	unidentified	sp. 17	pho
SS0505-GA282	013	DR001B	013DR001B-041	11173823	11	173	823	Cnidaria	Alcyonacea	unidentified	unidentified	sp. 23	pho
SS0505-GA282	013	DR001B	013DR001B-042	11173824	11	173	824	Cnidaria	Alcyonacea	unidentified	unidentified	sp. 24	pho
SS0505-GA282	013	DR001B	013DR001B-043	11173816	11	173	816	Cnidaria	Alcyonacea	unidentified	unidentified	sp. 16	pho
SS0505-GA282	013	DR001B	013DR001B-044	27500801	27	500	801	Crustacea	Cirripedia	unidentified	unidentified	sp. 1	pho
SS0505-GA282	013	DR001B	013DR001B-045	24080801	24	80	801	Mollusca	Gastropoda	Siliquariidae	Siliquaria	sp. 1	pho
SS0505-GA282	013	DR001B	013DR001B-046	10180802	10	180	802	Porifera	Demospongiae	unidentified	unidentified	sp. 2	pho
SS0505-GA282	013	DR001B	013DR001B-047	99901008	99	901	8					sieved sample	
SS0505-GA282	013	DR001B	013DR001B-048	19150801	19	150	801	Brachiopoda	Articulata	unidentified	unidentified	sp. 1	pho
SS0505-GA282	013	DR001B	013DR001B-049	22062802	22	62	802	Annelida	Polychaeta	Polynoidae	unidentified	sp. 2	pho
SS0505-GA282	013	DR001B	013DR001B-050	11229802	11	229	802	Cnidaria	Actinaria	unidentified	unidentified	sp. 2	pho
SS0505-GA282	013	DR001B	013DR001B-051	10180000	10	180	0	Porifera	Demospongiae	unidentified	unidentified	unidentified	
SS0505-GA282	013	DR001B	013DR001B-052	28843801	28	843	801	Crustacea	Anomura	Porcellanidae	unidentified	sp. 1	pho
SS0505-GA282	013	DR001B	013DR001B-053	25160803	25	160	803	Echinodermata	Ophiuroidea	unidentified	unidentified	sp. 3	pho
SS0505-GA282	013	DR001B	013DR001B-054	28840801	28	840	801	Crustacea	Anomura	Galatheidae	unidentified	sp. 1	pho
SS0505-GA282	013	DR001B	013DR001B-055	28840802	28	840	802	Crustacea	Anomura	Galatheidae	unidentified	sp. 2	pho
SS0505-GA282	013	DR001B	013DR001B-056	28840803	28	840	803	Crustacea	Anomura	Galatheidae	unidentified	sp. 3	pho
SS0505-GA282	013	DR001B	013DR001B-057	28926801	28	926	801	Crustacea	Brachyura	Pilumnidae	unidentified	sp. 1	pho
SS0505-GA282	013	DR001B	013DR001B-058	28765802	28	765	802	Crustacea	Caridea	Alpheidae	unidentified	sp. 2	pho
SS0505-GA282	013	DR001B	013DR001B-059	28911802	28	911	802	Crustacea	Brachyura	Portunidae	Thalamita	sp. 1	pho
SS0505-GA282	013	DR001B	013DR001B-060	11229803	11	229	803	Cnidaria	Actinaria	unidentified	unidentified	sp. 3	pho
SS0505-GA282	013	DR001B	013DR001B-061	11077802	11	77	802	Cnidaria	Hydrozoa	Stylasteridae	unidentified	sp. 2	pho
SS0505-GA282	013	DR001B	013DR001B-062	20300801	20	300	801	Bryozoa	Cheilostomata	Porinidae	Porina	vertebralis	
SS0505-GA282	013	DR001B	013DR001B-063	20325801	20	325	801	Bryozoa	Cheilostomata	Quadricellariidae	Nellia	sp. 1	
SS0505-GA282	013	DR001B	013DR001B-064	20332801	20	332	801	Bryozoa	Cheilostomata	Candidae	Scrupocellaria	curvata	pho
SS0505-GA282	013	DR001B	013DR001B-065	20405802	20	405	802	Bryozoa	Cheilostomata	Adeonidae	Adeonella	sp. 2	pho
SS0505-GA282	013	DR001B	013DR001B-066	20405801	20	405	801	Bryozoa	Cheilostomata	Adeonidae	Adeonella	sp. 1	pho
SS0505-GA282	013	DR001B	013DR001B-067	20300000	20	300	0	Bryozoa	Cheilostomata	unidentified	unidentified	unidentified	
SS0505-GA282	014	GR023B	014GR023B-001	99901005	99	901	5					fine sample bulk	
SS0505-GA282	015	GR024B	015GR024B-001	99901005	99	901	5					fine sample bulk	
SS0505-GA282	015	GR024B	015GR024B-002	10180000	10	180	0	Porifera	Demospongiae	unidentified	unidentified	unidentified	
SS0505-GA282	015	GR025B	015GR025B-001	99901005	99	901	5					fine sample bulk	
SS0505-GA282	015	GR025B	015GR025B-002	22000804	22	0	804	Annelida	Polychaeta	unidentified	unidentified	sp. 4	pho
SS0505-GA282	015	BS004B	015BS004B-001	99901005	99	901	5					fine sample bulk	
SS0505-GA282	015	BS004B	015BS004B-002	23207802	23	207	802	Mollusca	Bivalvia	Nuculanidae	unidentified	sp. 2	pho
SS0505-GA282	015	BS004B	015BS004B-003	28805803	28	805	803	Crustacea	Thalassinidea	Upogebiidae	unidentified	sp. 3	pho
SS0505-GA282	015	BS004B	015BS004B-004	28030802	28	30	802	Crustacea	Stomatopoda	unidentified	unidentified	sp. 2	pho
SS0505-GA282	015	BS004B	015BS004B-005	37428804	37	428	804	Chordata	Pisces	Gobiidae	unidentified	sp. 4	pho
SS0505-GA282	015	BS004B	015BS004B-006	28803804	28	803	804	Crustacea	Thalassinidea	Callianassidae	unidentified	sp. 4	pho
SS0505-GA282	015	BS004B	015BS004B-007	99901003	99	901	3					debris-shells	
SS0505-GA282	016	GR026B	016GR026B-001	24191801	24	191	801	Mollusca	Gastropoda	Epitoniidae	unidentified	sp. 1	pho
SS0505-GA282	016	GR026B	016GR026B-002	11314803	11	314	803	Cnidaria	Scleractinia	Caryophylliidae	unidentified	sp. 3	pho
SS0505-GA282	016	GR026B	016GR026B-003	99901003	99	901	3					debris-shells	
SS0505-GA282	016	GR026B	016GR026B-004	11317801	11	317	801	Cnidaria	Scleractinia	Turbinoliidae	unidentified	sp. 1	pho
SS0505-GA282	016	GR027B	016GR027B-001	99901005	99	901	5					fine sample bulk	
SS0505-GA282	016	GR027B	016GR027B-002	28765803	28	765	803	Crustacea	Caridea	Alpheidae	unidentified	sp. 3	pho
SS0505-GA282	016	GR027B	016GR027B-003	28711802	28	711	802	Crustacea	Penaeoidea	Penaeidae	unidentified	sp. 2	pho
SS0505-GA282	017	GR028B	017GR028B-001	22000000	22	0	0	Annelida	Polychaeta	unidentified	unidentified	unidentified	
SS0505-GA282	017	GR029B	017GR029B-001	99901005	99	901	5					fine sample bulk	
SS0505-GA282	017	GR029B	017GR029B-002	22000000	22	0	0	Annelida	Polychaeta	unidentified	unidentified	unidentified	
SS0505-GA282	017	GR029B	017GR029B-003	25160804	25	160	804	Echinodermata	Ophiuroidea	unidentified	unidentified	sp. 4	pho

SS0505-GA282	017	GR029B	017GR029B-004	28799000	28	799	0	Crustacea	Thalassinidea	unidentified	unidentified	unidentified	
SS0505-GA282	018	GR030B	018GR030B-001	28840804	28	840	804	Crustacea	Anomura	Galatheidae	unidentified	sp. 4	pho
SS0505-GA282	018	GR030B	018GR030B-002	28900801	28	900	801	Crustacea	Brachyura	Corystidae	unidentified	sp. 1	pho
SS0505-GA282	018	GR030B	018GR030B-003	23199801	23	199	801	Mollusca	Bivalvia	unidentified	unidentified	sp. 1	pho
SS0505-GA282	018	GR031B	018GR031B-001	99901005	99	901	5					fine sample bulk	
SS0505-GA282	018	GR031B	018GR031B-002	25160000	25	160	0	Echinodermata	Ophiuroidea	unidentified	unidentified	unidentified	
SS0505-GA282	018	GR031B	018GR031B-003	22030801	22	30	801	Annelida	Polychaeta	Onuphidae	unidentified	sp. 1	pho
SS0505-GA282	018	GR031B	018GR031B-004	14000801	14	0	801	Nemertea		unidentified	unidentified	sp. 1	pho
SS0505-GA282	018	DR002B	018DR002B-001	11173000	11	173	0	Cnidaria	Alcyonacea	unidentified	unidentified	unidentified	
SS0505-GA282	018	DR002B	018DR002B-002	20487801	20	487	801	Bryozoa	Cheilostomata	Phidoloporidae	Triphyllozoon	sp. 1	
SS0505-GA282	018	DR002B	018DR002B-003	99901005	99	901	5					fine sample bulk	
SS0505-GA282	019	GR032B	019GR032B-001	99901005	99	901	5					fine sample bulk	
SS0505-GA282	019	GR033B	019GR033B-001	28220803	28	220	803	Crustacea	Isopoda	Cirolanidae	unidentified	sp. 3	pho
SS0505-GA282	019	GR033B	019GR033B-002	28226801	28	226	801	Crustacea	Isopoda	Sphaeromatidae	unidentified	sp. 1	pho
SS0505-GA282	019	GR033B	019GR033B-003	28926801	28	926	801	Crustacea	Brachyura	Pilumnidae	unidentified	sp. 1	
SS0505-GA282	019	GR033B	019GR033B-004	25160000	25	160	0	Echinodermata	Ophiuroidea	unidentified	unidentified	unidentified	
SS0505-GA282	019	GR033B	019GR033B-005	22000000	22	0	0	Annelida	Polychaeta	unidentified	unidentified	unidentified	
SS0505-GA282	019	GR033B	019GR033B-006	28880802	28	880	802	Crustacea	Brachyura	Majidae	unidentified	sp. 2	pho
SS0505-GA282	019	GR033B	019GR033B-007	11173000	11	173	0	Cnidaria	Alcyonacea	unidentified	unidentified	unidentified	
SS0505-GA282	019	GR033B	019GR033B-008	11284801	11	284	801	Cnidaria	Zoanthinaria	unidentified	unidentified	sp. 1	pho
SS0505-GA282	019	GR033B	019GR033B-009	11290801	11	290	801	Cnidaria	Scleractinia	unidentified	unidentified	sp. 1	pho
SS0505-GA282	019	GR033B	019GR033B-010	99901005	99	901	5					fine sample bulk	
SS0505-GA282	019	DR003B	019DR003B-001	99901005	99	901	5					fine sample bulk	
SS0505-GA282	020	GR034B	020GR034B-001	11173000	11	173	0	Cnidaria	Alcyonacea	unidentified	unidentified	unidentified	plac
SS0505-GA282	020	GR035B	020GR035B-001	99901005	99	901	5					fine sample bulk	
SS0505-GA282	020	GR035B	020GR035B-002	11160801	11	160	801	Cnidaria	Antipatharia	unidentified	unidentified	sp. 1	pho
SS0505-GA282	020	GR035B	020GR035B-003	11173825	11	173	825	Cnidaria	Alcyonacea	unidentified	unidentified	sp. 25	pho
SS0505-GA282	020	GR035B	020GR035B-004	25001802	25	1	802	Echinodermata	Crinoidea	unidentified	unidentified	sp. 2	pho
SS0505-GA282	020	DR005B	020DR005B-001	25001801	25	1	801	Echinodermata	Crinoidea	unidentified	unidentified	sp. 1	
SS0505-GA282	020	DR005B	020DR005B-002	25001802	25	1	802	Echinodermata	Crinoidea	unidentified	unidentified	sp. 2	pho
SS0505-GA282	020	DR005B	020DR005B-003	25171803	25	171	803	Echinodermata	Ophiuroidea	Gorgonocephalidae	unidentified	sp. 3	pho
SS0505-GA282	020	DR005B	020DR005B-004	25160805	25	160	805	Echinodermata	Ophiuroidea	unidentified	unidentified	sp. 5	pho
SS0505-GA282	020	DR005B	020DR005B-005	19150802	19	150	802	Brachiopoda	Articulata	unidentified	unidentified	sp. 2	pho
SS0505-GA282	020	DR005B	020DR005B-006	19150801	19	150	801	Brachiopoda	Articulata	unidentified	unidentified	sp. 1	pho
SS0505-GA282	020	DR005B	020DR005B-007	25171802	25	171	802	Echinodermata	Ophiuroidea	Gorgonocephalidae	unidentified	sp. 2	pho
SS0505-GA282	020	DR005B	020DR005B-008	22116801	22	116	801	Annelida	Polychaeta	Flabelligeridae	unidentified	sp. 1	pho
SS0505-GA282	020	DR005B	020DR005B-009	28770801	28	770	801	Crustacea	Caridea	Pandalidae	unidentified	sp. 1	pho
SS0505-GA282	020	DR005B	020DR005B-010	99901005	99	901	5					fine sample bulk	
SS0505-GA282	020	DR005B	020DR005B-011	11229804	11	229	804	Cnidaria	Actinaria	unidentified	unidentified	sp. 4	pho
SS0505-GA282	020	DR005B	020DR005B-012	11314804	11	314	804	Cnidaria	Scleractinia	Caryophylliidae	unidentified	sp. 4	pho
SS0505-GA282	020	DR005B	020DR005B-013	11290801	11	290	801	Cnidaria	Scleractinia	unidentified	unidentified	sp. 1	pho
SS0505-GA282	020	DR005B	020DR005B-014	11001803	11	1	803	Cnidaria	Hydrozoa	unidentified	unidentified	sp. 3	pho
SS0505-GA282	020	DR005B	020DR005B-015	20487801	20	487	801	Bryozoa	Cheilostomata	Phidoloporidae	Triphyllozoon	sp. 1	
SS0505-GA282	020	DR005B	020DR005B-016	11001802	11	1	802	Cnidaria	Hydrozoa	unidentified	unidentified	sp. 2	pho
SS0505-GA282	020	DR005B	020DR005B-017	11160802	11	160	802	Cnidaria	Antipatharia	unidentified	unidentified	sp. 2	pho
SS0505-GA282	020	DR005B	020DR005B-018	22000000	22	0	0	Annelida	Polychaeta	unidentified	unidentified	unidentified	
SS0505-GA282	020	DR005B	020DR005B-019	25171801	25	171	801	Echinodermata	Ophiuroidea	Gorgonocephalidae	unidentified	sp. 1	pho
SS0505-GA282	020	DR005B	020DR005B-020	11196804	11	196	804	Cnidaria	Alcyonacea	Plexauridae	unidentified	sp. 4	pho
SS0505-GA282	020	DR005B	020DR005B-021	11173826	11	173	826	Cnidaria	Alcyonacea	unidentified	unidentified	sp. 26	pho
SS0505-GA282	020	DR005B	020DR005B-022	11173000	11	173	0	Cnidaria	Alcyonacea	unidentified	unidentified	unidentified	
SS0505-GA282	020	DR005B	020DR005B-023	25160000	25	160	0	Echinodermata	Ophiuroidea	unidentified	unidentified	unidentified	
SS0505-GA282	020	DR005B	020DR005B-024	27500801	27	500	801	Crustacea	Cirripedia	unidentified	unidentified	sp. 1	
SS0505-GA282	020	DR005B	020DR005B-025	99901008	99	901	8					seived sample bulk	
SS0505-GA282	020	DR005B	020DR005B-026	25200801	25	200	801	Echinodermata	Echinoidea	unidentified	unidentified	sp. 1	pho
SS0505-GA282	021	GR037B	021GR037B-001	99901005	99	901	5					fine sample bulk	
SS0505-GA282	021	GR037B	021GR037B-002	25160000	25	160	0	Echinodermata	Ophiuroidea	unidentified	unidentified	unidentified	
SS0505-GA282	022	GR038B	022GR038B-001	99901005	99	901	5					fine sample bulk	
SS0505-GA282	022	GR038B	022GR038B-002	28765804	28	765	804	Crustacea	Caridea	Alpheidae	unidentified	sp. 4	pho
SS0505-GA282	022	GR038B	022GR038B-003	11169801	11	169	801	Cnidaria	Octocorallia	unidentified	unidentified	sp. 1	pho
SS0505-GA282	022	GR039B	022GR039B-001	99901005	99	901	5					fine sample bulk	
SS0505-GA282	023	GR040B	023GR040B-001	11197801	11	197	801	Cnidaria	Alcyonacea	Primnoidae	unidentified	sp. 1	pho
SS0505-GA282	023	GR041B	023GR041B-001	99901005	99	901	5					fine sample bulk	
SS0505-GA282	023	GR042B	023GR042B-001	99901005	99	901	5					fine sample bulk	
SS0505-GA282	023	GR042B	023GR042B-002	28205802	28	205	802	Crustacea	Isopoda	Anthuridae	unidentified	sp. 2	pho
SS0505-GA282	023	GR042B	023GR042B-003	28765805	28	765	805	Crustacea	Caridea	Alpheidae	unidentified	sp. 5	pho

SS0505-GA282	023	GR042B	023GR042B-004	28803805	28	803	805	Crustacea	Thalassinidea	Callianassidae	unidentified	sp. 5	pho
SS0505-GA282	023	DR006B	023DR006B-001	25001801	25	1	801	Echinodermata	Crinoidea	unidentified	unidentified	sp. 1	
SS0505-GA282	023	DR006B	023DR006B-002	25160000	25	160	0	Echinodermata	Ophiuroidea	unidentified	unidentified	unidentified	
SS0505-GA282	023	DR006B	023DR006B-003	11173000	11	173	0	Cnidaria	Alcyonacea	unidentified	unidentified	unidentified	
SS0505-GA282	023	DR006B	023DR006B-004	11320801	11	320	801	Cnidaria	Scleractinia	Dendrophylliidae	unidentified	sp. 1	pho
SS0505-GA282	024	GR043B	024GR043B-001	99901005	99	901	5					fine sample bulk	
SS0505-GA282	024	GR044B	024GR044B-001	99901005	99	901	5					fine sample bulk	
SS0505-GA282	024	GR044B	024GR044B-002	23207802	23	207	802	Mollusca	Bivalvia	Nuculanidae	unidentified	sp. 2	pho
SS0505-GA282	025	GR045B	025GR045B-001	99901005	99	901	5					fine sample bulk	
SS0505-GA282	025	DR007B	025DR007B-001	99901005	99	901	5					fine sample bulk	
SS0505-GA282	025	DR007B	025DR007B-002	19150803	19	150	803	Brachiopoda	Articulata	unidentified	unidentified	sp. 3	pho
SS0505-GA282	026	GR046B	026GR046B-001	99901005	99	901	5					fine sample bulk	
SS0505-GA282	027	GR047B	027GR047B-001	99901005	99	901	5					fine sample bulk	
SS0505-GA282	027	GR048B	027GR048B-001	99901005	99	901	5					fine sample bulk	
SS0505-GA282	027	GR048B	027GR048B-002	25180801	25	180	801	Echinodermata	Ophiuroidea	Ophiodermatidae	unidentified	sp. 1	pho
SS0505-GA282	028	GR049B	028GR049B-001	99901005	99	901	5					fine sample bulk	
SS0505-GA282	028	GR049B	028GR049B-002	25160806	25	160	806	Echinodermata	Ophiuroidea	unidentified	unidentified	sp. 6	pho
SS0505-GA282	028	GR050B	028GR050B-001	99901005	99	901	5					fine sample bulk	
SS0505-GA282	029	GR051B	029GR051B-001	99901005	99	901	5					fine sample bulk	
SS0505-GA282	029	GR052B	029GR052B-001	99901005	99	901	5					fine sample bulk	
SS0505-GA282	029	GR052B	029GR052B-002	20330801	20	330	801	Bryozoa	Cheilostomata	Beaniidae	Beania	sp. 1	pho
SS0505-GA282	030	GR053B	030GR053B-001	99901005	99	901	5					fine sample bulk	
SS0505-GA282	030	GR054B	030GR054B-001	99901005	99	901	5					fine sample bulk	
SS0505-GA282	030	GR054B	030GR054B-002	23207803	23	207	803	Mollusca	Bivalvia	Nuculanidae	unidentified	sp. 3	pho
SS0505-GA282	031	BS005B	031BS005B-001	99901005	99	901	5					fine sample bulk	
SS0505-GA282	031	BS005B	031BS005B-002	11191802	11	191	802	Cnidaria	Alcyonacea	Nephtheidae	unidentified	sp. 2	pho
SS0505-GA282	032	BS006B	032BS006B-001	99901005	99	901	5					fine sample bulk	
SS0505-GA282	032	BS006B	032BS006B-002	28803806	28	803	806	Crustacea	Thalassinidea	Callianassidae	unidentified	sp. 6	pho
SS0505-GA282	032	BS006B	032BS006B-003	28803807	28	803	807	Crustacea	Thalassinidea	Callianassidae	unidentified	sp. 7	pho
SS0505-GA282	032	BS006B	032BS006B-004	28922801	28	922	801	Crustacea	Brachyura	Goneplacidae	unidentified	sp. 1	pho
SS0505-GA282	032	BS006B	032BS006B-005	28206801	28	206	801	Crustacea	Isopoda	Paranthuridae	unidentified	sp. 1	pho
SS0505-GA282	032	BS006B	032BS006B-006	99901007	99	901	7					coarse sample bulk	
SS0505-GA282	032	BS006B	032BS006B-007	99901003	99	901	3					debris-shells	
SS0505-GA282	032	BS006B	032BS006B-008	14000802	14	0	802	Nemertea		unidentified	unidentified	sp. 2	pho
SS0505-GA282	034	BS007B	034BS007B-001	99901005	99	901	5					fine sample bulk	
SS0505-GA282	034	BS007B	034BS007B-002	22000805	22	0	805	Annelida	Polychaeta	unidentified	unidentified	sp. 5	pho
SS0505-GA282	034	BS007B	034BS007B-003	99901007	99	901	7					coarse sample bulk	
SS0505-GA282	036	BS008B	036BS008B-001	99901005	99	901	5					fine sample bulk	
SS0505-GA282	037	GR056B	037GR056B-001	99901005	99	901	5					fine sample bulk	
SS0505-GA282	037	GR056B	037GR056B-002	24207801	24	207	801	Mollusca	Gastropoda	Volutidae	Volutoconus	sp. 1	pho
SS0505-GA282	037	GR056B	037GR056B-003	11077801	11	77	801	Cnidaria	Hydrozoa	Stylasteridae	unidentified	sp. 1	pho
SS0505-GA282	037	GR057B	037GR057B-001	99901005	99	901	5					fine sample bulk	
SS0505-GA282	037	GR057B	037GR057B-002	99901003	99	901	3					debris-shells	
SS0505-GA282	038	GR058B	038GR058B-001	99901007	99	901	7					coarse sample bulk	
SS0505-GA282	038	GR058B	038GR058B-002	11001804	11	1	804	Cnidaria	Hydrozoa	unidentified	unidentified	sp. 4	pho
SS0505-GA282	038	GR058B	038GR058B-003	10180803	10	180	803	Porifera	Demospongiae	unidentified	unidentified	sp. 3	pho
SS0505-GA282	038	GR059B	038GR059B-001	99901005	99	901	5					fine sample bulk	
SS0505-GA282	038	GR059B	038GR059B-002	10180805	10	180	805	Porifera	Demospongiae	unidentified	unidentified	sp. 5	pho
SS0505-GA282	038	GR059B	038GR059B-003	10180804	10	180	804	Porifera	Demospongiae	unidentified	unidentified	sp. 4	pho
SS0505-GA282	038	GR059B	038GR059B-004	11173825	11	173	825	Cnidaria	Alcyonacea	unidentified	unidentified	sp. 25	pho
SS0505-GA282	038	GR059B	038GR059B-005	11173827	11	173	827	Cnidaria	Alcyonacea	unidentified	unidentified	sp. 27	pho
SS0505-GA282	038	GR059B	038GR059B-006	11173828	11	173	828	Cnidaria	Alcyonacea	unidentified	unidentified	sp. 28	pho
SS0505-GA282	038	GR059B	038GR059B-007	25001803	25	1	803	Echinodermata	Crinoidea	unidentified	unidentified	sp. 3	pho
SS0505-GA282	038	GR060B	038GR060B-001	99901005	99	901	5					fine sample bulk	
SS0505-GA282	038	GR060B	038GR060B-002	11208801	11	208	801	Cnidaria	Pennatulacea	unidentified	unidentified	sp. 1	pho
SS0505-GA282	038	GR060B	038GR060B-003	25001803	25	1	803	Echinodermata	Crinoidea	unidentified	unidentified	sp. 3	
SS0505-GA282	038	GR060B	038GR060B-004	11173827	11	173	827	Cnidaria	Alcyonacea	unidentified	unidentified	sp. 27	
SS0505-GA282	038	DR009B	038DR009B-001	22000000	22	0	0	Annelida	Polychaeta	unidentified	unidentified	unidentified	
SS0505-GA282	038	DR009B	038DR009B-002	11173000	11	173	0	Cnidaria	Alcyonacea	unidentified	unidentified	unidentified	
SS0505-GA282	038	DR009B	038DR009B-003	11160000	11	160	0	Cnidaria	Antipatharia	unidentified	unidentified	unidentified	
SS0505-GA282	038	DR009B	038DR009B-004	11001804	11	1	804	Cnidaria	Hydrozoa	unidentified	unidentified	sp. 4	
SS0505-GA282	038	DR010B	038DR010B-001	25202801	25	202	801	Echinodermata	Echinoidea	Cidaridae	unidentified	sp. 1	pho
SS0505-GA282	038	DR010B	038DR010B-002	25000000	25	0	0	Echinodermata	Crinoidea	unidentified	unidentified	unidentified	whit
SS0505-GA282	038	DR010B	038DR010B-003	25000000	25	0	0	Echinodermata	Crinoidea	unidentified	unidentified	unidentified	brov
SS0505-GA282	038	DR010B	038DR010B-004	25171804	25	171	804	Echinodermata	Ophiuroidea	Gorgonocephalidae	unidentified	sp. 4	pho

SS0505-GA282	038	DR010B	038DR010B-005	11173829	11	173	829	Cnidaria	Alcyonacea	unidentified	unidentified	sp. 29	pho
SS0505-GA282	038	DR010B	038DR010B-006	10180806	10	180	806	Porifera	Demospongiae	unidentified	unidentified	sp. 6	pho
SS0505-GA282	038	DR010B	038DR010B-007	28840805	28	840	805	Crustacea	Anomura	Galatheidae	unidentified	sp. 5	pho
SS0505-GA282	038	DR010B	038DR010B-008	10180808	10	180	808	Porifera	Demospongiae	unidentified	unidentified	sp. 8	pho
SS0505-GA282	038	DR010B	038DR010B-009	10180807	10	180	807	Porifera	Demospongiae	unidentified	unidentified	sp. 7	pho
SS0505-GA282	038	DR010B	038DR010B-010	11191803	11	191	803	Cnidaria	Alcyonacea	Nephtheidae	unidentified	sp. 3	pho
SS0505-GA282	038	DR010B	038DR010B-011	25001801	25	1	801	Echinodermata	Crinoidea	unidentified	unidentified	sp. 1	
SS0505-GA282	038	DR010B	038DR010B-012	11077803	11	77	803	Cnidaria	Hydrozoa	Stylasteridae	unidentified	sp. 3	pho
SS0505-GA282	038	DR010B	038DR010B-013	11001804	11	1	804	Cnidaria	Hydrozoa	unidentified	unidentified	sp. 4	
SS0505-GA282	038	DR010B	038DR010B-014	10180802	10	180	802	Porifera	Demospongiae	unidentified	unidentified	sp. 2	
SS0505-GA282	038	DR010B	038DR010B-015	20322801	20	322	801	Bryozoa	Cheilostomata	Flustridae	unidentified	sp. 1	pho
SS0505-GA282	038	DR010B	038DR010B-016	11173830	11	173	830	Cnidaria	Alcyonacea	unidentified	unidentified	sp. 30	pho
SS0505-GA282	038	DR010B	038DR010B-017	25176802	25	176	802	Echinodermata	Ophiuroidea	Ophiuridae	unidentified	sp. 2	pho
SS0505-GA282	038	DR010B	038DR010B-018	11192801	11	192	801	Cnidaria	Alcyonacea	Nidaliidae	unidentified	sp. 1	
SS0505-GA282	038	DR010B	038DR010B-019	25202802	25	202	802	Echinodermata	Echinoidea	Cidaridae	unidentified	sp. 2	pho
SS0505-GA282	038	DR010B	038DR010B-020	23272801	23	272	801	Mollusca	Bivalvia	Spondylidae	Spondylus	sp. 1	pho
SS0505-GA282	038	DR010B	038DR010B-021	10180809	10	180	809	Porifera	Demospongiae	unidentified	unidentified	sp. 9	pho
SS0505-GA282	038	DR010B	038DR010B-022	28765806	28	765	806	Crustacea	Caridea	Alpheidae	unidentified	sp. 6	pho
SS0505-GA282	038	DR010B	038DR010B-023	22000000	22	0	0	Annelida	Polychaeta	unidentified	unidentified	unidentified	
SS0505-GA282	038	DR010B	038DR010B-024	11173811	11	173	811	Cnidaria	Alcyonacea	unidentified	unidentified	sp. 11	pho
SS0505-GA282	038	DR010B	038DR010B-025	11160805	11	160	805	Cnidaria	Antipatharia	unidentified	unidentified	sp. 5	pho
SS0505-GA282	038	DR010B	038DR010B-026	11160804	11	160	804	Cnidaria	Antipatharia	unidentified	unidentified	sp. 4	pho
SS0505-GA282	038	DR010B	038DR010B-027	11160803	11	160	803	Cnidaria	Antipatharia	unidentified	unidentified	sp. 3	pho
SS0505-GA282	038	DR010B	038DR010B-028	99901005	99	901	5					fine sample bulk	
SS0505-GA282	038	DR010B	038DR010B-029	27500802	27	500	802	Crustacea	Cirripedia	unidentified	unidentified	sp. 2	pho
SS0505-GA282	038	DR010B	038DR010B-030	10180810	10	180	810	Porifera	Demospongiae	unidentified	unidentified	sp. 10	pho
SS0505-GA282	038	DR010B	038DR010B-031	11320802	11	320	802	Cnidaria	Scleractinia	Dendrophylliidae	Balanophyllia	sp. 1	pho
SS0505-GA282	038	DR010B	038DR010B-032	11173000	11	173	0	Cnidaria	Alcyonacea	unidentified	unidentified	unidentified	
SS0505-GA282	038	DR010B	038DR010B-033	99901002	99	901	2					debris-rocks	
SS0505-GA282	038	DR010B	038DR010B-034	10180811	10	180	811	Porifera	Demospongiae	unidentified	unidentified	sp. 11	pho
SS0505-GA282	038	DR010B	038DR010B-035	35033801	35	33	801	Chordata	Urochordata	Styelidae	unidentified	sp. 1	pho
SS0505-GA282	038	DR010B	038DR010B-036	99901008	99	901	8					seived sample bulk	
SS0505-GA282	039	GR061B	039GR061B-001	99901005	99	901	5					fine sample bulk	
SS0505-GA282	039	GR061B	039GR061B-002	28840803	28	840	803	Crustacea	Anomura	Galatheidae	unidentified	sp. 3	pho
SS0505-GA282	039	GR061B	039GR061B-003	25178801	25	178	801	Echinodermata	Ophiuroidea	Ophiocomidae	unidentified	sp. 1	pho
SS0505-GA282	039	GR061B	039GR061B-004	10180812	10	180	812	Porifera	Demospongiae	unidentified	unidentified	sp. 12	pho
SS0505-GA282	039	GR061B	039GR061B-005	11173000	11	173	0	Cnidaria	Alcyonacea	unidentified	unidentified	unidentified	
SS0505-GA282	039	GR062B	039GR062B-001	99901005	99	901	5					fine sample bulk	
SS0505-GA282	039	GR062B	039GR062B-002	28840803	28	840	803	Crustacea	Anomura	Galatheidae	unidentified	sp. 3	pho
SS0505-GA282	039	GR062B	039GR062B-003	28730801	28	730	801	Crustacea	Caridea	unidentified	unidentified	sp. 1	pho
SS0505-GA282	039	GR062B	039GR062B-004	22024801	22	24	801	Annelida	Polychaeta	Eunicidae	Eunice	sp. 1	pho
SS0505-GA282	039	GR062B	039GR062B-005	10180813	10	180	813	Porifera	Demospongiae	unidentified	unidentified	sp. 13	pho
SS0505-GA282	039	GR062B	039GR062B-006	10180000	10	180	0	Porifera	Demospongiae	unidentified	unidentified	unidentified	
SS0505-GA282	039	GR062B	039GR062B-007	11173000	11	173	0	Cnidaria	Alcyonacea	unidentified	unidentified	unidentified	
SS0505-GA282	040	GR063B	040GR063B-001	99901005	99	901	5					fine sample bulk	
SS0505-GA282	040	GR064B	040GR064B-001	99901005	99	901	5					fine sample bulk	
SS0505-GA282	041	GR065B	041GR065B-001	99901005	99	901	5					fine sample bulk	
SS0505-GA282	041	GR066B	041GR066B-001	99901005	99	901	5					fine sample bulk	
SS0505-GA282	042	DR011B	042DR011B-001	11192802	11	192	802	Cnidaria	Alcyonacea	Nidaliidae	unidentified	sp. 2	pho
SS0505-GA282	042	DR011B	042DR011B-002	25404801	25	404	801	Echinodermata	Holothuroidea	Psolidae	unidentified	sp. 1	pho
SS0505-GA282	043	GR068B	043GR068B-001	99901005	99	901	5					fine sample bulk	
SS0505-GA282	043	GR069B	043GR069B-001	99901005	99	901	5					fine sample bulk	
SS0505-GA282	043	GR069B	043GR069B-002	11229805	11	229	805	Cnidaria	Actinaria	unidentified	unidentified	sp. 5	pho
SS0505-GA282	043	GR069B	043GR069B-003	25021801	25	21	801	Echinodermata	Crinoidea	Pentacrinitidae?	unidentified	sp. 1	pho
SS0505-GA282	043	GR069B	043GR069B-004	25160807	25	160	807	Echinodermata	Ophiuroidea	unidentified	unidentified	sp. 7	pho
SS0505-GA282	043	GR069B	043GR069B-005	19150804	19	150	804	Brachiopoda	Articulata	unidentified	unidentified	sp. 4	pho
SS0505-GA282	043	GR069B	043GR069B-006	28840806	28	840	806	Crustacea	Anomura	Galatheidae	unidentified	sp. 6	pho
SS0505-GA282	043	GR069B	043GR069B-007	99901007	99	901	7					coarse sample bulk	
SS0505-GA282	043	GR069B	043GR069B-008	99901009	99	901	9					debris - dead corals	
SS0505-GA282	043	DR012B	043DR012B-001	11280801	11	280	801	Cnidaria	Corallimorpharia	unidentified	unidentified	sp. 1	pho
SS0505-GA282	043	DR012B	043DR012B-002	10180814	10	180	814	Porifera	Demospongiae	unidentified	unidentified	sp. 14	pho
SS0505-GA282	043	DR012B	043DR012B-003	25160808	25	160	808	Echinodermata	Ophiuroidea	unidentified	unidentified	sp. 8	pho
SS0505-GA282	043	DR012B	043DR012B-004	20332801	20	332	801	Bryozoa	Cheilostomata	Candidae	Scrupocellaria	curvata	pho
SS0505-GA282	043	DR012B	043DR012B-005	25160000	25	160	0	Echinodermata	Ophiuroidea	unidentified	unidentified	unidentified	
SS0505-GA282	043	DR012B	043DR012B-006	27524801	27	524	801	Crustacea	Cirripedia	Scalpellidae	Arcoscalpellum	sp. 1	pho

SS0505-GA282	043	DR012B	043DR012B-007	27524802	27	524	802	Crustacea	Cirripedia	Scalpellidae	unidentified	sp. 1	pho
SS0505-GA282	043	DR012B	043DR012B-008	22000000	22	0	0	Annelida	Polychaeta	unidentified	unidentified	unidentified	
SS0505-GA282	043	DR012B	043DR012B-009	20300802	20	300	802	Bryozoa	Cheilostomata	unidentified	unidentified	sp. 1	pho
SS0505-GA282	043	DR012B	043DR012B-010	99901009	99	901	9					debris - dead corals	
SS0505-GA282	043	DR012B	043DR012B-011	10180000	10	180	0	Porifera	Demospongiae	unidentified	unidentified	unidentified	
SS0505-GA282	043	DR012B	043DR012B-012	25404801	25	404	801	Echinodermata	Holothuroidea	Psolidae	unidentified	sp. 1	
SS0505-GA282	044	GR070B	044GR070B-001	99901005	99	901	5					fine sample bulk	
SS0505-GA282	044	DR013B	044DR013B-001	11160803	11	160	803	Cnidaria	Antipatharia	unidentified	unidentified	sp. 3	pho
SS0505-GA282	044	DR013B	044DR013B-002	27500803	27	500	803	Crustacea	Cirripedia	unidentified	unidentified	sp. 3	pho
SS0505-GA282	044	DR013B	044DR013B-003	11001804	11	1	804	Cnidaria	Hydrozoa	unidentified	unidentified	sp. 4	
SS0505-GA282	044	DR013B	044DR013B-004	11190802	11	190	802	Cnidaria	Alcyonacea	Melithaeidae	unidentified	sp. 2	pho
SS0505-GA282	044	DR013B	044DR013B-005	10300802	10	300	802	Porifera	Hexactinellida	unidentified	unidentified	sp. 2	pho
SS0505-GA282	044	DR013B	044DR013B-006	10300801	10	300	801	Porifera	Hexactinellida	unidentified	unidentified	sp. 1	pho
SS0505-GA282	044	DR013B	044DR013B-007	24207000	24	207	0	Mollusca	Gastropoda	Volutidae	unidentified	unidentified	
SS0505-GA282	045	GR072B	045GR072B-001	25143801	25	143	801	Echinodermata	Asteroidea	Echinasteridae	unidentified	sp. 1	pho
SS0505-GA282	045	DR014B	045DR014B-001	11160801	11	160	801	Cnidaria	Antipatharia	unidentified	unidentified	sp. 1	
SS0505-GA282	045	DR014B	045DR014B-002	23401000	23	401	0	Mollusca	Bivalvia	Pholadidae	unidentified	unidentified	
SS0505-GA282	045	DR014B	045DR014B-003	17020801	17	20	801	Echiura		unidentified	unidentified	sp. 1	pho
SS0505-GA282	045	DR014B	045DR014B-004	20300803	20	300	803	Bryozoa	Cheilostomata	unidentified	unidentified	sp. 2	pho
SS0505-GA282	045	DR014B	045DR014B-005	20300804	20	300	804	Bryozoa	Cheilostomata	unidentified	unidentified	sp. 3	pho
SS0505-GA282	047	BS009B	047BS009B-001	99901005	99	901	5					fine sample bulk	
SS0505-GA282	047	BS009B	047BS009B-002	99901007	99	901	7					coarse sample bulk	
SS0505-GA282	047	BS009B	047BS009B-003	99901003	99	901	3					debris-shells	
SS0505-GA282	048	GR073B	048GR073B-001	99901005	99	901	5					fine sample bulk	
SS0505-GA282	048	GR073B	048GR073B-002	22000806	22	0	806	Annelida	Polychaeta	unidentified	unidentified	sp. 6	pho
SS0505-GA282	048	GR073B	048GR073B-003	25200801	25	200	801	Echinodermata	Echinoidea	unidentified	unidentified	sp. 1	
SS0505-GA282	048	GR074B	048GR074B-001	99901005	99	901	5					fine sample bulk	
SS0505-GA282	048	GR074B	048GR074B-002	25200801	25	200	801	Echinodermata	Echinoidea	unidentified	unidentified	sp. 1	pho
SS0505-GA282	049	GR075B	049GR075B-001	99901005	99	901	5					fine sample bulk	
SS0505-GA282	049	GR075B	049GR075B-002	25160809	25	160	809	Echinodermata	Ophiuroidea	unidentified	unidentified	sp. 9	pho
SS0505-GA282	049	GR075B	049GR075B-003	22000000	22	0	0	Annelida	Polychaeta	unidentified	unidentified	unidentified	
SS0505-GA282	049	GR076B	049GR076B-001	99901005	99	901	5					fine sample bulk	
SS0505-GA282	049	GR076B	049GR076B-002	11173000	11	173	0	Cnidaria	Alcyonacea	unidentified	unidentified	unidentified	
SS0505-GA282	049	GR077B	049GR077B-001	25160810	25	160	810	Echinodermata	Ophiuroidea	unidentified	unidentified	sp. 10	pho
SS0505-GA282	049	GR078B	049GR078B-001	99901005	99	901	5					fine sample bulk	
SS0505-GA282	049	GR078B	049GR078B-002	22116802	22	116	802	Annelida	Polychaeta	Flabelligeridae	unidentified	sp. 2	pho
SS0505-GA282	051	BS010B	051BS010B-001	99901005	99	901	5					fine sample bulk	
SS0505-GA282	050	BS011B	050BS011B-001	99901005	99	901	5					fine sample bulk	
SS0505-GA282	050	BS011B	050BS011B-002	99901007	99	901	7					coarse sample bulk	
SS0505-GA282	053	DR015B	053DR015B-001	28911803	28	911	803	Crustacea	Brachyura	Portunidae	Charybdis	sp. 1	pho
SS0505-GA282	053	DR015B	053DR015B-002	10180809	10	180	809	Porifera	Demospongiae	unidentified	unidentified	sp. 9	pho
SS0505-GA282	053	DR015B	053DR015B-003	10180811	10	180	811	Porifera	Demospongiae	unidentified	unidentified	sp. 11	
SS0505-GA282	053	DR015B	053DR015B-004	10300803	10	300	803	Porifera	Hexactinellida	unidentified	unidentified	sp. 3	pho
SS0505-GA282	053	DR015B	053DR015B-005	10180818	10	180	818	Porifera	Demospongiae	unidentified	unidentified	sp. 18	pho
SS0505-GA282	053	DR015B	053DR015B-006	10180815	10	180	815	Porifera	Demospongiae	unidentified	unidentified	sp. 15	pho
SS0505-GA282	053	DR015B	053DR015B-007	25001000	25	1	0	Echinodermata	Crinoidea	unidentified	unidentified	unidentified	
SS0505-GA282	053	DR015B	053DR015B-008	10180808	10	180	808	Porifera	Demospongiae	unidentified	unidentified	sp. 8	
SS0505-GA282	053	DR015B	053DR015B-009	11001804	11	1	804	Cnidaria	Hydrozoa	unidentified	unidentified	sp. 4	
SS0505-GA282	053	DR015B	053DR015B-010	11160804	11	160	804	Cnidaria	Antipatharia	unidentified	unidentified	sp. 4	
SS0505-GA282	053	DR015B	053DR015B-011	11160805	11	160	805	Cnidaria	Antipatharia	unidentified	unidentified	sp. 5	
SS0505-GA282	053	DR015B	053DR015B-012	10180816	10	180	816	Porifera	Demospongiae	unidentified	unidentified	sp. 16	pho
SS0505-GA282	053	DR015B	053DR015B-013	28926801	28	926	801	Crustacea	Brachyura	Pilumnidae	unidentified	sp. 1	
SS0505-GA282	053	DR015B	053DR015B-014	11314804	11	314	804	Cnidaria	Scleractinia	Caryophylliidae	unidentified	sp. 4	
SS0505-GA282	053	DR015B	053DR015B-015	22000000	22	0	0	Annelida	Polychaeta	unidentified	unidentified	unidentified	
SS0505-GA282	053	DR015B	053DR015B-016	28840807	28	840	807	Crustacea	Anomura	Galatheidae	unidentified	sp. 7	pho
SS0505-GA282	053	DR015B	053DR015B-017	23226801	23	226	801	Mollusca	Bivalvia	Arcidae	unidentified	sp. 1	pho
SS0505-GA282	053	DR015B	053DR015B-018	23301801	23	301	801	Mollusca	Bivalvia	Chamidae	Chama	sp. 1	pho
SS0505-GA282	053	DR015B	053DR015B-019	10180000	10	180	0	Porifera	Demospongiae	unidentified	unidentified	unidentified	
SS0505-GA282	053	DR015B	053DR015B-020	10180817	10	180	817	Porifera	Demospongiae	unidentified	unidentified	sp. 17	pho
SS0505-GA282	053	DR015B	053DR015B-021	11173000	11	173	0	Cnidaria	Alcyonacea	unidentified	unidentified	unidentified	
SS0505-GA282	053	GR080B	053GR080B-001	99901005	99	901	5					fine sample bulk	
SS0505-GA282	053	GR080B	053GR080B-002	25160000	25	160	0	Echinodermata	Ophiuroidea	unidentified	unidentified	unidentified	
SS0505-GA282	055	GR081B	055GR081B-001	99901005	99	901	5					fine sample bulk	
SS0505-GA282	056	BS012B	056BS012B-001	99901005	99	901	5					fine sample bulk	
SS0505-GA282	056	BS012B	056BS012B-002	20330801	20	330	801	Bryozoa	Cheilostomata	Beaniidae	Beania	sp. 1	

SS0505-GA282	057	BS013B	057BS013B-001	99901005	99	901	5					fine sample bulk	
SS0505-GA282	057	BS013B	057BS013B-002	25160000	25	160	0	Echinodermata	Ophiuroidea	unidentified	unidentified	unidentified	
SS0505-GA282	057	BS013B	057BS013B-003	99901003	99	901	3					debris-shells	
SS0505-GA282	060	BS014B	060BS014B-001	99901005	99	901	5					fine sample bulk	
SS0505-GA282	060	BS014B	060BS014B-002	11001805	11	1	805	Cnidaria	Hydrozoa	unidentified	unidentified	sp. 5	pho
SS0505-GA282	061	GR082B	061GR082B-001	99901005	99	901	5					fine sample bulk	
SS0505-GA282	061	GR082B	061GR082B-002	37000801	37	0	801	Chordata	Pisces	unidentified	unidentified	sp. 1	pho
SS0505-GA282	063	BS015B	063BS015B-001	99901005	99	901	5					fine sample bulk	
SS0505-GA282	063	BS015B	063BS015B-002	37065801	37	65	801	Chordata	Pisces	Nettastomatidae	unidentified	sp. 1	
SS0505-GA282	064	GR083B	064GR083B-001	17000801	17	0	801	Sipuncula		unidentified	unidentified	sp. 1	
SS0505-GA282	064	GR083B	064GR083B-002	22000807	22	0	807	Annelida	Polychaeta	unidentified	unidentified	sp. 7	pho
SS0505-GA282	064	GR083B	064GR083B-003	11173000	11	173	0	Cnidaria	Alcyonacea	unidentified	unidentified	unidentified	
SS0505-GA282	064	GR084B	064GR084B-001	28865801	28	865	801	Crustacea	Brachyura	Raninidae	unidentified	sp. 1	
SS0505-GA282	064	GR084B	064GR084B-002	28922802	28	922	802	Crustacea	Brachyura	Goneplacidae	unidentified	sp. 2	pho
SS0505-GA282	064	GR084B	064GR084B-003	28803802	28	803	802	Crustacea	Thalassinidea	Callianassidae	unidentified	sp. 2	pho
SS0505-GA282	064	GR084B	064GR084B-004	11314805	11	314	805	Cnidaria	Scleractinia	Caryophylliidae	unidentified	sp. 5	pho
SS0505-GA282	002	GR085B	002GR085B-001	22000000	22	0	0	Annelida	Polychaeta	unidentified	unidentified	unidentified	
SS0505-GA282	002	GR085B	002GR085B-002	24220802	24	220	802	Mollusca	Gastropoda	Turridae	unidentified	sp. 2	pho
SS0505-GA282	002	GR085B	002GR085B-003	28803801	28	803	801	Crustacea	Thalassinidea	Callianassidae	unidentified	sp. 1	pho
SS0505-GA282	002	GR085B	002GR085B-004	25160811	25	160	811	Echinodermata	Ophiuroidea	unidentified	unidentified	sp. 11	pho
SS0505-GA282	002	GR086B	002GR086B-001	25160801	25	160	801	Echinodermata	Ophiuroidea	unidentified	unidentified	sp. 1	
SS0505-GA282	002	GR086B	002GR086B-002	25191804	25	191	804	Echinodermata	Ophiuroidea	Amphiuridae	unidentified	sp. 4	pho

Appendix 6 (B)

Biological Photography by Karen Gowlett-Holmes

The images presented here in Appendix 6 were all taken by Karen Gowlett-Holmes and are subject to Commonwealth copyright. Macro invertebrates were photographed fresh before preservation to record colours. All specimens were photographed using a Nikon Coolpix 995 camera with an attached macro ring light mounted on a copystand. Specimens were placed on a black cloth background with a millimetre scale for photography. Fish were pinned to extend their fins, and the fins fixed in place using formalin painted on. The fish were then photographed using the same camera on a white background with a millimetre scale and a Kodak colour bar, according to standard CSIRO Marine Research fish photography protocols. The files were named with the specimen CAAB code, site/accession number and taxon identification and then arranged in directories taxonomically.

19150801-013DR001B-033a-Brachiopoda-sp1.tif

19150801-013DR001B-033b-Brachiopoda-sp1.tif

19150801-013DR001B-048a-Brachiopoda-sp1.tif

19150801-013DR001B-048b-Brachiopoda-sp1.tif

19150801-013DR001B-048c-Brachiopoda-sp1.tif

19150801-020DR005B-006-Brachiopoda-sp1.tif

19150802-020DR005B-005a-Brachiopoda-sp2.tif

19150802-020DR005B-005b-Brachiopoda-sp2.tif

19150803-025DR007B-002a-Brachiopoda-sp3.tif

19150803-025DR007B-002b-Brachiopoda-sp3.tif

19150804-043GR069B-005-Brachiopoda-sp4.tif

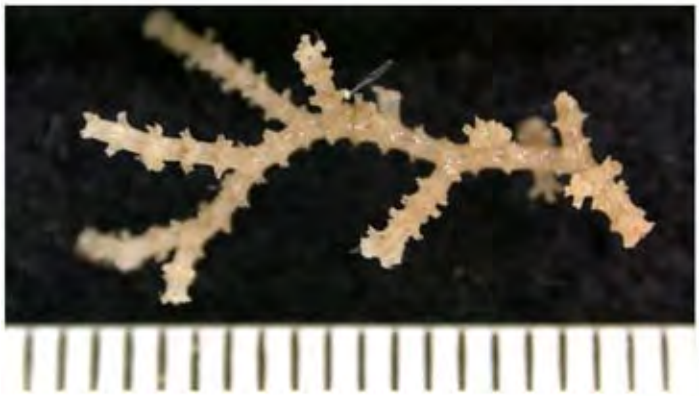

20300801-008GR012B-005-Porina-vertebralis.tif

20300802-043DR012B-009-Bryozoa-sp1.tif

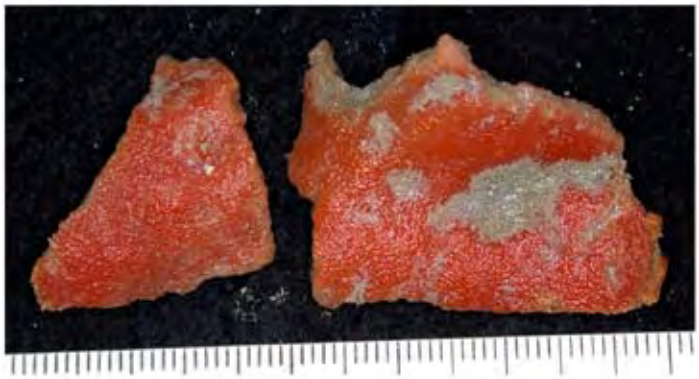

20300803-045DR014B-004-Bryozoa-sp2.tif

20300804-045DR014B-005-Bryozoa-sp3.tif

20322801-038DR010B-015-Flustridae-sp1.tif

20325801-008GR012B-004-Nellia-sp1.tif

20330801-029GR052B-002-Beania-sp1.tif

20332801-013DR001B-064-Scrupocellaria-curvata.tif

20332801-043DR012B-004-Scrupocellaria-curvata.tif

20405801-013DR001B-066-Adeonella-sp1.tif

20405802-013DR001B-065-Adeonella-sp2.tif

20487801-013DR001B-016-Triphyllozoon-sp1.tif

11229801-006GR009B-006a-Actinaria-sp1.tif

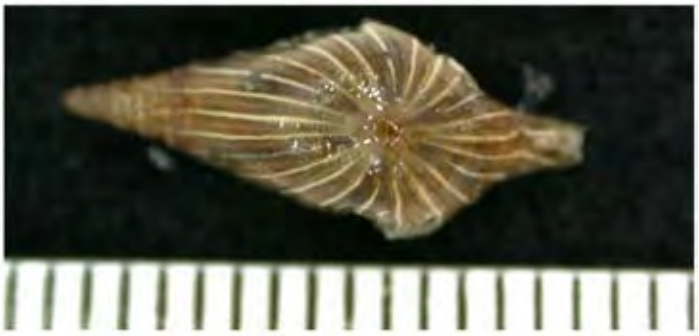

11229801-006GR009B-006b-Actinaria-sp1.tif

11229803-013DR001B-060b-Actinaria-sp3.tif

11229803-013DR001B-060a-Actinaria-sp3.tif

11229802-013DR001B-050-Actinaria-sp2.tif

11229805-043GR069B-002-Actinaria-sp5.tif

11229804-020DR005B-011a-Actinaria-sp4.tif

11229804-020DR005B-011b-Actinaria-sp4.tif

11280801-043DR012B-001a-Corallimorpharia-sp1.tif

11280801-043DR012B-001b-Corallimorpharia-sp1.tif

11284801-019GR033B-008-Zoanthinaria-sp1.tif

11160801-013DR001B-017-Antipatharia-sp1.tif

11160801-020GR035B-002-Antipatharia-sp1.tif

11160802-020DR005B-017-Antipatharia-sp2.tif

11160803-038DR010B-027-Antipatharia-sp3.tif

11160803-044DR013B-001-Antipatharia-sp3.tif

11160804-038DR010B-026-Antipatharia-sp4.tif

11160805-038DR010B-025-Antipatharia-sp5.tif

11001801-005GR006B-003a-Hydroida-sp1.tif

11001801-005GR006B-003b-Hydroida-sp1.tif

11001803-020DR005B-014a-Hydroida-sp3.tif

11001803-020DR005B-014b-Hydroida-sp3.tif

11001804-038GR058B-002a-Hydroida-sp4.tif

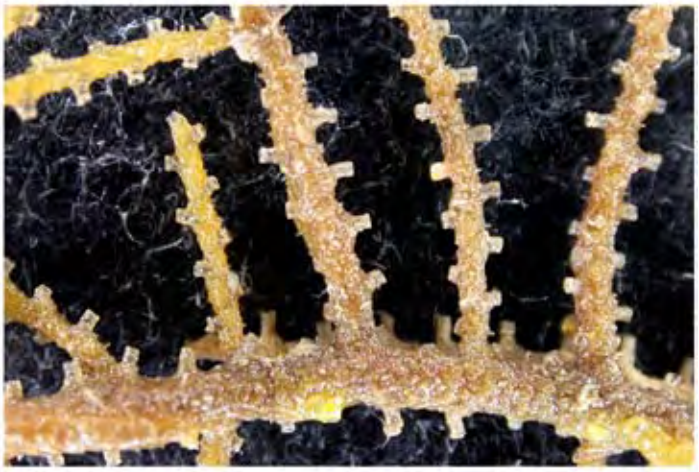

11001804-038GR058B-002b-Hydroida-sp4.tif

11001802-020DR005B-016-Hydroida-sp2.tif

11001805-060BS014B-002-Hydroida-sp5.tif

11077801-002GR002B-003-Stylasteridae-sp1.tif

11077801-003GR004B-004-Stylasteridae-sp1.tif

11077801-037GR056B-003-Stylasteridae-sp1.tif

11077802-013DR001B-061-Stylasteridae-sp2.tif

11077803-038DR010B-012a-Stylasteridae-sp3.tif

11077803-038DR010B-012b-Stylasteridae-sp3.tif

11169801-022GR038B-003a-Octocorallia-sp1.tif

11169801-022GR038B-003b-Octocorallia-sp1.tif

11173801-008GR012B-001a-Alcyonacea-sp1.tif

11173801-008GR012B-001b-Alcyonacea-sp1.tif

11173819-013DR001B-037-Alcyonacea-sp19.tif

11173828-038GR059B-006-Alcyonacea-sp28.tif

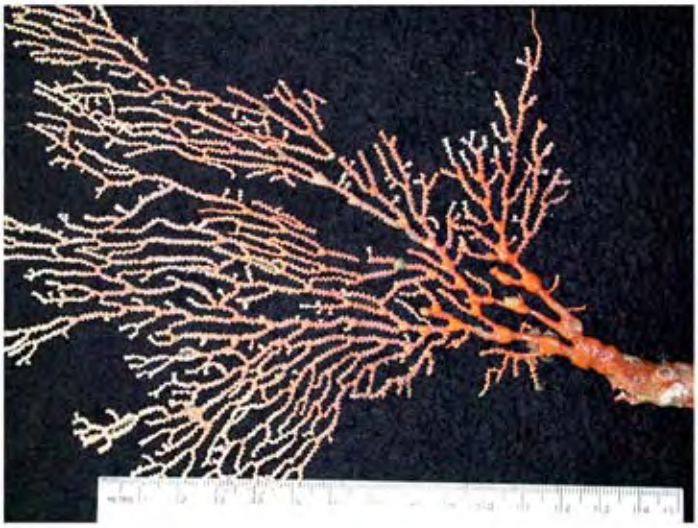

11173802-013DR001B-005a-Alcyonacea-sp2.tif

11173802-013DR001B-005b-Alcyonacea-sp2.tif

11173803-013DR001B-006a-Alcyonacea-sp3.tif

11173803-013DR001B-006b-Alcyonacea-sp3.tif

11173804-013DR001B-014a-Alcyonacea-sp4.tif

11173804-013DR001B-014b-Alcyonacea-sp4.tif

11173805-013DR001B-015a-Alcyonacea-sp5.tif

11173805-013DR001B-015b-Alcyonacea-sp5.tif

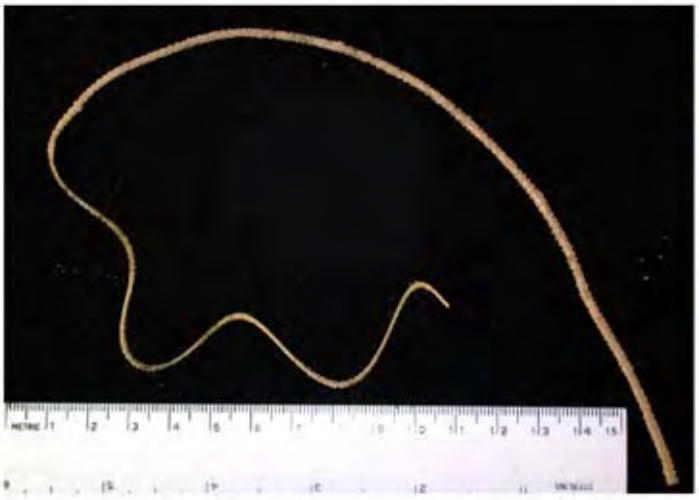

11173806-013DR001B-018a-Alcyonacea-sp6.tif

11173806-013DR001B-018b-Alcyonacea-sp6.tif

11173807-013DR001B-020a-Alcyonacea-sp7.tif

11173807-013DR001B-020b-Alcyonacea-sp7.tif

11173808-013DR001B-022a-Alcyonacea-sp8.tif

11173808-013DR001B-022b-Alcyonacea-sp8.tif

11173809-013DR001B-021a-Alcyonacea-sp9.tif

11173809-013DR001B-021b-Alcyonacea-sp9.tif

11173810-013DR001B-024a-Alcyonacea-sp10.tif

11173810-013DR001B-024b-Alcyonacea-sp10.tif

11173811-013DR001B-023a-Alcyonacea-sp11.tif

11173811-013DR001B-023b-Alcyonacea-sp11.tif

11173811-038DR010B-024a-Alcyonacea-sp11.tif

11173811-038DR010B-024b-Alcyonacea-sp11.tif

11173812-013DR001B-025a-Alcyonacea-sp12.tif

11173812-013DR001B-025b-Alcyonacea-sp12.tif

11173813-013DR001B-027a-Alcyonacea-sp13.tif

11173813-013DR001B-027b-Alcyonacea-sp13.tif

11173814-013DR001B-028a-Alcyonacea-sp14.tif

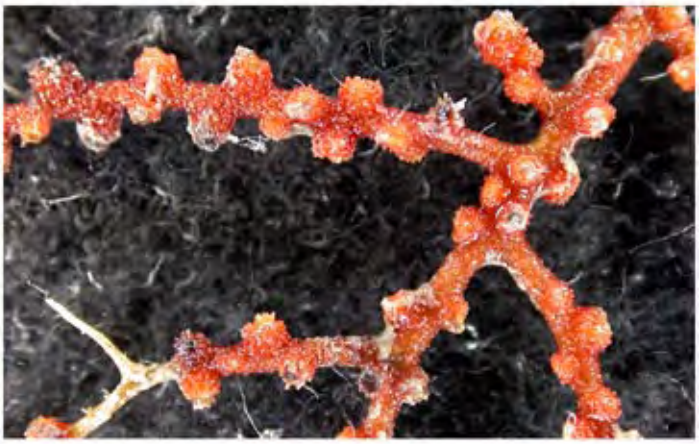

11173814-013DR001B-028b-Alcyonacea-sp14.tif

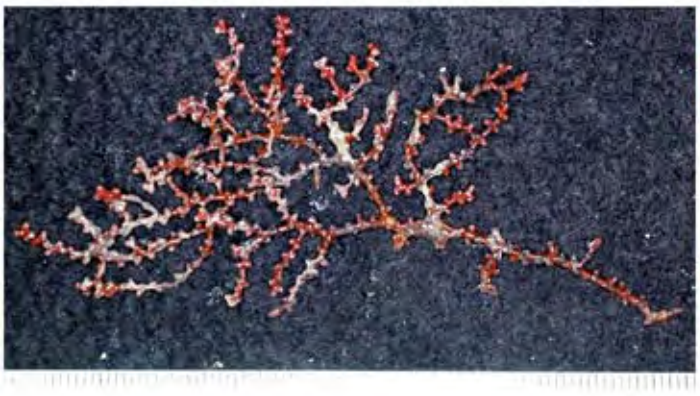

11173815-013DR001B-029a-Alcyonacea-sp15.tif

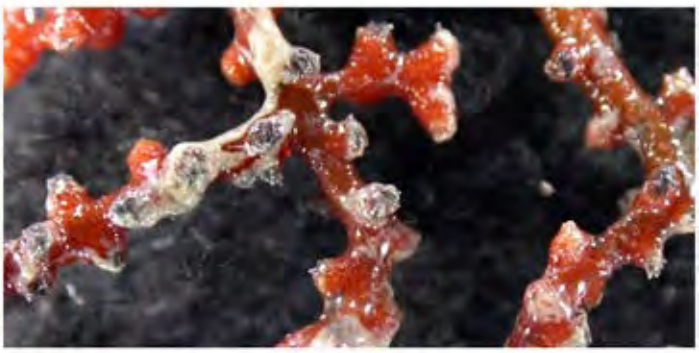

11173815-013DR001B-029b-Alcyonacea-sp15.tif

11173816-013DR001B-043a-Alcyonacea-sp16.tif

11173816-013DR001B-043b-Alcyonacea-sp16.tif

11173817-013DR001B-040a-Alcyonacea-sp17.tif

11173817-013DR001B-040b-Alcyonacea-sp17.tif

11173818-013DR001B-039a-Alcyonacea-sp18.tif

11173818-013DR001B-039b-Alcyonacea-sp18.tif

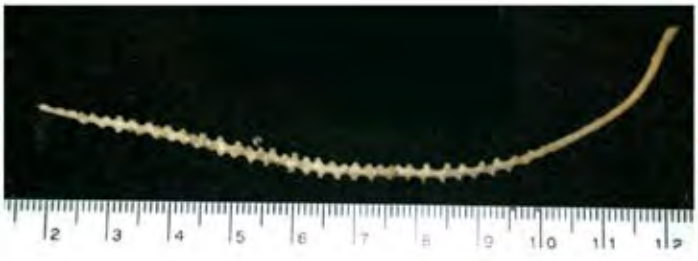

11173820-013DR001B-038a-Alcyonacea-sp20.tif

11173820-013DR001B-038b-Alcyonacea-sp20.tif

11173821-013DR001B-036a-Alcyonacea-sp21.tif

11173821-013DR001B-036b-Alcyonacea-sp21.tif

11173822-013DR001B-035a-Alcyonacea-sp22.tif

11173822-013DR001B-035b-Alcyonacea-sp22.tif

11173823-013DR001B-041a-Alcyonacea-sp23.tif

11173823-013DR001B-041b-Alcyonacea-sp23.tif

11173824-013DR001B-042a-Alcyonacea-sp24.tif

11173824-013DR001B-042b-Alcyonacea-sp24.tif

11173825-020GR035B-003a-Alcyonacea-sp25.tif

11173825-020GR035B-003b-Alcyonacea-sp25.tif

11173825-038GR059B-004a-Alcyonacea-sp25.tif

11173825-038GR059B-004b-Alcyonacea-sp25.tif

11173826-020DR005B-021a-Alcyonacea-sp26.tif

11173826-020DR005B-021b-Alcyonacea-sp26.tif

11173827-038GR059B-005a-Alcyonacea-sp27.tif

11173827-038GR059B-005b-Alcyonacea-sp27.tif

11173829-038DR010B-005a-Alcyonacea-sp29.tif

11173829-038DR010B-005b-Alcyonacea-sp29.tif

11173830-038DR010B-016a-Alcyonacea-sp30.tif

11173830-038DR010B-016b-Alcyonacea-sp30.tif

11190801-013DR001B-034-Melithaeidae-sp1.tif

11190802-044DR013B-004-Melithaeidae-sp2.tif

11191801-013DR001B-010a-Nephtheidae-sp1.tif

11191801-013DR001B-010b-Nephtheidae-sp1.tif

11191802-031BS005B-002a-Nephtheidae-sp2.tif

11191802-031BS005B-002b-Nephtheidae-sp2.tif

11191803-038DR010B-010a-Nephtheidae-sp3.tif

11192801-013DR001B-012a-Nidaliidae-sp1.tif

11192801-013DR001B-012b-Nidaliidae-sp1.tif

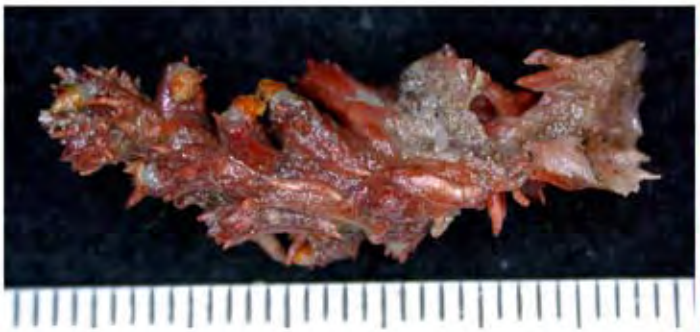

11192802-042DR011B-001a-Nidaliidae-sp2.tif

11192802-042DR011B-001b-Nidaliidae-sp2.tif

11196801-013DR001B-003a-Plexauridae-sp1.tif

11196801-013DR001B-003b-Plexauridae-sp1.tif

11196802-013DR001B-032a-Plexauridae-sp2.tif

11196802-013DR001B-032b-Plexauridae-sp2.tif

11196803-013DR001B-031a-Plexauridae-sp3.tif

11196803-013DR001B-031b-Plexauridae-sp3.tif

11196804-020DR005B-020a-Plexauridae-sp4.tif

11196804-020DR005B-020b-Plexauridae-sp4.tif

11197801-023GR040B-001a-Primnoidae-sp1.tif

11197801-023GR040B-001b-Primnoidae-sp1.tif

11208801-038GR060B-002-Pennatulacea-sp1.tif

11290801-019GR033B-009-Scleractinia-sp1.tif

11290801-020DR005B-013a-Scleractinia-sp1.tif

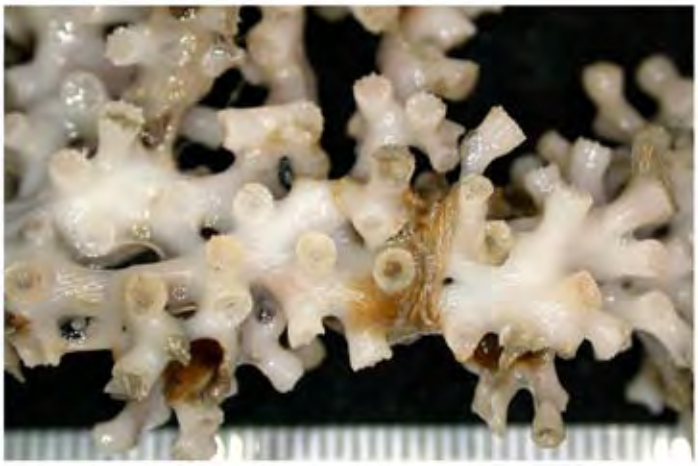

11290801-020DR005B-013b-Scleractinia-sp1.tif

11314801-002GR002B-003a-Caryophylliidae-sp1.tif

11314801-002GR002B-003b-Caryophylliidae-sp1.tif

11314801-002GR002B-003c-Caryophylliidae-sp1.tif

11314801-007GR011B-005a-Caryophylliidae-sp1.tif

11314801-007GR011B-005b-Caryophylliidae-sp1.tif

11314802-008GR012B-002a-Caryophylliidae-sp2.tif

11314802-008GR012B-002b-Caryophylliidae-sp2.tif

11314803-016GR026B-002-Caryophylliidae-sp3.tif

11314804-020DR005B-012a-Caryophylliidae-sp4.tif

11314804-020DR005B-012b-Caryophylliidae-sp4.tif

11320801-023DR006B-004-Dendrophylliidae-sp1.tif

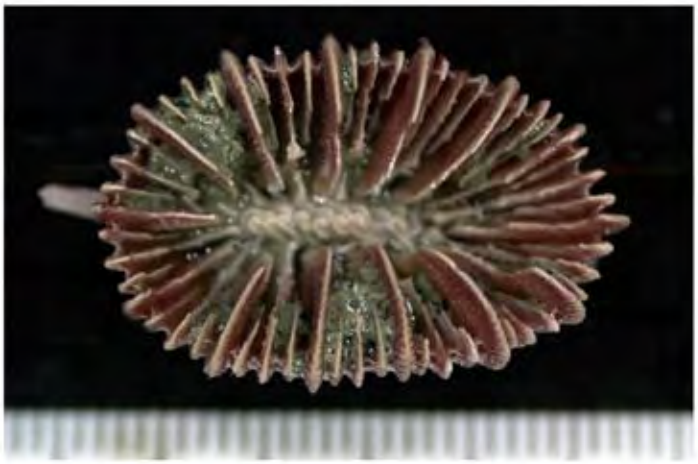

11314805-064GR084B-004b-Caryophylliidae-sp5.tif

11314805-064GR084B-004a-Caryophylliidae-sp5.tif

11317801-016GR026B-004b-Turbinoliidae-sp1.tif

11317801-016GR026B-004a-Turbinoliidae-sp1.tif

11320802-038DR010B-031a-Balanophyllia-sp1.tif

11320802-038DR010B-031b-Balanophyllia-sp1.tif

11328801-002GR001B-002a-Flabellum-sp1.tif

11328801-002GR001B-002b-Flabellum-sp1.tif

11328801-002GR001B-002c-Flabellum-sp1.tif

11328801-002GR001B-002d-Flabellum-sp1.tif

11328801-002GR001B-002e-Flabellum-sp1.tif

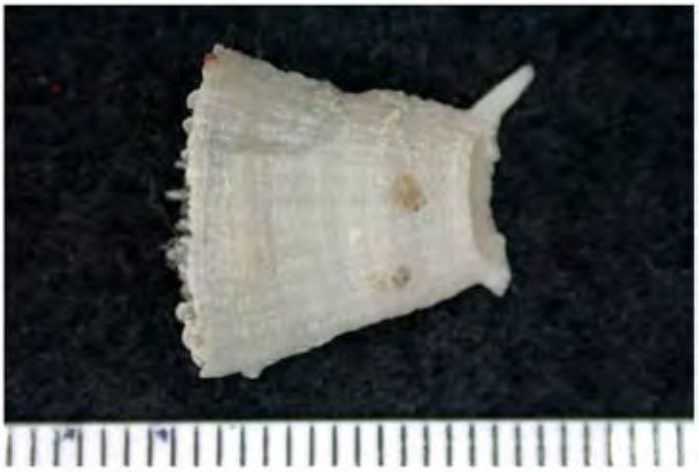

11328801-002GR001B-002f-Flabellum-sp1.tif

11328801-002GR001B-002g-Flabellum-sp1.tif

11328801-002GR001B-002h-Flabellum-sp1.tif

11328801-003GR004B-002-Flabellum-sp1.tif

28840801-013DR001B-054a-Galatheidae-sp1.tif

28840801-013DR001B-054b-Galatheidae-sp1.tif

28840802-013DR001B-055a-Galatheidae-sp2.tif

28840802-013DR001B-055b-Galatheidae-sp2.tif

28840803-013DR001B-056a-Galatheidae-sp3.tif

28840803-013DR001B-056b-Galatheidae-sp3.tif

28840803-039GR061B-002a-Galatheidae-sp3.tif

28840803-039GR061B-002b-Galatheidae-sp3.tif

28840803-039GR062B-002a-Galatheidae-sp3.tif

28840803-039GR062B-002b-Galatheidae-sp3.tif

28840804-018GR030B-001a-Galatheidae-sp4.tif

28840804-018GR030B-001b-Galatheidae-sp4.tif

28840004-013DR001B-013-Allogalathea-elegans.tif

28840805-038DR010B-007a-Galatheidae-sp5.tif

28840805-038DR010B-007b-Galatheidae-sp5.tif

28840805-038DR010B-007c-Galatheidae-sp5.tif

28840806-043GR069B-006a-Galatheidae-sp6.tif

28840806-043GR069B-006b-Galatheidae-sp6.tif

28840807-053DR015B-016-Galatheidae-sp7.tif

28843801-013DR001B-052-Porcellanidae-sp1.tif

28846801-002BS002-003a-Hippidae-sp1.tif

28846801-002BS002-003b-Hippidae-sp1.tif

28846801-003GR004B-002a-Hippidae-sp1.tif

28846801-003GR004B-002b-Hippidae-sp1.tif

28880801-013GR020B-001a-Majidae-sp1.tif

28880801-013GR020B-001b-Majidae-sp1.tif

28880801-013GR020B-001c-Majidae-sp1.tif

28880802-019GR033B-006a-Majidae-sp2.tif

28880802-019GR033B-006b-Majidae-sp2.tif

28911801-001BS001-001a-Portunus-sp1.tif

28911801-001BS001-001b-Portunus-sp1.tif

28911802-013DR011B-059a-Thalamita-sp1.tif

28911802-013DR011B-059b-Thalamita-sp1.tif

28911803-053DR015B-001a-Charybdis-sp1.tif

28911803-053DR015B-001b-Charybdis-sp1.tif

28900801-018GR030B-002a-Corystidae-sp1.tif

28900801-018GR030B-002b-Corystidae-sp1.tif

28926801-013DR001B-057a-Pilumnidae-sp1.tif

28926801-013DR001B-057b-Pilumnidae-sp1.tif

28926801-013DR001B-057c-Pilumnidae-sp1.tif

28922801-032BS006B-004a-Goneplacidae-sp1.tif

28922801-032BS006B-004b-Goneplacidae-sp1.tif

28922801-032BS006B-004c-Goneplacidae-sp1.tif

28922802-064GR084B-002a-Goneplacidae-sp2.tif

28922802-064GR084B-002b-Goneplacidae-sp2.tif

28922802-064GR084B-002c-Goneplacidae-sp2.tif

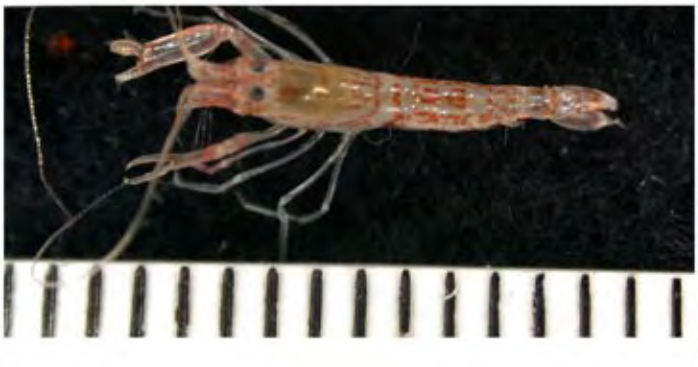

28765801-006GR009B-003a-Alpheidae-sp1.tif

28765801-006GR009B-003b-Alpheidae-sp1.tif

28765802-013DR001B-058a-Alpheidae-sp2.tif

28765802-013DR001B-058b-Alpheidae-sp2.tif

28765803-016GR027B-002a-Alpheidae-sp3.tif

28765803-016GR027B-002b-Alpheidae-sp3.tif

28765804-022GR038B-002a-Alpheidae-sp4.tif

28765804-022GR038B-002b-Alpheidae-sp4.tif

28765805-023GR042B-003a-Alpheidae-sp5.tif

28765805-023GR042B-003b-Alpheidae-sp5.tif

28765806-038DR010B-022a-Alpheidae-sp6.tif

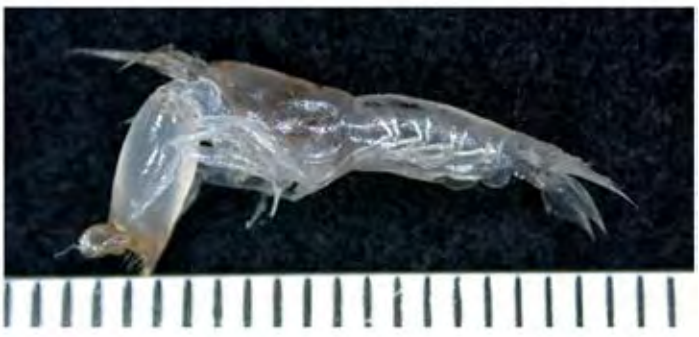

28765806-038DR010B-022b-Alpheidae-sp6.tif

27500801-013DR001B-044a-Cirripedia-sp1.tif

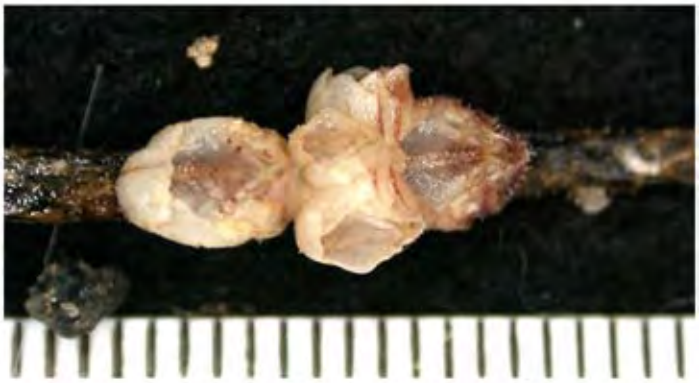

27500801-013DR001B-044b-Cirripedia-sp1.tif

27500802-038DR010B-029-Cirripedia-sp2.tif

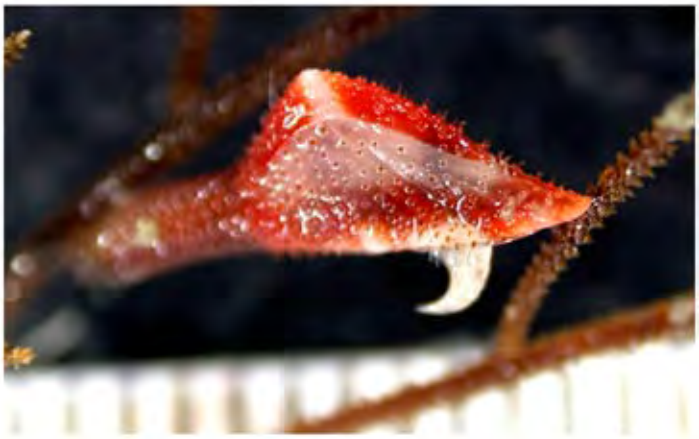

27500803-044DR013B-002-Cirripedia-sp3.tif

27524801-043DR012B-006a-Arcoscalpellum-sp1.tif

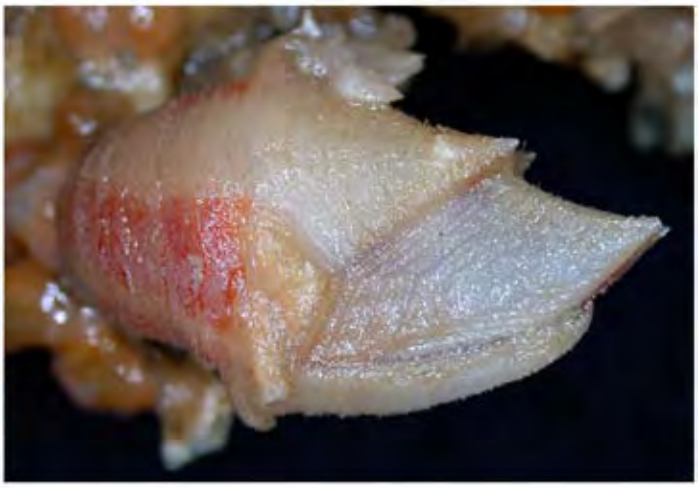

27524801-043DR012B-006b-Arcoscalpellum-sp1.tif

27524801-043DR012B-006c-Arcoscalpellum-sp1.tif

27524802-043DR012B-007a-Scalpellidae-sp1.tif

27524802-043DR012B-007b-Scalpellidae-sp1.tif

27524802-043DR012B-007c-Scalpellidae-sp1.tif

28220801-007BS003-006-Cirolanidae-sp1.tif

28220802-010GR017B-003a-Cirolanidae-sp2.tif

28220802-010GR017B-003b-Cirolanidae-sp2.tif

28220803-019GR033B-001-Cirolanidae-sp3.tif

28226801-019GR033B-002-Sphaeromatidae-sp1.tif

28400801-001BS001-005-Gammaridea-sp1.tif

28711801-007BS003-004a-Penaeidae-sp1.tif

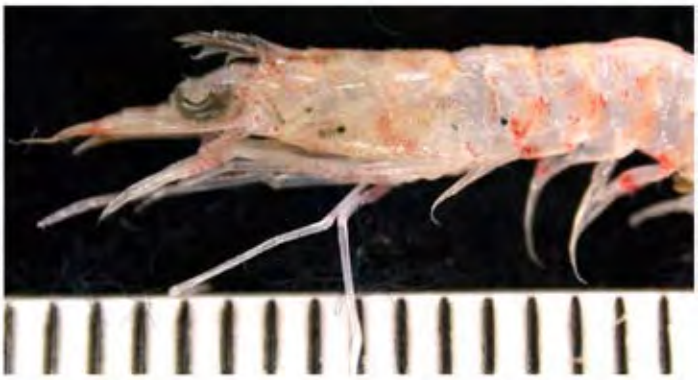

28711801-007BS003-004b-Penaeidae-sp1.tif

28711802-016GR027B-003a-Penaeidae-sp2.tif

28711802-016GR027B-003b-Penaeidae-sp2.tif

28730801-039GR062B-003a-Caridea-sp1.tif

28730801-039GR062B-003b-Caridea-sp1.tif

28770801-020DR005B-009a-Pandalidae-sp1.tif

28770801-020DR005B-009b-Pandalidae-sp1.tif

28030801-005GR006B-001-Stomatopoda-sp1.tif

28030802-006GR009B-001-Stomatopoda-sp2.tif

28030802-015BS004B-004-Stomatopoda-sp2.tif

28030803-007GR010B-001a-Stomatopoda-sp3.tif

28030803-007GR010B-001b-Stomatopoda-sp3.tif

28105801-001BS001-004-Tanaidacea-sp1.tif

28105802-007BS003-012-Tanaidacea-sp2.tif

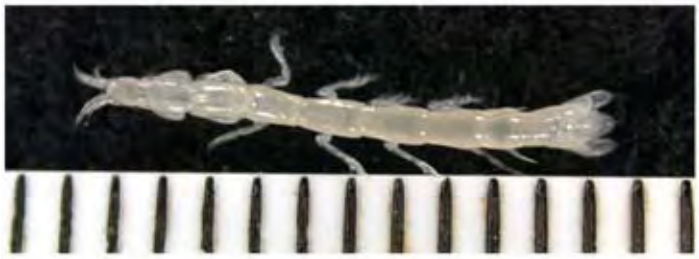

28205801-007BS003-007-Anthuridae-sp1.tif

28205802-023GR042B-002-Anthuridae-sp2.tif

28206801-032BS006B-005a-Paranthuridae-sp1.tif

28206801-032BS006B-005b-Paranthuridae-sp1.tif

28803801-002GR001B-001a-Callianassidae-sp1.tif

28803801-002GR001B-001b-Callianassidae-sp1.tif

28803801-002GR001B-001c-Callianassidae-sp1.tif

28803801-002GR001B-001d-Callianassidae-sp1.tif

28803801-002GR085B-003a-Callianassidae-sp1.tif

28803801-002GR085B-003b-Callianassidae-sp1.tif

28803801-005GR006B-002a-Callianassidae-sp1.tif

28803801-005GR006B-002d-Callianassidae-sp1.tif

28803802-007GR011B-004a-Callianassidae-sp2.tif

28803802-007GR011B-004b-Callianassidae-sp2.tif

28803802-064GR084B-003a-Callianassidae-sp2.tif

28803802-064GR084B-003b-Callianassidae-sp2.tif

28803803-007GR011B-003-Callianassidae-sp3.tif

28803804-015BS004B-006a-Callianassidae-sp4.tif

28803804-015BS004B-006b-Callianassidae-sp4.tif

28803804-015BS004B-006c-Callianassidae-sp4.tif

28803805-023GR042B-004a-Callianassidae-sp5.tif

28803805-023GR042B-004b-Callianassidae-sp5.tif

28803806-032BS006B-002a-Callianassidae-sp6.tif

28803806-032BS006B-002b-Callianassidae-sp6.tif

28803807-032BS006B-003a-Callianassidae-sp7.tif

28803807-032BS006B-003b-Callianassidae-sp7.tif

28805801-002BS002-002a-Upobebiidae-sp1-m.tif

28805801-002BS002-002b-Upobebiidae-sp1-m.tif

28805801-002BS002-002c-Upobebiidae-sp1-f.tif

28805801-002BS002-002d-Upobebiidae-sp1-f.tif

28805802-003GR005B-002a-Upobebiidae-sp2.tif

28805802-003GR005B-002b-Upobebiidae-sp2.tif

28805802-003GR005B-002c-Upobebiidae-sp2.tif

28805803-015BS004B-003a-Upobebiidae-sp3.tif

28805803-015BS004B-003b-Upobebiidae-sp3.tif

25143801-045GR072B-001-Echinasteridae-sp1.tif

25404801-042DR011B-002a-Psolidae-sp1.tif

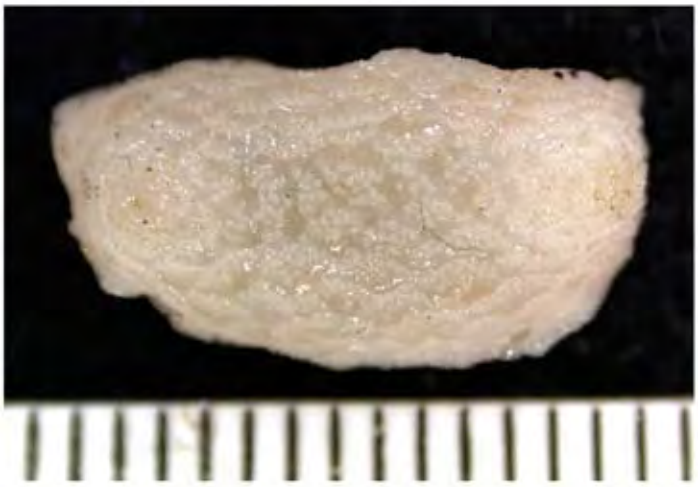

25404801-042DR011B-002b-Psolidae-sp1.tif

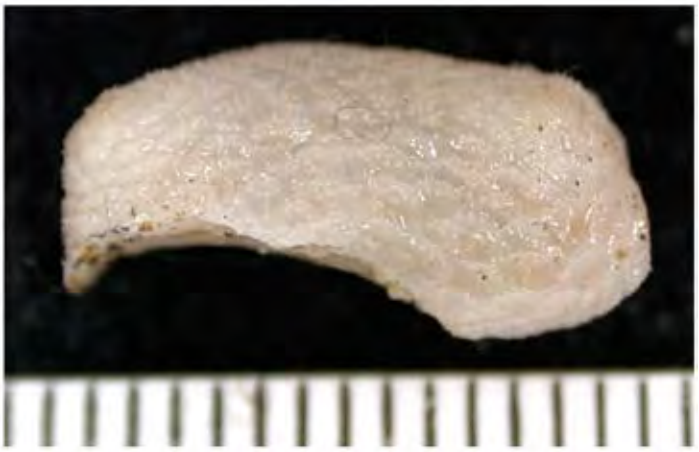

25404801-042DR011B-002c-Psolidae-sp1.tif

25404801-042DR011B-002d-Psolidae-sp1.tif

25001801-013DR001B-001a-Crinoidea-sp1.tif

25001801-013DR001B-001b-Crinoidea-sp1.tif

25001802-020DR005B-002-Crinoidea-sp2.tif

25001802-020GR035B-004a-Crinoidea-sp2.tif

25001802-020GR035B-004b-Crinoidea-sp2.tif

25021801-043GR069B-003-Pentacrinitidae-sp1.tif

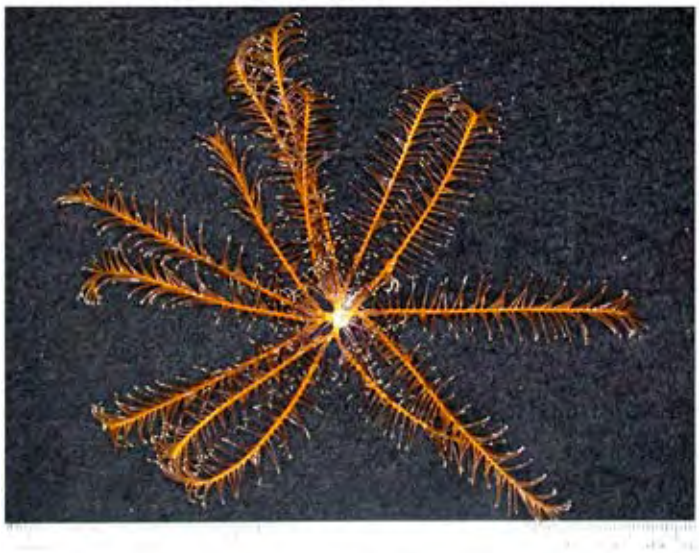

25001803-038GR059B-007a-Crinoidea-sp3.tif

25001803-038GR059B-007b-Crinoidea-sp3.tif

25039801-013DR001B-007a-Colobometridae-sp1.tif

25039801-013DR001B-007b-Colobometridae-sp1.tif

25039802-013DR001B-008-Colobometridae-sp2.tif

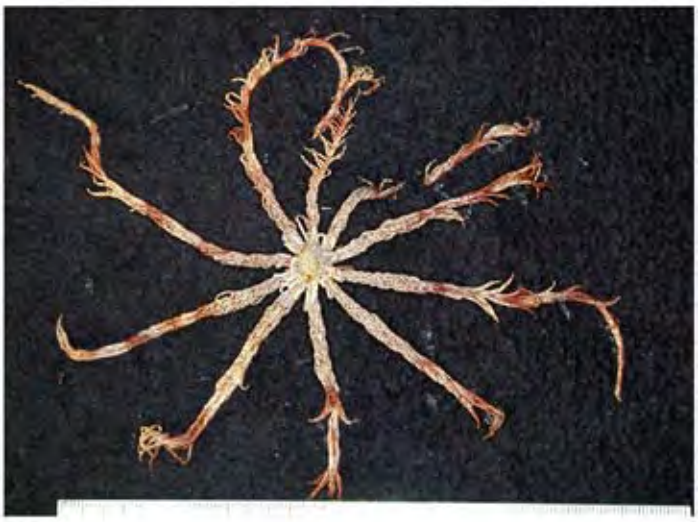

25039803-013DR001B-009-Colobometridae-sp3.tif

25200801-020DR005B-026a-Echinoidea-sp1.tif

25200801-020DR005B-026b-Echinoidea-sp1.tif

25200801-020DR005B-026c-Echinoidea-sp1.tif

25200801-048GR074B-002a-Echinoidea-sp1.tif

25200801-048GR074B-002b-Echinoidea-sp1.tif

25200801-048GR074B-002c-Echinoidea-sp1.tif

25200801-048GR074B-002d-Echinoidea-sp1.tif

25202801-038DR010B-001a-Cidaridae-sp1.tif

25202801-038DR010B-001b-Cidaridae-sp1.tif

25202801-038DR010B-001c-Cidaridae-sp1.tif

25202802-038DR010B-019a-Cidaridae-sp2.tif

25202802-038DR010B-019b-Cidaridae-sp2.tif

25160801-001BS001-003a-Ophiuroidea-sp1.tif

25160801-001BS001-003b-Ophiuroidea-sp1.tif

25160801-001BS001-003c-Ophiuroidea-sp1.tif

25160801-001BS001-003d-Ophiuroidea-sp1.tif

25160802-007BS003-014a-Ophiuroidea-sp2.tif

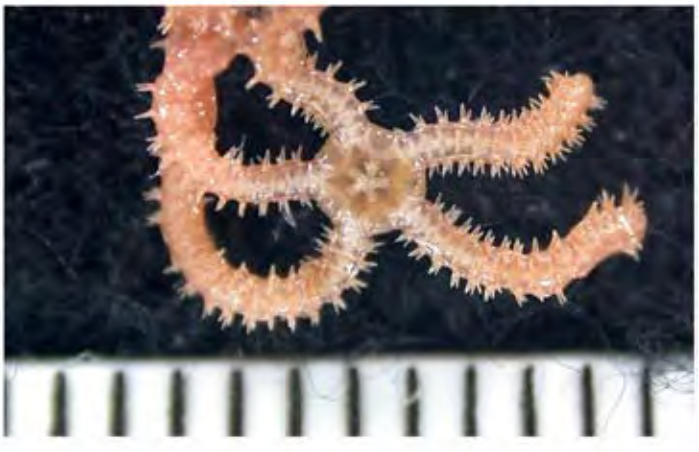

25160802-007BS003-014b-Ophiuroidea-sp2.tif

25160803-013DR001B-053a-Ophiuroidea-sp3.tif

25160803-013DR001B-053b-Ophiuroidea-sp3.tif

25160804-017GR029B-003a-Ophiuroidea-sp4.tif

25160804-017GR029B-003b-Ophiuroidea-sp4.tif

25160804-017GR029B-003c-Ophiuroidea-sp4.tif

25160805-020DR005B-004a-Ophiuroidea-sp5.tif

25160805-020DR005B-004b-Ophiuroidea-sp5.tif

25160805-020DR005B-004c-Ophiuroidea-sp5.tif

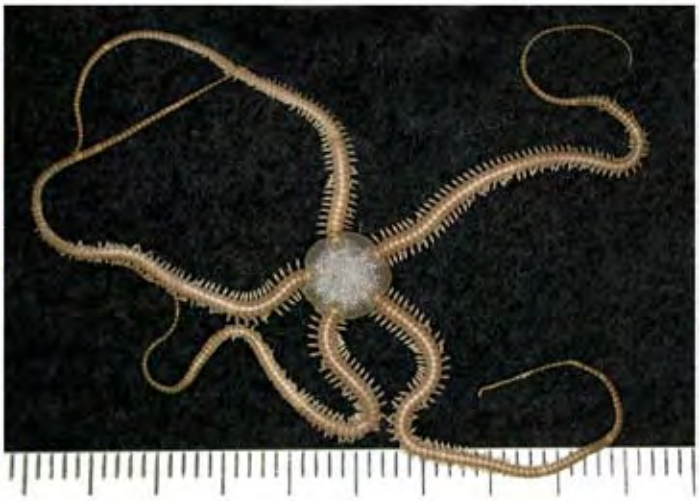

25160806-028GR049B-002a-Ophiuroidea-sp6.tif

25160806-028GR049B-002b-Ophiuroidea-sp6.tif

25160806-028GR049B-002c-Ophiuroidea-sp6.tif

25160807-043GR069B-004a-Ophiuroidea-sp7.tif

25160807-043GR069B-004b-Ophiuroidea-sp7.tif

25160807-043GR069B-004c-Ophiuroidea-sp7.tif

25160808-043DR012B-003a-Ophiuroidea-sp8.tif

25160808-043DR012B-003b-Ophiuroidea-sp8.tif

25160808-043DR012B-003c-Ophiuroidea-sp8.tif

25160809-049GR075B-002a-Ophiuroidea-sp9.tif

25160809-049GR075B-002b-Ophiuroidea-sp9.tif

25160810-049GR077B-001a-Ophiuroidea-sp10.tif

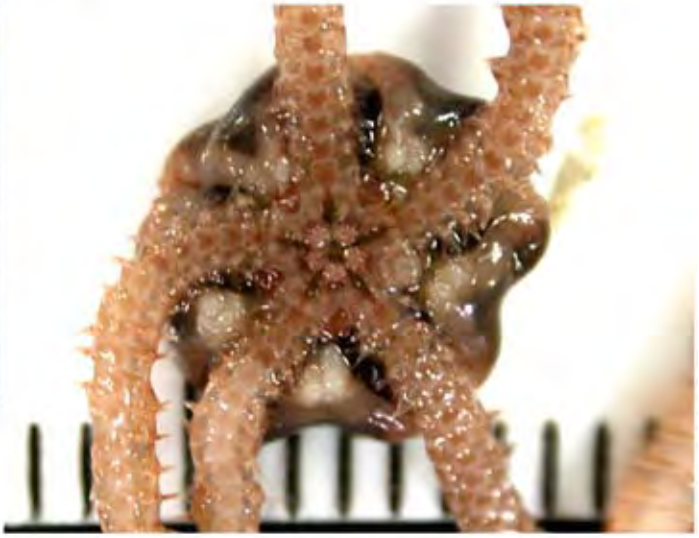

25160810-049GR077B-001b-Ophiuroidea-sp10.tif

25160810-049GR077B-001c-Ophiuroidea-sp10.tif

25160811-002GR085B-004a-Ophiuroidea-sp11.tif

25160811-002GR085B-004b-Ophiuroidea-sp11.tif

25160811-002GR085B-004c-Ophiuroidea-sp11.tif

25171801-013DR001B-002a-Gorgonocephalidae-sp1.tif

25171801-013DR001B-002b-Gorgonocephalidae-sp1.tif

25171801-013DR001B-002c-Gorgonocephalidae-sp1.tif

25171801-020DR005B-019a-Gorgonocephalidae-sp1.tif

25171801-020DR005B-019b-Gorgonocephalidae-sp1.tif

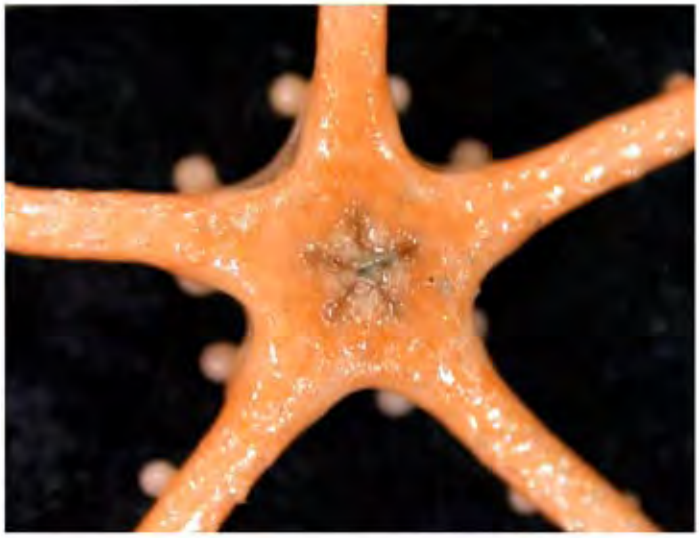

25171801-020DR005B-019c-Gorgonocephalidae-sp1.tif

25171802-020DR005B-007a-Gorgonocephalidae-sp2.tif

25171802-020DR005B-007b-Gorgonocephalidae-sp2.tif

25171802-020DR005B-007c-Gorgonocephalidae-sp2.tif

25171803-020DR005B-003a-Gorgonocephalidae-sp3.tif

25171803-020DR005B-003b-Gorgonocephalidae-sp3.tif

25171803-020DR005B-003c-Gorgonocephalidae-sp3.tif

25171804-038DR010B-004a-Gorgonocephalidae-sp4.tif

25171804-038DR010B-004b-Gorgonocephalidae-sp4.tif

25171804-038DR010B-004c-Gorgonocephalidae-sp4.tif

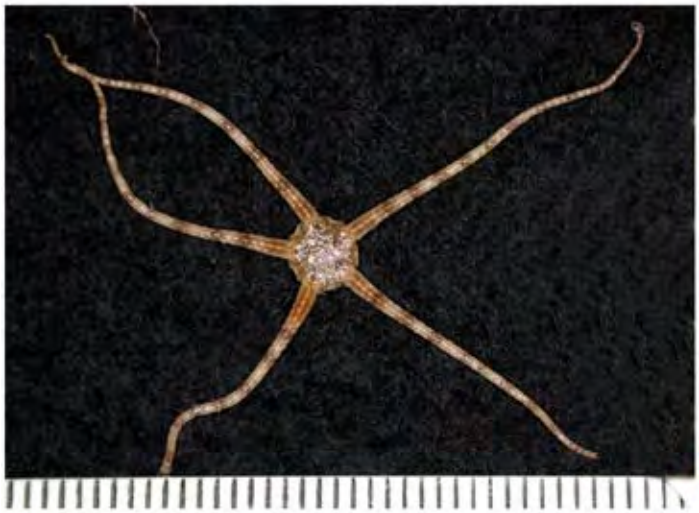

25176801-003GR004B-001a-Ophiuridae-sp1.tif

25176801-003GR004B-001b-Ophiuridae-sp1.tif

25176801-003GR004B-001c-Ophiuridae-sp1.tif

25176802-038DR010B-017a-Ophiuridae-sp2.tif

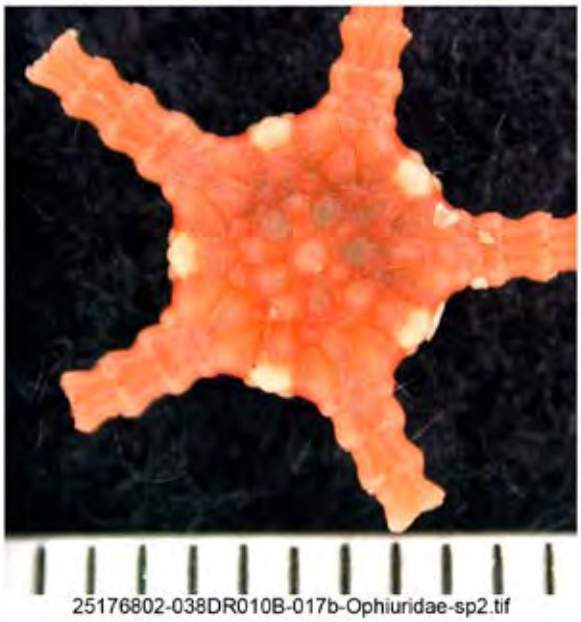

25176802-038DR010B-017b-Ophiuridae-sp2.tif

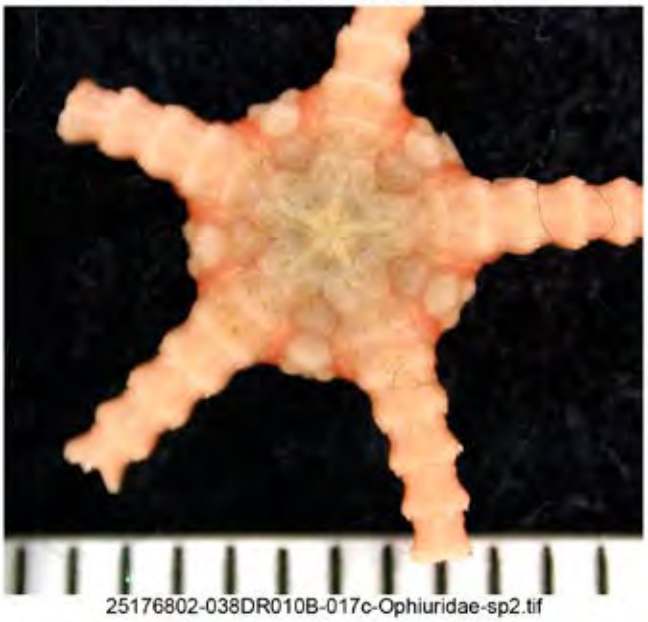

25176802-038DR010B-017c-Ophiuridae-sp2.tif

25178801-039GR061B-003a-Ophiocomidae-sp1.tif

25178801-039GR061B-003b-Ophiocomidae-sp1.tif

25178801-039GR061B-003c-Ophiocomidae-sp1.tif

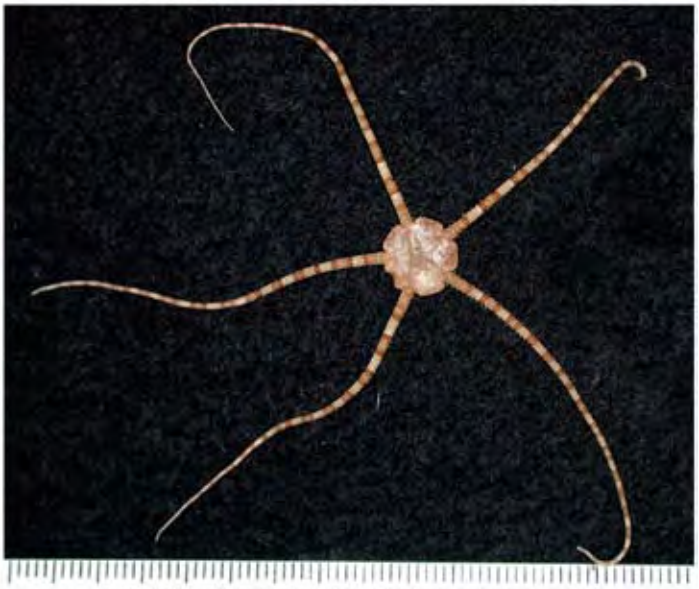

25180801-027GR048B-002a-Ophiodermatidae-sp1.tif

25180801-027GR048B-002b-Ophiodermatidae-sp1.tif

25180801-027GR048B-002c-Ophiodermatidae-sp1.tif

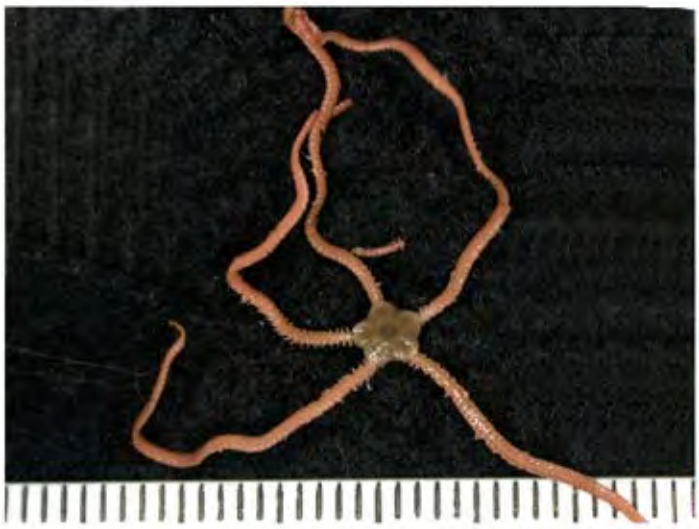

25191801-005GR007B-004a-Amphiuridae-sp1.tif

25191801-005GR007B-004b-Amphiuridae-sp1.tif

25191801-005GR007B-004c-Amphiuridae-sp1.tif

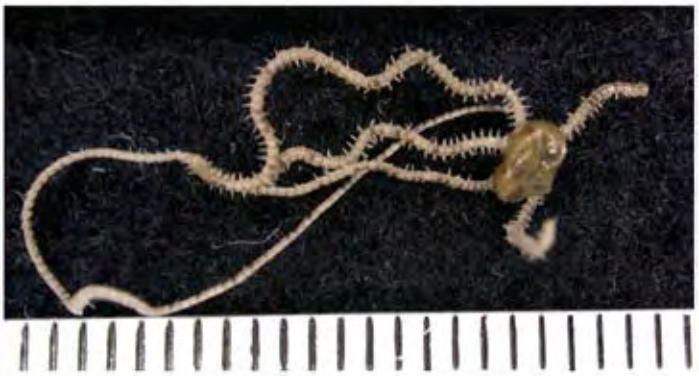

25191802-007BS003-013a-Amphiuridae-sp2.tif

25191802-007BS003-013b-Amphiuridae-sp2.tif

25191802-007BS003-013c-Amphiuridae-sp2.tif

25191803-011GR018B-002a-Amphiuridae-sp3.tif

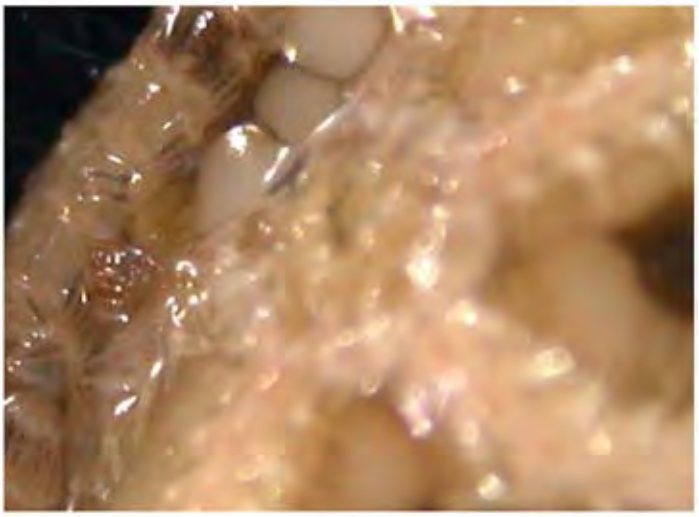

25191803-011GR018B-002b-Amphiuridae-sp3.tif

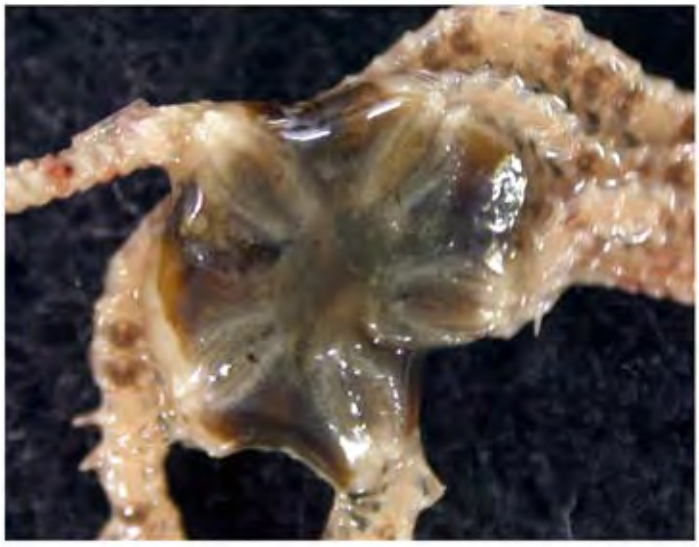

25191803-011GR018B-002c-Amphiuridae-sp3.tif

25191804-002GR086B-002a-Amphiuridae-sp4.tif

25191804-002GR086B-002b-Amphiuridae-sp4.tif

25191804-002GR086B-002c-Amphiuridae-sp4.tif

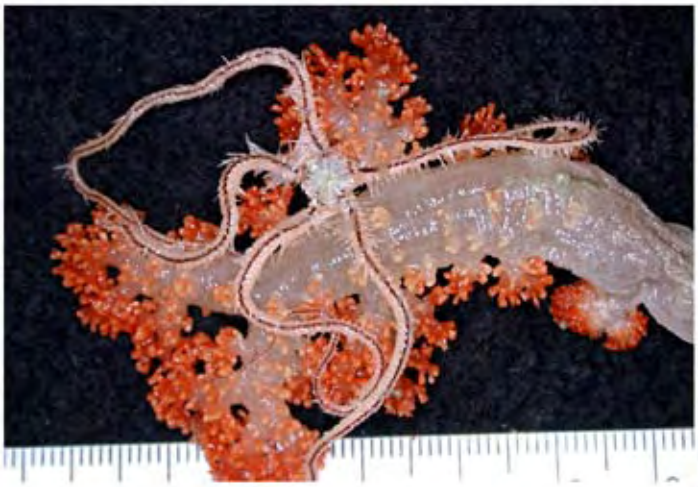

25192801-013DR001B-011a-Ophiothrix-sp1.tif

25192801-013DR001B-011b-Ophiothrix-sp1.tif

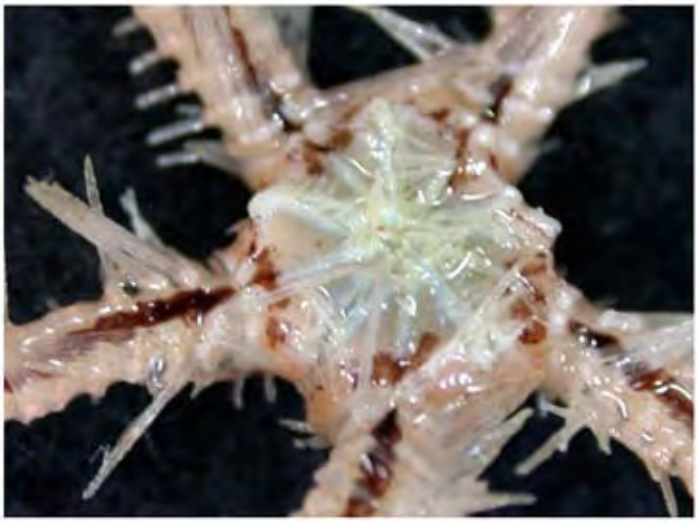

25192801-013DR001B-011c-Ophiothrix-sp1.tif

37000801-007BS003B-002-Fish-sp1.tif

37000801-061GR082B-002-Fish-sp1.tif

37065801-002GR003B-001-Nettastomatidae-sp1.tif

37428801-005GR007B-002-Gobiidae-sp1.tif

37428802-010GR017B-002-Gobiidae-sp2.tif

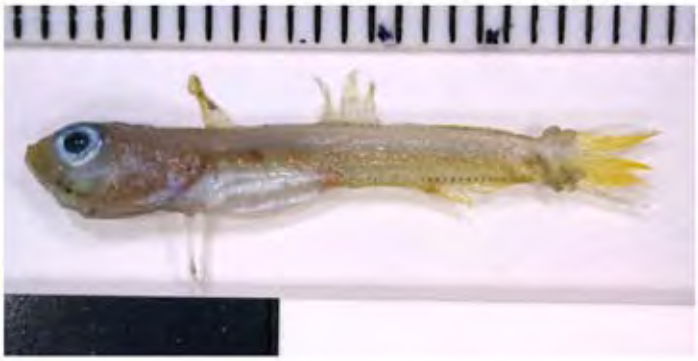

37428803-013GR021B-002-Gobiidae-sp3.tif

37428804-015BS004B-005-Gobiidae-sp4.tif

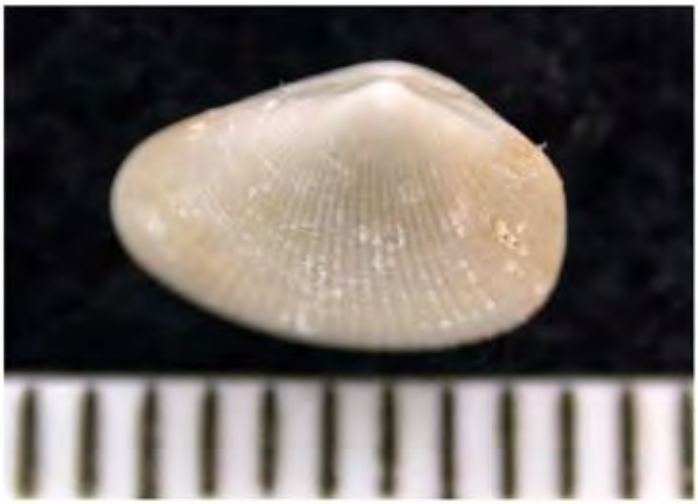

23199801-018GR030B-003-Bivalvia-sp1.tif

23207801-001BS001-006-Nuculanidae-sp1.tif

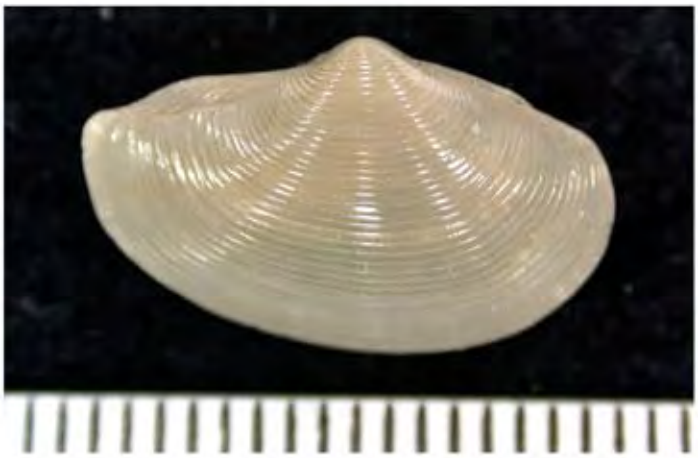

23207802-015BS004B-002-Nuculanidae-sp2.tif

23207802-024GR044B-002-Nuculanidae-sp2.tif

23207803-030GR054B-002-Nuculanidae-sp3.tif

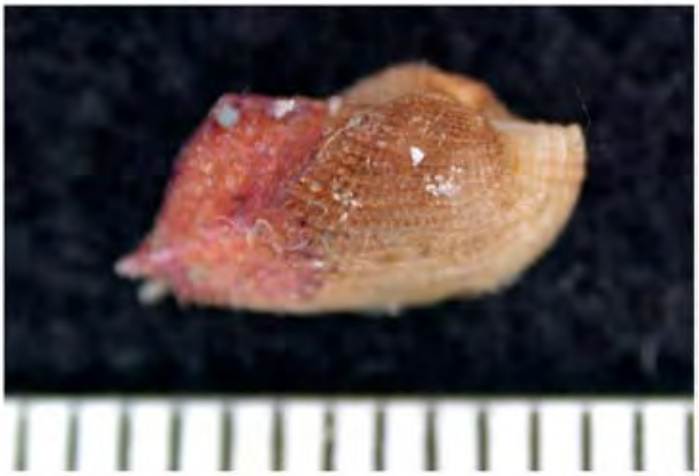

23226801-053DR015B-017-Arcidae-sp1.tif

23272801-038DR010B-020-Spondylus-sp1.tif

23301801-053DR015B-018a-Chama-sp1.tif

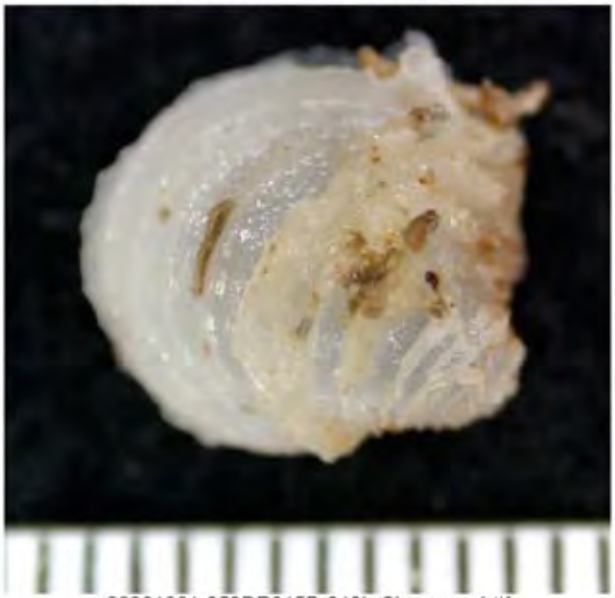

23301801-053DR015B-018b-Chama-sp1.tif

23355801-007BS003-009-Tellinidae-sp1.tif

23410801-002GR001B-005-Thraciidae-sp1.tif

24080801-013DR001B-045-Siliquaria-sp1.tif

24191801-016GR026B-001-Epitoniidae-sp1.tif

24207801-037GR056B-002a-Volutoconus-sp1.tif

24207801-037GR056B-002b-Volutoconus-sp1.tif

24221801-009GR014B-001a-Terebridae-sp1.tif

24221801-009GR014B-001b-Terebridae-sp1.tif

24202801-001BS001-007-Fasciolariinae-sp1.tif

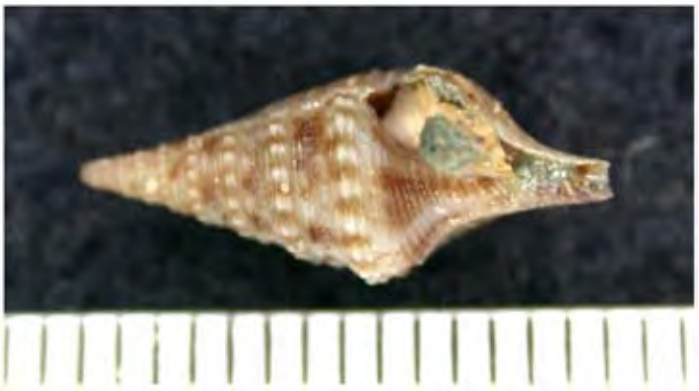

24220801-006GR009B-005a-Turridae-sp1.tif

24220801-006GR009B-005b-Turridae-sp1.tif

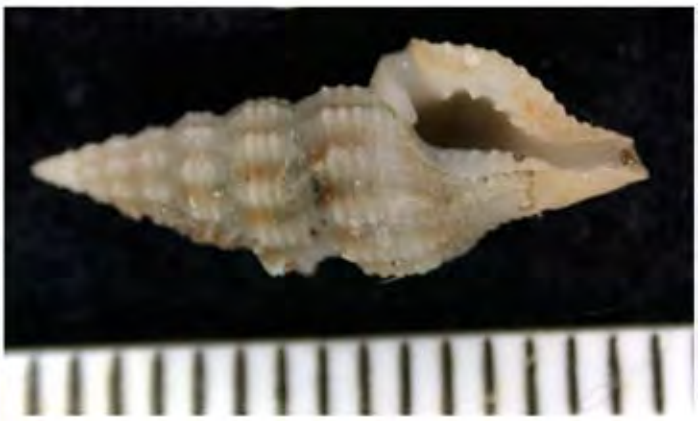

24220802-002GR085B-002a-Turridae-sp2.tif

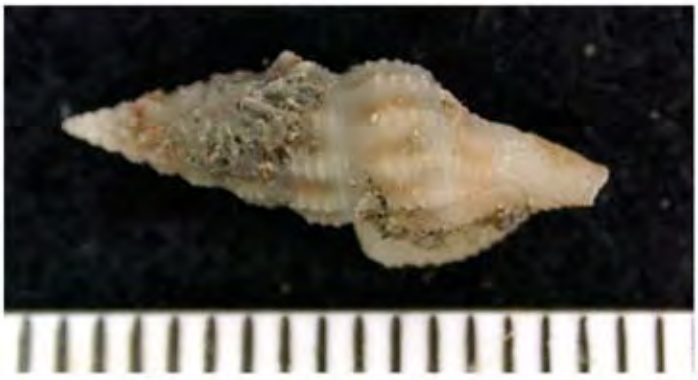

24220802-002GR085B-002b-Turridae-sp2.tif

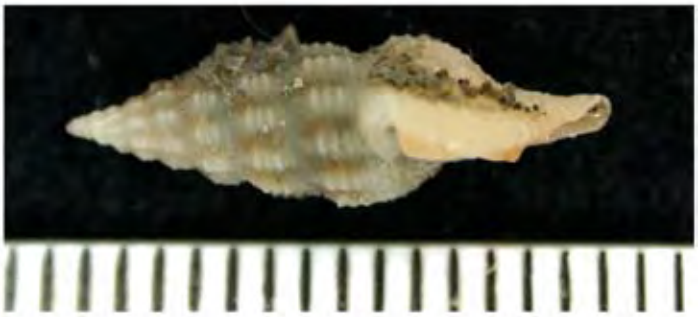

24220802-002GR085B-002c-Turridae-sp2.tif

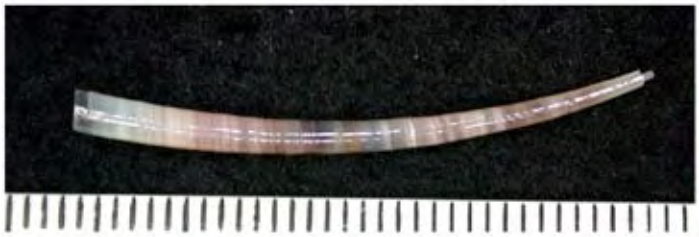

23499801-008GR013B-001a-Scaphopoda-sp1.tif

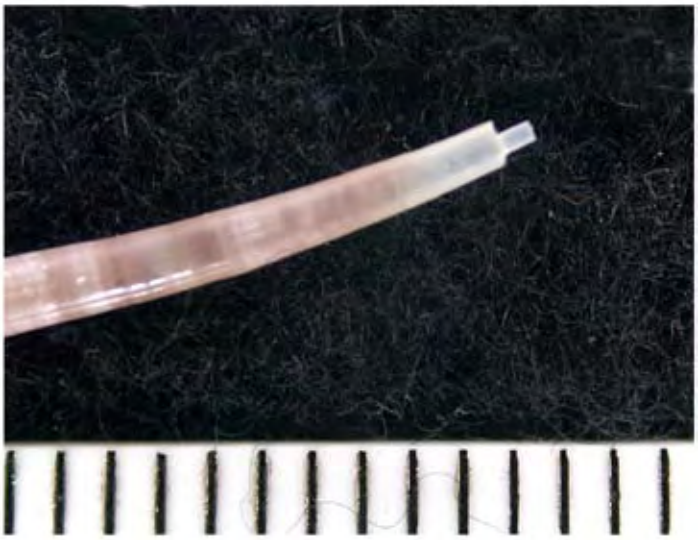

23499801-008GR013B-001b-Scaphopoda-sp1.tif

10300801-044DR013B-006a-Hexactinellida-sp1.tif

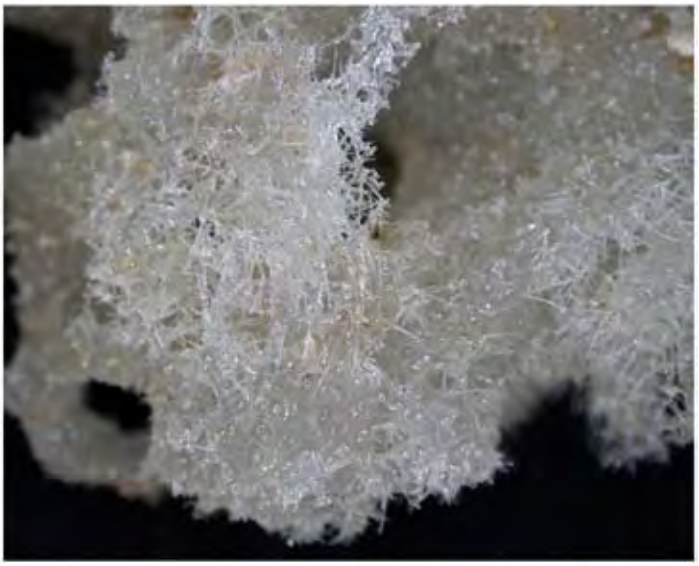

10300801-044DR013B-006b-Hexactinellida-sp1.tif

10300802-044DR013B-005a-Hexactinellida-sp2.tif

10300802-044DR013B-005b-Hexactinellida-sp2.tif

10300803-053DR015B-004a-Hexactinellida-sp3.tif

10300803-053DR015B-004b-Hexactinellida-sp3.tif

10180801-013DR001B-027-Demospongiae-sp1.tif

10180802-013DR001B-046a-Demospongiae-sp2.tif

10180802-013DR001B-046b-Demospongiae-sp2.tif

10180803-038GR058B-003-Demospongiae-sp3.tif

10180804-038GR059B-003-Demospongiae-sp4.tif

10180805-038GR059B-002-Demospongiae-sp5.tif

10180806-038DR010B-002-Demospongiae-sp6.tif

10180807-038DR010B-009-Demospongiae-sp7.tif

10180808-038DR010B-008-Demospongiae-sp8.tif

10180809-038DR010B-021-Demospongiae-sp9.tif

10180809-053DR015B-002-Demospongiae-sp9.tif

10180810-038DR010B-030-Demospongiae-sp10.tif

10180811-038DR010B-034a-Demospongiae-sp11.tif

10180811-038DR010B-034b-Demospongiae-sp11.tif

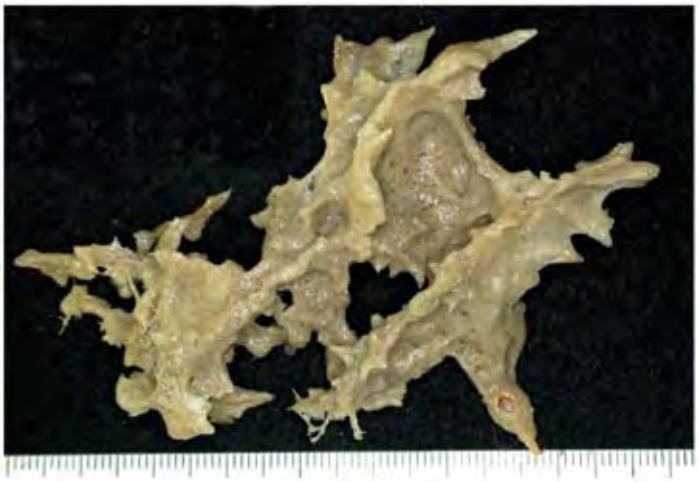

10180812-039GR061B-004-Demospongiae-sp12.tif

10180813-039GR062B-005a-Demospongiae-sp13.tif

10180813-039GR062B-005b-Demospongiae-sp13.tif

10180814-043DR012B-002-Demospongiae-sp14.tif

10180815-053DR015B-006a-Demospongiae-sp15.tif

10180815-053DR015B-006b-Demospongiae-sp15.tif

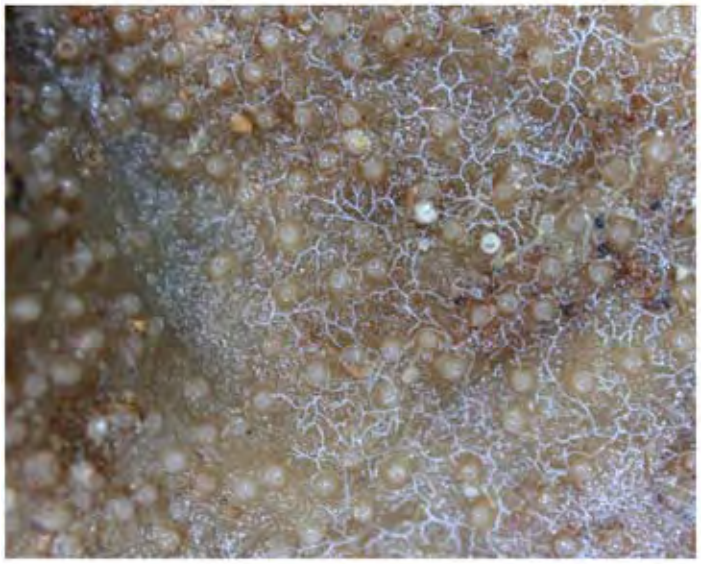

10180815-053DR015B-006c-Demospongiae-sp15.tif

10180816-053DR015B-012-Demospongiae-sp16.tif

10180817-053DR015B-020a-Demospongiae-sp17.tif

10180817-053DR015B-020b-Demospongiae-sp17.tif

10180818-053DR015B-005-Demospongiae-sp18.tif

35033801-038DR010B-035-Styelidae-sp1.tif

14000801-018GR031B-004a-Nemertea-sp1.tif

14000801-018GR031B-004b-Nemertea-sp1.tif

14000802-032BS006B-008-Nemertea-sp2.tif

17000801-012GR019B-002a-Sipuncula-sp1.tif

17000801-012GR019B-002b-Sipuncula-sp1.tif

17001801-009GR015B-002a-Sipunculus-sp1.tif

17001801-009GR015B-002b-Sipunculus-sp1.tif

17020801-045DR014B-003-Echiura-sp1.tif

22000801-001BS001-002a-Polychaeta-sp1.tif

22000801-001BS001-002b-Polychaeta-sp1.tif

22000801-005GR007B-003a-Polychaeta-sp1.tif

22000801-005GR007B-003b-Polychaeta-sp1.tif

22000801-010GR016B-001a-Polychaeta-sp1.tif

22000801-010GR016B-001b-Polychaeta-sp1.tif

22000802-001BS001-008-Polychaeta-sp2.tif

22000803-007GR011B-002-Polychaeta-sp3.tif

22000804-015GR025B-002a-Polychaeta-sp4.tif

22000804-015GR025B-002b-Polychaeta-sp4.tif

22000805-034BS007B-002-Polychaeta-sp5.tif

22000806-048GR073B-002-Polychaeta-sp6.tif

22000807-064GR083B-002-Polychaeta-sp7.tif

22024801-039GR062B-004-Eunice-sp1.tif

22062801-007BS003-005a-Polynoidae-sp1.tif

22062801-007BS003-005b-Polynoidae-sp1.tif

22062802-013DR001B-049a-Polynoidae-sp2.tif

22062802-013DR001B-049b-Polynoidae-sp2.tif

22030801-018GR031B-003-Onuphidae-sp1.tif

22116801-020DR005B-008-Flabelligeridae-sp1.tif

22116802-049GR078B-002a-Flabelligeridae-sp2.tif

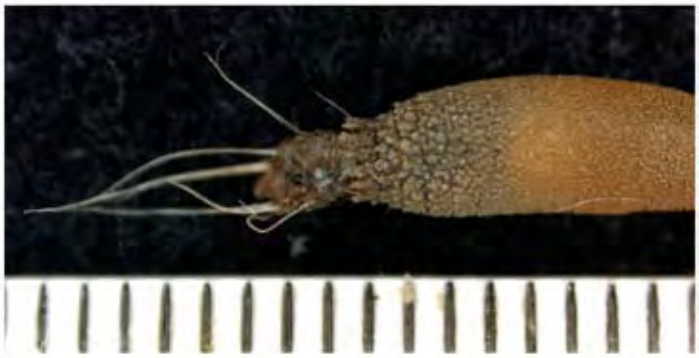

22116802-049GR078B-002b-Flabelligeridae-sp2.tif

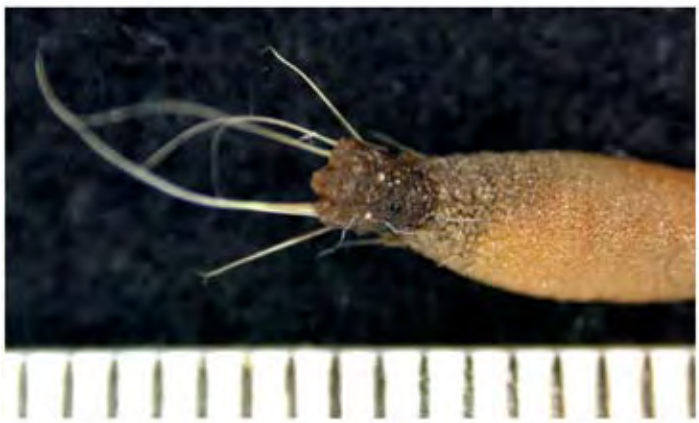

22116802-049GR078B-002c-Flabelligeridae-sp2.tif

22116802-049GR078B-002d-Flabelligeridae-sp2.tif